Dahanayake, Manilal

SURFACE CHEMISTRY: FUNDAMENTAL THERMODYNAMIC AND SURFACE PROPERTIES OF HIGHLY PURIFIED MODEL SURFACTANTS. ELUCIDATION OF INTERRELATIONSHIPS BETWEEN SURFACTANT CHEMICAL STRUCTURE, MECHANISMS OF ADSORPTION, AND PROPERTIES OF IMPORTANCE IN PRACTICAL APPLICATIONS

City University of New York PH.D. 1985

Surface Chemistry

Fundamental thermodynamic and surface properties of highly purified model surfactants.

Elucidation of interrelationships between surfactant chemical structure, mechanisms of adsorption, and properties of importance in practical applications.

by

Manilal Dahanayake

A thesis
presented to the Graduate Faculty in Chemistry
in partial fulfillment of the
requirements for the degree of
Doctor of Philosophy
in
City University of New york

1985

This manuscript has been read and accepted for the Graduate Faculty in Chemistry in satisfaction of the dissertation requirement for the degree of Doctor of Philosophy.

12/7/84
date

Chairman of Examining Committee

12/11/84
date

Executive Officer

Seymour Aronson

C. J. Todaro

Supervisory Committee

The City University of New York

Abstract

FUNDAMENTAL THERMODYNAMIC AND SURFACE PROPERTIES OF HIGHLY PURIFIED MODEL SURFACTANTS

by

Manilal Dahanayake

Advisor: Professor Milton J. Rosen

The interrelationships between surfactant chemical structure, mechanism of adsorption, and properties of importance in practical application for well purified, well characterized surfactants of all charge types are elucidated. Properties measured are critical micelle concentration (cmc), maximum surface excess concentration and minimum area per molecule at aqueous solution/air interface, efficiency and effectiveness of surface tension reduction, standard thermodynamic parameters of micellization and of adsorption, effectiveness in foaming and textile wetting time.

Anionic surfactants of homogenous structure, $C_{12}H_{25}(OC_2H_4)_xOH$, where x = 2-8, were investigated. The standard free energy of

micellization was found to increase with increase in the length of the oxyethylene chain. On the other hand, the effect of this change on the standard free energy of adsorption was found to be almost insignificant.

Of the two cationic surfactants, N-dodecylpyridinium bromide was found to be somewhat more surface active than the corresponding chloride in all properties investigated. The difference appears to be due to the greater degree of hydration of the chloride ion compared to the bromide. Micellization appears to involve more dehydration of the counterion than adsorption at the aqueous solution-air interface.

Zwitterionic surfactants of structure, R $N(CH_2C_6H_5)(CH_3)CH_2COO^-$, where R is an alkyl chain of 10 or 12 carbon atoms, and $RN(CH_2C_6H_5)(CH_3)CH_2CH_2SO_3$ where R is 8, 10 and 12 carbon atoms, were synthesized. The surface areas per molecule for the glycines are comparable to those of the corresponding N-alkyl,N,N-dimethylglycines and 2-(trimethylammonium)alkanoates. On the other hand, the cmc for the glycines are found to be considerably smaller than for the corresponding N-alkyl,N,N-dimethylglycines and 2-(trimethylammonium)alkanoates.

Two series of anionic surfactants of type $C_{12}H_{25}(OC_2H_4)_iOSO_3Na$, where i = 1 and 2, and $C_nH_{2n+1}(OC_2H_4)_iSO_3Na$, where i = 0 or 1, and

n = 10 and 12 were investigated. In contrast to the polyethenoxylated nonionics, increases in the negative standard free energies of micellization and adsorption were observed with introduction of oxyethylene units into both these types of compounds. The complexation of the counterion with the oxyethylene groups of these polyethenoxylated anionic surfactants is suggested as an explanation for these results.

Dedication

To my parents, for their support and encouragement throughout my studies.

Acknowledgements

I would like to express my sincere thanks:

to Professor Milton J. Rosen for his excellent guidence, accessibility, encouragement, understanding and friendship throughout this work. I am proud to have worked under such a fine research scientist; his expert knowledge and helpfulness have made my learning experience all the more rewarding.

to Professor S. Aronson and Dr. E.D. Goddard, members of my examining and advisory committee for their time and advice.

to Dr. Padmanabhan Parayanthal, for sharing his knowledge of computerized text -editing ,

to Ramani, my wife, for seeing me through these years with understanding, support, friendship and love (not to mention typing).

Contents

TABLES

FIGURES

Chapter I

Introduction.

1.1 Surface - active agents

Surface-active agents, now commonly called surfactants, are among the most versatile of the products of the chemical industry. This is shown by their application as detergents in laundary cleaning compounds , dispersing agents in pharmaceutical preparation, flotation agents in the concentration of ores, emulsifying agents in food products, insecticides, polishes, and metal cutting oils, wetting agents in textile scouring and dyeing, and bonding agents in asphaltic applications. Soaps of long chain fatty acid salts have been known for their cleaning properties since the Roman empire. The advent of World War I and the scarcity of natural fats and oils in Germany led to the development of synthetic surface-active agents,(1).

Realization of the technical and commercial potentialities of surface-active agents during the interwar years produced intense

activity and interest in surface-active agents in Germany and in other countries. The years of the second World War and the years that followed saw enormous advances in industrial and household detergent markets, mainly due to the improvements in chemical technology rather than to new discoveries in chemical synthesis. Synthetic surface-active agents during the post war years have continued to develop at the expense of the soap-based products which are known to be inferior in their resistant to hard water containing calcium and magnesium ions.

Presently, the consumption of synthetic detergents is estimated to exceed seven billion pounds and by 1991 is expected to grow to 8.3 billion pounds (2). It is not only in the tonnage on a value basis that progress has been notable over the last few years, but especially in the development of new applications for surface-active agents and in commercial production of new products. More recently, there has been intense interest in the use of surfactants in micellar polymer flooding for enhanced oil recovery.

In spite of this wealth of experience in the area of surfactant chemistry, there have been relatively few studies of structure/property relationships, mechanisms of adsorption, and performance properties of well-defined surfactant model compounds. Lack of physicochemical data on well-characterized model compounds has hampered a rational approach

to the practical application of surfactants and to the development of improved products for industrial and biochemical applications. The objective of this investigation is to remedy that situation by providing physicochemical and performance data on well-purified , well-characterized surfactants of all charge types: anionic, cationic,, nonionic, and zwitterionic.

1.2 Adsorption at interfaces (3,4)

In general, the utility of surface-active agents in their appliciations is due to two characteristic fundamental properties: 1) their spontaneous adsorption at interfaces and 2) their aggregation in solution to form micelles.

Surface active agents (surfactants) have the property of adsorbing onto the surfaces or interfaces of the system and of altering the free energies of these surfaces and interfaces. The term interface indicates a boundary between any two immiscible phases. A general prerequisite for the stable existence of an interface between two phases is that the free energy of formation of the interface be positive.

In terms of potential function the total surface energy E^s, of a system where n_i and n_s are the number of nearest neighbours in the interior of the liquid and the surface region, respectively could be expressed by the following formula,

$$E^s = (N_o \varepsilon/2)(n_i - n_s)$$

Where ε is the interaction energy and N_o is Avogadro's number. Since the surface molecules have fewer nearest neighbours than the molecules in bulk phase, $n_s < n_i$; therefore the potential energy of a surface molecule is higher than that of a bulk molecule.

In general, $n_s = (0.6 \quad 0.8)n_i$ which means that E^s is 20-40% greater than E_i. Therefore a knowledge of the potential function for the interaction between molecules allows the calculation of the total surface energy, and this as a function of temperature will give us the surface free energy, which is the minimum amount of energy to create that surface or interface.

Surface or interfacial tension is the minimum amount of work required to create a unit area of the interface or to expand it by unit area. When we measure the surface tension of a liquid, we are measuring the interfacial free energy per unit area of the boundary between the liquid and the air above it. When we expand an interface, the minimum work, W, required to create the additional amount of the

interface is the product of the interfacial tension, γ times the increase in the area, A, of the interface, $W = \gamma x A$.

It was pointed out earlier that the molecules at the surface have higher potential energies than those in the interior. The surface free energy can be regarded as the work of bringing a molecule from the interior of a liquid to the surface and this will cause an extension of the surface. The structure of surfactants is such that when they are present in low concentration they are adsorbed at some or all of the interfaces in the system and significantly decrease the work required to bring molecules to the surface, thereby decreasing the surface free energy.

Surface-active agents have a characteristic molecular structure consisting of a hydrophobic group, which has very little attraction for the solvent, together with a hydrophilic group that has strong attraction for the solvent. Compounds having this structure are called amphipathic molecules. When amphipathic molecules are dissolved in water their hydrophobic groups disrupt the structure of water and thereby increase the free energy of the system. This in turn, will decrease the work required for the extension of the surface, since less work is required to bring a molecule of surfactant than a water molecule to the surface or interface. Their lyophilic groups, due to their

affinity for the solvent, will prevent the whole molecule from being expelled completely from the solvent as a separate phase. In addition, this amphipathic nature will allow the molecule to orientate at the interface with the lyophilic group towards the solvent and the lyophobic group away from it. This orientation is a very important factor in changing the properties of the interface.

1.2.1 Surface Thermodynamic Quantities

When adsorption takes place at an interface the surface tension changes, and one of the main objectives of surface chemistry is to determine the amount of material that is adsorbed at an interface. In this respect, the Gibbs adsorption equation is very useful in determining the surface concentration at liquid-liquid and liquid -vapour systems.

In the Gibbs treatment, the interface is regarded as a mathematical dividing plane (the Gibbs surface) (3,4).

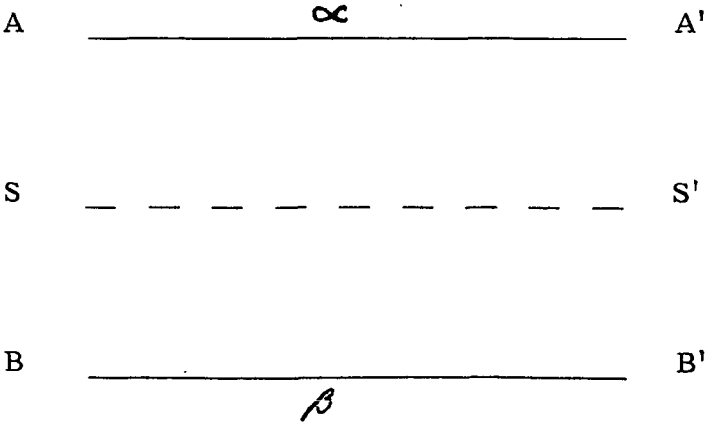

This is illustrated in the figure above where α and β are homogenous up to the phase AA' and BB' respectively. SS' represent the dividing surface having zero thickness and volume situated at some arbitary position between AA' and BB'. The amount of adsorption of component i is measured by its surface excess, defined as the amount of i in unit area of the region between AA' and BB' less the amount of i in the same region of α and β extended unchanged to SS'.

The total internal energy of the system comprising α $\beta$and interface, s, is the sum of the internal energies of each of the phases and so,

$$U = U^{\alpha} + U^{\beta} + U^{s} \tag{1}$$

where U^{α}, U^{β} and U^{s} are the internal energies of α β and the interface respectively. Correspondingly for a small reversible change,

$$dU = dU^{\alpha} + dU^{\beta} + dU^{s} \tag{2}$$

$$dU = \sum_{a} TdS^{a} - \sum_{a} PdV^{a} + \gamma dA + \sum_{a}\sum_{i} \mu_i dn_i^{a} \tag{3}$$

where $\sum_{a}$ denotes summation over all the phases present in the system, γ is the tension and A the area of the interface, μ is the chemical potential of component i, and n_i , the number of moles of i in the system $\sum_{i}$ denotes the summation over all species 1 to i.

For the surface alone,

$$dU^s = TdS^s - PdV + \gamma dA + \sum_i \mu_i dn_i^s \quad (4)$$

$$dU^s = TdS^s + \gamma dA + \sum_i \mu_i dn_i^s \quad (5)$$

as $dV = O$, from the Gibbs convention for the surface.

Integration of equation (5), holding constant the intensive properties T, μ_i and γ, we obtain

$$U^s = TS^s + \gamma A + \sum_i \mu_i n_i^s \quad (6)$$

On differentiation, this equation becomes

$$dU^s = TdS^s + S^s dT + \sum_i \mu_i dn_i^s + \sum_i n_i^s d\mu_i + \gamma dA + Ad\gamma \quad (7)$$

The comparison of equation (5) with (7) gives,

$$S^s dT + \sum_i n_i^s d\mu_i + A\, d\gamma = O \quad (8)$$

or per unit area,

$$d\gamma = -S^s dT - \sum_i \Gamma d\mu_i \quad (9)$$

For a two component system at constant temperature equation (9) reduces to,

$$d\gamma = -\Gamma_1 d\mu_1 - \Gamma_2 d\mu_2. \quad (10)$$

Γ_1 and Γ_2 are surface excesses and the usual convention (Gibbs) is to place the dividing surface such that $\Gamma_1 = O$ and the excess of component 2 is written Γ_2' to denote this. Therefore,

$$-d\gamma = \Gamma_2' d\mu_2 \qquad (11)$$

An alternate method of locating the dividing surface is to assume a finite thickness for the surface. Then Γ_1 and Γ_2 in equation (10) represent total surface concentrations (Written Γ_1^s and Γ_2^s).

By use of the Gibbs - Duhem relationship,

$$N_1 d\mu_1 + N_2 d\mu_2 = O,$$

where N_1 and N_2 are the mole fractions of components 1 and 2, respectively, equation (10) becomes

$$-d\gamma = [\Gamma_2^s - (N_2/N_1)\Gamma_1^s] d\mu_2. \qquad (12)$$

For dilute solutions of strongly adsorbing substances, such as surfactants, Γ_1^s is negligibly small and equation (12) can be written

$$-d\gamma = \Gamma_2^s d\mu_2 \qquad (13)$$

$$d\mu_2 = RT d \ln a_2 \qquad (14)$$

where a_2 is the activity of the component 2. Therefore, the expression for the surface excess concentration is:

$$\Gamma_2^s = -1/RT \cdot d\gamma/d \ln a_2, \qquad (15)$$

or

$$d\gamma = -RT\Gamma_2^s d \ln a_2 \qquad (16)$$

Therefore, the Gibbs adsorption equation (16) is a thermodynamic expression which relates the surface concentration or surface excess of a species to both the interfacial tension, γ and the bulk activity, a, or fugacity of the adsorbate.

From equation (16) it follows that

$$d\gamma = -RT\Gamma_2 d\ (\ln X_2 + \ln f_2) \qquad (17)$$

where X_2 is the mole fractions of any component in the bulk phase and f_2 its activity coefficient. For a dilute solution (10^{-2}M or less), containing only one nondissociating surface active solute, the activity coefficient of the solute can be considered to be constant and the mole fraction of the solute X_2 may be replaced by it's molar concentration.

$$d\gamma = -RT\ \Gamma_2 d\ \ln\ C_2 \qquad (18)$$

Equation (18) is the form in which the Gibbs equation in commonly used for solutions of nonionic surfactants.

In systems where γ is directly and simply measurable (i.e, liquid-liquid and liquid-vapour systems), the Gibbs adsorption equation is used to calculate the surface concentration.

The Gibbs adsorption equation (16) for 1 : 1 ionic compounds can be written as:

$$-d\gamma = RT\ (\Gamma_{N^+} d\ \ln\ a_{N^+} + \Gamma_{X^-} d\ \ln\ a_{X^-}) \qquad (19)$$

Where Γ_{N^+} and Γ_{X^-}, are the surface excess concentrations of the N^+ surfactant ion and the counter ion, X^-, respectively, and a_{N^+} and a_{X^-} their respective bulk phase activities.

For solutions of surfactant in pure water, $\Gamma_{N,^+max} = \Gamma_{X^-,max}$ and thus,

$d \ln a_{N^+} + d \ln a_{X^-} = 2d(\ln C_{N^+X^-} + \ln f_{\pm})$, where $C_{N^+X^-}$, is the molar concentration of the surfactant and $f_{\pm}$ is the mean activity coefficient of the surfactant. When Γ_{N^+} has reached it's maximum value,

$$-d\gamma = d\pi = 2RT\Gamma_{N^+X^-,max} d(\ln C_{N^+X^-} + \ln f_{\pm}). \quad (20)$$

$\Gamma_{N^+X,^-max}$ is the maximum surface excess concentration of the surfactant and π is the surface pressure. In these cases the activity coefficients may be evaluated (5) from the Debye-Huckel equation

$$\log f_2 = -B|z_+z_-| I^{1/2} / 1 + 0.33 \alpha I^{1/2} \quad (21)$$

Where $B = 1.825x106x(DT)^{3/2}$. Here, I is the ionic strength based on the free ions in the solution, α is the mean distance of approach of the ions, in A° (5), and D is the dielectric constant of solvent. α is taken as 0.6 for the surfactant ion and 0.3 for the counter ions. log $f_{\pm}$ in equation (20) is assumed to equal (log f_++log f_)/2.

From equation (20),

$$\Gamma_{N^+X^-,\,max} = 1/4.606RT.\ [d\pi/d(\log C_{N^+X^-} + \log f_{\pm})]_{max} \qquad (22)$$

or

$$\Gamma_{N^+X^-,max} = -1/4.606RT.\ [d\gamma/d(\log C_{N^+X^-} + \log f_{\pm})]_{max}. \qquad (22a)$$

The surface excess concentration , Γ_2, for a dilute solution of a 1:1 ionic surfactant in the presence of a swamping amount of electrolyte containing a common non-surfactant ion, from equation (19), is

$$\Gamma_{N^+X^-,max} = \Gamma_{N^+,max} = 1/2.3RT\ .\ [d\pi/d(\log C_{N^+} + \log f_{+})], \qquad (23)$$

since under these conditions there is no change in the activity of the counterion with adsorption.

Surface excess concentrations can consequently be obtained from the slopes of plots of γ vs log a at constant temperature. For surface-active solutes, the surface excess concentration, Γ_2, can be considered to be equal to the actual surface concentration without significant error.

The slope of a typical surface pressure, π vs log a curve is essentially constant below but near the cmc and from equations (22) and (23) it is evident that the surface excess concentration has reached a constant maximum value in this region.

The surface excess concentration at surface saturation, Γ_{max}, is a useful measure of the effectiveness (6) of adsorption of a surfactant at the interface since it is the maximum value to which adsorption can attain.

From the surface excess concentration, another very useful surface parameter, the area per molecule, A, at the interface in nm^2, is calculated from the relationship:

$$A = 10^{14}/N\Gamma_2, \tag{24}$$

where N = Avogadro's number and Γ_2 is in moles/cm^2.

The area per molecule at the interface gives us information regarding the packing and the orientation of the adsorbed surfactant molecule at the interface, when compared with the dimensions of the molecule as obtained by use of molecular models. The area that a molecule of surfactant will occupy at the interface will depend on the nature of the hydrophobic group and on the position and the nature of the hydrophilic group.

1.2.2 Standard Thermodynamic Parameters

The evaluation of standard thermodynamic functions of adsorption for surface-active solutes provides an excellent means of quantifying subtle differences in adsorption. For instance, standard free energies of adsorption give us information that allow us to compare different types of surfactants as to their efficiency of adsorption at various interfaces, their extent of adsorption, and the role played by different structural units in the surfactant adsorption. On the other hand, standard enthalpy and entropy data provide information concerning the mechanism of the adsorption process.

Thermodynamic functions of adsorption for surface-active solutes at the aqueous/air interface have been calculated by a number of different methods, making use of data from surface tension measurements (7-13).

For very dilute solutions of surface-active agents, where activity coefficients closely approximate unity, the variation of surface pressure (π) with molar bulk phase concentration (C) of surface-active agent is linear, i.e:

$$(d\pi/dc)_{c->o} = \alpha \qquad (25)$$

This rule was pointed out by Langmuir (14), who showed that equation (25) is true when the surface phase obeys an equation of state which is analogous to a 2-dimensional ideal gas law:

$$\pi A = kT, \tag{26}$$

where A is the surface area per molecule, k is the Boltzmann constant, and T is the absolute temperature.

Betts and Pethica (15,16), defined a surface fugacity, π^* , as follows:

$$\pi^* A = kT = \pi f A \tag{27}$$

where f is the fugacity coefficient. In the ideal region, where Traube's relation applies, values of f approach unity, and values of π may, therefore, be considered equal to surface fugacities. Thus, in the dilute region where bulk activities can be replaced by concentrations and where Traube's law applies, if the standard state is chosen as one of unit fugacity (1 dyne/cm) the chemical potentials for the surface and the bulk phases are as follows:

$$\mu^{\beta} = \mu_o^{\beta} + RT \ln C \tag{28}$$

$$\mu^{s} = \mu_o^{s} + RT \ln \Pi, \tag{29}$$

where s and β refer to surface and bulk, respectively, and μ_o to the standard states. Hence, at equilibrium,

$$\mu_o^{\beta} - \mu_o^{s} = -\Delta G^{\circ} = RT \ln \Pi/C. \tag{30}$$

Since $\Pi = \alpha C$,

$$-\Delta G^\circ = RT \ln \alpha \quad (31)$$

and $$d \ln \alpha / dT = -\Delta H^\circ / RT^2, \quad (32)$$

where ΔH° is the standard heat of adsorption.

Posner et al (8), following Ward and Tordai (17,18), have given a somewhat different expression for the standard free energy of adsorption. Their choice of a standard state was in terms of a monolayer thickness of one molecule in the surface phase. Since

$$\mu_s = \mu_s^\circ + kT \ln a_s \quad (33)$$

$$\mu_\beta = \mu_\beta^\circ + kT \ln a_\beta, \quad (34)$$

where a_s and a_β refer to surface and bulk activity, respectively, under equilibrium conditions at, high dilutions where activity coefficients approximate unity,

$$\mu_s^\circ + kT \ln C_s/\delta = \mu_\beta^\circ + kT \ln C_\beta \quad (35)$$

and

$$\mu_\beta^\circ - \mu_s^\circ = -\Delta G^\circ = kT \ln (C_s/C_\beta\delta) \quad (36)$$

Here, the surface concentration of the solute is expressed as a two dimentional concentration of molecules cm^{-2}, and δ is the thickness of the surface phase.

From Traube's relationship, $\pi = \alpha C$, and from the equation of state for a dilute interfacial film, $\pi = kTC_s$, substituting for C_s and then for π/C_β in equation (36),

$$\Delta G^\circ = -2.303\ kT \log \alpha/kT\ \delta\ . \qquad (37)$$

Therefore, if Traube's constant is known and if the value for the monolayer thickness, δ , can be estimated, the free energy of transfer of the solute molecule from the bulk to the monolayer may be calculated.

Betts and Pethica (15) have criticized this choice of a standard state in terms of thickness as arbitrary and have indicated difficulties when applied to ionized surfaces, in view of the variation of the diffuse double layer thickness with salt concentration.

Although the above methods of determining standard thermodynamic parameters have the best theoretical foundations, they involve determining the surface tension of solutions of the surface-active solute at very low concentrations where $(d\pi/dC)_{c-->o}$ is a constant i.e, where the surface tension of the solvent is depressed by just a few mNm^{-1}(dyn cm^{-1}). Unfortunately, good data in this very dilute region are difficult to generate, since surface tension values in this region are markedly affected by traces of impurities that may be present in the solution, or in the gas phase. Secondly, most of the studies dealing with surface tension have been performed for the purpose of

determining critical micelle concentration and as a result there are only a few studies reported in the literature on the region where Traube's rule can be applied. By making some assumptions, it is possible to use surface tension data in the vicinity of the cmc reported in the literature to calculate free energies of adsorption, and a number of investigators have done so by use of the Szyszkowski equation, (3,19).

$$\gamma_o - \gamma = K \log (C/B + 1) \qquad (38)$$

where K and B are constants, C is the concentration of solute in mol dm^{-3} in the aqueous phase, and γ_o the surface tension of the solvent.

The Szyszkowski equation has been shown (20) to arise from the combination of the Langmuir equation

$$\Gamma = \Gamma_{max}\, C/(C+B) \qquad (39)$$

where Γ is the surface concentration of the surfactant (Γ_{max} at surface saturation) with the Gibbs adsorption equation in the form

$$-d\gamma = 2.303\ RT\ \Gamma\ d \log C \qquad (40)$$

The constant, K, in the Szyszkowski equation is related to the terms in the Gibbs equation by the expression,

$$K = 2.303\ RT\ \Gamma_{max} \qquad (41)$$

The standard state in this case is defined as one in which the surface is half filled, ie., $\Gamma=\Gamma_{max}/2$, and the standard free energy of adsorption is given by

$$\Delta G^{\circ} = 2.303\ RT \log B \qquad (42)$$

This permits calculation of a standard free energy change of adsorption when the Szyszkowski equation fits the surface tension data. The applicability of the Szyszkowski equation to the system being investigated can be tested by calculating values for B over a wide range of concentrations and noting whether it remains constant.

The strict application of the Langmuir adsorption isotherm approach requires absence of interactions between the molecules adsorbed at the interface. Therefore, the interactions between surfactant molecules are not included in the free energy parameters and this is a serious drawback to the Langmuir isotherm approach for the calculation of thermodynamic parameters.

In order to estimate standard free energies of adsorption making use of surface tension data in the range where γ has values of 20 mNm^{-1}, (dynes/cm) and greater, a new standard state has been defined recently (20). It uses a hypothetical standard state in which the surface is filled with a monolayer of surface-active agent, i.e, $\Gamma=\Gamma_{\alpha}$, but at a surface pressure of zero.

The equilibrium between surface and bulk phase is given by

$$\overset{\circ}{\mu}_{\beta} + RT \ln a_{\beta} = \overset{\circ}{\mu}_{s} + RT \ln a_{s} \qquad (43)$$

At maximum surface saturation, Γ_{max}, the Gibbs equation, (16) for a nonionized solute becomes,

$$d\pi/d\mu = \Gamma_{max} = 1/A_{min} \quad (44)$$

where A_{min} is the minimum area per mole of the surface-active agent. The change in chemical potential in going from a surface pressure π to zero surface pressure is, then, equal to πA_{min} and the standard free energy of adsorption is given by,

$$\Delta G^{\circ}_{ad} = 2.303\ RT \log a_{\pi} - \pi A_{min}, \quad (45)$$

where a_{π} is the activity of the surfactant in the bulk phase at surface pressure, π

For nonionic surfactants, activities can be replaced by the molar concentrations, and for ionic surfactants equation (45) will take the form.

$$\Delta G^{\circ}_{ad} = 2.3\ RT[\log C_{N^+} + \log f_+ + \log C_{X^-} + \log f_-] - 0.6023\ \pi\ A_{min} \quad (46)$$

Activity coeficients for the ions can be evaluated (5) from the Debye-Huckel equation (28).

Unlike the Langmuir isotherm approach to the determination of ΔG°_{ad}, here the interaction between surfactant molecules is included in the free energy parameters.

Standard free energies of adsorption at the aqueous solution/air interface for primary alcohols at 25 and 20°C calculated by the Traube's constant method, using equation (31), and by the above method using equation (45), have been compared (20) and shown to yield similar values for the standard free energy of a methylene group.

The standard entropies and enthalpies of adsorption, ΔS°_{ad} and ΔH°_{ad}, can be calculated from the relationship:

$$d(\Delta G^\circ)/dT = -\Delta S^\circ \qquad (47)$$

and

$$\Delta H^\circ = \Delta G^\circ + T\Delta S^\circ \qquad (48)$$

1.3 Micelle formation in Aqueous solution by Surfactants (21,22,23,24)

Another property of surfactants, apart from adsorption at interfaces, is their ability to aggregate into clusters to form micelles. Here, too, the built in asymmetry or amphipathic nature of surfactant monomers is the cause of this phenomenon. Micelle formation, or micellization, is responsible for such properties of surfactants as

solubilization and detergency. In addition, micellization indirectly influences the surface and interfacial tension reduction of the solvent by surfactants.

In ionic micelles, the interior region is surrounded by a region that contains the ionic head groups, the Stern layer of the electrical double layer, where most of the counterions are associated. The remaining counter ions are contained in the Gouy Chapman portion of the double layer that extends further into the aqueous phase. For polyoxyethylenated nonionics, the structure is essentially the same, except that the outer region contains no counterions, but includes coils of hydrated polyoxyethylene chains. From recent investigations (25,26,27), it appears that there is some bound water associated with the first few methylene groups adjacent to the hydrophilic head group.

In hydrocarbon media, the structure of the micelle in similar but reversed, with the hydrophilic heads comprising the interior region surrounded by an outer region containing the hydrophobic groups and hydrocarbon. Changes in temperature, structure and concentration of surfactant, and additives in the liquid phase are known to change the size, shape, the aggregation number of the micelle, with the structure varying from spherical through rod or disclike to lamellar in shape (22).

The aggregation of monomers to form micelles frequently sets in over a remarkably narrow range of solute concentration, usually denoted as the critical micelle concentration. A plot of the surface tension of a surfactant solution against the logarithem of inverse concentration shows a discontinuity in the region where the critical micelle concentration is reached. This is a popular method for determining the critical micelle concentration. Similar breaks in almost every measurable physical property that depend on the size or number of particles in solution are shown by all types of surfactants:nonionic, anionic, cationic and zwitterionic.

Consequently, there are a large number of other possible methods for determining the cmc (24) and they vary with respect to their precision, accuracy and usefullness. The reliability of the cmc is of great importance in the evaluation of quantitative aspects of the monomer-micellar equilibrium. Other methods commonly used for the determination of the cmc are electrical conductivity, light scattering or refractive index. Spectral changes associated with added ionic dyes of opposite charge to the surfactant ion, though a popular method for determination of the cmc, give substantially inaccurate results due to the dye being able to act as a surface-active impurity (10). An excellent critical evaluation of the methods for determining cmc is given by Mukerjee and Mysels (24).

The tendency of the hydrocarbon part of the surfactant monomer to associated with itself rather than to be solvated by water is the primary driving force for micelle formation. In spite of considerable attention in recent years, the nature of hydrophobic bonding still remains incompletely understood. Initially, the formation of micelles was regarded primarily as an interfacial energy effect (27 to 29) and the minimization of the interfacial free energy was believed to provide the driving force for micellization. Aggregation occured, according to this view, when the energy available from the hydrocarbon - water interface exceeded the electrical energy due to the repulsion of the ionic heads in the micelle. The above model predicted micelle formation to be predominently an energy effect and the process to be exothermic.

However, enthalpy changes determined from calorimetric (29-31) measurements and temperature variation of the cmc (31-36), were shown to be positive and small, at least at lower temperatures. Goddard et al (31,32), explained this positive, but small, enthalpy change in terms of ordering of water molecules around the surfactant monomers in solution , thus lowering the enthalpy and entropy of the pre-micellar system. When such a monomer becomes part of a micelle, its frozen water molecules are released to the bulk water state. This accounts for the positive ΔH°_{mic} values and also the increase in randomness of the post-micellar system. In the description of energetics of micellar formation it

is assumed that the environment of the hydrophilic head group of the surfactant ions remains unchanged prior to and after micellization. Hence, the main contribution to the process is expected to be from the hydrocarbon chain. Recent studies (21) show that there is a substantial influence of the hydrophilic head group on the free energy of micellization. This arises due to the compact nature of the micelle which forces the hydrophilic head groups to be closely packed and oriented, and therefore, to interact with each other. These interactions are influenced by the hydration, steric and size factors of the hydrophilic head groups. So far, these interactions have been treated only semi-quantitatively. Therefore the interpretation of experimental heat changes in terms of hydrocarbon chain contributions alone is not completely valid (21).

Although the energy changes associated with micelle formation have been studied extensively (37-48,30,35), no universally accepted set of thermodynamic relationships has evolved. This lack of consistency in the thermodynamic treatment is due to incomplete understanding of the process of micellization.

Two general approaches have been developed: in the first, micellization is regarded as a phase separation which commences at the cmc (49,40,42); in the second, micelles and the single surfactant ions

are considered to be in association-dissociation equilibrium (37,50,51,52) and the law of mass action is applied.

a) Mass action model (21,37,46,53)

Here, the following equilibrium is considered;

$$n(N^+) + m(X^-) \dashrightarrow (M)^{n-m},$$

Where N^+ is the surfactant ion and X^- its counter ion. The equlibrium constant for the above is:

$$K = a_M / (a_{N^+})^n (a_{X^-})^m \qquad (49)$$

where the micelle, M, is thought to be an aggregate of n surfactant ions with m firmly bound anions.

Assuming no deviation of activity coefficients from unity, the standard free energy of micellization, per mole of monomeric surfactant, ΔG°_{mic} is given by

$$\Delta G^\circ_{mic} = RT(-\log [M]/n + \ln [N^+] + m/n \ln [X^-]) \qquad (50)$$

When the aggregation number n is large (greater than 20) (52), -log[M]/n is generally very small compared to other terms on the right hand side of the equation (54) and is often omitted, yielding

$$\Delta G^\circ_{mic} = RT (\ln[N^+] + m/n \ln [X^-]) \qquad (51)$$

For nonionic surfactant, equation (55) simplifies to,

$$\Delta G^{\circ}_{mic} = RT \ln cmc \qquad (52)$$

as the monomer concentration $[N^+]$ is the cmc.

The situation for ionic surfactants, where activity coefficients are expected to deviate significantly from unity, is:

$$\Delta G^{\circ}_{mic} = 2.3\ RT[\log a_{N^+,cmc} + m/n(\log a_{X^-})] \qquad (53)$$

$$= 2.3\ RT\ [\log\ cmc + \log f_+ + m/n(\log C_{X^-} + \log f_-)] \qquad (54)$$

The counterion concentration at the cmc is the concentration of all counterions, including any added electrolyte.

The most popular method of estimating the m/n fraction in equation (50) is due to Corrin (53). The logarithm of the cmc of ionic association colloids normally is found to vary linearly with the logarithm of the total counterion concentration. Under these circumstances the slope of such a curve should give the m/n value. Values of m/n (the degree of association of the counter ion), have been experimentally determined from measurements of electromotive force (54,55,56), electrical conductivity (57) and light scattering (58).

b) Phase Separation Model (40,42,49,50,51,52)

This approach, considers the micelles to be a separate phase. Here, the cmc is regarded as the saturation solubility of the single species, which if exceeded, leads to the production of a new phase.

If n moles of surfactant and m moles of solvent aggregate to form one mole of micelles, then,

$$n\mu_i + m\mu_o = \mu_n \tag{55}$$

where μ_i and μ_n are the chemical potentials of the monomeric and micellized surfactants, respectively, and μ_o the chemical potential of the solvent. The standard free energy for micelle formation is then,

$$\Delta G_i^o = \mu_n^o - (n\mu_i^o + m\mu^o) = RT\ (n \ln a_i + m \ln a_o - \ln a_n), \tag{56}$$

where the zero superscripts denote the standard chemical potentials for the hydrated monomer, the hydrated micelle and the solvent (at unit mole fraction) and a refers to their respective activities.

Since in dilute solution $a_o = 1$, as the micelle is treated as a separate phase, a_n must be constant at unity and the equation (56) simplifies to

$$\Delta G_1^o/n = \Delta G^o = RT \ln a_i \tag{57}$$

For a dilute solution of a non electrolyte surfactant, equation (57) will become,

$$\Delta G^\circ = RT \ln C_i,$$

or

$$\Delta G^\circ = RT \ln cmc, \tag{58}$$

where ΔG° is the standard free energy per mole of micellized monomers and C_i the mole fraction of monomer at the cmc.

The standard enthalpy of micellization ΔH°_{mic} is given by

$$\Delta H^\circ = -RT^2 \, d \ln cmc/dT \tag{59}$$

In the above treatment, the micellar phase is defined as comprising both the charged surfactant ions and the counter ions in the diffuse double layer and the system is described in terms of uncharged components.

The basic assumption of the two phase model is that the monomer activity remains constant above the cmc, while in the mass action model for a finite value of n, the monomer activity must increase above the cmc, however slowly (43). Constant activity of the monomer above the cmc would lead to a constant activity of the micelle, too. In contrast, to this, however, it has been found that the vapor pressures and freezing points of solutions of association colloids decrease above the

cmc (34,58,59), indicating that the activity of the monomer increases. This variation in activity above the cmc has been further substantiated by dialysis experiments (60).

Evidence in favour of constant monomer activity above the critical micelle concentration are surface tension data above the cmc, where it has been often reported that the surface tension remains constant. The mass action model would predict a slow decrease. On the other hand, surface tension is very sensitive to surface-active impurities and furthermore surface tension data above cmc is generally confined to the region just above the cmc, consequently, it is difficult to evaluate these data. From the data available on well purified surfactants (61,62), there is evidence to confirm the slow decrease of surface tension above the cmc. Due to lack of substantial surface tension data on purified surfactants, the monomer activity above cmc is assumed to remain constant in the mass action model for the treatment of micellization. Whenever n is large, errors arising from this approximation can be considered to be negligibly small.

Whereas both these approaches are sound for the treatment of nonionic systems, provided the nonideality effects are small, the question arises whether these two models apply to ionic association colloids. In the mass action model there is doubt whether all effects of

the ionic interactions of the micelles are included in the fraction m/n of counter ions bound to the micelle and what value of m/n to use (43). On the other hand, there is doubt as to whether the effect of counterions can be ignored, as done in the two phase model. To overcome these two approaches, the two phase model has been modified by Pethica et al, to take into account the counterion effect on micellar formation (52).

By treating the micelle as a separate phase, they have shown that the enthalpy of micellization can be calculated from the temperature dependence of the activity of micelle-forming species by use of the relationship:

$$-\Delta H = \alpha(d \ln (cmc)/dT)_{\Delta G} \qquad (60)$$

assuming activity coefficients to be unity. For pure ionic detergents in the absence of electrolyte, $\alpha = 2$; and in the presence of swamping amount of electrolyte, $\alpha = 1$. $\Delta H = H^m - H^w$, where H^m and H^w are the partial molar heat contents of the surfactant in the micellar phase and in the water phase, respectively. The ΔH values calculated from these equations for sodium dodecyl sulfate with and without added salt, are found to be in agreement with the values obtained from calorimetric determinations for the same compounds, (32,40,63).

To reconcile the two approaches, the mass action and the phase separation models, Shinoda (42,64) has treated the micellar phase as a charged entity and has derived the following equations.

$$\Delta H_m/T = -(1+Kg)RT(d \ln cmc/dT) \qquad (61)$$

Kg is an experimental constant and is equivalent to the m/n fraction obtained in the mass action model.

In the absence of salt,

$$\Delta H_m/T = -kT[(d \ln X_2/dT)_{\Delta G_m} + Kg\ (d \ln X_3/dT)_{\Delta G_m}] \qquad (62)$$

where X_2 and X_3 are the concentrations of surfactant ion and counterion, respectively.

In the presence of a swamping amount of electrolyte, X_3 is a constant and the equation (62), will become,

$$\Delta H_m/T = -kT\ (d \ln X_2/dT)_{\Delta G, X_3} \qquad (63)$$

In this extension, thermodynamic calculations for the phase separation model are brought much closer to those based on the mass action approach.

1.4 Surface Tension Reduction by Surfactants

Surface tension reduction in aqueous media depends upon the replacement of water molecules at the surface by surface-active molecules from the bulk phase of the solution. In discussing surface activity and the relationship between the structure of the surfactant and its reduction of surface tension, it is necessary to distinguish between the a) the efficiency (65) of a surfactant, measured by the bulk phase concentration of surfactant required to produce some significant reduction in the surface tension of the water, and b) its effectiveness (66), measured by the maximum surface pressure (minimum surface tension) to which the surfactant can lower the surface tension, since these two parameter are often found to run counter to each other.

1.4.1 a) Efficiency of Surface Tension Reduction

It has been proposed by Rosen (65) that the log of the reciprocal of the concentration, C_{20}, in moles cm^{-3}, of surfactant necessary to produce an interfacial pressure of 20 dyne cm^{-1} i.e. log $(1/C_{20})$ or

pC_{20}, be considered as a measure of the efficiency of a surfactant in reducing interfacial tension. Furthermore, this quantity can be shown to be related to the free energy of adsorption, which itself is a measure of the efficiency of adsorption of a surfactant. From equation (45),

$$\Delta G^{\circ}_{ad} = RT \ln C_{\pi} - \pi A_{min} \tag{64}$$

At a surface pressure of 20 dynes cm^{-1},

$$\Delta G^{\circ}_{ad} = 2.303\ RT \log C_{20} - 20\ A_{min} \tag{65}$$

or

$$\Delta G^{\circ}_{ad} = -2.303RT\ pC_{20} - 20A_{min},$$

(where $pC_{20} = -\log C_{20}$)

and

$$pC_{20} = -(\Delta G^{\circ}_{ad}/2.303\ RT) - (20\ A_{min}/2.303\ RT) \tag{66}$$

When the interfacial pressure has reached a value of 20 dyne cm^{-1}, the surface concentration is usually close to its maximum value and therefore the area per molecule, A_{min}, is a constant. When different

surfactant molecules have the same hydrophilic group, or similar A_{min} then,

$$pC_{20} = -\Delta G^{\circ}_{ad} / 2.303\ RT - K \qquad (67)$$

For a straight chain surfactant of structure, $CH_3(-CH_2-)_nW$, where W is the hydrophilic portion of the molecule, ΔG°_{ad} is given by the relationship,

$$\Delta G^{\circ}_{ad} = \Delta G^{\circ}(-W) + m\ \Delta G^{\circ}(-CH_2-) + K_1, \qquad (68)$$

where m = the total number of carbon atoms (n+1) in the hydrocarbon chain and K_1, the difference in free energy of transfer between the terminal ($-CH_3-$) and ($-CH_2-$) group, thus,

$$pC_{20} = (-\Delta G^{\circ}(-CH_2-)/2.3RT)m + (-\Delta G^{\circ}(-W))/2.3RT + K_2 \qquad (69)$$

Under conditions where $\Delta G^{\circ}(-W)$ is independent of the length of the hydrophobic group, for a homologous series of straight chain

surfactants with the same hydrophilic group at some specified temperature,

$$pC_{20} = (-\Delta G^{\circ}(-CH_2-)/2.3RT)m + K_3, \qquad (70)$$

where K_2 and K_3 are constants.

As seen from equation (70), the pC_{20} value should increase with increase in the number of carbon atoms in a straight chain hydrophobic group, and this is found to be true experimentally (65).

The value of the free energy decrease per methylene group, $-\Delta G^{\circ}_{ad}$ $(-CH_2-)$ can be obtained (66) from the slope of the plot of pC_{20} vs m, equation (69).

The pC_{20} value is found to increase by 0.55-0.6 for every increase of $2(-CH_2-)$ groups for the aqueous solution/air and aqueous solution/heptane interface (66).

In the case of poloxyethyleneated nonionics at the aqueous solution/air interface and for ionic surfactants at 0.1M NaCl aqueous solution/air interface, pC_{20} is increased by about 0.9 and 0.7, respectively, when the chain length is increased by $2(-CH_2-)$ groups.

1.4.2 b) Effectiveness in Surface or Interfacial Tension Reduction (66)

The surface pressure at the cmc is the maximum pressure, π_{cmc}, an aqueous solution of a well purified surfactant can achieve, and its value at this point is therefore a suitable measure of the effectiveness of a surfactant in reducing surface or interfacial tension.

If the cmc exceeds the solubility of the surfactant at a particular temperature, then the maximum surface pressure will be achieved at the point of maximum solubility.

The following equation has been derived (66), showing the relationship between, Γ_{max}, cmc, C_{20}, and the effectiveness of adsorption, (π_{cmc}),

$$-\Delta\gamma_{cmc} = \pi_{cmc} = 20 + 2.3\ RT\Gamma_{max} \log\ cmc/C_{20} \qquad (71)$$

The larger the maximum surface concentration, the larger the critical micelle concentration and the smaller the C_{20} value, that is, the larger the cmc/C_{20} ratio, the greater the surface pressure, π at the cmc.

1.5 Surface tension data

Impurities are a major problem in surface chemistry. In adsorption at any interface, solid/gas, solid/liquid, liquid/gas or liquid/liquid, the presence in the system of even a trace of impurity that is more surface-active than the material whose adsorption is being measured makes the data obtained very unreliable. The presence of these impurities is the cause of a minimum in the surface tension-concentration curve, as shown by Miles (67,68).

In the determination of surface properties and thermodynamic parameters of surface-active agents, and for intercomparison of different surfactants, reliable surface tension data are of prime importance. The standard free energy of a adsorption, ΔG°_{ad}, of surfactants at the aqueous solution/air or aqueous solution/hydrocarbon interface is most often calculated from surface tension data on dilute aqueous solution of the compounds under investigation. The standard free energy of micellization, ΔG°_{mic}, of surfactants is obtained from the cmc. Though cmc values may be obtained by a variety of methods, the use of surface tension is one of the methods most free of criticism (24). A major advantage of the use of surface tension for determining the free energy of adsorption or micellization or surface properties is that data that are invalid due to the presence of highly surface-active

impurities are easily detected by the presence of a minimum in the surface-tension concentration curve and also by the very slow approach to equilibrium surface tension.

The values reported for the same substance in the literature often show disagreement, and this is illustrated by the paper by Vijayendran (69), where six purchased samples of sodium dodecyl sulfate, supposedly pure enough for surface chemical research, all showed surface tension minima and five of the six could not be purified, by extensive use of conventional methods, as shown by their values for the cmc. Because the methods of preparing surfactants generally result in the presence in them of highly surface - active impurities that are difficult to remove to a degree sufficient for reliable chemical investigations, much of the surface chemical data on surfactants in the scientific literature is of doubtful reliability (24,42). A compilation of critical micelle concentration issued a few years ago considers only about 600 of the 5000 entries listed therein as reliable (24).

In spite of the tremendous advances made during the past few decades or so in separation and purification techniques, the purification of surfactants for surface chemical investigation is generally still performed by methods developed in the 1940's (69). These generally involved tedious solvent extraction and multiple crystallization from

various solvents. These difficulties have made it almost impossible to calculate reliable thermodynamic parameters of adsorption and micellization or to relate chemical structure to application properties and consequently have hampered the aquisition of a fundamental understanding of these phenomena.

In the past few years, a reversed phase liquid chromatography procedure, coupled with more conventional methods of purification, has been developed for the purification of surfactants (70). This procedure has been shown to remove specifically the highly surface-active impurities from surfactant solutions under investigation. These highly surface-active impurities are removed from aqueous solution of both ionic and non-ionic surfactants by passing the solution through small, 13 x 10mm, prepacked, high density, chromatographic columns of octadecylsilanized silica gel, (SEP - Pak C18 Cartridge, Water Assoc., Midford, Mass.). Since these columns operate by reverse phase liquid chromatography, they retain most strongly the most hydrophobic impurities, allowing the surfactant, free of these, to pass through in the aqueous phase. Solution of surfactants treated by the above procedure were found to have no minima in surface tension concentration curves and equilibrium surface tension was reached within one hour.

1.6 Current state of knowledge on physical chemical properties of surfactants.

Nonionic Surfactants

Nonionic detergents account for approximately a fifth of the total detergent market (2). Their compatibility with all other types of surfactants, resistance to hard water and polyvalent cations, and solubility in both water and in hydrocarbon solvents has made them very attractive for industrial applications. In recent years, nonionic surfactants based on polyoxyethylenated C_{12} to C_{18} alcohols have become very attractive as low temperature laundry detergents.

Among the nonionic detergents, polyoxyethylenated materials have the special advantage that their physico-chemical properties can be modified considerably by simply changing the length of the polyoxyethylene groups to give a range of products of varying surface and micellar properties. As a result, these polyoxyethylenated nonionics have become the subject of considerable investigation in the last few decades. Unfortunately, most of the published work on polyoxyethylenated nonionics has been carried out using commercial or rather impure materials due to the difficulties in preparation of pure homogenous material and the lack of a procedure for the purification of the commercially available nonionic surfactants.

The present knowledge of the surface and micellar properties of a series of pure ethenoxylated compounds is limited to p-tert-$C_8H_{17}C_6H_4(OC_2H_4)_xOH$, where x = 1 - 10 (71,72), $C_mH_{2m+1}(OC_2H_4)_6OH$ where m = 8, 12, and 16 (73) and $C_nH_{2n+1}(OCH_2CH_2)_8OH$, where n = 10 to 15 (74).

From these investigations, it is evident that the cross-sectional area of the molecule increases with the number of oxyethylene units and that the effectiveness of adsorption of these compounds appears to increase with increase in the length of the hydrophobic group (71).

In earlier investigations on polyoxyethylenated nonylphenols with averages of 10.5, 15, 20, and 30 oxyethylene units (75), the cmc was observed to increase linearly with increase in oxyethylene content. Subsequent studies on pure polyoxyethylenated nonionic compounds (71), indicated that there is no apparent linearity for molecules with less than twenty oxyethylene units; on the other hand, for a series of p-tert-octylphenoxypoly(ethenoxy)ethanols, Crook et al (71) observed a minimum cmc at oxyethylene content of four, as the number of oxyethylene units in the molecule increased from one to ten.

From studies on the temperature dependence of the cmc, Crook et al (72) determined the change in the enthalpy and entropy of micellization for the series, p-tert-octylphenoxypoly(ethenoxy)ethanol.

For the molecules with oxyethylene units greater than four, ΔH°_{mic} and ΔS°_{mic} were positive and found to increase with increasing oxyethylene contents. Increase in temperature caused both ΔH°_{mic} and ΔS°_{mic}, values to become less positive. For molecules with less than four oxyethylene units, the ΔH°_{mic} and ΔS°_{mic} were both negative, although they still increased with temperature.

From cmc studies on the homologous series, $C_nH_{2n+1}(OC_2H_4)_6OH$ with n = 8,12 and 16, the ΔG°_{mic} per methylene group was shown to be 1.1 kT by Corkill et al, using unit mole fraction as the reference state (73). The contribution to the total free energy of micellization of the oxyethylene unit has been estimated by them to be one tenth the change in ΔG° per methylene group ($-CH_2-$), with opposite sign.

More recently, Meguro et al (74), from studies on the homologous series $C_nH_{2n+1}(OCH_2CH_2)_8H$, where n = 10 to 15, have calculated the separate contributions made by the hydrophilic and hydrophobic groups. From the large positive $\Delta H^{\circ}_m(-W)$ value obtained for the hydrophilic head group they concluded that the hydrophilic head group in these molecules opposes micellization. The contribution of $\Delta H_m(-W)$ value to the total free energy of micellization was found to be more significant than the contribution made by $\Delta S_m(-W)$.

In the current investigation, a systematic study of the surface and thermodynamic properties of well characterized and purified surfactants of structure $C_{12}H_{25}(OC_2H_4)_xOH$, where x = 1-8, is undertaken in order to obtain a broader understanding of structure to property relationship of this class of surfactants.

Zwitterionic Surfactants

The use of zwitterionic surfactants commercially has increased dramatically in recent years (76) because of their unique properties, such as compatibility and synergism when used in conjunction with most other types of surfactants. This type of surfactant is used in textile processing aids, cosmetic products, cleaning agents, and as antistatic agents. The sulfobetaines have been found to be very good lime soap dispersants (77).

Inspite of this wide applicability, a survey of the literature reveals that, compared to ionic and nonionic surfactants, there have been relatively few investigations of their surface and thermodynamic properties. Investigation has been hampered by the nonavailability of pure compounds and proper analytical techniques to determine their concentration in solution.

The micellar properties of a series of 2-trimethylammonium alkanoates were studied by Tori (78 to 82), and N-alkyl-N,N-dimethylglycines were studied by Beckett and Woodward (83) and Tori (81). From studies of the temperature dependence of the cmc, Tori et al were able to calculate ΔH°_{mic} values. Herrmann (84) studied C_{10}, C_{12} and C_{16} N-alkylsulfobetaines of the type, $R\text{-}\overset{+}{N}(CH_3)_2CH_2CH_2SO_3^-$ with regard to the effects on the cmc of chain length and ionic strength variation. He calculated the standard free energy contribution to micellization of a methylene group to be 0.61 Kcal mol^{-1}, and thereby concluded that the internal structure of the micelles of these zwitterionics is similar to that of all other ionic and nonionic surfactants studied. Thermodynamic parameters of micellization have also been investigated by Molyneux (85), and Swarbrick (86). They were able to estimate the standard free energy contribution to micellization of the head group of N-alkyl and C-alkylbetaines to be +3.3 and +2.7 Kcal mol^{-1}, respectively. Molyneux et al (85) found the plot of log cmc vs 1/T for dodecyl N-methylbetaines to be linear, whereas Swarbrick et al (86) observed a minimum in the curve for the corresponding decyl and undecyl betaines. From these data, these workers were able to estimate the standard enthalpies and entropies of micellization and to compare these results with other nonelectrolyte amphophiles.

In contrast to this, there is little information available (87), on the thermodynamics of adsorption of alkylbetaines and no data on the thermodynamic parameters of adsorption or micellization for sulfobetaines.

In the present work, we have synthesised two betaines and three sulfobetaines in very pure form and have determined their surface and thermodynamic properties of micellization and adsorption. From these data on the two classes of zwitterionics, energetics of micellization and adsorption of the hydrophilic head groups have been estimated and compared to those of other types of zwitterionic and nonionic surfactants.

Cationic Surfactants

Cationic surfactants first became important when the commercial potential of their bacteriostatic properties was recognized (88). Today, cationic surface-active agents with antibacterial properties continue to play an important role as sanitizing and antiseptic agents, as components in cosmetic formulations, as textile softners, corrosion inhibitors, form depressents, flotation chemicals, and asphalt and petroleum additives.

From a theoretical viewpoint, these cationic surfactants are of considerable interest to researchers as they represent excellent models for studies on the effect of hydrophilic head groups on surface and micellar properties. Studies of the physical properties of micellar solutions of surface-active agents have indicated that the counterion influences the micellar properties (89 to 92). Subsequent studies by Anacker (93) and Tamaki (94) on a variety of univalent counterions indicated the dependence of the micellar properties on the hydration size of the hydrated counterions. Micellar charge determination from light scattering data for dodecylpyridinium chloride showed the ion-binding ability to decrease in the order I >Br >Cl (90).

On the other hand, there have been very few studies of the thermodynamic parameters of adsorption or micellization of these cationic surfactants. Increments of ΔG°_{mic} attributed to methyl and methylene groups, as well as polar groups, have been reported (94,95), but not the values of ΔH°_{mic} and ΔS°_{mic}. Therefore, for an explicit understanding of the thermodynamic of adsorption and micellization of these surface-active agents, and to compare the counter-ion effect, thermodynamic parameters of dodecylpyridinium chloride and bromide were investigated at three different temperatures and at three different ionic strengths.

Anionic Surfactants

Anionic surfactants represent the largest single charge type of the surfactant market. Among anionic surfactants, linear alkylbenzenesulfonates, alpha olefin sulfonates, sulfated alcohols, and sulfated ether alcohols are the most widely used. As a result of their extensive utility in industry, their physicochemical properties have been studied more than any other class of surfactants.

In recent years, sulfated ether alcohols (polyoxyethyleneglycol n-alkyl ethers) have become increasingly important industrially due to their high water solubility, high detergency, and lime soap dispersing ability, when compared to linear alkyl sulfates (2).

From the few investigations (96 to 99) on this class of compounds, it appears that the oxyethylene groups in these compounds have unique properties. Early investigations have shown (96) the sodium salts of sulfated ethenoxylated tallow alcohols with low oxyethylene content to be very much more water soluble than the corresponding alcohol sulfates. Subsequent work by Weil et al (97) on sodium hexadecyl sulfates, $C_{16}H_{17}(OC_2H_4)_nOSO_3Na$, where n = 1,2 and 4 (synthesised by reacting the alkyl halide with the corresponding oxyethyleneglycol) showed the cmc to decrease with increase in ethenoxy content. Since nonionic surfactants are known to have low cmcs, they interpreted the above

decrease in cmc as increase in the nonionic character of the sulfated polyoxyethylenated alcohols.

Tokiwa et al (98), from investigations done on a series of compounds, $C_nH_{2n+1}(OC_2H_4)OSO_3Na$, where n = 1 to 10 (average ethenoxy content), have estimated the micellar hydration and aggregation numbers. For the first two members in the series the aggregation number and the hydration numbers were found to be very similar to those of sodium dodecyl sulfate. Increase in the polyoxyethylene chain beyond n = 2 increased the hydration number and decreased the micellar aggregation numbers.

These studies indicate the dependence of micellar and hydration properties on the oxyethylene chain of these compounds, as found for nonionic polyoxethylenated alcohols. The oxyethylene units in the nonionic polyoxyethylenated alcohols are known to increase the water solubility of the molecule and this is explained in terms of the hydrogen bonding of the nucleophilic ether oxygens to the water molecules. Also, the increase in oxyethylene content decreases the tendency in these molecules to forming micelles (72,75,99). The decrease in cmc of the ethenoxylated alcohol sulfates, on one hand, and their increase in solubility, on the other, with increase in the length of the polyoxyethylene chain in these compounds remain to be understood. No

studies have been done on the energetics of adsorption and micellization of these compounds.

In view of the lack of understanding of the mechanism of adsorption and micellization of these sulfated ethenoxylated alcohols, two series of compounds, $C_{12}H_{25}(OC_2H_4)_iOSO_3Na$, where i = 1 and 2 and $C_nH_{2n+1}(OC_2H_4)_iSO_3Na$, where i = 0 or 1, and n = 10 and 12 were investigated. The results of these studies are compared to those on the corresponding nonionic polyoxyethylenated alcohols and a mechanism is suggested to explain the behavior of the oxyethylene groups in these ionic surfactants.

Chapter II

Experimental

2.1 Materials

Sodium decyl ($C_{10}S$) , dodecyl sulfonate ($C_{12}S$), and dodecyl sulfate ($C_{12}SO$), were purchased (Research Plus, Bayonne, N.J., >98% purity), 2-Dodecyloxypoly(ethenoxyethanol)s, $C_{12}H_{25}(OC_2H_4)_xOH$, (EOX) where x = 1-8 were purchased from (Nikko Chemical Co., Tokyo, Japan. > 98%). These compounds were further purified by repeatedly passing their aqueous solutions through octadecylsilanized columns (70) prior to been used for surface tension measurements.

N-methylbenzylamine (98% purity), chloroacetic acid (Eastman, practical grade), 2-chloroethanesulfonic acid, sodium salt monohydrate, (Aldrich, 98%, dehydrated to constant weight in an oven at 110°C prior to been used), sodium isethionate (GAF Corporation), chlorosulfonic acid (Matheson Coleman and Bell), pyridine (Baker, Analysed Reagent, dried over KOH), 1-chlorododecane (Fluka AG, >99% purity), 1-bromooctane, (Aldrich, 99% purity), 1-bromododecane (Fluka, purissima grade >99% purity), 1-bromodecane (Eastman, >99% purity).

were used as received, except where indicated. Sodium chloroacetate was prepared from chloroacetic acid by adding 4 g (0.1 moles) of NaOH, dissolved in 95% ethanol, to 9.5 g of (0.1 moles), of chloroacetic acid. Sodium chloride (Fisher, Cert. ACS), and sodium bromide (Baker, analysed reagent), were baked for several hours in a porcelain casserole at red heat. Anhydrous sodium carbonate (Fisher, Cert. ACS), sodium sulfate,anhydrous (Baker, analysed reagent), sodium hydroxide (J.T. Baker), potassium carbonate (Baker, Analysed reagent), activated carbon, (Darco G-60, ICI Americas), and methanol (reagent grade) were used without further purification.

Micro analyses were done by MicAnal microanalytical laboratory, Tuscon, Arizona.

Spectra

NMR spectra were determined on a Varian Associates model T-60 spectrometer. All chemical shifts are given in terms of δ scale relative to tetramethylsilane. IR spectra were obtained with Perkin-Elmer model 267 spectrophotometer. The molar absorptivities were made either with a Beckman DU(Gilford modified) or Cary 17 Spectrophotometer.

Computations

Calculations were carried out on an IBM 360-50 computer and PL/C compiler.

2.2 Synthesis

2.2.1 Preparation of sodium 2-alkoxyethanesulfonates, $C_nH_{2n+1}OC_2H_4SO_3^-Na^+$

These syntheses were based on the Williamson synthesis

The synthetic schemes are as follows:

$CH_3OH + Na(metal) \longrightarrow CH_3O^-Na^+$

$CH_3O^-Na^+ + HO\text{-}CH_2CH_2SO_3^-Na^+ \longrightarrow NaOCH_2CH_2SO_3^-Na^+$

$NaOCH_2CH_2SO_3^-Na^+ + RBr \longrightarrow R\text{-}OCH_2CH_2SO_3^-Na^+$

($R = n\text{-}C_{10}H_{21}$ or $n\text{-}C_{12}H_{25}$)

2.2.1.1 Sodium 2-decyloxyethylenesulfonate. $C_{10}H_{21}OC_2H_4SO_3^-Na^+$ ($C_{10}EOS$)

Sodium methoxide (0.11 moles) was prepared by accurately weighing out 2.51 g (0.11 M), of freshly cut sodium metal, dividing it into small pieces, and dissolving it in 50 ml of methanol in a 250 ml, three-necked, round-bottom flask previously cooled in a ice bath. After all

the sodium metal had reacted, the excess of methanol was removed by rotary evaporator and the product was dissolved in 250 ml of dimethyl-sulfoxide. The flask was assembled with a magnetic stirrer, dropping funnel and a refluxing condenser protected by a calcium chloride tube, and was heated by a heating mantle to 80 to 90°C for a period of two hours, as the sodium methoxide showed a limited solubility in methanol. The final solution appeared cloudy. Sodium salt of isethionic acid (GAF), 17.7 g (0.12 moles), dissolved in 100 ml of DMSO at 90°C, was added from the dropping funnel over a period of half an hour. Some solid matter precipitated out and an additional 100 ml of DMSO was added to the reaction mixture. The reaction mixture was distilled (30 torr), by rotary evaporater and approximately 40 ml of solution was removed. This procedure was to remove the methanol formed in the reaction.

The three-necked flask (equipped with magnetic stirrer, dropping funnel, and condenser protected by calcium chloride tube) with the reactants was heated to 85° to 90°C, using a heating mantle. Bromodecane (26.2 g, 0.12 moles), was added from the dropping funnel at the slowest possible dropping rate. A dropping time of 4 to 5 hours was required. Upon addition of the bromodecane the solution cleared. After addition of the bromodecane was completed, the mixture was stirred and heated at 80°C overnight. The solution was found to be

neutral by testing with indicater paper. The solution was then cooled for two hours in an ice-water bath and filtered. The residue was washed with 40 ml of n-butanol. A yellow solid was obtained.

The filtrate was placed in a one-litre flask and concentrated to one third the volume by vacuum distillation (75°C, 20 torr). Solid appeared on cooling and was filtered. The two batches of insoluble product were combined. Yield of crude product, 15.6 gms. (49% of the theoretical yield).

The dried yellow solid was dissolved in 250 ml of n-butanol and the solution was filtered while hot to remove a small amount of insoluble matter. The solution was allowed to cool for two hours at room temperature, then in an ice-water bath, and filtered. The residue was washed with 50 ml of cold n-butanol; a pale yellow crystalline product was obtained, 10.5 g (33% of the theoretical yield).

The filtrate from the above was concentrated to 100 ml and the solution was cooled in ice. The precipitated solid was filtered and washed with 50 ml of cold n-butanol and combined with the rest of the solid. The faint yellow crystalline product was twice recrystallized from a 100 ml portions of n-butanol, and then, twice from 50 ml portions of a mixture of isopropanol and n-butanol (2:1), and finally from 30-ml of quartz-distilled water.

Yield of the pure, white product was 5.5 g (17.5% yield). The purity was shown to be 99.0% by two phase titration of the product with Hyamine 1622, using mixed indicator (100).

2.2.1.2 Sodium 2-dodecyloxyethylenesulfonate.

$C_{12}H_{25}OC_2H_4SO_3^-Na^+$, ($C_{12}$EOS)

The procedure used was basically the same as for the previous compound. However, slight modifications were made to try to improve the yield.

Metallic sodium (2.9 g, 0.13 moles) was placed in a flask with 60 ml of cold reagent methanol. The methanol was subsequently removed by reduced pressure evaporation and dry sodium methoxide obtained . The solid sodium methoxide was dissolved in 200 ml DMSO. One objective in this synthesis was to use as little DMSO as possible, so that product might precipitate. Sodium salt of isethionic acid 17.8 g (0.12 moles), was dissolved in 80 ml of DMSO, at 90°C, the solution was filtered by gravity and added to the sodium methoxide solution in DMSO. The reaction mixture was distilled (25 torr) using a rotary evaporator and approximately 45 ml of solution was removed. The remaining solution was placed in a 3-necked, 500-ml round-bottom flask equipped with a condenser, $CaCl_2$ drying tube, thermometer and dropping funnel. Dodecylbromide (Tridom, purissima grade, >99%),

32.4 g (0.13 moles), was weighed directly into the dropping funnel. The halide was dropped into the reaction mixture over a period of 2 hours, and the reaction flask allowed to proceed overnight. The reaction mixture was yellow brown and there was an abundance of a yellowish, gelatinous material.

The reaction mixture was cooled in an ice-water bath and filtered to yield a brown solid. Evaporation of the filtrate to half its original volume, followed by cooling in an ice-water bath and removal of the precipitate by filtration, gave a total of 20 g (53% of the theoretical). The product was recrystallised twice from 60-ml portions of n-butanol. The white crystalline product, $C_{12}H_{25}OC_2H_4SO_3Na$, was dissolved in quartz distilled water (8 gms in 200 ml of water), and filtered hot. The filtrate was allowed to cool, filtered, and the residue was washed with 50 ml of ice-cold water. This procedure was repeated twice and yielded a white crystalline product, 7.2 g, (23% of the theoretical).

Purity was shown to be 99.5%, by two-phase titration with Hyamine 1622, using mixed indicator (100).

2.2.2 Preparation of sodium dodecyloxyethylene sulfates.

2.2.2.1 Sodium dodecylmonooxyethylene sulfate.

$C_{12}H_{25}OC_2H_4SO_4^-Na^+$ ($C_{12}EOSO$)

Monoethyleneglycol dodecyl ether (Nikko Chemical Co., Tokyo, Japan.>99%), 11 g (0.05 moles), was added to 100 ml of chloroform (dried over calcium chloride), in a 250 ml, three-necked, round-bottom flask equipped with a magnetic stirrer, a dropping funnel, a thermometer and a reflux condneser protected by a calcium chloride drying tube, and cooled by an ice-water bath to 8°C.

Freshly distilled chlorosulfonic acid, 6.9 g (0.06 moles), was added from the dropping funnel at the slowest possible dropping rate and the temperature of the reaction mixture was maintained below 10°C.

After the addition of the chlorosulfonic acid was complete (two hours), the mixture was stirred for an hour at room temperature. During this time nitrogen was passed in to remove hydrogen chloride formed during the reaction. The reaction mixture was neutralized with 4 g (0.1 moles), of sodium hydroxide dissolved in 40 ml of ethanol. The chloroform was removed at reduced pressure by using a rotary evaporator, 100 ml of absolute ethanol was added, and the reaction mixture was heated to 60°C and filtered hot to remove insoluble matter.

The filtrate was cooled to room temperature, then in an ice-water bath, and filtered.

Crystallization of the residue four times from 40-ml portions of 2-propanol gave 4.2g (25% of the theoretical), of white, crystalline product, after drying to constant weight in a dessicator over phosphorus pentoxide.

2.2.2.2 Sodium dodecyl diethoxyethylene sulfate

$C_{12}H_{25}(OC_2H_4)_2SO_4^+Na^-$, ($C_{12}EO_2SO$)

The apparatus and the procedure used was the same as for the previous compound. To 9 g (0.02 moles) of diethyleneglycol dodecyl ether in 100 ml of dry chloroform at 8°C, 3.5 g (.03 moles) of freshly distilled chlorosulfonic acid was added from a dropping funnel, with constant stirring. After the addition of all the chlorosulfonic acid, the reaction mixture was allowed to warm up to room temperature and stirred for two hours.

After neutralization of the reaction mixture, 100 ml of ethanol was added. The solution remained cloudy on warming and was difficult to filter due to the dispersion of the sodium chloride and sodium sulfate in the solution.

The ethanol was removed and the product was redissolved in 75 ml of n-propyl alcohol and centrifuged at 40°C. The clear supernatant was concentrated under reduced pressure, using a rotary evaporator. The residue was dissolved in isopropyl alcohol and gave a clear solution on warming. Upon cooling in an ice-water bath, the solution yielded a white product which was recystallized four times from 50 ml portions of 2-propanol. After being dried overnight in a dessicator with phosphorus pentoxide, the product weighed 1.8 g (24% of the theoretical). Purity was 99.0%, as determined by two-phase titration with Hyamine 1622 using mixed indicator (100).

2.2.3 Preparation of N-alkyl, N-benzyl, N-methylglycines, $C_nH_{2n+1}\overset{+}{N}(CH_2C_6H_5)(CH_3)CH_2COO^-$

Two homologues, in which n = 10 (C_{10}BMG) and 12 (C_{12}BMG), were synthesized. The synthetic schemes are as follows:

$$C_6H_5CH_2NH(CH_3) + ClCH_2COO^-Na^+ \longrightarrow C_6H_5CH_2N(CH_3)CH_2COO^-Na^+$$

$$C_6H_5CH_2N(CH_3)CH_2COO^-Na^+ + RBr \longrightarrow C_6H_5CH_2\overset{+}{N}(CH_3)(R)CH_2COO^-$$

(where R = n-$C_{10}H_{21}$ or $C_{12}H_{25}$).

2.2.3.1 N-dodecyl N-benzyl N-methyglycine

$C_{12}H_{25}\overset{+}{N}(CH_2C_6H_5)(CH_3)CH_2COO^-$, ($C_{12}$BMG)

N-methylbenzylamine, 36 g (0.3 moles), in 100 ml of 95% ethanol in a 500 ml, three-necked, round-bottom flask equipped with magnetic mixing stirrer, a dropping funnel and a reflux condenser, was heated by an heating mantle to reflux temperature. Sodium chloroacetate, 11.6 (0.1 moles), partially dissolved in 100 ml of 95% ethanol, was added from the dropping funnel overnight to the reaction flask maintained at 60°C.

To the resulting solution was added 100 ml of water and Na_2CO_3 (0.5 moles), and the mixture was steam distilled to remove the excess N-methylbenzylamine. After 4 hours, the distillate was found to be neutral to litmus. The water was removed under reduced pressure, using a rotary evaporater and the crude residue was dissolved in 200 ml absolute ethanol and filtered hot to remove the sodium chloride. Ethanol was removed from the filtrate by distillation under reduced pressure and the product was recrystallized from 100 ml isopropyl alcohol. The yield of the tertiary amine, $C_6H_5N(CH_3)CH_2COO^-Na^+$, 15 g (70% of the theoretical).

The tertiary amine, 15.0 g (0.07 mole), thus obtained, was dissolved in 200 ml of absolute ethanol and was reluxed for two days with five molar percent excess of the bromododecane (Humphrey

Chemical, North Haven, Conn., 97%). Solvent was removed by rotary evaporator and the residue was dissolved in 100 ml of 10 per cent aqueous sodium carbonate solution and extracted three times with 50-ml portions of hexane to remove any unreacted bromododecane. The product, the N-alkyl,N-benzyl,N-methylglycine, was extracted into 75 ml of chloroform from the aqueous layer. Solvent was stripped off to obtain 22 g (80% of the theoretical) of a viscous product. The well-dried product was recrystallized thrice from 25-ml portions of carbon tetrachloride and twice from 30-ml portions of THF/$CHCl_3$(60:40v/v), mixture to yield 15 g (50% of the theoretical) of white, crystalline product.

IR (CCl_4);$\nu_{c=o}$ = 1575 cm^{-1}

H^1NMR (CCl_4);7.45 (5H,s), 4.9(2H,d), 3.6(2H,s), 3.4-3.0(5H,m) 2-0 - 1.0(20H,m), 0.8(3H,t)

Calc, for $C_{12}H_{25}\overset{+}{N}(CH_2C_6H_5)(CH_3)CH_2COO^-$: C,75.19;H.10.41;N,4.38; Found: C,74.48; H,10.82;N,4.32;

The molar absorptivity of the compound is listed in Table I.

2.2.3.2 N-decyl,N-benzyl,N-methylglycine.

$C_{10}H_{21}\overset{+}{N}(CH_2C_6H_5)(CH_3)CH_2COO^-$ (C_{10}BMG)

The well dried tertiary amine, 10 g (0.05 moles), (obtained from the procedure described above for C_{12}BMG), was dissolved in 125 ml of hot ethanol and refluxed with 5 molar percent excess of the bromodecane (Humphrey Chemical, North Haven, Conn.,97%,) for 24 hours. The solvent was stripped off, and the residue was dissolved in 100 ml of 10% aqueous sodium carbonate solution and extracted four times with 50 ml portions of hexane. The product was next extracted into 75 ml of chloroform from the aqueous layer. Removal of the solvent gave of viscous product, 14 g (82% of the theoretical).

The well dried product was recrystallized twice from 50-ml portions of carbon tetrachloride and twice from 40 ml portions of a mixture (60:40v/v) of THF/CHCl to obtain a white, crystalline product, 9 g (53% of the theoretical).

IR(CCl_4; $\nu_{c=o}$ = 1575 cm^{-1}

H^1NMR (CCl_4); 7.4(5H,s), 4.9(2H,d), 3.55(2H,s) 3.3-2.9(5H,m), 2.0-1.0(16H,m), 0.85(3H,t).

Anal Calc: C,76.03;H,10.73;N,4.03 Found: C,75.70;H,10.76;N,3.92

2.2.4 Preparation of N-alkyl,N-benzyl,N-methyltaurines.

$C_nH_{2n+1}N^+(CH_2C_6H_5)(CH_3)CH_2CH_2SO_3$

Three homologues, in which n = 8 (C_8BMT), 10 (C_{10}BMT), and 12 (C_{12}BMT), were synthesised by a procedure similar to that for the N-alkylbetaines

2.2.4.1 N-decyl,N-benzyl,N-methyl taurine

$C_{10}H_{21}N^+(CH_2C_6H_5)(CH_3)\ CH_2CH_2SO_3^-$ (C_{10}BMT).

N-methylbenzylamine, 30 g (0.15 moles), in 100 ml of 95% methanol in a 500 ml, three-necked flask equipped with a reflux condenser and dropping funnel, was heated to 50°C.

Sodium salt of chloroethanesulfonic acid, 8.32 g (0.05 moles), dissolved in 100 ml of 75% methanol, was added from the dropping funnel over a period of 6 hours, and the reaction was allowed to proceed for two days at reflux temperature.

Solvent was evaporated and the residue was dissolved in 100 ml of solution containing 10.6g(0.1 moles), of sodium carbonate. The mixture was steam distilled to remove excess N-methylbenzylamine. The water was removed by rotary evaporator from the residue and the the crude tertiary amine and salts were added to 200 ml of hot absolute ethanol,

the mixture was stirred for 5 minutes, and filtered. The ethanol was removed from the filtrate by vacuum distillation (5 torr), at room temperature, yielding 10.5 of yellow powder. The powder was dissolved in 100 ml of hot methanol, decolorised twiced with Norite, and the solution was filtered. The methanol was removed from the filtrate by distillation under reduced pressure (5 torr) at room temperature and the product $C_6H_5N(CH_3)CH_2CH_2SO_3^-Na^+$, 9.0g (72% of theoretical) was dried in vacuo at room temperature over phosphorus pentoxide.

The well dried $C_6H_5N(CH_3)CH_2CH_2SO_3^-Na^+$, 8.5 g (0.03 moles), was dissolved in 150 ml of hot ethanol (absolute), and was refluxed with five molar per cent excess of bromodecane (Humphrey Chemical, North Haven, Conn.,97%) for two days. Solvent was removed by distillation under reduced pressure, the residue was dissolved in 100 ml of 10% aqueous sodium carbonate solution and was extracted with four 50-ml portions of hexane to remove the unreacted bromodecane. The product was extracted into 100 ml of chloroform from the aqueous layer. The solvent was removed by vacuum distillation at room temperature. The crude, yellow product, 4.2 g (36% of the theoretical), was dried in vacuo at room temperature. The product was recrystallized twice from water and then dried over phosphorus pentoxide in vacuo at room temperature. The yield of product, $C_{10}H_{21}N^+(CH_2C_6H_5)(CH_3)CH_2CH_2SO_3^-$ was 3.0 g (25% of the theoretical).

H^1NMR (D_2O): 7.3(5H,m), 4.8(2H,s), 4.1-3.65(4H,broad), 2.85(5H,m), 2.0-1.0(16H,m), 0.85(3H,t).

Calc: C,64.99;H,9.55;N,3.79. Found: C,65.20;H,9.92;N,3.74.

The molar absorptivity of the compound is listed in Table I.

2.2.4.2 N-dodecyl,N-benzyl,N-methyltaurine.

$C_{12}H_{25}\overset{+}{N}(CH_2C_6H_5)(CH_3)CH_2CH_2SO_3^-$, ($C_{12}$BMT).

The apparatus and the procedure used was the same as for C_{10}BMT. The tertiary amine, 13 g (0.03 moles), was dissolved in hot ethanol (absolute), and refluxed with five molar percent excess of the bromododecane (Humphrey Chemical, North Haven, Conn.,97%), for two days. Solvent was stripped off at reduced pressure, using a rotary evaporator. The residue was dissolved in 100 ml of sodium carbonate (0.015 moles) solution, and extracted with four 50-ml portions of hexane. The product was extracted into 100 ml of chloroform. Solvent was removed and the crude product was recrystallized twice from water and twice from THF/$CHCl_3$(40:60) mixture. The white crystalline product obtained was dried over phosphorous pentoxide in vacuo at room temperature: the yield of product, $C_{12}H_{25}\overset{+}{N}(CH_2C_6H_5)(CH_3)CH_2CH_2SO_3^-$ was 3.4g (27% of the theoretical).

H^1NMR (D_2O): 7.4(5H,m), 4.8(2H,S), 4.2-3.6(4H,broad), 2.85(5H,m), 2-1.0(2OH,m), 1.85(3H,t)

Anal. Calc: C,66.45;H,9.89;N,3.52, Found: C,66.31;H,10.01;N,3.48,

The molar absorptivity the compound in aqueous solution is listed in Table I.

2.2.4.3 N-octyl,N-benzyl,N-methyltaurine

$C_8H_{17}\overset{+}{N}(CH_2C_6H_5)(CH_3)CH_2CH_2SO_3^-$, ($C_8$BMT)

The tertiary amine, $C_6H_5N(CH_3)CH_2CH_2SO_3^-Na^+$, 12 g (0.03 moles) was dissolved in 100 ml of hot ethanol (absolute) and refluxed with five molar per cent excess of bromooctane (Aldrich, 99%) for two days. Solvent was stripped off and the crude residue was dissolved in 100 ml of aqueous sodium carbonate (0.015 moles), and was extracted with four 50 ml portion of hexane. Next, the crude product was extracted into chloroform from the aqueous layer. Solvent was stripped off and the crude product was dried and recrystallized from THF/$CHCl_3$ (60:40) mixture. The white crystalline product obtained was dried in vacuo over P_2O_5 at room temperature. Yield:2.5 g (25% of the theoretical).

H^1NMR (D_2O); 7.4(5H,m), 4.8(2H,s), 4.1-3.65(4H,broad), 2.8(5H,m), 2-1.0(12H,m), 1.8(3H,t)

The molar absorptivity for the compound in aqueous solution is listed in Table I.

TABLE I: Molar absorptivities for $R\text{-}\overset{+}{N}(CH_2C_6H_5)(CH_3)CH_2COO^-$ and $R\text{-}\overset{+}{N}(CH_2C_6H_5)(CH_3)CH_2CH_2SO_3^-$.

Compd	λ_{max}	ε ($dm^3 mol^{-1} cm^{-1} \times 10^{-2}$)
C_{10}BMG	263	3.80
C_{12}BMG	263	3.55
C_8BMT	263	3.88
C_{10}BMT	263	3.80
C_{12}BMT	210	121.20

2.2.5 Preparation of N-dodecylpyridinium halides

N-dodecylpyridinium bromide (C_{12}NBr) and N-Dodecylpyridinium chloride (C_{12}NCl) were prepared by reacting the appropriate 1-halododecane with pyridine.

2.2.5.1 N-dodecylpyridinium bromide.

($C_{12}NBr$).

1-Bromododecane (Tridom, purissima grade, 99%),31 g (0.126 M), was refluxed at 115°C with 10 g (0.130 moles), of pyridine (Fisher, Certified ACS grade, dried over KOH), for two days. The excess pyridine was removed by rotary evaporater under reduced pressure. The crude N-dodecylpyridinium bromide was purified by recrystallization from 50 ml of acetone, then dissolved in 100 ml of hot methanol and treated with decolorizing carbon (Darco G-60, ICI America). The methanol was removed from the filtrate and the white solid residue was recrystallized thrice from 2-butanone. The white, crystalline product was dried in vacuo over P_2O_5 at room temperature. Yield: 20 g (50% of the theoretical).

The purity of the product was checked by 2-phase dye transfer titration with sodium dodecanesulfonate solution of known concentration, using mixed indicators (100). After three recrystallizations from 2-butanone, the purity of the product had reached a constant value of 99.5%.

2.2.5.2 N-dodecylpyridinium Chloride.

($C_{12}NCl$).

A procedure similar to that used for N-dodecylpyridinium bromide was used to prepare the crude product.

The crude N-dodecylpyridinium chloride (15g) was dissolved in 75 ml of hot 2-butanone treated with decolorizing carbon (Darco G-60), and the solution filtered hot. Cooling of the filtrate yielded a white, solid product that was recrystallized again from 2-butanone. After three crystallizations, the product 12 g (60% of the theoretical) had reached a constant purity of 100.08%, as determined by the two-phase dye transfer titration.

The molar absorptivities for the two compounds, $C_{12}NBr$ and $C_{12}NCl$, at λ max (259.0nm), in aqueous solutions containing various amounts of sodium halides, are listed in Table II.

TABLE 2: Molar Absorptivities of N-Dodecylpyridinium Bromide and Chloride at 259.0 nm

Compound	Solvent	e($dm^3 mol^{-1} cm^{-1} X10^{-3}$)
$C_{12}NBr$	H_2O	3.88
$C_{12}NBr$	0.1 M NaBr	3.84
$C_{12}NBr$	0.5 M NaBr	3.84
$C_{12}NCl$	H_2O	4.08
$C_{12}NCl$	0.1 M NaCl	4.11
$C_{12}NCl$	0.5 M NaCl	4.18

2.3 Purification and analysis of surfactants

Surfactants synthesised were all purified to >99% purity, as determined by analytical techniques, using conventional purification techniques. For surface tension measurements, the aqueous solutions of compounds of this purity were prepared with water that had first been deionized and then distilled twice, the last time from alkaline potassium permanganate through a three-foot high Vigreaux column with quartz condenser and receiver. These solutions were repeatedly passed

through columns of octadecylsilanized silica gel, (SEP-Pak C_{18} Cartridge, Water Assoc., Milford, Mass), until the surface tension-concentration curve of the material showed no minima in the vicinity of the CMC and, in addition, reached steady values of surface tension within one hour. Those solutions that required a time over one hour to reach equilibrium surface tension value were either discarded or re-treated by passage through the SEP-PAK columns. The concentrations of the effluent from these columns were determined either by ultraviolet absorbance in the case of betaines, sulfobetaines and dodecylpyridinium halides, by two-phase titration of anionic surfactants by Hyamine 1622 with mixed indicator in the case of anionic surfactants, and by tensammetric method, in the case of polyoxyethylenated alcohols.

The sodium bromide and sodium chloride used to increase the ionic strength of the solutions were analytical reagent grade materials which were baked for several hours in a porcelain casserole at red heat to remove traces of organic compounds. The surface tension of aqueous solutions of the baked salts was measured to ensure the absence of traces of surface-active impurities.

Tensammetric determination of polyoxyethylenated alcohols (101)

Differential double-layer capacitance vs potential measurements at the dropping mercury electrode was used for the determination of polyoxyethylenated n-dodecyl alcohols.

Sufficient lithium chloride was dissolved in the surfactant solution (containing 2.20 ppm surfactant) to give a 0.1 - 1 M lithium chloride solution. Fifty millimeters of the solution was transferred to the polarograph cell. The drop time of the dropping mercury electrode was adjusted to 3 s, and the differential capacitance of the desorption peak was recorded from -1 to -2 V. The height (Δh) in millimeters, of the highest desorption peak between -1 and -2V was measured. A calibration curve of Δh vs. surfactant concentration, C, was prepared for solutions of known surfactant concentration in the range of 2-20 ppm. The concentration of the unknown solution after purification was determined by the use of the calibration curve. A calibration curve was done each day surfactant concentrations were measured.

Two phase titration of anionic surfactant by Hyamine 1622 with mixed indicator, (100)

This procedure for the analysis of ionic surfactants is based upon the solubility of the dyestuff-salt complex in organic solvents, such as

chloroform. Here, one ionic type of surfactant is titrated against the opposite charge type in the presence of a mixed indicator.

Reagents;

Cationic titrating solution; 1.75 - 1.85g of Hyamine 1622 (diisobutylphenoxyethyldimethylbenzylammoniumchloride,) was weighed accurately into a 1 - litre volumetric flask, and the solution made to mark with distilled water. The concentration of the solution was checked by ultraviolet absorbance, using the molar absorptivity of 1.322 $dm^3 mol^{-1} cm^{-1} X 10^{-3}$ at λ = 247 nm.

Indicator: Dimidium bromide (Burroughs Wellcome Co., Ltd., London), 0.5g., was weighed into a 50 ml beaker. Disulphine Blue VN (Imperial Chemical Industries, Manchester), 0.25 g, was weighed into a second 50-ml beaker. Hot 10% (vol) ethanol (25ml) was added to each beaker. The solutions were stirred, transferred to a 250 ml graduated cylinder, and diluted to the mark with the same solvent.

Acid Indicator: 200 ml of distilled water was added to 20 ml of the above indicator in a 500 ml of graduated cylinder. 20 ml of 2.5 M sulfuric acid was added and diluted to 500 ml with distilled water.

To 20 ml of anionic surfactant of unknown concentration (approximately 0.002 M) in a 200 ml glass-stoppered conical flask, 15 ml of chloroform and 10 ml of acid indicator was added. This solution was

titrated against the cationic solution until the pink color was discharged from the chloroform layer. After each addition of titrating solution the mixture was shaken well and then the layers allowed to separate. At the end point, the lower layer has a gray color with no trace of pink.

2.4 Surface tension measurement

(102)

All surface tension measurements were made by the Wilhelmy vertical plate technique, using a sand-blasted platinum plate of approximately 5 cm perimeter. The plate was calibrated against quartz distilled water (specific conductivity, 1.11 mho, at 25.0°C) each day that a measurement was made. The correction for densities was ignored in the present work because, the weight per cent of surfactant in the solutions never exceeded 1 %, therefore, the densities are virtually the same as that of quartz-distilled water.

The surface tension apparatus consists of a circular dial-type torsion balance with a maximum capacity of 500 mg, readable to 0.2 mg. One of the arms was tared to approximately balance the platinum plate (and the cotton string supporting it) on the other end of the arm. The whole balance rests on a metal covered wood platform over a

constant temperature bath. The platform can be raised and lowered accurately by a machine-threaded hydraulic device.

The solution to be tested was kept in a 200 ml dish partially immersed in a constant temperature bath at the desired temperature ±0.02° C.

The procedure for measuring surface tension by the Wilhelmey plate technique was as follows:

1) The temperature of the water bath was adjusted to the desired temperature.

2) The 200 ml dish containing approximately 40 ml of the surfactant solution was placed in the water bath and equlibrated to the bath temperature.

3) The platinum plate was rinsed with quartz-distilled water, and was flamed the outer portion with a Bunsen burner flame until it was red, holding the plate vertically by a pair of tweezers.

4) The plate was suspended from the cotton thread suspended from the locked balance. The balance was unlocked and adjusted to read zero.

5) The balance was locked and lowered slowly until the lower edge of the plate almost reached its image reflected from the surface of the solution. The plate was checked and adjusted, if necessary, to lie parallel to the surface of the solution. The stirrer of the constant

temperature bath was shut off, the balance was unlocked and the assembly lowered until the plate was just pulled under the surface of the solution. The stirrer of the constant temperature bath was turned on.

6) The samples were aged at least for 15 minutes before readings were taken.

7) The readings were taken as follows: The stirrer of the constant temperature bath was shut off and the plate was restored to it's original position in space by moving the arm of the torsion balance until the pointer reached the zero position. Five successive readings were taken without detaching the plate from the surface of the solution. The plate was immersed again and left for ten to fifteen minutes before the next measurement was made.

Chapter III

Results and Discussion

3.1 2-Dodecoxypoly(ethenoxy)ethanols

3.1.1 Results

Plots of the surface tension (γ) at 10,25, and 40°C of aqueous solutions of EO2,EO3,EO4,EO5,EO7, and EO8 vs the log of their bulk phase concentration in mol dm^{-3} (log C) in water are shown in Figures I to VI.

Critical micelle concentrations were taken as the concentrations at the point of intersection of the two linear portions of the γ - log C plots. The slope of the linear portion of each curve below the CMC was determined by the method of least mean squares. Maximum surface excess concentration (Γ_{max}), in mol cm^{-2} and minimum area per molecule (A_{min}), in nm^{-2}, at the aqueous/air interface were calculated from equations (18) and (24), respectively. Values of CMC, Γ_{max}, A_{min} and π_{cmc} are listed in Table 3.

TABLE 3: Surface Properties of Surfactants of Structure

$C_{12}H_{25}(OC_2H_4)_xOH$

Compd	T (°C)	Cmc (mol dm^{-3} X 10^5)	Γ_{max} (mol cm^{-2} X 10^{10})	A_{min} (nm^2 X 100)	π_{cmc} (mNm^{-1})
EO2	10	3.8	5.34	31.3	47.4
	25	3.3	4.73	35.1	45.7
	40	3.3	4.72	35.2	43.6
EO3	10	6.3	4.01	39.3	45.4
	25	5.2	3.98	41.8	44.1
	40	5.6	3.90	42.5	43.1
EO4	10	8.2	3.96	42.0	43.9
	25	6.4	3.63	45.7	43.3
	40	5.9	3.41	48.7	42.0
EO5	10	9.0	3.42	48.6	41.9
	25	6.4	3.31	50.1	41.5
	40	5.9	3.28	50.6	41.2
EO7	10	12.1	2.85	58.3	38.3
	25	8.2	2.90	57.3	38.3
	40	7.3	2.77	59.9	38.5
EO8	10	15.6	2.56	64.9	37.4
	25	10.9	2.52	66.0	37.2
	40	9.3	2.46	67.4	37.3

TABLE 4: Thermodynamic parameters of micellization for Nonionics of structure $C_{12}H_{25}(OC_2H_4)_xOH$

Compd	T(°C)	$\Delta G°_{mic}$ (kJ mol^{-1})	$\Delta H°_{mic}$ (kJ mol^{-1})	$\Delta S°_{mic}$ (kJ mol^{-1}K^{-1})
EO_2	10	-23.9		
	25	-25.6	+4.2	+0.10
	40	-26.9		
EO_3	10	-22.8		
	25	-24.4	+5.9	+0.10
	40	-25.8		
EO_4	10	-22.1		
	25	-23.9	+8.8	+0.11
	40	-25.4		
EO_5	10	-21.9		
	25	-23.9	+9.9	+0.11
	40	-25.3		
EO_7	10	-21.2		
	25	-23.3	+12.5	+0.12
	40	-25.3		
EO_8	10	-20.6		
	25	-22.6	+13.2	+0.12
	40	-24.2		

TABLE 5: Thermodynamic Parameters of adsorption for Nonionics of Structure $C_{12}H_{25}(OC_2H_4)_xOH$

Compd	T(°C)	$\Delta G°_{ad}$ (kJ mol^{-1})	$\Delta H°_{ad}$ (kJ mol^{-1})	$\Delta S°_{ad}$ (kJ $mol^{-1}K^{-1}$)
EO_2	10	-32.8		
	25	-35.2	-1.4	+0.11
	40	-36.2		
EO_3	10	-33.5		
	25	-35.5	-0.3	+0.11
	40	-36.8		
EO_4	10	-33.3		
	25	-35.9	+0.4	+0.12
	40	-37.7		
EO_5	10	-34.2		
	25	-36.2	+0.6	+0.12
	40	-37.9		
EO_7	10	-34.7		
	25	-36.9	+2.4	+0.13
	40	-38.7		
EO_8	10	-35.2		
	25	-37.4	+3.3	+0.13
	40	-39.3		

TABLE 6: Structural Effects on micellization and adsorption for Noninics of structure $C_{12}H_{25}(OC_2H_4)_xOH$

Compd	T(°C)	$\Delta G°_{mic}-\Delta G°_{ad}$ (kJ mol^{-1})	$\Delta H°_{mic}-\Delta H°_{ad}$ (kJ mol^{-1})	$\Delta S°_{mic}-\Delta S°_{ad}$ (kJ $mol^{-1}K^{-1}$)
EO_2	10	+8.9		
	25	+9.6	+5.6	-3.9
	40	+9.3		
EO_3	10	+10.7		
	25	+11.1	+6.2	-4.8
	40	+11.0		
EO_4	10	+11.2		
	25	+12.0	+8.4	-3.6
	40	+12.3		
EO_5	10	+12.3		
	25	+12.4	+9.3	-3.0
	40	+12.6		
EO_7	10	+13.5		
	25	+13.6	+10.1	-3.6
	40	+13.9		
EO_8	10	+14.6		
	25	+14.8	+9.0	-5.0
	40	+15.1		

The ΔG°_{mic} values were calculated from equation (52). The ΔG°_{mic} values calculated in this manner at each of the three temperatures were plotted against the number of oxyethylene units in the molecule and smooth curves were drawn through the data points. From these three curves, ΔS°_{mic} and ΔH°_{mic} values at 25°C were calculated by use of equations (47) and (48), respectively. These thermodynamic parameters of micellization are listed in Table 4.

Table (5) lists the standard free energies, ΔG°_{ad}, enthalpies ΔH°_{ad} and entropies, ΔS°_{ad}, of adsorption. ΔG°_{ad} values were calculated by the use of equation (45), and ΔS°_{ad} and and ΔH°_{ad} from equations (47) and (48).

3.1.2 Discussion

The minimum area per molecule at the aqueous solution/air interface increases with increase in the number of oxyethylene units in the molecule. This is in agreement with the relationship observed for other polyoxyethylenated nonionics (103), that $A_{min}\ n^{-1/2}$ (=21.0-22.9 at 10°C; 21.7-24.8 at 25°C; 22.6-24.9 at 40°C), where n is the number of oxyethylene units in the chain, is almost a constant. There appears to be an sharp increase in area per molecule with the initial increase in oxyethylene units, followed by a moderate increase. The increase in area with the increase in oxyethylene units appear to be due to poor

packing at the air/water interface since the hydrated, coiled oxyethylene chains sweep out a greater surface area as their length increases.

The minimum area per molecule also increase with increase in temperature, as would be expected from the increased thermal agitation. This would result in poorer packing of the adsorbed molecules and a consequent increase in area per molecule. This increase in area due to thermal agitation is opposed by the effect of the dehydration of the oxyethylene chains with increase in temperature. With the series of polyoxyethylenated compounds studied, except possibly for the EO7 compound going from 10° to 25°C, the area-increasing effect due to thermal agitation predominates over the area-decreasing effect due to dehydration.

The critical micelle concentration values show an increase with increase in the number of oxyethylene groups in the molecule. This is in agreement with previous studies (72) with nonionic surfactants.

The critical micelle concentration is found to decrease with increase in temperature for all the members of the series. In contrast, Crook et al (72), found continuous increase in CMC with temperature for the series of compounds p-tert-octylphenoxypoly(ethenoxyethonol)s with oxyethylene units one to four, while for the compounds with

oxyethylene units from five to ten the CMC initially decreased, then increased as the temperature was increased. For the molecules with the lowest EO content, EO2 and EO3, the variation of the CMC with temperature appears to be very small, whereas for the rest of the members in the series, the variation seems to be significant, especially going from 10° to 25°C. As the oxyethylene content is increased, there is greater solvation and therefore the influence of the temperature on the dehydration process will be more marked with molecules of high oxyethylene content than of low oxyethylene content. The larger variation of the CMC in the temperature range of 10 to 25°C than of 25° to 40°C for all members in the series suggests that most of the dehydration is complete at 25°C and that there is less dehydration taking place between 25° and 40°C.

The effectiveness of surface tension reduction, measured by π_{cmc}, shows a steady decrease with increase in the number of oxyethylene units Figure VII. This behaviour is in contrast to that reported for p-tert-octylphenoxypoly(ethenoxyethanol)s (72), where a maximum was observed at three to six oxyethylene units, depending upon the temperature. As seen from the equation (71), the decrease in π_{cmc} with increase in oxyethylene content appears to be due to the large decrease in surface excess concentration with the increase in oxyethylene content in these molecules.

Temperature increase has two opposing effects on the surface properties of these nonionic polyoxyethylenated molecules.

1) Dehydration of the oxyethylene units, leading to more hydrophobicity for the molecule and, 2) Kinetic-thermal effects, which generally result in increase in solubility and larger area per molecule at the aqueous solution /air interface.

It is apparent from Figure VII that the molecules with lower oxyethylene content have a larger variation of π_{cmc} with temperature, while no significant change in π_{cmc} is shown by the higher oxyethylenated compounds at the temperatures studied.

For molecules with shorter oxyethylene chains, as shown by the decrease in π_{cmc} values with increase in temperature, the second effect plays a more important part than the first. Due to the fewer solvated oxygens in the oxyethylene units in these shorter polyoxyethylenated compounds, the dehydration effect is expected to be small. On the other hand, for the longer polyoxyethylenated molecules it appears that both effects are equally important, as shown by their almost similar π_{cmc} values at all the temperatures studied.

With the shorter polyoxyethylenated members, the π_{cmc} value of 43 to 45 mNm^{-1}, approaches the π_{max} values of long-chain alcohols

containing six to ten carbon atoms (45 mNm^{-1}) at 20°C (105) and of $C_8H_{17}OC_2H_4OH$ (45 mNm^{-1}) at 25°C (104), in aqueous solution. On the other hand Crook et al have reported a value of 37.4 mNm^{-1} for p-tert-$C_8H_{17}C_6H_4OC_2H_4OH$, which appears to be too low.

The $\Delta S°_{mic}$ values in Table 4 are all positive for all the members in the series, indicating increasing randomness in the system upon transformation of the nonionic surfactant molecules into micelles. This increase of entropy (positive) on micellization has been observed for ionic surfactants, too, and this has been attributed to the destruction of a considerable portion of the structured water about the monomeric units of surfactants during their incorporation into the micelle (31). Moreover, an increase in $\Delta S°_{mic}$ values with increase of oxyethylene units indicates the desolvation of oxyethylene units to be a contributing factor to the positive entropy change. On the other hand, the crowding of the oxyethylene units into the outer micellar shell might cause decrease in configurational entropy for the molecule compared to that of the free monomers, and this would cause an entropy decrease with increase in oxyethylene units. The small increase in $\Delta S°_{mic}$ observed with increase in oxyethylene units may be due to the combination of these two effects.

The ΔH°_{mic} values in Table 4 are positive for all the members in the series. This is in contrast to the negative ΔH°_{mic} values at 25°C observed for the p-tert-octylphenoxypoly(ethenoxy)ethanols containing less than four oxyethylene units (72). The increase in ΔH°_{mic} values with increase in oxyethylene content indicates that greater numbers of hydrogen bonds between polyoxyethylene chain oxygens and water molecules are broken in the micellization process as the number of oxyethylene units in the molecule increases.

The ΔS°_{ad} values are all positive, as in micellization but slightly greater than the ΔS°_{mic} values for the same compounds. This may reflect the greater freedom of motion of the oxyethylene chain units at the planar air/aqueous solution interface compared to the crowded outer shell of a micelle. The change in ΔS°_{ad} with increase in the number of oxyethylene units in the molecule, on the other hand, approximates that observed for ΔS°_{mic}. This is expected, since groups at the micellar surface would not experience the space restriction imposed upon groups extending into the interior.

The ΔH°_{ad} values are all less positive than ΔH°_{mic} values and become slightly more positive with increase in the number of oxyethylene units in the molecule. This shows that less bonds between polyoxyethylene chain oxygens and water molecules are broken in the

process of adsorption at the air/aqueous solution interface than in micellization, but that, as in micellization, the number of bonds broken increases with increase in the number of oxyethylene units in the molecule.

It is evident from Table 5 that most of the negative ΔG°_{ad} value comes from the ΔS°_{ad} value and that the contribution of the oxyethylene unit to the ΔG°_{ad} value is very small in these polyethenoxylated nonionic surfactants. Also, a $-\Delta G^\circ_{ad}$ value of 36 to 37 kJ mol^{-1} for oxyethylene chain lengths of five to eight units indicates that these compounds all have almost the same tendency to adsorb at the aqueous solution/air interface at 25°C. Their tendency for adsorption is comparable to those of $C_{12}H_{25}CH_2OH$ or $C_{12}H_{25}CHOHCH_2CH_2OH$, both of which have a ΔG°_{ad} value of 37.0 kJ mol^{-1} (20).

From equation (52) and (45) it follows that:

$$\Pi_{cmc}\, A_{cmc} \equiv \Pi_{cmc}\, A_{min} = \Delta G^\circ_{mic} - \Delta G^\circ_{ad}$$

The $\pi_{cmc}\, A_{min}$ product consequently expresses the work involved in transferring the surfactant molecule from a monolayer at zero surface pressure to the micelle. The $\Delta G^\circ_{mic} - \Delta G^\circ_{ad}$ values are listed in Table 6. It is apparent that these terms, which measure the ease of adsorption to form a monolayer at zero surface pressure relative to the

ease of micellization, are all positive and show little change with temperature in the 10-40°C range. From Tables 4 and 5 it appears that the positive contribution to the positive (ΔG°_{mic} - ΔG°_{ad}) value arises from 1) The greater positive entropy change upon adsorption than upon micellization and (2) the smaller positive enthalpy change upon adsorption than upon micellization.

From Table 6 it is seen that the entropy contribution to the ΔG°_{mic} - ΔG°_{ad} remains almost constant at 3 to 5 kJ mol^{-1} while the enthalpy contribution increases steadily with increase in the number of oxyethylene units in the molecule, showing the significance of the enthalpy factor in reducing the ease of micellization over adsorption. From the above observations and from the literature (105) it is known that steric factors inhibit micellization more than they do adsorption at the air/aqueous solution interface. In the case of these polyoxyethylenated nonionic alcohols, the structural elements in the surfactant molecule that may cause "steric inhibition" of micellization are (1) The alkyl chain and (2) the polyoxyethylene chain. The greater restriction on the motion of the alkyl chain in the relatively cramped interior of the micelle compared to the planar air/aqueous solution interface may be the cause for the entropy contribution to the positive value of the work of transfer. This contribution would be expected to remain essentially unchanged with increase in the number of

oxyethylene units in the surfactant molecule. On the other hand, the positive values for $\Delta H^\circ_{mic} - \Delta H^\circ_{ad}$ and their steady increase with the increase in the number of oxyethylene units in the molecule indicate that greater dehydration of the polyoxyethylene chain is required for micellization than for adsorption at the air/aqueous solution interface. This shows that the space available to the hydrophilic group at the surface of the micelle is more restricted than at the planar air/aqueous solution interface.

From equation (82) it follows that,

$$\pi_{cmc} = (\Delta G^\circ_{mic} - \Delta G^\circ_{ad})/A_{min}$$

Since, as discussed above, bulky hydrophilic groups inhibit micellization more than they do adsorption at the air/aqueous solution interface, π_{cmc}, the effectiveness of surface tension reduction, would normally increase as the bulkiness of the hydrophilic group is increased if A_{min} remained constant. In the present case, an increase of one in the number of oxyethylene units in the molecule cause an approxymately 15 % increase in A_{min}, while producing an increase of less than 10 % in the value of $\Delta G^\circ_{mic} - \Delta G^\circ_{ad}$, resulting in the observed decrease in π_{cmc} (Table 3) as the length of the polyoxyethylene chain is increased.

The percentage change in ($\Delta G^\circ_{mic} - \Delta G^\circ_{ad}$) with change in temperature from 10° to 40°C is more or less constant with increase in

the number of oxyethylene units in the surfactant molecule, while the percentage change in A_{min}, which at lesser oxyethylene content is greater than the percentage change in (ΔG°_{mic} - ΔG°_{ad}), decreases and approaches that of the latter when the molecule contains more than five oxyethylene units. This accounts for the convergence of three temperature curves in Figure VII to one, at that oxyethylene content.

3.2 Betaines and Sulfobetaines

3.2.1 Results

Plots of surface tension (γ) vs the log of the molar concentration, C, of the surfactant in the bulk phase at 10, 25 and 40°C for the N-alkylglycines and N-alkyltaurines are shown in figures VIII and IX, respectively.

Surface excess concentration, Γ_{max}, in mol cm^{-2} and area per molecule, A_{min} in nm^{-2}, at the liquid/air interface were calculated from equations (18) and (24) respectively. Values of the critical micelle concentration, cmc, minimum area per molecule A_{min}, π_{cmc}, the effectiveness of surface tension reduction, and pC_{20}, the efficiency of surface tension reduction, are listed in Table 7.

The standard free energies, $\Delta G°_{mic}$, entropies, $\Delta S°_{mic}$, and enthalpies, $\Delta H°_{mic}$, of micellization were calculated from equations (52),(47) and (48) respectively. These values are listed in Table 8. Table 9 lists the standard free energies, $\Delta G°_{ad}$, enthalpies $\Delta H°_{ad}$, and entropies, $\Delta S°_{ad}$, of adsorption. $\Delta G°_{ad}$ values were calculated by the use of equation (45), and $\Delta S°_{ad}$ and $\Delta H°_{ad}$ from equations (47) and (48) respectively.

TABLE 7: Surface Properties of betaines and sulfobetaines

Compd	T(°C)	Cmc mol dm^{-3} X 10^3	A_{min} nm^2 X 100	pC_{20}	Π_{cmc} mNm^{-1}	Cmc/C_{20}
C_{10}BMG	10	6.31	54.8	3.34	38.7	13.8
	25	5.25	56.9	3.36	38.0	12.0
	40	4.36	59.7	3.30	36.3	8.7
C_{12}BMG	10	0.60	56.2	4.42	39.7	15.8
	25	0.54	57.6	4.42	39.0	14.41
	40	0.52	59.7	4.32	37.6	11.0
C_8BMT	10	----	54.0	2.26	----	----
	25	----	60.9	2.23	----	----
	40	----	63.4	2.17	----	----
C_{10}BMT	10	----	55.8	3.40	----	----
	25	----	60.9	3.34	----	----
	40	4.57	64.0	3.22	33.8	7.6
C_{12}BMT	10	----	58.5	4.52	----	----
	25	----	61.2	4.44	----	----
	40	----	64.0	4.32	----	----

TABLE 8: Standard Thermodynamic Parameters of micellization for N-alkyl, N-benzyl, N-methylglycines

Compd	T(°C)	ΔG°_{mic} (kJ mol^{-1})	ΔH°_{mic} (kJ mol^{-1})	ΔS°_{mic} (kJ $mol^{-1}K^{-1}$)
C_{10}BMG	10	-11.5		
			+8.5	+0.070
	25	-13.0		
			+4.7	+0.044
	40	-13.9		
C_{12}BMG	10	-17.4		
			+4.6	+0.078
	25	-18.6		
			+0.9	+0.067
	40	-19.6		

TABLE 9: Standard Thermodynamic parameters of adsorption for zwitterionic compounds.

Compd	T(°C)	ΔG°_{ad} (kJ mol^{-1})	ΔH°_{ad} (kJ mol^{-1})	ΔS°_{ad} (kJ mol^{-1}K^{-1})
C_{10}BMG	10	-24.7		
			+0.2	+0.087
	25	-26.0		
			-2.6	+0.078
	40	-27.2		
C_{12}BMG	10	-30.9		
			-7.1	+0.082
	25	-32.1		
			-10.9	+0.071
	40	-33.2		
C_8BMT	10	-18.7		
			+5.9	+0.083
	25	-20.0		
			-9.2	+0.036
	40	-20.6		
C_{10}BMT	10	-25.1		
			-2.7	+0.079
	25	-26.3		
			-12.9	+0.045
	40	-27.0		

Cont'd

C_{12}BMT	10	-31.5		
			-10.6	+0.074
	25	-32.6		
			-14.8	+0.060
	40	-33.5		

3.2.2 Discussion

C_{10}BMG and C_{12}BMG were found to have high solubility in water, whereas the corresponding N-alkyltaurines were sparingly soluble in water. As a result, the only cmc determined in the latter series was for C_{10}BMT at 40°C. The cmc of C_8BMT was not determined due to its high cmc and insufficient material.

The areas per molecule for the glycines and for the taurines, when compared to the cross sectional areas of the compounds as obtained from molecular models, suggest that at the aqueous solution/air interface the ionic head groups, $-\overset{+}{N}(CH_2C_6H_5)(CH_3)CH_2CH_2SO_3^-$ in the case of taurines, and $-\overset{+}{N}(CH_2C_6H_5)(CH_3)CH_2COO^-$ in the case of glycines, are lying flat in the interface.

The taurines have a slightly larger area per molecule when compared to the glycines. The areas per molecule for the C_{10}BMG and C_{12}BMG are comparable to those of N-alkyl,N,N-dimethylglycines, (84,80) and for trimethylammonium alkanoates (82,80). Thus, the introduction of a benzylic group in C_{10}BMG and C_{12}BMG has a small effect on the area per molecule for these compounds.

From the only cmc obtained (for the C_8BMT at 40°C), it appears that the critical micelle concentration for the glycines and the taurines are comparable to each other.

On the other hand, the cmcs for the glycines are about three times smaller when compared to the corresponding N-alkyl,N,N-dimethyglycines (84), where 1.80×10^{-2} and 1.85×10^{-3} mol dm^{-3} been reported for the C_{10} and C_{12} compounds, respectively. Besides, the cmcs for the corresponding 2-(trimethylammonium)alkanoates (79,81) are 1.31×10^{-2} and 1.32×10^{-3} mol dm^{-3}, respectively. The very much lower cmcs for the C_{10}BMG and C_{12}BMG compounds appear to be due to the contribution of the benzylic group to the hydrophobicity in these molecules. Comparing the cmcs for C_{10}BMG and C_{12}BMG with the corresponding N-alkyl,N,N-dimethylglycines, it appears that the contribution of the benzene group to the hydrophobicity in these molecules is equivalent to about one half of a carbon atom in a straight hydrocarbon chain.

The efficiency of surface tension reduction, pC_{20}, for the betaines and their corresponding sulfobetaines is almost the same. On the other hand, this value is about a unit more than for the corresponding N-alkyl,N,N-trimethylammonium glycines (84): the pC_{20} values for the latter containing 10 and 12 carbon atom are 2.5 and 3.51, respectively, at 23°C. This increase is comparable to the increase in pC_{20} value for two methylene groups in a alkyl chain as seen from the difference of the pC_{20} values for the C_{10} and C_{12}BMG molecules. This shows the greater efficiency of the benzylic group in these compounds in

decreasing the surface tension at the aqueous solution/air interface than reducing the critical micelle concentration. The increase in hydrophobic character due to the $-CH_2C_6H_5$ group is counteracted in part in micellization by its steric inhibition of micellization.

Although the efficiencies of surface tension reduction for the betaines and the corresponding sulfobetaines are almost the same, the former appear to show greater effectiveness in surface tension reduction, as indicated by the π_{cmc} values. This appears to be due to the smaller area per molecule of the betaines as compared to the corresponding sulfobetaines. However, the corresponding N-alkyl,N,N-dimethylglycines show smaller π_{cmc} values: 36 and 32.5 mNm^{-1} for the C_{12} and C_{10} compounds, respectively. This greater effectiveness in surface tension reduction appears to be due to the larger cmc/C_{20} ratio for the C_{10}BMG and C_{12}BMG compounds compared to the corresponding N-alkyl,N,N-dimethylglycines.

Thus, the introduction of a more bulky hydrophobic group into the hydrophilic head group of the surfactant appears to cause a larger decrease in the C_{20} value than in the cmc value. Since, as mentioned above, this change in structure does not affect the value of A_{min} significantly, the increase in the value of cmc/C_{20} causes an increase in the effectiveness of the surfactant in reducing the surface tension.

Also, the very much larger decrease in C_{20} value compared to the cmc value for C_{10}BMG and C_{12}BMG, when compared to the corresponding N-alkyl,N,N-trimethylglycines, shows that steric factors have a greater effect on the process of micellization than on adsorption at the aqueous solution/air interface.

The ΔS°_{mic} values in Table 8 are all positive, indicating increased randomness in the system upon transformation of the zwitterionic surfactant molecules into micelles. The ΔH°_{mic} values, too, are positive, due to the endothermic desolvation associated with micellization. Smaller ΔH°_{mic} and ΔS°_{mic} values at 25-40° C than at 10-25°C are due to the smaller hydration of the monomers at the higher temperatures. In the temperature range studied no minimum in the variation of ΔH°_{mic} with temperature was observed, in agreement with the work of Swarbrick et al (86).

From the variation of the ΔH°_{mic} values for the two alkyl betaines it is seen that, for the shorter alkyl chain compounds, the enthalpy change is a significant factor in the process of micellization while, for the longer chain compounds, the free energy change is due almost entirely to the entropy change.

From the standard free energy of micellization of the N-alkylglycines, the ΔG°_{mic} per methylene group at 25°C is -2.80 kJ mol

$^{-1}$. This is in close agreement with the corresponding value of -2.85 kJ mol^{-1} at 20°C obtained by Molyneux et al (85).

From the data, in Table 9, $\Delta G°_{ad}$ per methylene group at 25°C is -3.05 kJ mol^{-1} for the glycines and -3.15 kJ mol^{-1} for the taurines. These are in agreement with values of -3.15 kJ mol^{-1} for long-chain alcohols and 1,3-diols (20).

The $\Delta H°_{ad}$ values are less positive than the $\Delta H°_{mic}$ values for the same alkyl glycines. This shows less dehydration of the surfactant required for adsorption at the aqueous solution/air interface than for the process of micellization. This is consistant with the observations on polyoxyethylenated nonionics, above, and alkylpyridinium halides, below.

The $\Delta S°_{ad}$ values are all slightly more positive than the $\Delta S°_{mic}$ values for the same compound, reflecting the greater restriction of space in the micelle than at the aqueous solution/air interface.

The $\Delta S°_{ad}$ values and $\Delta H°_{ad}$ values are both more positive for the betaines than for the corresponding sulfobetaines. This shows that the sulfobetaines require less dehydration for adsorption at the aqueous solution/air interface.

Using $\Delta G^{\circ}(-CH_3) = \Delta G^{\circ}(-CH_2-) - 5.56$ kJ mol^{-1}, on the basis of solubility data (106) for liquid N-alkanes in water at 25°C, standard free energies of adsorption and micellization, $\Delta G^{\circ}_{ad}(-W)$ and $\Delta G^{\circ}_{mic}(-W)$ respectively, for the hydrophilic head groups, $-\overset{+}{N}(CH_3)(CH_2C_6H_5)CH_2CH_2SO_3^-$ and $-\overset{+}{N}(CH_2C_6H_5)(CH_3)CH_2COO^-$, were calculated. These values are listed in Table 10 together with standard free energy values for the hydrophilic head groups for the N-alkyl,N,N-dimethylglycines (84), 2(trimethylammonium)alkanoates (82), and some polyoxyethylenated nonionics and 1,3-diols (107),(108).

From the solubility data of N-decane in water, the enthalpy for the process n-decane (H_2O)--> n-decane (pure) at 25°C has been estimated by Goddard et al (31) to be -5.85 kJ mol^{-1}. Subtracting this value from the calculated ΔH° at 25°C values for C_{10}BMG and C_{10}BMT, in Tables 8 and 9, the $\Delta H^{\circ}(-W)$ values for micellization and for adsorption at the aqueous solution/air interface at 25°C are estimated. These values are shown in Table 11 together with the values for the hydrophilic head groups of N-alkyl,N,N-dimethylglycines and 2(trimethylammonium)alkanoates.

The $\Delta G^{\circ}(-W)$ values for the two N-benzylglycine and taurines are comparable to each other, and are less positive than for the N-alkyl,N,N-dimethylglycines and 2-(trimethylammonium)alkanoates.

TABLE 10:

Standard Thermodynamic Parameters of Adsorption and Micellization of various head groups (-W) at 25 C

-W	ΔG°_{ad} (kJ mol^{-1})	ΔG°_{mic} (kJ mol^{-1})
$-N^{+}(CH_2C_6H_5)(CH_3)CH_2COO^{-}$	10.0	20.5
$-N^{+}(CH_2C_6H_5)(CH_3)CH_2CH_2SO_3^{-}$	10.6	----
$-CH(+N(CH_3)_3)-COO^{-}$	15.2	22.7
$-N^{+}(CH_3)_2CH_2COO^{-}$	16.4	23.6
$-CH(OH)CH_2CH_2OH$	7.4	10.1
$-(OCH_2CH_2)_8OH$	5.8	16.5

TABLE 11:

Standard Thermodynamic Parameters of Adsorption and Micellization of various head groups (-W) at 25°C

-W	ΔH^0_{ad}	ΔS^0_{ad}	ΔH^0_{mic}	ΔS^0_{mic}
$-\overset{+}{N}(CH_2C_6H_5)(CH_3)CH_2COO^-$	4.6	-0.018	12.4	-0.027
$-\overset{+}{N}(CH_2C_6H_5)(CH_3)CH_2CH_2SO_3^-$	-1.9	-0.042	----	----
$-CH(+N(CH_3)_3)-COO^-$	----	----	8.4	-0.047
$-\overset{+}{N}(CH_3)_2CH_2COO^-$	----	-----	9.6	-0.047

The more positive ΔH°_{mic} values (Table 11) for the N-benzyl,N-methylglycine head groups than for the N,N-dimethylglycine and 2-(trimethylammonium)alkanoates sugest the greater requirement of heat to desolvate the former. This is reflected in the less negative ΔS°_{mic} value for the N-benzyl,N-methylglycine head group.

In the case of dimethyl ammonium glycines, the replacement of a methyl group by a benzylic group as in N-methyl,N-benzylglycines, will assist in the further removal of the hydrophilic head group out of the water and into the micelle core. This will account for the greater heat of desolvation of the hydrophilic head groups of the N-benzyl,N-methylglycines. The effect is similar to that of lengthening the hydrocarbon chains and it facilitates micelle formation and lowers the cmc, as observed. The relevent contribution to the negative free energy of micellization is about 3kJ mol^{-1}.

From the ΔH°_{ad} (-W) term for the two types of hydrophilic groups, it is evident that there is an exothermic effect in the transfer of $-N^{+}(CH_2C_6H_5)(CH_3)CH_2CH_2SO_3^{-}$ from aqueous medium to the interface. This exothermic enthalpy term, together with a larger negative entropy term for the N-alkyltaurines head group, is possibly due to the partial neutralization of the oppositely charged groups in the hydrophilic heads due to their arrangement in checkerboard fashion at the aqueous

solution/air interface, as suggested by Beckett and Woodward (83). In the case of the N-alkylglycines, endothermic dehydration of the hydrophilic head may outweigh the neutralization effect, thus making ΔH°_{ad} (-W) positive.

3.3 Dodecylpyridinium halides

3.3.1 Results

Plots of γ versus log $C_{N^+X^-}$ in quartz-condensed, distilled water and in electrolyte solution of 0.1 M or 0.5 M total ionic strength at 10,25 and 40°C for $C_{12}NBr$ and $C_{12}NCl$ are shown in Figures X and XI, respectively. Plots of surface pressure, π versus (log $C_{N^+X^-}$ + log $f_\pm$) for solution in pure water or versus (log $_{N^+}$ + log f_+) for 0.1 M and 0.5 M total ionic strength solution are shown in figures XII and XIII, for $C_{12}NBr$ and $C_{12}NCl$, respectively. The activity coefficients were evaluated from the extended Debye - Huckel equation (21). In the absence of added salt, $f_\pm$ was assumed to equal (log f_+ + log f_-)/2. Tables A1 to A18 (Appendix) list the calculated values for the activity coefficients, the activities for the ions, together with the respective surface pressure, π ,values for the two compounds.

Maximum surface excess concentrations for compounds in pure water were calculated from the maximum slopes of the π vs (log $C_{N^+X^-}$ + log $f_\pm$) curves for the compounds (equation 22) and π vs (log C_{N^+} + log f_+) curves (equation 23) in the case of solutions containing swamping amounts of electrolytes. The area per molecule, A_{min}, was calculated by use of equation 24. These values together with the cmc, π_{cmc}, the effectiveness of the surface tension reduction, pC_{20}, the

efficiency of the surface tension reduction, and cmc/C_{20} ratios are listed in Table 12.

Conductance , W, square root of concentration, $C^{1/2}$, together with the calculated values for conductivity, k, and equivalent conductivity Λ ,are listed in Tables A19 to A24. Plots of $C^{1/2}$ versus equivalent conductivity, Λ ,in quartz distilled water for $C_{12}NBr$ and $C_{12}NCl$, are shown in figure XIV and XV, respectively. The critical micelle concentrations obtained at the intersection of the two, linear portions of the plot just above and below the discontinuity are shown in Table 12.

TABLE 12:

Surface Properties of N-dodecylpyridinium bromide and chloride

Compd	T(°C)	Cmc, (mol dm^{-3} X 10^3)	$\Gamma_{N^+X^-,max}$ (mol cm^{-2} X 10^{10})	A_{min} (nm^2 X 100)	pC_{20}	Cmc/C_{20}	π cmc (mNm^{-1})
In quartz-condensed, distilled water							
$C_{12}NBr$	10	11.7	3.5	48	2.365	2.7	34.6
		11.7(cond)					
	25	11.5	3.3	50	2.33	2.5	32.9
		11.3(cond)					
	40	11.0	3.2	52	2.29	2.1	30.8
		11.4(cond)					
$C_{12}NCl$	10	11.2	2.7	61	2.12	2.3	29.6
		17.7(cond)					
	25	16.2	2.7	62	2.095	2.0	28.3
		17.8(cond)					
	40	15.5	2.6	63	2.065	1.8	26.9
		18.5(cond)					

TABLE 12: (cont'd)

Surface Properties of N-dodecylpyridinium bromide and chloride

Compd	T(°C)	Cmc, (mol dm^{-3} X 10^3)	$\Gamma_{N^+X^-,max}$ (mol cm^{-2} X 10^{10})	A min (nm^2 X 100)	pC_{20}	Cmc/C_{20}	π cmc (mNm^{-1})
In NaX solution of 0.1 M total ionic strength							
$C_{12}NBr$	10	2.75	3.7	45	3.48	8.3	36.9
	25	2.75	3.5	48	3.40	6.9	35.2
	40	2.85	3.3	51	3.30	5.7	33.5
$C_{12}NCl$	10	5.5	3.1	54	3.03	5.9	31.8
	25	4.8	3.0	55	2.98	4.6	30.4
	40	4.5	2.9	57	2.92	3.8	29.1
In NaX solution of 0.5 M total ionic strength							
$C_{12}NBr$	10	1.07	3.8	44	4.02	11.3	38.7
	25	1.08	3.5	47	3.91	8.9	37.2
	40	1.16	3.3	50	3.80	7.3	35.6
$C_{12}NCl$	10	1.9	3.2	52	3.55	6.8	34.1
	25	1.78	3.1	54	3.49	5.5	32.8
	40	1.78	3.0	55	3.43	4.8	31.6

TABLE 13: Standard thermodynamic parameters of micellization for N-dodecylpyridinium bromide and chloride

Compd	T(°C)	$\Delta G°_{mic}$ (kJ mol^{-1})	$\Delta H°_{mic}$ (kJ mol^{-1})	$\Delta S°_{mic}$ (kJ $mol^{-1}K^{-1}$)
$C_{12}NBr$	10	-19.1		
			+0.2	+0.068
$C_{12}NBr$	25	-20.1		
			-6.0	+0.047
$C_{12}NBr$	40	-20.8		
$C_{12}NCl$	10	-17.7		
			+4.8	+0.079
$C_{12}NCl$	25	-18.9		
			-0.8	+0.061
$C_{12}NCl$	40	-19.8		

TABLE 14: Standard thermodynamic parameters of adsorption for N-dodecylpyridinium halides

Compd	T(°C)	ΔG°_{ad} (kJ mol^{-1})	ΔH°_{ad} (kJ mol^{-1})	ΔS°_{ad} (kJ mol^{-1}K^{-1})
In quartz-condensed, distilled water				
$C_{12}NBr$	10	-31.4		
			-10.6	+0.073
	25	-32.5		
			-8.7	+0.080
	40	-33.7		
$C_{12}NCl$	10	-30.6		
			-11.7	+0.067
	25	-31.6		
			-11.7	+0.067
	40	-32.6		
In NaX of 0.1 M total ionic strength				
$C_{12}NBr$	10	-30.5		
			-7.9	+0.080
	25	-31.7		
			-7.9	+0.080
	40	-32.9		
$C_{12}NCl$	10	-29.1		
			-8.3	+0.073
	25	-30.2		

			-8.3	+0.073
	40	-31.3		
In NaX of 0.5 M total ionic strength				
$C_{12}NBr$	10	-30.0		
			-3.6	+0.093
	25	-31.4		
			-9.5	+0.073
	40	-32.5		
$C_{12}NCl$	10	-28.9		
			-4.8	+0.085
	25	-30.2		
			-12.8	+0.056
	40	-31.1		

Standard free energies of micellization were calculated by the use of equation (54). The activity coefficients were evaluated from Debye-Huckel equation (21), where α is taken as 0.6 for the surfactant ion and 0.3 for the counter ions. The calculated f_+ and f_- values, together with log cmc values in water, 0.1 M NaCl and 0.5 M NaCl are tabulated in Tables A25 and A26 for $C_{12}NBr$ and $C_{12}NCl$, respectively. The electrical coefficient of micellization, m/n, was obtained from the slope of the plot of (log cmc + log f_+) versus (log C_{X^-} + log f_-) shown in Figure XVI. These values are listed in Table A27. The linearity of the plots is good evidence for the assumption that ΔG°_{mic} is constant with change in ionic strength of the solution. Values of ΔG°_{mic}, together with ΔH°_{mic} and ΔS°_{mic} values calculated by equations (47) and (48), are listed in Table 13.

The standard free energies of adsorption at the aqueous solution/air interface were calculated by equation (46). The π_{cmc} values, together with log cmc, activity, and activity coefficients for the ions at cmc in water, 0.1 M NaCl, and 0.5 M NaCl, required for the calculation of ΔG°_{ad}, are listed in Table 14. ΔH°_{ad} and ΔS°_{ad} values, calculated by use of equations (47) and (48), are listed in the same table.

3.3.2 Discussion

The minimum areas per molecule for $C_{12}NBr$ and $C_{12}NCl$ show a smaller area per molecule for $C_{12}NBr$ than for $C_{12}NCl$, under the same conditions of temperature and ionic strength. At higher ionic strength of the solution there is a decrease in the A_{min} due to the compression of the electrical double layer at the aqueous solution/air interface and the consequent reduced repulsion between the similarly charged hydrophilic heads of the surfactant ions. The difference in A_{min} for $C_{12}NBr$ and $C_{12}NCl$ becomes smaller at higher ionic strength than in aqueous medium. With increase in temperature from 10 to 40°C there is a steady increase in the minimum area per molecule at the aqueous solution/air interface, reflecting the increased thermal motion of the molecules. The increase for dodecylpyridinium bromide is about twice that shown for the corresponding chloride under the same conditions.

At all ionic strengths dodecylpyridinium bromide has a lower critical micelle concentration than the chloride. At higher ionic strength the critical micelle concentration decreases as expected but this decrease in cmc is greater for the $C_{12}NCl$ than for the $C_{12}NBr$ at both 0.1 M and 0.5 M salt concentrations. The effect of temperature change in the range investigated for these two compounds appears to be almost insignificant, and no general trend is apparent. The critical micelle

concentrations at 25°C for $C_{12}NBr$ and $C_{12}NCl$ are less than for the corresponding trimethylammonium bromide (1.6×10^{-2} mol dm^{-3}) and chloride (2.0×10^{-3} mol dm^{-3}) (110). This appears to be due to the bulkiness of the trimethylammonium hydrophilic head group, which may create a steric barrier for micellization, while the planar pyridinium group can pack more closely. The ability of the alkyl pyridinium group to pack closely compared to the trimethylammonium is shown by the larger A_{min} for dodecyltrimethylammonium bromide ($61 \times 10^{-2} nm^2$), (92), compared to $C_{12}NBr$ in water at 25°C.

The efficiency of surface tension reduction, given by the pC_{20} value, is larger for the $C_{12}NBr$ than for $C_{12}NCl$. The pC_{20} values for both compounds decrease with increasing temperature, indicating decreased efficiency in surface tension reduction.

The effectiveness in surface tension reduction, given by π_{cmc}, is also larger for the $C_{12}NBr$ than for $C_{12}NCl$. With increase of temperature from 10 to 40°C, there is a steady decrease of π_{cmc} for both compounds and this appears to be due to both the decrease in Γ_{max} and in the cmc/c_{20} ratio with temperature. Due to the increase in cmc/C_{20} values, π_{cmc} values, for both compounds increase with increase in the ionic strength of the solution.

The π_{cmc} values for $C_{12}NCl$ in 0.1 M NaCl at 25°C (30.4 mNm^{-1}) is smaller than for the corresponding trimethylammonium chloride (42 mNm^{-1}) (109). The bulky hydrophilic headgroup in trimethylammonium chloride inhibits micellization, as evidenced by its greater cmc/C_{20} ratio (9.5), compared to that of $C_{12}NCl$, and thus increases the value of π_{cmc}.

It is apparent from all the surface properties in Table 12 that N-dodecylpyridinium bromide, in all properties investigated, is some-what more surface-active than the corresponding chloride. At all ionic strengths, it has a lower cmc, larger pC_{20}, and larger π_{cmc} value than the latter compound under the same conditions of temperature and ionic strength. It is, therefore, more prone to form micelles and is more efficient and more effective at reducing the surface tension of the solvent than the chloride.

From the data in Table 12, it is seen that, in the temperature range of 10 to 25°C, both ΔH° and ΔS° values are positive for both the compounds, indicating the significance of the entropy contribution to the negative free energy of micellization at these temperatures. The positive heats of micellization have also been inferred from calorimetric measurement of heat of dilution and solution for anionic surfactants, (31). At higher temperatures, the ΔH°_{mic} values for both compounds become negative, thus contributing to the process feasibility.

The positive ΔH°_{mic} and ΔS°_{mic} values at low temperature are due presumably to desolvation of structured water about the hydrocarbon chain and the hydrophilic head groups. Due to the dehydration of the molecules at the lower temperatures, as the temperature is raised the ΔH°_{mic} values become more negative and the ΔS°_{mic} values less positive. Therefore, these data substantiate the observations made by other investigators (31) that at low temperatures the process of micellization is predominently due to the entropy effect, whereas the contribution of enthalpy to the process of micellization becomes significantly more important as the temperature is increased.

The larger entropy of micellization for $C_{12}NCl$ and its more positive enthalpy of micellization in both temperature ranges investigated indicate that, in the micellization process, more bonds to water molecules are being broken for the chloride than for the bromide. This is expected since, in the monomeric form of the surfactant, chloride ion is more highly hydrated than bromide ion. The higher equivalent conductivity of $C_{12}NBr$, compared to $C_{12}NCl$, at concentrations below their cmc, observed in the measurement of their cmcs by conductance, shows the low mobility of chloride ion compared to bromide ion, presumably due to its larger hydration sphere. The higher degree of hydration of chloride than of bromide ion has also been observed by others (111).

The change in ΔH°_{mic} from a small positive value in the 10-25°C range to a small negative value in the 25 - 40C° range for both $C_{12}NBr$ and $C_{12}NCl$ appears to indicate that the degree of dehydration of the hydrophobic group and of the halide ion necessary for incorporation into micelle is accomplished readily at room temperature. This is also consistant with the apparent trend of the ΔG°_{mic} values of the two compounds to approach each other as the temperature is increased.

The significance of the dehydration of the counterions upon micellization is again reflected in the m/n values (Table A27) for these two compounds. If the counterions associated with the micelle were hydrated, chloride ion would be held less tightly to the micelle than the smaller hydrated bromide ion, and its m/n value would be expected to be smaller. On the other hand, the dehydrated chloride ion is smaller than the dehydrated bromide ion and would be expected to be more completely associated with the micelle, thus giving a large m/n value for the $C_{12}NCl$ compared to the $C_{12}NBr$.

As in the case of the ΔG°_{mic} values, the ΔG°_{ad} values should be constant with change in ionic strength. The values calculated in the absence of added electrolyte are almost 1 kJ mol^{-1} more negative than those values and this is believed to be due to the assumption that, in pure water, the surface concentration of counterion equals that of the

adsorbed surfactant ions. However, recent studies (112) show that the counterion/adsorbed surfactant ion ratio in the absence of added electrolyte decreases with the increase in the surface area of adsorbed surfactant ion. Therefore, the essentially constant values at 0.1 M and 0.5 M ionic strength are probably more reliable than those calculated in pure water solution.

The ΔG°_{ad} values are slightly more negative for the bromide than for the chloride, showing the greater tendency of $C_{12}NBr$ to adsorb at the interface than $C_{12}NCl$.

ΔH°_{ad} values for both $C_{12}NBr$ and $C_{12}NCl$ are all negative and show little or no variation with increase in temperature from 10° to 25°C range to the 25° to 40°C range. The variation of ΔH°_{ad} at 0.5 M ionic strength is not considered significent. The consistantly negative ΔH°_{ad} values appear to indicate that adsorption at the planar aqueous solution/air interface is occuring with less dehydration of the hydrophilic head group of the surfactant ion and of the counter-ion than occurs in micellization.

The less negative ΔH°_{ad} and more positive ΔS°_{ad} values for $C_{12}NBr$ compared to $C_{12}NCl$ indicate the closeness of approach of the bromide ion, compared to the chloride ion, to the charged head group of the surfactant cation at the aqueous solution/air interface. A bromide with

its smaller sphere of hydration is desolvated on approach to the hydrophilic head groups. Whereas the chloride ion, with the larger sphere of hydration appears to remain further away from the ionic head groups at the aqueous solution/air interface.

The larger the distance of closest approach of the chloride ion, the smaller will be the screening action on the charged interface and this in turn is reflected in the larger area per molecule for $C_{12}NCl$ compared to $C_{12}NBr$. Thus, the more positive ΔH°_{mic} and ΔS°_{mic} values for $C_{12}NCl$ compared to $C_{12}NBr$, and the less negative ΔH°_{ad} and more positive ΔS°_{ad} for $C_{12}NBr$ compared to $C_{12}NCl$, indicate the greater requirement of dehydration of the counter ions for the process of micellization than for adsorption at the aqueous/air interface.

3.4 Anionic Surfactants

3.4.1 Results

Plots of the surface tension, (γ) ,of aqueous solutions of $C_{10}S, C_{12}S, C_{10}EOS, C_{12}EOS, C_{12}EOSO, C_{12}EO_2SO$ vs log of their bulk concentration in mol dm^{-3} (log C) in quartz-condensed distilled water and in electrolyte solution of 0.1 M or 0.5 M total ionic strength at 10,25 and 40°C are shown in Figures XVII to XXII.

Plots of surface pressure (π), versus (log $C_{R^-X^+}$ + log $f_{\pm}$) for solution in pure water or versus (log C_{R^-} + log f_-) for 0.1 M or 0.5 M total ionic strength solution are shown in Figures XXIII to XXVIII. The activity coefficients were evaluated from the extended Debye - Huckel equation (21). For surfactant solution in pure water $f_{\pm}$ was assumed to equal (log f_+ + log f_-)/2. Activity coefficients and the activity for the ions, together with the corresponding surface pressure values, are listed in Tables A28 to A81.

Maximum surface excess concentrations for compounds in water were calculated from equation (22), making use of the maximum slopes of the π vs (log $C_{R^-X^+}$ + log $f_{\pm}$) curve for the compounds. The corresponding equation (23) and the slopes of the curves π vs (log C_{R^-} + log f_-) were used for the calculation of surface excess concentrations for surfactant solutions of 0.1 M and 0.5 M ionic strength. Area per molecule, A_{min} was obtained from equation (24). Tables 15 to 20 list cmc values, Γ_{max} and A_{min}, together with π_{cmc}, the effectiveness of surface tension reduction, pC_{20}, the efficiency of surface tension reduction, and cmc/C_{20} ratios.

The standard free energies of micellization were calculated by the use of equation (54). The f_+,f_- values together with log cmc values in water, 0.1 M NaCl and 0.5 M NaCl are tabulated in Tables A82 to A86 for the compounds. From the slope of (log cmc + log f_-) versus (log

C_{X^+} + log f_+) (Figures XXVIX to XXXIII), the m/n values were determined. These values are listed in Table A27. The linearity of the plots is good evidence for the assumption that ΔG°_{mic} is constant with change in the ionic strength of the solution.

Values of ΔG°_{mic}, together with ΔH°_{mic}, and ΔS°_{mic}, calculated by equation (47) and (48), are listed in Table 21.

The standard free energies of adsorption at the aqueous solution/air interface were calculated by equation (46). For the compounds $C_{10}S$, $C_{10}EOS$, $C_{12}EOSO$ and $C_{12}EO_2SO$, the maximum surface pressure, π_{cmc}, values were used in equation (46) together with the activities at the critical micelle concentration for the calculation of ΔG°_{ad} values. For the compounds $C_{12}S$ and $C_{12}EOS$, where the cmc could not be reached due to their poor solubility, the activity and A_{min} values at π = 20 were used in equation (46).

TABLE 15:
Surface Properties of $C_{10}S$

Compd	Medium	Temp (°C)	Cmc (mol dm^{-3} X 10^3)	Γ_{max} (mol cm^{-3} X 10^{10})	A_{min} (nm^2 X 100)	pC_{20}	π_{cmc} (mNm^{-1})	Cmc/C_{20}
$C_{10}S$	H_2O	10	47.90	3.37	49.2	1.70	33.0	2.4
		25	42.70	3.22	51.8	1.69	31.0	2.1
		40	39.80	3.05	54.4	1.66	29.2	1.8
	0.1 M	10	25.70	4.06	40.9	2.29	34.4	5.01
		25	21.10	3.85	43.1	2.29	32.6	4.11
		40	18.20	3.67	45.2	2.27	31.1	3.39
	0.5 M	10	7.94	4.46	37.2	2.89	38.1	6.16
		25	7.33	4.24	40.6	2.87	37.1	5.43
		40	6.53	4.04	41.1	2.84	35.7	4.51

TABLE 16:
Surface Properties of $C_{12}S$

Compd	Medium	Temp (°C)	Cmc (mol dm^{-3} X 10^3)	Γ_{max} (mol cm^{-3} X 10^{10})	A_{min} (nm^2 X 100)	pC_{20}	π_{cmc} (mNm^{-1})	Cmc/C_{20}
$C_{12}S$	H_2O	10	----	3.02	54.9	2.38	----	----
		25	12.40	2.93	56.7	2.36	33.0	2.84
		40	11.40	2.78	59.7	2.33	31.0	2.40
	0.1 M	10	----	3.92	42.4	3.41	----	----
		25	2.47	3.76	44.2	3.38	36.4	5.90
		40	2.42	3.55	46.8	3.30	34.8	4.80
	0.5 M	10	----	3.98	41.7	4.11	----	----
		25	----	3.85	41.7	4.06	----	----
		40	0.79	3.60	43.8	3.93	39.00	6.75

TABLE 17:
Surface Properties of $C_{10}EOS$

Compd	Medium	Temp (°C)	Cmc (mol dm^{-3} X 10^3)	Γ_{max} (mol cm^{-3} X 10^{10})	A_{min} (nm^2 X 100)	pC_{20}	π_{cmc} (mNm^{-1})	Cmc /C_{20}
$C_{10}EOS$	H_2O	10	20.50	3.37	49.2	2.04	32.9	2.24
		25	15.90	3.22	51.5	2.10	30.8	2.00
		40	15.40	3.12	53.3	2.06	28.8	1.70
	0.1 M	10	6.49	4.21	39.4	2.93	36.5	5.52
		25	5.46	3.85	43.1	2.92	34.7	4.54
		40	5.01	3.67	45.2	2.87	33.0	3.70
	0.5 M	10	----	4.43	37.5	3.60	----	----
		25	2.04	4.30	38.6	3.54	39.0	7.10
		40	2.00	4.00	41.5	3.45	37.7	5.58

TABLE 18:
Surface Properties of $C_{12}EOS$

Compd	Medium	Temp (°C)	Cmc (mol dm^{-3} X 10^3)	Γ_{max} (mol cm^{-3} X 10^{10})	A_{min} (nm^2 X 100)	pC_{20}	π_{cmc} (mNm^{-1})	Cmc /C_{20}
$C_{12}EOS$	H_2O	10	----	3.07	54.0	2.76	----	----
		25	----	2.92	56.9	2.75	----	----
		40	----	2.74	60.5	2.67	----	----
	0.1 M	10	----	3.93	42.2	4.14	----	----
		25	----	3.73	44.3	4.07	----	----
		40	----	3.57	46.5	3.98	----	----
	0.5 M	10	----	4.22	39.4	4.76	----	----
		25	----	3.97	41.8	4.68	----	----
		40	----	3.81	43.6	4.60	----	----

TABLE 19:
Surface Properties of $C_{12}SO$ and $C_{12}EOSO$

Compd	Medium	Temp (°C)	Cmc (mol dm^{-3} X 10^3)	Γ max (mol cm^{-3} X 10^{10})	A min (nm^2 X 100)	pC_{20}	π cmc (mNm^{-1})	Cmc / C_{20}
$C_{12}SO$	H_2O	25	7.94	3.16	52.5	2.51	32.5	2.6
	0.1 M	22	1.29	4.03	41.2	3.67	38.0	6.03
$C_{12}EOSO$	H_2O	10	4.73	3.07	54.1	2.82	35.6	3.12
		25	3.91	2.91	56.8	2.83	32.8	2.60
		40	4.14	2.80	59.2	2.72	30.4	2.17
	0.1 M	10	0.48	4.03	41.2	4.29	40.6	7.80
		25	0.43	3.81	43.6	4.23	38.6	7.30
		40	0.49	3.60	46.1	4.09	36.4	6.02
	0.5 M	10	0.14	4.61	36.0	4.93	44.4	11.60
		25	0.13	4.41	37.6	4.80	42.4	8.26
		40	0.15	4.14	40.1	4.67	40.8	7.10

TABLE 20:
Surface Properties of $C_{12}EO_2SO$

Compd	Medium	Temp (°C)	Cmc (mol dm^{-3} X 10^3)	T_{max} (mol cm^{-3} X 10^{10})	A_{min} (nm^2 X 100)	pC_{20}	π_{cmc} (mNm^{-1})	Cmc/C_{20}
$C_{12}EO_2SO$	H_2O	10	3.09	2.76	60.0	2.96	32.6	2.80
		25	2.88	2.62	63.2	2.92	30.6	2.49
		40	2.78	2.50	66.4	2.86	28.6	2.01
	0.1 M	10	0.32	3.65	45.5	4.40	38.0	7.9
		25	0.29	3.46	47.9	4.36	36.5	6.7
		40	0.28	3.30	50.3	4.23	34.8	4.8
	0.5 M	10	0.11	3.95	42.0	5.04	41.5	12.1
		25	0.10	3.78	43.9	4.98	40.2	10.0
		40	0.10	3.57	46.5	4.89	38.6	7.9

TABLE 21: Standard Thermodynamic parameters of micellization for Anionic Surfactants.

Compd	T(°C)	$\Delta G°_{mic}$ (kJ mol^{-1})	$\Delta H°_{mic}$ (kJ mol^{-1})	$\Delta S°_{mic}$ (kJ mol^{-1}K^{-1})
$C_{10}S$	10	-14.77		
			2.56	0.060
	25	-15.69		
			2.40	0.061
	40	-16.60		
$C_{12}S$	10	--.--		
			--.--	--.--
	25	-21.00		
			2.06	0.74
	40	-22.15		
$C_{10}EOS$	10	-17.37		
			1.10	0.065
	25	-18.35		
			0.925	0.064
	40	-19.36		
$C_{12}SO$	25	-21.97	-0.05	0.073
$C_{12}EOSO$	10	-24.06		
			-1.4	0.080
	25	-25.26		
			-7.2	0.060
	40	-26.17		

$C_{12}EO_2SO$	10	-24.26		
			2.64	0.095
	25	-25.74		
			0.48	0.083
	40	-27.06		

TABLE 22: Standard Thermodynamic parameters of adsorption for Anionic Surfactants

Compd	T(°C)	ΔG°_{ad} (kJ mol^{-1})	ΔH°_{ad} (kJ mol^{-1})	ΔS°_{ad} (kJ mol^{-1}K^{-1})
$C_{10}S$	10	-23.64		
			2.4	0.092
	25	-25.02		
			-1.8	0.078
	40	-26.16		
$C_{12}S$	10	30.20		
			-3.7	0.093
	25	-31.61		
			-5.7	0.087
	40	-32.70		
$C_{10}EOS$	10	-27.11		
			-0.7	0.093
	25	-28.50		
			-2.7	0.086
	40	-29.81		
$C_{12}EOS$	10	-34.48		
			-6.9	0.096
	25	-35.48		
				0.086
			-9.7	
	40	-36.78		

$C_{12}SO$	25	-32.25	--.--	--.--
$C_{12}EOSO$	10	-34.35		
			-5.1	0.103
	25	-35.90		
			-12.5	0.078
	40	-37.00		
$C_{12}EO_2SO$	10	-35.69		
			-4.9	0.109
	25	-37.32		
			-5.8	0.106
	40	-38.91		

The ΔG°_{ad} values, together with the ΔH°_{ad} and ΔS°_{ad} values calculated from equation (47) and (48), are listed in Table 22.

3.4.2 Discussion

At all ionic strengths, the cmc values for the sulfates are slightly lower than for the corresponding sulfonates. The cmc values decrease with the inclusion of oxyethylene groups into the alkyl sulfate or alkanesulfonate molecule, confirming earlier investigations (97,98) on ethenoxylated sulfates. This is in contrast to the situation in nonionic ethenoxylated alcohols, where increase in oxyethylene content of the molecule increases the cmc, attributed to greater steric inhibition for micellization by the oxyethylenated products.

The A_{min} values for the alkyl sulfates and the ethenoxylated sulfates are comparable to those of the corresponding sulfonates under the same conditions of ionic strength and temperature. The introduction of one oxyethylene group into the alkyl sulfates or alkane sulfonates have little effect on the area per molecule as seen by the comparable A_{min} values for $C_{10}S$ and $C_{10}EOS$, $C_{12}S$ and $C_{12}EOS$, and $C_{12}SO$, and $C_{12}EOSO$ respectively. The introduction of a second oxyethylene group, however, increases the A_{min}, as seen for $C_{12}EO_2SO$.

The investigation of the series $C_{12}H_{25}\ (OC_2H_4)_nOSO_3^-Na^+$, where n = 0 to 4, by Lange et al (99) , showed that the area increase with increasing n was smaller for n < 2 than for n > 2. In addition, this

increase in area per molecule for the above series was found to be smaller at n = 0 to n = 2, and larger at n > 2, than for the corresponding nonionic compounds.

The efficiency of surface tension reduction, as measured by the pC_{20} value, is greater for the sulfates than for the corresponding sulfonates. Efficiency in surface tension reduction increases with the introduction of an oxyethylene unit for both sulfates and sulfonates. For the ethenoxylated sulfates, the increase in efficiency is greater for the introduction of the first oxyethylene unit than for the second. This agrees with the results of Lange et al (99) on polyethenoxylated sulfates. Their work also shows the relative increase in pC_{20} value to be smaller going from n = 2 to 4 than from n = 1 to 2.

The effectiveness of surface tension reduction, given by π_{cmc}, is almost same in pure water for the mono oxyethylenated compounds and their corresponding non ethenoxylated compounds. This appears to be due to the similar surface areas and cmc/C_{20} values for these compounds. On the other hand the π_{cmc} value is very much smaller for the $C_{12}EO_2SO$ due to its larger area per molecule and smaller cmc/C_{20} at the aqueous solution/air interface.

In contrast to what is observed in pure water, the monoxyethylenated sulfate, $C_{12}EOSO$, shows a larger π_{cmc} value in 0.1 M NaCl than its alkyl sulfate, $C_{12}SO$. This is also true for the

alkanesulfonate $C_{10}S$, and its monoxyethylenated derivatives, $C_{10}EOS$. This greater effectiveness in surface tension reduction appears to be due to the larger cmc/C_{20} ratios, for ethenoxylated compounds in solutions of high ionic strengths. As molecules pack more closely together bulky oxyethylene groups show steric effect in micellization more than in adsorption.

From the above surface and micellar properties it appears that the inclusion of oxyethylene units adjacent to the hydrophilic head groups results in an increase in the hydrophobicity both for the process of micellization and for adsorption at aqueous solution/air interface of these types of ionic molecules. These trends in surface properties are very well reflected in the thermodynamic properties of micellization and adsorption for the compounds.

The standard free energies of micellization for the ethenoxylated sulfates and sulfonates are more negative than those for the corresponding nonethenoxylated compounds. This is in contrast to the effect in nonionic polyethenoxylated alcohols, where ΔG°_{mic} was found to become less negative with the increase in oxyethylene content of the molecule. On the other hand, for the process of adsorption at the aqueous solution/air interface, we see a significant increase in the negative value of the standard free energy of adsorption with increase in oxyethylene content, whereas for the nonionic polyethenoxylated

alcohols the increase in the negative standard free energy of adsorption was found to be relatively small (108).

From the information obtained in the present study, the following mechanism is postulated to explain the surface and micellar properties of these ethenoxylated anionic surfactants.

The increase in the solubility in water upon inclusion of oxyethylene units into polyoxyethylenated sulfates and sulfonates and into nonionic polyoxyethylenated alcohols suggests that the oxyethylene units of these molecules are solvated by water molecules. In the case of the ionic surfactants, the counter ions will also be solvated by water molecules. On micelle formation or adsorption at the interface, where less hydration is expected, it is likely for favourably-positioned ether oxygens of the oxyethylene units to coordinate with the positive counterions.

On complexation, the oxyethylene units and the counter ions are dehydrated and the extent of dehydration is determined by the closeness of the approach of the oxygens of the oxyethylene units to the primary coordination site of the counterions. As the oxyethylene units get further away from the hydrophilic head group the oxyethylene chains have to bend around (or crown) in order for their oxygens to approach the counterions for coordination but this will lead to some loss of configurational entropy for the molecules.

From molecular models it is seen that, for the monoethenoxylated sulfonates, the ether oxygens of the oxyethylene units can approach the counterions with little change in configuration of the alkyl chain or the oxyethylene units, i.e., there is little difference in the area/molecule of the ethenoxylated sulfonate with this configuration and the unethenoxylated sulfonate. On the other hand, these models show a larger area per molecule for the monoethenoxylated sulfate $C_{12}EO_2SO$, and a still larger area for the diethenoxylated compound, $C_{12}EO_2SO$, with their oxyethylene units in close approach to the counterion, compared to the unethenoxylated sulfate. This is consistant with the experimental results (Table 23).

TABLE 23

Compound	A* (nm^2 x 100)	A_{min} (nm^2 x 100)
$C_{10}S$	31.2	51.8
$C_{12}S$	32.0	56.7
$C_{10}EOS$	34.5	51.5
$C_{12}EOS$	35.0	56.9
$C_{12}SO$	32.6	52.5
$C_{12}EOSO$	40.4	56.8
$C_{12}EO_2SO$	50.2	63.2

* Area per molecule determined from molecular models, with the oxyethylene units, for oxyethylenated compounds, approaching the polar head group.

The cordination of counterions to the oxyethylene groups upon micellization will release the hydrogen bonded water molecules from the ether oxygens and the counterions to the bulk phase, making the

process energetically more favourable. This is apparent from the ΔH°_{mic} values in Tables 97 to 101, where for both sulfates and sulfonates the ΔH°_{mic} values are less positive for the ethenoxylated materials, when compared to the nonethenoxylated ones. These trends in enthalpy are also observed for the process of adsorption (Table 22). Here, exothermic bond formation between counterions and ether oxygens may facilitate the desolvation of the hydrated ether oxygens of the ethenoxylated sulfates and sulfonates.

For the series $C_{12}(EO)_nSO$, where n = 0,1 and 2, the ΔG°_{mic} value increases by 3.3 kJ mol^{-1} from n = 0 to 1 and by only 3.7 kJ mol^{-1} from n = 0 to 2. Therefore, as the oxyethylene units get further away from the hydrophilic head group it appears that their contribution to the free energy of micellization becomes less. The smaller effect of the second oxyethylene group is due mainly to the greater heat of desolvation involved in transfering a β oxyethylene unit from the bulk phase to the micelle. The observed increase in the ΔH°_{mic} value is expected, due to the smaller ability of the β oxyethylene unit to complex with the counter ion, because of its less favorable position with respect to it. This increase in enthalpy for $C_{12}EO_2SO$ is also observed for the process of adsorption at aqueous solution/air interface, as seen from the more positive ΔS°_{ad} and ΔH°_{ad} values for $C_{12}EO_2SO$, compared to $C_{12}EOSO$. The ΔH°_{ad} values are less

positive for $C_{10}EOS$ and $C_{12}EOS$ than for their corresponding non ethenoxylated compounds, but, these differences are much smaller than for the process of micellization, indicating that less bonds between polyoxyethylene chains and water molecules are broken in the process of adsorption than in micellization.

The changes in ΔS°_{mic} values on the other hand are insignificant for the ethenoxylated sulfate and sulfonates, when compared to their corresponding nonethenoxylated compounds. This may be due to two opposing effects, the loss of configurational entropy on one hand and the gain of entropy due to the release of solvated water molecules from the ether oxygens on micellization.

The dehydration of the oxyethylene chains as a result of the complexation of the counterions to the ether oxgens in the sulfates on micellization is substantiated by studies on the hydration properties of polyoxyethylenated sulfates. Tokiwa et al (98), from intrinsic viscocity and frictional ratio measurements, have shown that the hydration behavior of the mono- and diethenoxylated dodecylsulfates is similar to dodecylsulfates, the oxyethylene units showing no influence. Beyond two oxyethylene units, the hydration behavior was found to increase in a linear manner up to 10 oxyethylene content.

Further evidence for this mechanism of complexation comes from the influence of electrolyte on the cmc and C_{20} values. The influence of

electrolyte on the cmc and on C_{20} is expressed as a ratio of these values in the absence of electrolyte and in the presence of 0.1 M NaCl. As shown in Table 106, these ratios are considerably larger for the ethenoxylated sulfates and sulfonates than for their corresponding nonethenoxylated compounds. With increase in ionic strength, approach of the cations to the complexation sites will be closer. This will cause a greater degree of dehydration of the oxyethylene chains at the aqueous solution/air interface and on micellization, resulting in smaller values of cmc and C_{20} and therefore larger ratios for the above surface properties of the ethenoxylated sulfates and sulfonates, compared to the corresponding nonethenoxylated compounds.

TABLE 24

Compound	Cmc/cmc(0.1M)	C_{20}/C_{20}(0.1M)
$C_{10}S$	2.02	3.98
$C_{10}EOS$	2.92	6.59
$C_{12}S$	---	10.27
$C_{12}EOS$	---	20.89
$C_{12}SO$	5.08	10.37
$C_{12}EOSO$	9.09	25.15
$C_{12}EO_2SO$	9.76	27.57

Recent studies on binary mixtures of surfactants, (113), in which the effect of the ionic strength of the solution on, β , the parameter measuring the interaction between two different surfactants at the aqueous solution/air interface, further substantiate the complexation theory.

The values of β for three systems are shown in Table 25. The nonionic - cationic interaction is found to decrease steadily with increase in NaCl content of the solution, and this has been explained in terms of the compression of the double layer with increase in salt concentration. For the nonionic - anionic systems, there is an increase in the interaction between the surfactants with increase in the ionic strength of the solution to 0.1 M. This increase in β has been explained as being due to complexation of sodium ions with the ether oxygens of the polyoxyethylene chain of the nonionic surfactant, thereby producing an electrostatic interaction between the now positively charged nonionic and the anionic surfactant. The close presence of the negatively charged head group of the anionic is expected to be necessary for this complexing of sodium ions with the ether oxygens. Therefore, in the case of the polyethenoxylated nonionic-alkyl pyridinium system (EO8 - $C_{12}NCl$) this interaction will be absent due to the lack of a negatively charged head group in close proximity to the ether oxygens of the polyoxyethylenated nonionic alcohols. An ethenoxylated sulfate or sulfonate is similar in nature to an anionic-polyoxyethylenated nonionic mixture and therefore should show similar complexation behavior for sodium ions.

TABLE 25

Effect of Ionic Strength Solution on β

System	Medium	β
EO8-C_{12}NCl	H_2O	-2.8
EO8-C_{12}NCl	0.1 M T.I.S. (NaCl)	-2.2
EO8-C_{12}NCl	0.5 M T.I.S. (NaCl)	-1.5
EO8-C_{12}SO	H_2O	-2.7
EO8-C_{12}SO	0.1 M T.I.S. (NaCl)	-3.5
EO8-C_{12}SO	0.5 M T.I.S. (NaCl)	-3.1
EO8-C_{12}S	H_2O	-1.5
EO8-C_{12}S	0.1 M T.I.S. (NaCl)	-2.6
EO8-C_{12}S	0.5 M T.I.S. (NaCl)	-2.0

An alternative to the complexation theory presented above for explaining the micellar and surface properties of the polyoxyethylenated anionic compounds is the electrostatic self-potential theory, first suggested by Stigter (114), This theory has been useful in explaining the differences in the critical micelle concentrations of ionic surfactants in terms of the closeness of the hydrophilic head groups to the α carbon atom of the alkyl chain of the surfactant molecule.

Klevens (115) has compared the cmc data for several homologous series of ionic surfactants, and concluded that ln cmc varies linearly with the total length of the surfactant ion, including the distance between the α carbon and head group charge. However, subsequent investigation by Stigter on ionic surfactants containing five different hydrophilic terminal groups found that, Klevens' empirical relationship is a very approximate one. For the five different ionic surfactants investigated, it was found that the cmc is higher when the ionic charge on the head group is closer to the α carbon atom in the alkyl chain. A correlation between the ln cmc and the distance between the carbon was explained quantitatively by Stigter in terms of the increase in electrostatic self potential of the surfactant ion when, in micellization, the head group moves from bulk water, which has a higher dielectric constant, to the vicinity of the low dielectric constant, non polar core of the micelle. This theory is based on the assumption that the

methylene group of the surfactant ion is contained in the micelle core and that the core-water interface is located at a distance of 0.4 to 1.2 A from the center of the α carbon atom. On the basis of this theory, the closer distance of the ionic charge of a sulfonate to its α carbon atom, compared to a sulfate, requires more work to move its electric charge to a medium of lower dielectric constant. This explains the less negative ΔG°_{mic} values for the sulfonates when compared to the corresponding sulfates.

This same argument could be extended to explain the more negative standard free energies of micellization of the ethenoxylated sulfates and sulfonates, when compared to their corresponding nonethenoxylated compounds. For the monoethenoxylated sulfates and sulfonates it is possible that on micellization, the oxyethylene unit is not transferred to the micelle core, but instead, remains extended into the bulk phase. As such, the ionic charge of the $C_{12}EOS$ and $C_{12}EOSO$ will be further away from the α carbon atom or the micelle core than the corresponding charge on $C_{12}S$ and $C_{12}SO$. This, in turn, would reduce the electrostatic self potential involved in bringing the ionic head group of $C_{12}EOS$ or $C_{12}EOSO$ to the vicinity of the micelle core, and consequently make their ΔG°_{mic} values more negative than those for the corresponding nonethenoxylated materials.

Although either of these models could explain the thermodynamic parameters, it is also very likely that both these theories could complement each other. On the other hand, the data on the effect of ionic strength on cmc and C_{20} values, the interaction parameters for anionic-polyoxyethylenated nonionic binary mixtures, and the micellar hydration numbers show that there is definite interaction between the ether oxygens and the counterions of the polyoxyethylenated ionic surfactant, therefore placing more emphasis on the complexation theory presented above.

Chapter IV

Chemical Structure - Property relationships of surfactants

In this section a brief study was made of chemical structure-performance property relationships in the ionics and betaine-type of surfactants discussed in part I.

4.1 Textile wetting in aqueous solution

4.1.1 Experimental :-

The performance rating of the surfactant was determined using the Draves test (116). Standard cotton skeins of gray, unboiled, 2 ply yarn folded to form 18-in loops, each skein weighing 5.00g, were purchased from Test Fabrics, Inc., Middlesex, N.J., and used as received.

Solutions of surfactants of concentration of 1 g/L were made with deionized distilled water. Subsequent concentrations were made by diluting this stock solution. A 500 ml graduated cylinder was filled to

the mark with the surfactant solution. Temperature control was maintained at ±1°C by placing the graduated cylinder in a large thermostatted water bath. A 3-g stainless steel hook and 50-g anchor were attached to one end of the skein. The skein, together with the hook and anchor, was released vertically into the surfactant solution. The skein is completely immersed in the solution, but is buoyed up by the attached air bubbles. The wetting out time (WOT) is the time (in sec) for the fully immersed skein to start to sink. This is usually taken as that between the skein release time and the time when the hook starts to sink in the solution. Wetting out times (WOT) at concentrations of 1 g/L or lower were done at least in duplicate, generally in triplicate.

4.1.2 Discussion

The wetting out times for the surfactants studied are listed in Table 26 together with the corresponding π values. Log - log plots of WOT (in sec) as a function of initial concentration (C) of surfactant (in mol L^{-1}) at 25°C for $C_{12}EOSO$, $C_{12}EO_2SO$, $C_{12}S$ and $C_{12}SO$ are shown in Figure XXXIV.

TABLE: 26 Performance Properties of Purified Surfactants
Draves Wetting at 25°C

Compd	Medium	C, (mol dm^{-3} X 10^3)	C, (g/l)	π (mNm^{-1})	WOT (sec)
$C_{10}S$	H_2O	4.01	1.00	4.0	> 300
	0.1 M	4.01	1.00	18.0	93.0
	0.2 M	4.01	1.00	----	65.0
$C_{12}S$	H_2O	3.67	1.00	18.0	28.0
	"	3.31	0.90	16.8	40.7
	"	3.02	0.80	16.0	50.1
	"	2.76	0.75	14.0	68.0
	"	1.84	0.50	----	73.0
$C_{12}SO$	H_2O	3.4	1.00	22.0	7.5
	"	1.7	0.50	14.0	40.0
$C_{12}EOSO$	H_2O	2.92	1.00	28.6	6.0
	"	2.17	0.75	23.8	9.0
	"	1.46	0.50	18.6	16.0
	0.1 M	2.57	0.88	38.6	6.1
	"	2.07	0.71	38.6	8.5
	"	1.62	0.55	38.6	12.0
	"	1.45	0.50	38.6	14.0

cont'd

TABLE: 26 Performance Properties of Purified Surfactants Draves Wetting at 25°C

Compd	Medium	C, (mol dm^{-3} X 10^3)	C, (g/l)	Π (mNm^{-1})	WOT(sec)
$C_{12}EO_2SO$	H_2O	2.66	1.00	30.0	11.1
	"	2.00	0.75	25.9	14.0
	"	1.33	0.50	17.0	23.1
	0.1 M	2.66	1.00	36.5	13.0
	"	2.18	0.82	36.5	15.5
	"	1.45	0.55	36.5	24.1
$C_{12}NCl$	H_2O	3.52	1.00	28.3	250
$C_{12}NBr$	H_2O	3.04	1.00	32.9	250
$C_{10}BMG$	H_2O	3.13	1.00	38.0	250
$C_{12}BMG$	H_2O	2.87	1.00	39.0	250

The concentrations in pure water at which WOT were determined were all below the cmc for the respective compounds. Log-log plots of WOT (in sec) vs bulk concentration show a linear relationship in the range of 0.5-1.0 g/L (Figure XXXIV), for $C_{12}SO$, $C_{12}EOSO$ and $C_{12}EO_2SO$. Of the three sulfates studied, the most effective wetting agent appears to be $C_{12}EOSO$.

Although the reduction in surface tension by $C_{12}EOSO$ at 1 g/L is substantially greater than that of $C_{12}SO$, the difference in WOT is relatively small. $C_{12}EO_2SO$, although it produces a larger surface tension reduction than $C_{12}SO$ or $C_{12}EOSO$ at 1 g/L, shows a larger wetting time. Equilibrium surface tension is therefore apparently not the controlling factor.

Since adsorption and diffusion are known to have negligible effect on the rates of wetting (117) by ionic surfactants, it is probable that in this case the differences in WOT are due to the dynamic surface tension values.

The bulkiness of the hydrophilic heads, due to the hydration of the ether oxygens in the oxyethylenated sulfates, may retard the diffusion of the surfactant to the wetting front, thus, overcoming any potential reduction in WOT due to the static (equilibrium) surface tension value.

For the two ethenoxylated sulfates in 0.1 M NaCl, the WOT values are almost comparable to those in pure water at the same concentration (in g/L), even though the π_{cmc} values, are substantially larger in 0.1 M NaCl. Since the concentrations at which WOT values were taken in 0.1 M NaCl are all above the cmc (in 0.1M NaCl) of the compounds, the data confirm the observation made by others (117,118) that, for low cmc surfactants, diffusion and dissociation of micelles into monomers appears to be the slow rate-controlling process in wetting.

For $C_{10}S$, there is a sharp decrease in wetting time going from pure water to 0.1 M NaCl. All solutions were below the cmc of the material. The data indicate that wetting for this high cmc product is primarily a function of the surface tension reduction at the wetting front.

The WOT results in Table 26 show that both cationic and zwitterionic surfactants are poor wetting agents.

The cationic surfactants are known to be poor wetting agents due to their adsorption onto the negatively charged sites on the textile fibres. Such adsorption will make the surface of the substrate more hydrophobic due to the orientation of the hydrophobic tails of the cationic surfactants towards the aqueous phase, and will also deplete the surfactant at the wetting front. Both these factors will result in an increase in interfacial tension between the substrate and the aqueous phase.

The surface properties of zwitterionic betaines in water are known to be determined in part by the concentration of the protonated cationic form in equilibrium with the zwitterionic (119). The poor wetting properties of the betaines appear to be due to the interaction of the cationic species with the negatively charged sites on the cellulose skeins, in a manner similar to that of the alkylpyridinium halides.

4.2 Foaming in aqueous solution.

The effectiveness of the surfactants as foaming agents was determined by use of the Ross-Miles method (120).

4.2.1 Experimental

The apparatus and procedure used were those of A.S.T.M method D1173-53 (121). The foam cylinder used had an internal diameter of 4.89 ± 0.1cm at 60°C. The foam cylinder was cleaned by passing hot 1:9 HNO_3 -H_2SO_4 mixture down the walls, followed by rinsing with distilled water, and finally with quartz-distilled water.

The wall of the foam cylinder was rinsed with a 60 ml of the surfactant solution whose foaming properties were to be measured. The stopcock at the bottom of the cylinder was adjusted so that the solution

filled exactly to the 50 ml mark in the foam cylinder. Water at 60°C was circulated through the outer jacket of the foam cylinder. The graduated pipet was filled exactly to the 200 ml mark, at room temperature, and was placed at the top of the foam cylinder. The solution in the pipet was allowed to drain into the foam cylinder by opening the stopcock of the pipet.

Initial foam height of the solution was taken as the height of the foam after the last drop of the solution had drained from the pipet. A second reading of the foam height was taken 5 minutes after the initial foam height had been measured.

TABLE: 27. Foaming effectiveness of aqueous surfactant solution

Surfactant	C*(mol dm^{-3} X 10^3)	π_{cmc} ($40^{\circ}C$)	Foam Height (mm) Initial	After 5 mins
$C_{10}S$	28.10	29.2	160	5
$C_{12}S$	12.00	31.0	190	125
$C_{12}SO$	7.85	28.0	220	200
$C_{12}EOSO$	4.28	30.4	246	241
$C_{12}EO_2SO$	2.81	28.6	180	131
$C_{12}NBr$	11.30	30.8	135	3
$C_{10}BMG$	4.50	36.3	35	2
$C_{12}BMG$	5.30	37.6	50	2

* Here, the concentrations at cmc were used for the respective compounds, in the determination of their foaming properties.

4.2.2 Discussion

Table 27 lists the foaming effectiveness of the surfactants in aqueous solution. Of the three sulfates, $C_{12}SO$, $C_{12}EOSO$ and $C_{12}EO_2SO$, $C_{12}EOSO$ shows the greatest foam heights and foam stabilities, followed closely by $C_{12}SO$. On the other hand, $C_{12}EO_2SO$ produces considerably less initial foam and shows much poorer foam stability than $C_{12}SO$ or $C_{12}EOSO$.

The larger area per molecule for $C_{12}EO_2SO$ will reduce the intermolecular cohesive forces in the interfacial film, thus, reducing the stability of the foam produced; the smaller π_{cmc} for this compound will result in less initial foam.

The cationic surfactant, dodecyl pyridinium bromide, produces less initial foam and a much less stable foam than do the anionic surfactants in aqueous medium. This appears to be mainly due to the adsorption of cationic surfactant onto the negatively charged sites on the surface of the glass tube used in the test, thus making the tube hydrophobic. This , in addition to increasing the interfacial tension between the tube and the aqueous solution, will also reduce the effective concentration of the surfactant for the film formation. Evidence for this was the breaking of the foam from the tube surface inward towards the center.

The foaming data for the two betaines, C_{10}BMG and C_{12}BMG, show these compounds to have poor foaming capacities, poorer than the nonionics, and even poorer than the cationic. The absence of a significant electrical charge on the two surfaces of the foam film, to help stabilization of the foam film by mutual repulsion of the two surfaces, is probably the cause of the poor foaming properties of these materials. In addition, the adsorption of the protonated cationic species of these betaines onto the glass wall of the tube will both decrease the concentration of the surfactant in the bulk phase as well as increase the interfacial tension, thereby making for poor film volume and stability.

Appendix

TABLE: A1 Surface pressure vs. activity data

Compd	Temp:	Medium	γ° (mNm^{-1})	
$C_{12}NBr$	10°C	H_2O	74.25	
-log C	-log f_{N^+}	-log f_{X^-}	-log a	π(mNm^{-1})
1.5304	0.0637	0.0729	1.5987	34.78
1.8318	0.0486	0.0538	1.8830	34.43
2.0389	0.0400	0.0434	2.0806	21.15
2.0847	0.0382	0.0414	2.1245	29.78
2.1895	0.0345	0.0370	2.2252	25.25
2.3437	0.0229	0.0314	2.3742	21.23
2.5191	0.0246	0.0259	2.5444	15.15
2.8046	0.0182	0.0189	2.8232	8.51
3.3783	0.0098	0.0100	3.3882	1.83
3.4531	0.0090	0.0092	3.4621	1.28
3.5107	0.0084	0.0086	3.5192	1.16
3.6623	0.0071	0.0072	3.6695	1.35

TABLE: A2 Surface pressure vs. activity data

Compd	Temp:	Medium	γ° (mNm^{-1})
$C_{12}NBr$	25°C	H_2O	72.80

-log C	-log f_{N^+}	-log f_{X^-}	-log a	π(mNm^{-1})
1.5304	0.0652	0.0747	1.6004	32.90
1.8318	0.0498	0.0551	1.8843	32.82
2.0071	0.0422	0.0460	2.0512	31.10
2.0389	0.0409	0.0445	2.0816	29.58
2.0847	0.0391	0.0424	2.1255	28.57
2.1895	0.0353	0.0379	2.2260	24.09
2.2986	0.0316	0.0337	2.3313	20.16
2.3437	0.0303	0.0321	2.3749	19.83
2.5191	0.0265	0.0265	2.5450	13.67
2.5348	0.0248	0.0261	2.5603	14.25
2.6937	0.0210	0.0219	2.7152	10.14
2.8046	0.0187	0.0194	2.8236	7.13
3.0936	0.0137	0.0141	3.1075	3.56
3.1919	0.0123	0.0126	3.2043	2.36
3.2991	0.0109	0.0112	3.3101	2.06
3.3783	0.0100	0.0102	3.3884	1.82
3.4531	0.0092	0.0094	3.4624	1.65
3.5107	0.0086	0.0088	3.5194	1.22
3.5557	0.0082	0.0083	3.5640	1.10
3.6623	0.0073	0.0074	3.6696	1.29

TABLE: A3 Surface pressure vs. activity data

Compd	Temp:	Medium	γ° (mNm^{-1})	
$C_{12}NBr$	40°C	H_2O	69.63	
-log C	-log f_{N^+}	-log f_{X^-}	-log a	π(mNm^{-1})
1.4984	0.0690	0.0794	1.5726	30.73
1.8318	0.0513	0.0568	1.8858	30.83
2.0389	0.0421	0.0458	2.0829	27.98
2.0847	0.0403	0.0436	2.1267	26.90
2.1895	0.0363	0.0390	2.2272	21.07
2.3437	0.0311	0.0331	2.3758	18.41
2.5191	0.0260	0.0273	2.5458	12.41
2.8046	0.0192	0.0200	2.8242	6.81
3.1919	0.0126	0.0130	3.2047	2.09
3.3783	0.0103	0.0105	3.3887	1.38
3.4531	0.0095	0.0097	3.4627	1.73
3.5107	0.0089	0.0095	3.5197	0.95
3.6123	0.0075	0.0076	3.6699	1.23

TABLE: A4 Surface pressure vs. activity data

Compd	Temp	Medium	-log f_{X^-}	γ°(mNm^{-1})
$C_{12}NBr$	10°C	0.1 M NaBr	0.0967	74.66

-log C_{N^+}	-log a_{N^+}	π(mNm^{-1})
2.1930	2.2897	36.96
2.4148	2.5115	36.75
2.4148	2.5115	37.01
2.4940	2.5907	36.76
2.5969	2.6876	36.32
2.7158	2.8125	34.06
2.8919	??.??	30.82
3.1930	3.2897	25.31
3.4940	3.5907	19.91
3.8919	3.9886	13.44
4.1930	4.2897	9.24
4.2899	4.3866	8.13
4.2899	4.3866	8.43
4.5909	4.6876	5.09
4.8128	4.9095	3.52
4.9888	5.0855	2.14

TABLE: A5 Surface pressure vs. activity data

Compd	Temp.	Medium	-log f_{X^-}	γ°(mNm^{-1})
$C_{12}NBr$	25°C	0.1 M NaBr	0.0990	72.40

-log C_{N^+}	-log a_{N^+}	π(mNm^{-1})
2.1930	2.9200	35.24
2.4148	2.5138	35.18
2.4148	2.5138	35.28
2.4940	2.5930	35.19
2.5909	2.6899	34.73
2.7158	2.8148	32.47
2.8919	2.9909	28.76
3.1930	3.2092	23.37
3.4940	3.5930	18.56
3.8919	3.9909	12.51
4.1930	4.2936	7.72
4.2899	4.3889	6.56
4.2926	4.3916	7.60
4.5909	4.6890	3.64
4.8128	4.9118	2.37
4.9888	5.0878	1.50

TABLE: A6 Surface pressure vs. activity data

Compd	Temp	Medium	-log f_{X^-}	γ°(mNm^{-1})
$C_{12}NBr$	40°C	0.1 M NaBr	0.0990	70.02

-log C_{N^+}	-log a_{N^+}	π(mNm^{-1})
2.1930	2.2949	33.57
2.4148	2.5167	33.47
2.2415	2.5167	33.56
2.4940	2.5959	33.47
2.5909	2.6928	32.64
2.7158	2.8177	30.50
2.8919	2.9938	27.00
3.1930	3.2949	21.80
3.4940	3.5959	16.31
3.8919	3.9938	10.43
4.1930	4.2949	6.16
4.2899	2.3918	5.217
4.2899	4.3918	5.74
4.5909	4.6928	2.997
4.8128	4.9147	1.71
4.8128	4.9147	2.18
4.9888	5.0907	1.26

TABLE: A7 Surface pressure vs. activity data

Compd	Temp	Medium	-log f_{X^-}	γ°(mNm^{-1})
$C_{12}NBr$	10°C	0.5 M NaBr	0.1464	75.09

-log C_{N^+}	-log a_{N^+}	π(mNm^{-1})
2.4332	2.5796	38.72
2.7343	2.8807	38.82
2.8312	2.9776	38.54
3.1322	3.2786	36.36
3.4332	3.5796	30.82
3.7343	3.8807	25.72
3.9517	4.0981	21.59
4.1322	4.2786	17.76
4.4332	4.5796	12.86
4.4332	4.5796	12.996
4.5301	4.6765	12.19
4.8312	4.9776	7.70
5.0530	5.1994	5.26
5.2291	5.3759	3.69
5.3540	5.5004	2.65
5.3540	5.5004	2.996

TABLE: A8 Surface pressure vs. activity data

Compd	Temp	Medium	-log f_{X^-}	γ°(mNm^{-1})
$C_{12}NBr$	25°C	0.5 M NaBr	0.1500	72.82

-log C_{N^+}	-log a_{N^+}	π(mNm^{-1})
2.4332	2.5832	37.05
2.7343	2.8843	37.38
2.8312	2.9812	36.99
2.9512	3.1017	37.42
3.1322	3.2822	34.08
3.4332	3.5832	28.65
3.7343	3.8843	23.47
3.4517	4.1017	19.42
4.1322	4.2822	15.01
4.4332	4.5832	11.02
4.4332	4.5832	11.36
4.7328	4.6828	10.86
4.8312	4.9812	5.92
5.0530	5.2030	4.11
5.2291	5.3791	2.56
5.3540	5.5040	1.47
5.3549	5.5040	2.54

TABLE: A9 Surface pressure vs. activity data

Compd	Temp	Medium	-log f_{X^-}	γ° (mNm^{-1})
$C_{12}NBr$	40°C	0.5 M NaBr	0.1544	70.42

-log C_{N^+}	-log a_{N^+}	π (mNm^{-1})
2.4332	2.5876	35.53
2.7343	2.8887	35.78
2.8312	2.9856	35.59
3.1322	3.2866	31.42
3.4332	3.5876	26.36
3.7343	3.8887	21.22
3.9517	4.1061	17.40
4.1322	4.2866	13.43
4.4332	4.5876	8.76
4.4332	4.5876	9.03
4.5328	4.6872	8.59
4.8312	4.9856	4.49
5.0530	5.2074	2.74
5.2291	5.3835	1.83
5.3540	5.5084	1.28
5.3540	5.5084	1.24

TABLE: A10 Surface pressure vs. activity data

Compd	Temp:	Medium	γ° (mNm^{-1})
$C_{12}NCl$	10°C	H_2O	74.25

-log C	-log f_{N^+}	-log f_{X^-}	-log a	π(mNm^{-1})
1.3706	0.0728	0.0852	1.4496	29.49
1.7782	0.0511	0.0569	1.8322	29.55
1.8711	0.0469	0.0517	1.9204	26.12
2.0690	0.0388	0.0421	2.1094	21.50
2.1959	0.0342	0.0368	2.2314	17.97
2.5599	0.0236	0.0248	2.5841	9.33
2.7027	0.0203	0.0212	2.7235	7.33
2.9921	0.0149	0.0154	3.0072	3.55
3.2050	0.0118	0.0121	3.2170	2.49
3.3229	0.0104	0.0106	3.3333	1.53
3.5090	0.0084	0.0085	3.5274	1.24

TABLE: A11 Surface pressure vs. activity data

Compd	Temp:	Medium	γ° (mNm^{-1})	
$C_{12}NCl$	25°C	H_2O	72	
-log C	-log f_{N^+}	-log f_{X^-}	-log a	π(mNm^{-1})
1.3706	0.0746	0.0872	1.4515	28.27
1.7782	0.0523	0.0583	1.8335	28.26
1.8711	0.0482	0.0531	1.9218	25.95
2.0690	0.0397	0.0431	2.1104	21.22
2.1959	0.0351	0.0376	2.2323	17.02
2.5599	0.0242	0.0242	2.5850	9.00
2.7027	0.0215	0.0215	2.7243	4.20
2.9536	0.0159	0.0159	2.9698	3.45
2.9921	0.0153	0.0153	3.0076	2.43
3.2050	0.0121	0.0121	3.2173	2.25
3.3229	0.0106	0.0106	3.3336	1.55
3.5190	0.0086	0.0086	3.5676	1.14

TABLE: A12 Surface pressure vs. activity data

Compd	Temp:	Medium	γ° (mNm^{-1})	
$C_{12}NCl$	40°C	H_2O	69.63	
-log C	-log f_{N^+}	-log f_{X^-}	-log a	π(mNm^{-1})
1.3706	0.0768	0.0898	1.4539	26.73
1.7782	0.0539	0.0600	1.8351	26.76
1.8711	0.0494	0.0545	1.9231	25.55
2.0690	0.0409	0.0443	2.1116	20.29
2.1959	0.0361	0.0388	2.2330	16.01
2.5599	0.0249	0.0261	2.5854	7.97
2.7027	0.0221	0.0223	2.7249	6.17
2.9921	0.0157	0.0162	3.0081	3.21
3.3229	0.0109	0.0112	3.3339	1.45
3.5190	0.0088	0.0090	3.5279	1.25

TABLE: A13 Surface pressure vs. activity data

Compd	Temp	Medium	-log f_{X^-}	γ°(mNm^{-1})
$C_{12}NCl$	10°C	0.1 M NaCl	.0967	74.56

-log C_{N^+}	-log a_{N^+}	π(mNm^{-1})
2.1324	2.2291	31.85
2.2573	2.3540	31.58
2.2573	2.3540	31.85
2.4334	2.5301	28.98
2.6095	2.7062	26.04
2.8314	2.9281	22.72
3.4334	3.5301	13.76
3.5303	3.6270	12.76
3.6553	3.7520	10.94
3.8314	3.9281	8.95
4.7324	4.2291	6.53
4.530	4.6270	3.45
4.5303	4.6270	3.69
4.8314	4.9281	2.21
5.1324	5.2291	1.35
5.1324	5.2291	1.59

TABLE: A14 Surface pressure vs. activity data

Compd	Temp	Medium	-log f_{X^-}	γ°(mNm^{-1})
$C_{12}NCl$	25°C	0.1 M NaCl	0.0990	72.30

-log C_{N^+}	-log a_{N^+}	π(mNm^{-1})
2.1324	2.2314	30.40
2.2573	2.3563	30.31
2.2573	2.3563	30.38
2.4334	2.5324	28.69
2.6095	2.7085	25.55
2.8314	2.9304	22.50
3.4334	3.5324	13.14
3.5303	3.6293	12.40
3.6553	3.7542	10.26
3.8314	3.9304	8.33
4.1324	4.2314	6.02
4.5303	4.6293	3.12
4.5303	4.6293	3.59
4.8314	4.9304	2.14
5.1324	5.2314	1.10
5.1324	5.2314	1.39

TABLE: A15 Surface pressure vs. activity data

Compd	Temp	Medium	-log f_{X^-}	$\gamma^{\circ}(mNm^{-1})$
$C_{12}NCl$	40°C	0.1 M NaCl	0.1019	69.92

-log C_{N^+}	-log a_{N^+}	$\pi(mNm^{-1})$
2.1324	2.2343	29.07
2.2573	2.3592	29.14
2.2573	2.3592	29.20
2.4334	2.5353	27.85
2.6095	2.0814	24.24
2.8314	2.9333	21.61
3.4334	3.5353	12.08
3.5303	3.6322	11.11
3.6553	3.7572	9.23
3.8314	3.9333	7.72
4.1324	4.2343	5.57
4.5303	4.6322	2.80
4.5303	4.6322	2.71
4.8314	4.9333	1.74
5.1324	5.2343	1.72
5.1324	5.2343	1.16

TABLE: A16 Surface pressure vs. activity data

Compd	Temp	Medium	-log f_{X^-}	γ°(mNm^{-1})
$C_{12}NCl$	10°C	0.5 M NaCl	0.1464	75.13

-log C_{N^+}	-log a_{N^+}	π(mNm^{-1})
2.4822	2.6286	34.11
2.7418	2.8882	33.92
2.7418	2.8882	34.30
2.8277	2.9741	32.07
2.9526	3.0990	30.06
2.9526	3.0990	30.33
3.2434	3.3898	25.13
3.5444	3.6908	19.76
4.9423	3.9918	15.99
3.9423	4.0887	14.99
4.2434	4.3898	11.23
4.5444	4.6908	7.16
4.9423	5.0887	5.13
5.1812	5.3276	2.96
5.2434	5.3898	2.98
5.2434	5.3898	2.98

TABLE: A17 Surface pressure vs. activity data

Compd	Temp	Medium	-log f_{X^-}	γ°(mNm^{-1})
$C_{12}NCl$	25°C	0.5 M NaCl	0.1500	72.85

-log C_{N^+}	-log a_{N^+}	π(mNm^{-1})
2.4822	2.6322	32.76
2.4822	2.6322	32.83
2.7418	2.6322	32.83
2.7418	2.8918	32.85
2.7418	2.8918	32.75
2.8277	2.9777	31.85
2.9526	3.1026	29.37
2.9526	3.1026	29.87
3.2434	3.3934	24.05
3.5444	3.6944	19.05
3.8454	3.9954	14.96
3.9423	4.0923	14.43
4.2434	4.3934	10.00
4.5444	4.6944	7.02
4.9423	5.0923	4.24
5.1812	5.3312	2.41
5.1812	5.3312	2.18
5.2434	5.3934	2.32

TABLE: A18 Surface pressure vs. activity data

Compd	Temp	Medium	-log f_{X^-}	γ°(mNm^{-1})
$C_{12}NCl$	40°C	0.5 M NaCl	0.1544	70.45

-log C_{N^+}	-log a_{N^+}	π(mNm^{-1})
2.4822	2.6366	31.53
2.4822	2.6366	31.61
2.7418	2.8962	31.62
2.7418	2.8962	31.64
2.8277	2.9821	30.25
2.9526	3.1070	27.84
2.9526	3.1070	28.43
3.2434	3.3978	23.05
3.5444	3.6988	17.85
3.8454	3.9998	13.81
3.9423	4.0967	13.04
4.2434	4.3978	9.06
4.5444	4.6988	6.18
4.9923	5.0967	3.66
5.1812	5.3356	1.93
5.1812	5.3356	2.05
5.2434	5.3978	1.93
5.2434	5.3978	1.89

TABLE: A19. Conductance data for $C_{12}NBr$ at 10°C

$C^a x10^2$	$W^b x10^3$	$k^c x10^3$	$\Lambda^d x10^3$	$C^{1/2}$
2.5378	2.3162	0.9266	36.51	0.159
1.6900	2.2783	0.9113	53.86	0.130
1.4927	2.2030	0.8812	59.03	0.122
1.2353	2.0742	0.8291	67.09	0.111
1.0536	1.8758	0.7500	71.21	0.103
0.9548	1.7100	0.6849	71.63	0.098
0.6564	1.1940	0.4776	75.75	0.081
0.8631	2.2050	0.9061	104.99	0.093

TABLE: A20 Conductance data for $C_{12}NBr$ at 25°C

$C^a x10^2$	$W^b x10^3$	$k^c x10^3$	$\Lambda^d x10^3$	$C^{1/2}$
2.5373	3.4600	1.4220	56.03	0.1590
1.6918	3.3200	1.3640	80.62	0.1300
1.2084	2.9400	1.2080	99.99	0.1090
1.0536	2.6650	1.0950	103.95	0.1030
0.8631	2.2050	0.9060	104.99	0.0930
0.9548	2.4260	0.9974	104.43	0.0980
0.6564	1.6868	0.6930	105.60	0.0810

a. mol dm^{-3}

b. Ohm^{-1}

c. $Ohm^{-1}cm^{-1}$

d. $Ohm^{-1}cm^2$ equiv $^{-1}$

TABLE: A21 Conductance data for $C_{12}NBr$ at 40°C

$C^a x10^2$	$W^b x10^3$	$k^c x10^3$	$\Lambda^d x10^3$	$C^{1/2}$
2.5378	4.8700	2.0360	80.21	0.1590
1.6918	4.5800	1.9140	113.16	0.1300
1.2080	3.9760	1.6620	137.53	0.1090
1.0536	3.5180	1.4710	139.57	0.1030
0.8631	2.9100	1.2170	140.42	0.0930
0.9548	3.2620	1.3380	140.17	0.0980
6.5642	2.2310	0.9320	142.06	0.0810

TABLE: A22 Conductance data for $C_{12}NCl$ at 10°C

$C^a x10^2$	$W^b x10^3$	$k^c x10^3$	$\Lambda^d x10^3$	$C^{1/2}$
2.5430	3.2030	1.2262	48.24	0.1590
2.2113	3.2570	1.2471	56.41	0.1490
1.9560	3.1800	1.2179	62.26	0.1400
1.8160	3.0890	1.1830	65.75	0.1350
1.3075	2.2800	0.8650	66.78	0.1140
1.1670	2.0630	0.7901	67.70	0.1080
0.9902	1.7750	0.6798	68.60	0.0990

a. mol dm^{-3}

b. Ohm^{-1}

c. $Ohm^{-1}cm^{-1}$

d. $Ohm^{-1}cm^2$ equiv $^{-1}$

TABLE: A23, Conductance data for $C_{12}NCl$ at 25°C

$C^a x10^2$	$W^b x10^3$	$k^c x10^3$	$\Lambda^d x10^3$	$C^{1/2}$
1.0910	2.7670	1.0708	98.24	0.1040
2.5430	4.5440	1.7580	69.13	0.1590
2.2113	4.5540	1.7624	76.69	0.1490
1.9560	4.4240	1.7121	87.53	0.1400
1.8160	4.2950	1.6620	91.52	0.1350
1.3075	3.5220	3.2522	96.26	0.1140
1.1671	2.9472	1.1410	97.74	0.1080
0.9902	2.5350	1.7750	68.60	0.0990

TABLE: A24, Conductance data for $C_{12}NCl$ at 40°C

$C^a x10^2$	$W^b x10^3$	$k^c x10^3$	$\Lambda^d x10^3$	$C^{1/2}$
2.2113	6.2040	2.4009	108.57	0.149
1.9560	5.9700	2.3100	118.12	0.140
1.8160	5.7680	2.2320	122.92	0.135
1.3075	4.2922	1.6610	127.04	0.114
1.1670	3.9140	1.5150	129.82	0.108
0.9902	1.7750	0.6798	131.60	0.093
0.8598	2.9450	1.1400	132.60	0.093

a. mol dm^{-3}

b. Ohm^{-1}

c. $Ohm^{-1}cm^{-1}$

d. $Ohm^{-1}cm^2$ $equiv^{-1}$

TABLE: A25

log (CMC.f_+) vs log (C_{X^-}.f_-) data for $C_{12}NBr$

T	I	-log CMC	-log C_{X^-}	-log f_+	-log f_-
10	H_2O	1.9315	1.9315	0.0443	0.0486
	0.1 M	2.5607	1.0000	0.0966	0.0120
	0.5 M	2.9706	0.3010	0.1464	0.2067
25	H_2O	1.9390	1.9390	0.0450	0.0494
	0.1 M	2.5607	1.000	0.9660	0.1226
	0.5 M	2.9666	0.3010	0.1500	0.2117
40	H_2O	1.9582	1.9582	0.0455	0.0498
	0.1 M	2.5452	1.0000	0.1019	0.1262
	0.5 M	2.9355	0.3010	0.1544	0.2179

TABLE: A26

log (cmc.f_+) vs log (C_{X^-}.f_-) data for $C_{12}NCl$

T	I	-log CMC	-log C_{X^-}	-log f_+	-log f_-
10	H_2O	1.7641	1.7641	0.0517	0.0577
	0.1 M	2.2596	1.0000	0.0966	0.1200
	0.5 M	2.7212	0.3010	0.1464	0.2067
25°C	H_2O	1.7901	1.7901	0.0517	0.0575
	0.1 M	2.3188	1.0000	0.9900	1.226
	0.5 M	2.7296	0.3010	0.1500	0.2117
40°C	H_2O	1.8090	0.8090	0.0523	0.0580
	0.1 M	2.3468	1.0000	0.1019	0.1262
	0.5 M	2.7496	0.3010	0.1544	0.2179

TABLE: A27,% Effective electrical coefficients of micellization for the surfactants.

Compd	m/n 10°C	25°C	40°C
$C_{12}NBr$	0.78	0.77	0.73
$C_{12}NCl$	0.80	0.79	0.77
$C_{10}S$	0.94	0.89	0.89
$C_{12}S$	-.--	0.88	0.85
$C_{10}EOS$	0.84	0.74	0.73
$C_{12}EOSO$	0.89	0.83	0.82
$C_{12}EO_2SO$	0.78	0.77	0.76

TABLE: A28 Surface pressure vs. activity data

Compd	Temp:	Medium	γ° (mNm^{-1})
$C_{10}S$	10°C	H_2O	74.24

-log C	-log f_{R^-}	-log f_{X^+}	-log a	π(mNm^{-1})
1.2294	.0815	0.0973	1.3188	33.10
1.3300	.0754	0.0887	1.4119	32.52
1.4026	.0709	0.0826	1.4790	29.62
1.4084	.0706	0.0821	1.4850	29.42
1.5125	.0647	0.0742	1.5820	26.66
1.8135	.0495	0.0549	1.8657	15.20
1.9896	.0419	0.0457	2.0334	11.16
1.1108	.0373	0.0402	2.1496	8.95
2.2110	.0337	0.0361	2.2467	6.93
2.4300	.0269	0.0285	2.4578	3.00
2.5124	.0248	0.0261	2.5379	3.31
2.6100	.0224	0.0235	2.6330	2.10
2.7300	.0197	0.0205	2.7500	1.39
2.9100	.0163	0.0684	2.9270	1.13
3.2115	.0117	0.0120	3.2230	0.59

TABLE: A29 Surface pressure vs. activity data

Compd	Temp:	Medium	γ^{o} (mNm^{-1})	
$C_{10}S$	25°C	H_2O	72	
-log C	-log f_{R^-}	-log f_{X^+}	-log a	π(mNm^{-1})
1.2294	0.0835	0.0996	1.3210	31.10
1.3300	0.7720	0.0908	1.4140	30.96
1.4030	0.0726	0.0846	1.4812	29.53
1.4080	0.0723	0.0841	1.4866	29.51
1.5130	0.0662	0.0760	1.5836	26.93
1.8130	0.0507	0.0562	1.8669	15.59
1.9900	0.0468	2.0340	2.0340	10.87
2.1110	0.0382	0.0412	2.1505	8.52
2.2120	0.0346	0.0370	2.2476	6.49
2.4300	0.0276	0.0291	2.4584	3.49
2.5120	0.0254	0.0267	2.5385	3.17
2.6100	0.0230	0.0241	2.6335	2.52
2.7300	0.0201	0.0210	2.7506	1.73
2.9100	0.1167	0.0173	2.9270	1.13
3.2120	0.0120	0.0123	3.2237	0.63

TABLE: A30 Surface pressure vs. activity data

Compd	Temp:	Medium	γ° (mNm^{-1})	
$C_{10}S$	40°C	H_2O	69.63	
-log C	-log f_{R^-}	-log f_{X^+}	-log a	π(mNm^{-1})
1.2294	0.0835	0.0996	1.3211	31.10
1.3300	0.0772	0.0908	1.4140	30.96
1.4030	0.0726	0.0846	1.4810	29.53
1.4080	0.0723	0.0841	1.4900	29.51
1.5130	0.0662	0.0760	1.5840	26.93
1.8130	0.0507	0.0562	1.8670	15.59
1.9900	0.0429	0.0468	2.0340	10.87
2.1110	0.0382	0.0412	2.1510	8.52
2.2120	0.0346	0.0370	2.2480	6.49
2.4300	0.0276	0.0292	2.4580	3.49
2.5120	0.0254	0.0267	2.5390	3.17
2.6100	0.2298	0.0241	2.6340	2.52
2.7300	0.0201	0.0211	2.7506	1.73
2.9100	0.0167	0.0173	2.9270	1.13
3.2120	0.0120	0.0123	3.2240	0.63

TABLE: A31 Surface pressure vs. activity data

Compd	Temp	Medium	-log f_{X^+}	γ°(mNm^{-1})
$C_{10}S$	10°C	0.1 M NaCl	0.0967	74.45

-log C_{R^-}	-log a_{R^-}	π(mNm^{-1})
1.4140	1.5107	34.29
1.5073	1.6040	34.47
1.6500	1.7467	33.43
1.7292	1.8259	31.49
1.8083	1.9050	29.43
1.8100	1.9067	29.65
1.8911	1.9878	27.22
1.9844	2.0811	26.39
2.1094	2.2061	23.51
2.2100	2.3067	21.85
2.4140	2.5107	16.85
2.5073	2.6040	15.43
2.7290	2.8257	12.38
2.9052	3.0019	10.01
3.0302	3.1269	8.08
3.2063	3.3030	6.21
3.5073	3.6040	3.25
3.6042	3.7009	3.07
3.7011	3.7978	2.33
3.7591	3.8558	1.95

TABLE: A32 Surface pressure vs. activity data

Compd	Temp	Medium	-log f_{X^+}	γ°(mNm^{-1})
$C_{10}S$	25°C	0.1 M NaCl	0.099	72.19

-log C_{R^-}	-log a_{R^-}	π(mNm^{-1})
1.4140	1.5130	32.69
1.5073	1.6060	32.78
1.6500	1.7490	32.41
1.7290	1.8280	32.31
1.8080	1.9070	29.78
1.8100	1.9090	30.49
1.8910	1.9900	27.12
1.9840	2.0830	26.16
2.1090	2.2080	24.32
2.2100	2.3090	21.10
2.4140	2.5730	17.19
2.5070	2.6060	15.42
2.7290	2.8280	12.67
2.9050	3.0040	9.65
3.0300	3.1290	7.91
3.2060	3.3050	6.03
3.5070	3.6060	3.61
3.6040	3.7030	3.09
3.7010	3.8000	2.08
3.7590	3.8580	1.96

TABLE: A33 Surface pressure vs. activity data

Compd	Temp	Medium	-log f_{X^+}	γ°(mNm^{-1})
$C_{10}S$	40°C	0.1 M NaCl	0.1019	69.81

-log C_{R^-}	-log a_{R^-}	π(mNm^{-1})
1.4140	1.5159	30.91
1.5073	1.6092	31.05
1.6500	1.7519	30.98
1.7292	1.8311	31.36
1.8083	1.9102	29.64
1.8100	1.9119	28.79
1.8911	1.9930	26.68
1.9844	2.0863	25.93
2.1094	2.2113	23.72
2.2100	2.3119	22.01
2.4140	2.5159	16.94
2.5073	2.6092	14.60
2.7290	2.8309	11.36
2.9052	3.0071	8.78
3.0302	3.1321	7.06
3.2063	3.3082	5.22
3.5073	3.5092	3.89
3.6042	3.7061	3.31
3.7011	3.8030	2.12
3.7591	3.8610	2.11

TABLE: A34 Surface pressure vs. activity data

Compd	Temp	Medium	-log f_{X^+}	γ°(mNm^{-1})
$C_{10}S$	10°C	0.5 M NaCl	0.1464	74.87

-log C_{R^-}	-log a_{R^-}	π(mNm^{-1})
2.2729	2.4193	33.53
2.4490	2.5954	29.37
2.5739	2.7203	26.51
2.6700	2.8164	24.85
2.9719	3.1183	18.64
3.1268	3.2732	15.90
3.2717	3.4181	12.97
3.3700	3.5164	12.47
3.6696	3.8160	7.56
3.9707	4.1171	3.77
4.0676	4.2140	3.04
4.1645	4.3109	2.46
4.2220	4.3684	1.95
4.2894	4.4358	1.71

TABLE: A35 Surface pressure vs. activity data

Compd	Temp	Medium	-log f_{X^+}	γ°(mNm^{-1})
$C_{10}S$	25°C	0.5 M NaCl	0.1500	72.60

-log C_{R^-}	-log a_{R^-}	π(mNm^{-1})
2.2729	2.4229	33.79
2.4490	2.5990	29.37
2.5739	2.7239	26.60
2.6700	2.8200	25.35
2.9719	3.1219	17.84
3.1268	3.2768	15.16
3.2717	3.4217	12.37
3.3700	3.5200	12.14
3.6696	3.8196	6.98
3.9707	4.1207	3.50
4.0676	4.2176	2.62
4.1645	4.3145	2.63
4.2220	4.3720	1.70
4.2894	4.4394	1.65

TABLE: A36 Surface pressure vs. activity data

Compd	Temp	Medium	-log f_{X^+}	γ^o(mNm^{-1})
$C_{10}S$	40°C	0.5 M NaCl	0.1544	70.21

-log C_R-	-log a_R-	π(mNm^{-1})
2.2729	2.4273	33.83
2.4490	2.6034	28.57
2.5739	2.7283	24.65
2.6700	2.8244	24.16
2.9719	3.1263	16.69
3.1268	3.2812	13.61
3.2717	3.4261	11.03
3.3700	3.5244	11.38
3.6696	3.8240	6.91
3.9709	4.1253	3.11
4.0676	4.2220	2.06
4.1645	4.3189	1.92
4.2220	4.3764	1.45
4.2894	4.4438	0.99
2.4490	2.5954	29.37
2.5739	2.7203	26.51
2.6700	2.8164	24.85
2.9719	3.1183	18.64
3.1268	3.2732	15.90
3.2717	3.4181	12.97

3.3700	3.5164	12.47
3.6696	3.8160	7.56
3.9707	4.1171	3.77
4.0676	4.2140	3.04
4.1645	4.3109	2.46
4.2220	4.3684	1.95
4.2894	4.4358	1.71

TABLE: A37 Surface pressure vs. activity data

Compd	Temp:	Medium	γ° (mNm^{-1})	
$C_{12}S$	10°C	H_2O	74.25	
-log C	-log f_{R^-}	-log f_{X^+}	-log a	π(mNm^{-1})
2.2309	0.0331	0.0354	2.2651	24.44
2.2716	0.0318	0.0339	2.3045	20.92
2.4862	0.0255	0.0269	2.5124	16.45
2.5319	0.0243	0.0256	2.5568	16.06
2.7538	0.0193	0.0200	2.7735	10.10
2.9299	0.0159	0.0165	2.9461	6.15
3.1319	0.0128	0.0131	3.1449	3.08
3.2309	0.0115	0.0118	3.2425	2.01
3.3278	0.0103	0.0105	3.3382	1.73
3.4003	0.0095	0.0097	3.4099	1.56
3.4528	0.0090	0.0916	3.4619	1.17
3.5320	0.0082	0.0084	3.5403	0.97
2.2800	0.0314	0.0335	2.3125	23.51

TABLE: A38 Surface pressure vs. activity data

Compd	Temp:	Medium	γ^{o} (mNm^{-1})
$C_{12}S$	25°C	H_2O	72

-log C	-log f_{R^-}	-log f_{X^+}	-log a	π(mNm^{-1})
2.2309	0.03388	0.0363	2.2660	24.20
2.2716	0.03256	0.0348	2.3053	21.22
2.4862	0.02613	0.0275	2.5130	16.20
2.5319	0.0249	0.0262	2.5575	15.76
2.7538	0.0197	0.0205	2.7739	9.47
2.9299	0.0163	0.0169	2.9465	6.34
3.1319	0.0131	0.0135	3.1452	3.23
3.2309	0.0118	0.0120	3.2428	1.83
3.3328	0.0106	0.0108	3.3385	1.73
3.4003	0.0098	0.0996	3.4102	1.38
3.4528	0.0092	0.0094	3.4621	1.58
3.5320	0.0084	0.0086	3.5405	0.76
2.2800	0.0322	0.0343	2.3132	22.60
2.1090	0.3822	0.0413	2.1487	26.55
2.4220	0.2791	0.0295	2.4507	17.89
2.6210	0.0227	0.0237	2.6442	12.90
1.9380	0.0451	0.0494	2.9852	31.95
2.0666	0.0398	0.0432	2.1081	29.02
1.5830	0.06232	0.0709	1.6496	32.91
1.6370	0.0594	0.0672	1.7003	32.83

TABLE: A39 Surface pressure vs. activity data

Compd	Temp:	Medium	γ° (mNm^{-1})	
$C_{12}S$	40°C	H_2O	69.63	
-log C	-log f_{R^-}	-log f_{X^+}	-log a	π(mNm^{-1})
2.2309	0.0349	0.0373	2.2670	22.90
2.2716	0.0335	0.0358	2.3063	20.33
2.4862	0.0269	0.0283	2.5138	14.32
2.5319	0.0256	0.0270	2.5582	14.07
2.7538	0.0203	0.0211	2.7745	8.51
2.9299	0.0168	0.0174	2.9470	4.63
3.1319	0.0135	0.0139	3.1456	2.42
3.2309	0.0121	0.0124	3.2431	1.93
3.3278	0.0109	0.0112	3.3388	1.29
3.4003	0.0100	0.0102	3.4104	1.19
3.4528	0.0095	0.9659	3.4624	1.25
3.5320	0.0087	0.0088	3.5408	0.86
2.2800	0.0331	0.0353	2.3142	21.09
2.0666	0.0411	0.0444	2.1093	28.03
1.9380	0.0464	0.0508	1.9866	30.34
1.5830	0.0642	0.0730	1.6516	30.87
1.6370	0.0612	0.0692	1.7022	30.87

TABLE: A40 Surface pressure vs. activity data

Compd	Temp	Medium	-log f_{X^+}	γ°(mNm^{-1})
$C_{12}S$	10°C	0.1 M NaCl	0.0967	74.38

-log C_{R^-}	-log a_{R^-}	π(mNm^{-1})
3.8199	3.9165	13.85
3.9748	4.0714	10.61
4.1209	4.2175	8.17
4.3428	4.4394	5.34
4.5188	4.6154	3.75
4.6757	4.7723	2.59
4.8199	4.9165	1.92
4.9748	5.0714	1.24
4.9748	5.0714	1.11
5.1209	5.2175	0.71
5.1209	5.2175	0.77
3.2800	3.3767	22.74
3.4370	3.5337	19.78
3.5830	3.6797	16.88

TABLE: A41 Surface pressure vs. activity data

Compd	Temp	Medium	-log f_{X^+}	$\gamma°$(mNm^{-1})
$C_{12}S$	25°C	0.1 M NaCl	0.0990	72.13

-log C_{R^-}	-log a_{R^-}	π(mNm^{-1})
3.8199	3.9189	13.45
3.9748	4.0738	9.74
4.1209	4.2199	7.44
4.3428	4.4418	4.69
4.5188	4.6178	3.38
4.6757	4.7747	2.37
4.8199	4.9189	1.72
4.9748	5.0738	1.10
4.9748	5.0738	1.33
5.1209	5.2199	0.85
5.1209	5.2199	0.92
3.2800	3.3790	21.82
3.4370	3.5360	18.79
3.5830	3.6820	15.83
2.5407	2.6397	36.29
2.5819	2.6809	36.58
2.8829	2.9819	30.86
3.1048	3.2038	26.33
2.6199	2.7189	36.18

TABLE: A42 Surface pressure vs. activity data

Compd	Temp	Medium	-log f_{X^+}	γ°(mNm^{-1})
$C_{12}S$	40°C	0.1 M NaCl	0.1019	69.76

-log C_{R^-}	-log a_{R^-}	π(mNm^{-1})
3.8199	3.9218	12.36
3.9748	4.0767	8.89
4.1209	4.2228	6.54
4.3428	4.4447	3.99
4.5188	4.6207	2.86
4.6757	4.7776	2.03
4.8199	4.9218	1.54
4.9749	5.0767	0.92
4.9748	5.0767	0.99
5.1209	5.2228	0.69
5.1209	5.2228	0.69
3.2800	3.3819	19.91
3.4370	3.5389	16.75
3.5830	3.6849	14.11
2.5407	2.6426	34.71
2.5819	2.6838	34.67
2.8829	2.9847	29.32
3.1048	3.2067	23.31
2.6199	2.7218	34.32

TABLE: A43 Surface pressure vs. activity data

Compd	Temp	Medium	-log f_{X^+}	γ^o(mNm^{-1})
$C_{12}S$	10°C	0.5 M NaCl	0.1464	75.17

-log C_{R^-}	-log a_{R^-}	π(mNm^{-1})
4.0560	4.2024	21.13
4.2110	4.3573	17.63
4.3570	4.5034	15.20
4.5789	4.7253	11.87
4.7550	4.9014	9.05
4.9099	5.0563	6.10
4.9769	5.1233	4.82
5.0560	5.2024	4.13
5.2110	5.3573	2.56
5.3570	5.5034	1.71
5.5789	5.7253	0.74
3.5830	3.7294	31.52
3.7379	3.8843	28.31
3.8840	4.0304	24.80

TABLE: A44 Surface pressure vs. activity data

Compd	Temp	Medium	$-\log f_{X^+}$	$\gamma^\circ(mNm^{-1})$
$C_{12}S$	25°C	0.5 M NaCl	0.1500	72.89

$-\log C_{R^-}$	$-\log a_{R^-}$	$\pi(mNm^{-1})$
4.0560	4.2060	20.12
4.2110	4.3609	16.60
4.3570	4.5070	13.87
4.5789	4.7289	10.16
4.7550	4.9050	7.53
4.9099	5.0599	5.30
4.9769	5.1269	4.05
5.0560	5.2060	3.53
5.2110	5.3609	2.06
5.3570	5.5070	1.43
5.5789	5.7289	0.81
3.5830	3.7330	30.60
3.7379	3.8879	26.73
3.8840	4.0340	23.06

TABLE: A45 Surface pressure vs. activity data

Compd	Temp	Medium	-log f_{X^+}	γ° (mNm^{-1})
$C_{12}S$	40°C	0.5 M NaCl	0.1544	70.49

-log C_{R^-}	-log a_{R^-}	π (mNm^{-1})
4.0560	4.2104	17.69
4.2110	4.3653	14.24
4.3570	4.5114	11.69
4.5789	4.7333	8.65
4.7550	4.9094	6.21
4.9099	5.0643	4.30
4.9769	5.1313	3.01
5.0560	5.2104	2.61
5.2110	5.3653	1.37
5.3570	5.5114	0.99
5.5789	5.7333	0.24
3.5830	3.7374	27.89
3.7379	3.8923	24.60
3.8840	4.0384	21.08
2.7940	2.9484	39.04
2.6850	2.8394	38.94
2.9860	3.1404	38.56
3.1620	3.3164	37.72
3.4172	3.5716	32.43

TABLE: A46 Surface pressure vs. activity data

Compd	Temp:	Medium	γ° (mNm^{-1})	
$C_{10}EOS$	10°C	H_2O	74.24	
-log C	-log f_{R^-}	-log f_{X^+}	-log a	π(mNm^{-1})
1.6380	0.0580	0.0656	1.6997	33.01
1.7980	0.0517	0.0557	1.8510	28.47
2.2199	0.0334	0.0358	2.2550	14.60
2.1110	0.0373	0.0402	2.1497	17.26
1.9801	0.0423	0.0462	2.0241	21.98
1.9050	0.0454	0.0499	1.9530	24.91

TABLE: A47 Surface pressure vs. activity data

Compd	Temp:	Medium	γ° (mNm^{-1})	
$C_{10}EOS$	25°C	H_2O	72	
-log C	-log f_{R^-}	-log f_{X^+}	-log a	π(mNm^{-1})
1.6380	0.0594	0.0671	1.7012	30.99
1.7980	0.0514	0.0571	1.8522	30.40
2.2199	0.0343	0.0367	2.2550	16.69
2.1111	0.0381	0.0412	2.1506	19.60
1.9000	0.0467	0.0514	1.9490	27.21
1.9800	0.0433	0.0473	2.0250	24.21
2.0600	0.0401	0.0435	2.1017	21.40

TABLE: A48 Surface pressure vs. activity data

Compd	Temp:	Medium	γ° (mNm^{-1})
$C_{10}EOS$	40°C	H_2O	69.63

-log C	-log f_{R^-}	-log f_{X^+}	-log a	π(mNm^{-1})
1.6380	0.0611	0.0691	1.7031	28.85
1.7980	0.0529	0.0588	1.8538	28.89
2.2199	0.0353	0.0378	2.2564	15.51
2.2111	0.0393	0.0424	2.1518	18.25
1.8701	0.0495	0.0546	1.9220	27.58
1.9800	0.0446	0.0487	2.0266	22.83
1.5811	0.0643	0.0732	1.6497	28.95

TABLE: A49 Surface pressure vs. activity data

Compd	Temp	Medium	-log f_{X^+}	γ°(mNm^{-1})
$C_{10}EOS$	10°C	0.1 M NaCl	0.0967	74.36

-log C_{R^-}	-log a_{R^-}	π(mNm^{-1})
2.1101	2.2071	36.55
2.4000	2.4970	31.43
2.8071	2.9040	22.27
2.9041	3.0010	20.45
2.6341	2.7271	26.80
2.1601	2.2571	36.63

TABLE: A50 Surface pressure vs. activity data

Compd	Temp	Medium	-log f_{X^+}	γ°(mNm^{-1})
C_{10}EOS	25°C	0.1 M NaCl	0.0990	72.11

-log C_{R^-}	-log a_{R^-}	π(mNm^{-1})
2.1101	2.2089	34.71
2.4000	2.4991	35.51
2.8071	2.9061	22.51
2.9043	3.0031	20.62
2.6301	2.7291	26.95
2.1600	2.2591	34.77

TABLE: A51 Surface pressure vs. activity data

Compd	Temp	Medium	-log f_{X^+}	γ°(mNm^{-1})
C_{10}EOS	40°C	0.1 M NaCl	0.1019	69.74

-log C_{R^-}	-log a_{R^-}	π(mNm^{-1})
2.1101	2.2120	32.96
2.4001	2.5021	30.67
2.8071	2.9091	21.25
2.9043	2.0060	19.30
2.6301	2.7320	25.66
2.1600	2.2621	33.08

TABLE: A52 Surface pressure vs. activity data

Compd	Temp	Medium	-log f_{X^+}	γ°(mNm^{-1})
C_{10}EOS	10°C	0.5 M NaCl	0.1464	75.20

-log C_R-	-log a_R-	π(mNm^{-1})
2.8200	2.9664	36.52
3.1201	3.2661	29.61
3.4305	3.5760	23.30
2.9370	3.8200	33.93

TABLE: A53 Surface pressure vs. activity data

Compd	Temp	Medium	-log f_{X^+}	γ°(mNm^{-1})
C_{10}EOS	25°C	0.5 M NaCl	0.1500	72.93

-log C_R-	-log a_R-	π(mNm^{-1})
2.5670	2.7170	38.96
2.8200	2.9700	36.34
3.1202	3.2710	29.28
3.4311	3.5800	23.04
2.6400	2.7901	38.95
2.9371	3.0872	33.49

TABLE: A54 Surface pressure vs. activity data

Compd	Temp	Medium	-log f_{X^+}	γ°(mNm^{-1})
C_{10}EOS	40°C	0.5 M NaCl	0.1544	70.76

-log C_{R^-}	-log a_{R^-}	π(mNm^{-1})
2.5670	2.7214	33.10
2.8210	2.9744	35.77
3.1200	3.2744	27.83
3.4300	3.5844	21.49
2.6401	2.7944	37.75
2.9370	3.0914	32.10

TABLE: A55 Surface pressure vs. activity data

Compd	Temp:	Medium	γ° (mNm^{-1})	
$C_{12}EOS$	10°C	H_2O	74.25	
-log C	-log f_{R^-}	-log f_{X^+}	-log a	π(mNm^{-1})
2.5374	0.0242	0.0254	2.5623	27.27
2.6050	0.0254	0.0236	2.6281	25.14
2.7160	0.0201	0.0889	2.7365	21.46
2.8511	0.0174	0.0179	2.8677	17.10
2.9810	0.0151	0.0156	2.9954	12.95

TABLE: A56 Surface pressure vs. activity data

Compd	Temp:	Medium	γ° (mNm^{-1})	
$C_{12}EOS$	25°C	H_2O	72	
-log C	-log f_{R^-}	-log f_{X^+}	-log a	π(mNm^{-1})
2.4522	0.0272	0.0286	2.4800	29.66
2.5374	0.0247	0.0261	2.5630	26.74
2.5700	0.0239	0.0251	2.5945	26.02
2.7160	0.0205	0.0213	2.7369	21.18
2.8511	0.0178	0.0184	2.8681	16.59
2.9810	0.0154	0.0159	2.9957	12.62

TABLE: A57 Surface pressure vs. activity data

Compd	Temp:	Medium	γ° (mNm^{-1})
$C_{12}EOS$	40°C	H_2O	69.63

-log C	-log f_{R^-}	-log f_{X^+}	-log a	π(mNm^{-1})
2.5374	0.0255	0.0268	2.4808	27.23
2.7160	0.0211	0.0220	2.5636	24.71
2.7160	0.0183	0.0189	2.7376	18.82
2.8501	0.0159	0.0164	2.8686	14.33
2.9800	0.0495	0.0545	2.9962	10.76

TABLE: A58 Surface pressure vs. activity data

Compd	Temp	Medium	-log f_{X^+}	γ°(mNm^{-1})
$C_{12}EOS$	10°C	0.1 M NaCl	0.0967	74.36

-log C_{R^-}	-log a_{R^-}	π(mNm^{-1})
3.8667	3.9634	25.69
4.0325	4.1309	22.43
4.1677	4.2644	19.51
4.2650	4.3613	17.31
4.3895	4.4863	14.61

TABLE: A59 Surface pressure vs. activity data

Compd	Temp	Medium	-log f_{X^+}	γ°(mNm^{-1})
C_{12}EOS	25°C	0.1 M NaCl	0.0990	74.36

-log C_{R^-}	-log a_{R^-}	π(mNm^{-1})
3.8667	3.9657	25.21
4.0325	4.1332	21.29
4.1677	4.2667	18.39
4.2650	4.3636	16.14
4.3895	4.4885	13.63

TABLE: A60 Surface pressure vs. activity data

Compd	Temp	Medium	-log f_{X^+}	γ°(mNm^{-1})
C_{12}EOS	40°C	0.1 M NaCl	0.1019	69.74

-log C_{R^-}	-log a_{R^-}	π(mNm^{-1})
3.5656	3.6676	28.18
3.8667	3.9686	22.04
4.0325	4.1361	18.79
4.1677	4.2696	15.75
4.2650	4.3665	14.03
4.3895	4.4916	11.74

TABLE: A61 Surface pressure vs. activity data

Compd	Temp	Medium	-log f_{X^+}	γ°(mNm^{-1})
C_{12}EOS	10°C	0.5 M NaCl	0.1464	75.20

-log C_{R^-}	-log a_{R^-}	π(mNm^{-1})
4.5377	4.6841	25.50
4.6346	4.7810	22.82
4.6926	4.8389	21.47
4.8387	4.9851	18.48
4.9356	5.0820	16.72

TABLE: A62 Surface pressure vs. activity data

Compd	Temp	Medium	-log f_{X^+}	γ°(mNm^{-1})
C_{12}EOS	25°C	0.5 M NaCl	0.1500	72.93

-log C_{R^-}	-log a_{R^-}	π(mNm^{-1})
4.5377	4.6876	23.90
4.6346	4.7845	21.55
4.6926	4.8426	19.90
4.8387	4.9887	17.13
4.9356	5.0856	15.17

TABLE: A63 Surface pressure vs. activity data

Compd	Temp	Medium	-log f_{X^+}	$\gamma^{\circ}(mNm^{-1})$
$C_{12}EOS$	40°C	0.5 M NaCl	0.1544	70.76

-log C_{R^-}	-log a_{R^-}	$\pi(mNm^{-1})$
4.2366	4.3910	28.37
4.5377	4.6921	21.20
4.6346	4.7889	19.19
4.6926	4.8469	17.67
4.8387	4.9931	14.96
4.9356	5.0900	12.98

TABLE: A64 Surface pressure vs. activity data

Compd	Temp:	Medium	γ^{o}(mNm^{-1})	
C_{12}EOSO	10°C	H_2O	74.20	
-log C	-log f_{R^-}	-log f_{X^+}	-log a	π(mNm^{-1})
1.9748	.04250	.04643	2.0193	35.55
2.1189	.03696	.0399	2.1573	35.40
2.2748	.03162	.03375	2.3075	35.16
2.4089	.02762	.02923	2.4373	33.46
2.5582	.02367	.02484	2.5824	28.00
2.6459	.02159	.02256	2.6680	25.73
2.6496	.02151	.02247	2.6716	25.41
2.6986	.02043	.02129	2.7195	23.80
2.7928	.01848	.01919	2.8116	20.80
3.0287	.01434	.01476	3.0432	14.95
3.2017	.01187	.01216	3.2137	13.38
3.2400	.01138	.01164	3.2515	10.38
3.2400	.01138	.01164	3.2515	11.18
3.2800	.01089	.01113	3.2910	10.09
3.3028	.01062	.01085	3.3135	9.48
3.3476	.01012	.01032	3.3578	8.81
3.3500	.01008	.01029	3.3602	8.72
3.4303	.00922	.00940	2.4396	6.34
3.4303	.00922	.00940	3.4396	5.70
3.5800	.00781	.00793	3.5879	4.32

3.6835	.00695	.00705	3.6905	3.30
3.7528	.00644	.00652	3.7593	3.01
3.8825	.00556	.00563	3.8880	1.82

TABLE: A65 Surface pressure vs. activity data

Compd	Temp:	Medium	γ° (mNm^{-1})	
$C_{12}EOSO$	25°C	H_2O	72	
-log C	-log f_{R^-}	-log f_{X^+}	-log a	π(mNm^{-1})
1.9748	.0435	.04755	2.0203	3.30
2.1189	.0378	.04086	2.1583	32.88
2.2748	.0324	.03456	2.3083	32.59
2.4089	.0283	.02994	2.4380	32.38
2.5582	.0242	.02544	2.5830	27.83
2.6459	.0221	.02311	2.6685	26.05
2.6496	.0220	.02301	2.6721	26.00
2.6986	.0209	.02180	2.7199	23.24
3.0287	.0147	.01511	3.0436	14.00
3.2400	.0116	.01192	3.2518	9.15
3.2400	.0116	.01192	3.2518	9.87
3.2800	.0111	.01140	3.2913	8.67
3.3028	.0109	.01110	3.3138	8.61
3.3476	.0103	.01057	3.3580	7.73
3.3500	.0103	.01054	3.3604	7.61
3.4303	.0095	.00962	3.4398	5.27
3.4303	.0094	.00962	3.4398	5.14
3.5800	.0080	.00812	3.5880	3.87
3.6835	.0071	.00722	3.6907	2.61
3.7528	.0066	.00668	3.7594	2.39

TABLE: A66 Surface pressure vs. activity data

Compd	Temp:	Medium	γ° (mNm^{-1})	
$C_{12}EOSO$	40°C	H_2O	69.63	
-log C	-log f_R^-	-log f_X^+	-log a	π(mNm^{-1})
1.9748	.04481	.04895	2.0216	30.56
2.1189	.03897	.04210	2.1594	30.43
2.2748	.03333	.03558	2.3093	30.17
2.4089	.02912	.03082	2.4385	29.43
2.5582	.02496	.02619	2.5938	24.82
2.6459	.02268	.02380	2.6692	22.93
2.6496	.02268	.02370	2.6728	22.28
2.6986	.02154	.02245	2.7206	20.72
2.7928	.01949	.02023	2.8127	17.87
3.0287	.01511	.01556	3.0155	11.43
3.2400	.01200	.01227	3.2521	6.94
3.2400	.01200	.01227	3.2521	6.33
3.2800	.01148	.01174	3.2916	7.12
3.3028	.01120	.01144	3.3141	6.81
3.3476	.01066	.01088	3.3584	6.18
3.3500	.01063	.01085	3.3607	5.81
3.4303	.00972	.00991	3.4401	3.85
3.4303	.00973	.00991	3.4401	3.78
3.5800	.00823	.00836	3.5883	2.17
3.6835	.00733	.00744	3.6909	1.98

3.7528	.00679	.00687	3.7596	1.95
3.8825	.00587	.005933	3.8884	1.28

TABLE: A67 Surface pressure vs. activity data

Compd	Temp	Medium	-log f_{X^+}	γ°(mNm^{-1})
C_{12}EOSO	10°C	0.1 M NaCl	0.0967	74.36

-log C_R-	-log a_R-	π(mNm^{-1})
2.5518	2.6485	40.66
2.8570	2.9537	40.51
2.8570	2.9537	40.80
2.9580	3.0547	40.62
3.2520	3.3487	40.62
3.3520	3.4487	40.17
3.4097	3.5064	38.91
3.5558	3.6525	35.31
3.8580	3.9547	29.21
3.9301	4.0268	27.73
4.0787	4.1754	24.08
4.1590	4.2557	23.15
4.3490	4.4457	18.47
4.5320	4.6287	16.20
4.7540	4.8507	12.20
4.9301	5.0268	9.45
5.0850	5.1817	7.78
5.2310	5.3277	6.04
5.3280	5.4247	4.35
5.4529	5.5496	3.34

5.6290	5.7257	2.17
5.9301	6.0268	1.16
6.3280	6.4247	0.33

TABLE: A68 Surface pressure vs. activity data

Compd	Temp	Medium	-log f_{X^+}	γ°(mNm^{-1})
C_{12}EOSO	25°C	0.1 M NaCl	0.0990	72.11

-log C_{R^-}	-log a_{R^-}	π(mNm^{-1})
2.5518	2.6508	38.67
2.8570	2.9560	38.52
2.9580	3.0570	38.78
2.9580	3.0570	38.56
3.2520	3.3510	38.50
3.3520	3.4510	38.33
3.4097	3.5087	37.50
3.5558	3.6548	34.12
3.8580	3.9570	27.60
3.9301	4.0291	26.67
4.0787	4.1777	22.43
4.1590	4.2580	21.46
4.3490	4.4480	17.08
4.5320	4.6310	14.64
4.7540	4.8530	10.70
4.9301	4.0291	26.67
5.0850	5.1840	6.73
5.2310	5.3300	5.36
5.3280	5.4270	3.73
5.4529	5.5519	2.87

5.6290	5.7280	1.82
5.9301	6.0291	0.88
6.3280	6.4270	0.14

TABLE: A69 Surface pressure vs. activity data

Compd	Temp	Medium	-log f_{X^+}	$\gamma°(mNm^{-1})$
$C_{12}EOSO$	40°C	0.1 M NaCl	0.1019	69.74

-log C_{R^-}	-log a_{R^-}	$\pi(mNm^{-1})$
2.5518	2.6537	36.54
2.8570	2.9589	36.30
2.8570	2.9589	36.48
2.9580	3.0599	36.43
3.2520	3.3539	36.39
3.3520	3.4539	36.23
3.4097	3.5116	34.54
3.4097	3.5116	34.35
3.5558	3.6577	30.82
3.5558	3.6577	31.09
3.8580	3.9599	23.93
3.9301	4.0320	23.60
4.0787	4.1806	20.06
4.1590	4.2609	18.92
4.3490	4.4509	14.59
4.5320	4.6339	12.43
4.7540	4.8559	8.92
4.9301	5.0320	6.47
5.0850	5.1869	4.74
5.2310	5.3329	3.95

5.3280	5.4299	3.04
5.4529	5.5548	2.16
5.6290	5.7309	1.46
5.9301	6.0320	0.48
6.3280	6.4299	0.14

TABLE: A70 Surface pressure vs. activity data

Compd	Temp	Medium	-log f_{X^+}	γ°(mNm^{-1})
C_{12}EOSO	10°C	0.5 M NaCl	0.1464	75.20

-log C_{R^-}	-log a_{R^-}	π(mNm^{-1})
3.0277	3.1741	44.66
3.3287	3.4751	44.66
3.3287	3.4751	44.19
3.6300	3.7764	32.08
3.9087	4.0551	43.41
3.9087	4.0551	44.10
3.9787	4.1251	42.90
4.1037	4.2501	38.78
4.1829	4.3293	37.05
4.2798	4.4262	34.41
4.4000	4.5464	32.06
4.5808	4.7272	26.94
4.8819	5.0283	21.66
5.1829	5.3293	15.03
5.4047	5.5511	10.36
5.5808	5.7272	7.92
5.6778	5.8242	6.12
5.6778	5.8242	6.61
5.7850	5.9314	5.08
5.8819	6.0283	4.15

5.9485	6.0949	2.90
5.9485	6.0949	3.14
6.0277	6.1741	2.03

TABLE: A71 Surface pressure vs. activity data

Compd	Temp	Medium	-log f_{X^+}	$\gamma°(mNm^{-1})$
$C_{12}EOSO$	25°C	0.5 M NaCl	0.1500	73.11

-log C_{R^-}	-log a_{R^-}	$\pi(mNm^{-1})$
3.0277	3.1777	43.10
3.3287	3.4787	43.00
3.3287	3.4787	42.46
3.6300	3.4787	42.57
3.8819	4.0319	42.42
3.9087	4.0587	41.89
3.9087	4.0587	42.54
3.9787	4.1287	41.04
4.1037	4.2537	37.18
4.1829	4.3329	35.22
4.2798	4.4298	32.85
4.4000	4.5500	29.97
4.5808	4.7308	25.36
4.8819	5.0319	19.64
5.1829	5.2219	13.45
5.4047	5.5547	9.41
5.5808	5.7308	6.91
5.6778	5.8278	5.26
5.6778	5.8278	6.01
5.7850	5.9350	4.25

5.8819	6.9319	3.22
5.9485	6.0985	2.51
5.9485	6.0985	2.72
6.0277	6.1777	1.80

TABLE: A72 Surface pressure vs. activity data

Compd	Temp	Medium	-log f_{X^+}	$\gamma°(mNm^{-1})$
$C_{12}EOSO$	40°C	0.5 M NaCl	0.1544	70.76

-log C_{R^-}	-log a_{R^-}	$\pi(mNm^{-1})$
3.0277	3.1821	40.84
3.3287	3.4831	40.68
3.6300	3.7844	40.68
3.8819	4.0363	39.42
3.9087	4.0631	38.50
3.9087	4.0631	38.59
3.9787	4.1331	37.19
4.1037	4.2581	33.74
4.1829	4.3373	32.21
4.2798	4.4342	29.56
4.4000	4.5544	28.55
4.5808	4.7352	22.11
4.8819	5.9363	16.49
5.1829	5.3373	11.15
5.4047	5.5591	6.96
5.5808	5.7351	5.03
5.6778	5.8322	3.79
5.6778	5.8322	4.11
5.7850	5.9394	3.11
5.8819	6.0363	2.52

5.9485	6.1029	1.64
5.9485	6.1029	1.83
6.0277	6.1821	1.46

TABLE: A73 Surface pressure vs. activity data

Compd	Temp:	Medium	γ° (mNm^{-1})
$C_{12}EO_2SO$	10°C	H_2O	74.25

-log C	-log f_{R^-}	-log f_{X^+}	-log a	π(mNm^{-1})
2.1258	0.0367	0.0396	2.1639	32.60
2.4145	0.0275	0.0270	2.4428	32.59
2.6137	0.0223	0.0234	2.6370	29.43
2.7030	0.0203	0.0220	2.7238	25.13
2.7136	0.0201	0.0209	2.7341	27.95
2.8226	0.0179	0.0185	2.8408	22.46
2.8782	0.0169	0.0174	2.8954	21.84
2.9818	0.0151	0.0155	2.9971	19.53
3.1220	0.0129	0.0133	3.1351	18.16
3.2610	0.0111	0.0114	3.2722	14.50
3.3356	0.0102	0.0105	3.3459	12.94
3.4040	0.0095	0.0097	3.4136	8.92
3.6946	0.0069	0.0070	3.7015	6.05
3.7051	0.0068	0.0069	3.7119	7.02
3.8446	0.0058	0.0059	3.8504	3.40
3.9599	0.0051	0.0051	3.9650	3.70
4.0843	0.0044	0.0045	4.0888	2.07
4.1876	0.0039	0.0039	4.1916	1.66
4.3179	0.0034	0.0342	4.3213	1.76

TABLE: A74 Surface pressure vs. activity data

Compd	Temp:	Medium	γ° (mNm^{-1})	
$C_{12}EO_2SO$	25°C	H_2O	72	
-log C	-log f_{R^-}	-log f_{X^+}	-log a	π(mNm^{-1})
2.1258	0.0376	0.0406	2.1649	30.50
2.4145	0.0281	0.0297	2.4434	30.60
2.6132	0.0229	0.0239	2.6371	29.09
2.7030	0.2082	0.0219	2.7243	24.96
2.7136	0.0206	0.0214	2.7346	26.38
2.8226	0.0183	0.0190	2.8413	22.91
2.8782	0.0173	0.0179	2.8958	21.20
2.9818	0.0154	0.0159	2.9975	19.08
3.1220	0.0133	0.1362	3.1354	16.77
3.2610	0.0114	0.0116	3.2725	13.94
3.3356	0.0105	0.0107	3.3462	12.12
3.4040	0.0097	0.0099	3.4138	10.10
3.6946	0.0070	0.0071	3.7017	4.53
3.1051	0.0069	0.0070	3.7121	6.28
3.8446	0.0059	0.0060	3.8506	3.06
3.9599	0.0052	0.0053	3.9651	3.24
4.0843	0.0045	0.0046	4.0889	1.79
4.1876	0.0040	0.0041	4.1917	1.55
4.3179	0.0029	0.0035	4.3211	1.51

TABLE: A75 Surface pressure vs. activity data

Compd	Temp:	Medium	γ° (mNm^{-1})	
$C_{12}EO_2SO$	40°C	H_2O	69.63	
-log C	-log f_{R^-}	-log f_{X^+}	-log a	π(mNm^{-1})
2.1258	0.0387	0.0418	2.1660	28.77
2.4145	0.0290	0.0306	2.4443	28.53
2.6137	0.0235	0.0246	2.6378	27.21
2.7030	0.0214	0.0223	2.7249	23.08
2.7136	0.0212	0.0221	2.7316	23.77
2.8226	0.0189	0.0196	2.8418	20.93
2.8782	0.0178	0.0184	2.8963	18.57
2.9813	0.0159	0.0164	2.9980	17.09
3.1220	0.0137	0.0140	3.1358	13.83
3.2610	0.0117	0.0120	3.2729	11.48
3.3356	0.0108	0.1102	3.3465	10.52
3.4040	0.0100	0.0102	3.4141	8.38
3.5544	0.0085	0.0086	3.5629	6.78
3.6946	0.0072	0.0073	3.7019	6.75
3.8446	0.0061	0.0062	3.8508	2.04
3.9599	0.0054	0.0054	3.9653	2.59
4.0843	0.0467	0.0047	4.0889	1.49
4.1876	0.0042	0.0042	4.1918	1.19
4.3179	0.0035	0.0036	4.3215	1.39

TABLE: A76 Surface pressure vs. activity data

Compd	Temp	Medium	-log f_{X^+}	γ°(mNm^{-1})
$C_{12}EO_2SO$	10°C	0.1 M NaCl	0.0967	74.37

-log C_{R^-}	-log a_{R^-}	π(mNm^{-1})
2.5518	2.6485	40.66
3.2170	3.3137	38.07
3.3419	3.4386	37.91
3.5180	3.6147	36.99
3.6149	3.7116	35.02
3.7399	3.8366	32.90
3.9160	4.0127	29.04
4.2070	4.3037	23.47
4.4388	4.5355	19.47
4.5180	4.6147	18.81
4.6150	4.7117	16.30
4.7400	4.8367	14.51
4.9160	5.0127	12.34
5.2170	5.3137	8.26
5.3139	5.4106	7.17
5.5400	5.6367	4.40
5.6149	5.7116	3.78
5.7118	5.8085	3.09
5.8368	5.9335	2.36
6.0130	6.1097	1.02

TABLE: A77 Surface pressure vs. activity data

Compd	Temp	Medium	-log f_{X^+}	γ°(mNm^{-1})
$C_{12}EO_2SO$	25°C	0.1 M NaCl	0.0990	72.28

-log C_{R^-}	-log a_{R^-}	π(mNm^{-1})
3.2170	3.3160	36.70
3.3419	3.4409	36.40
3.5180	3.6170	36.28
3.6149	3.7139	34.54
3.7399	3.8389	31.73
3.9160	4.0150	28.26
4.2070	4.3060	22.63
4.4388	4.5378	18.55
4.5780	4.6170	17.49
4.6150	4.7140	15.51
4.7400	4.8390	13.58
4.9160	5.0150	11.16
5.2170	5.3160	7.43
5.3139	5.4129	6.44
5.5400	5.6390	3.76
5.6149	5.7139	3.07
5.7118	5.8108	2.57
5.8368	5.9358	2.06
6.0100	6.1090	1.14
6.3130	6.4129	0.44

TABLE: A78 Surface pressure vs. activity data

Compd	Temp	Medium	-log f_{X^+}	$\gamma°$(mNm^{-1})
$C_{12}EO_2SO$	40°C	0.1 M NaCl	0.1019	69.80

-log C_{R^-}	-log a_{R^-}	π(mNm^{-1})
3.2170	3.3189	34.78
3.3419	3.4438	34.84
3.5180	3.6199	34.75
3.6149	3.7168	32.84
3.7399	3.8418	29.93
3.9160	4.0179	26.60
4.2070	4.3089	21.05
4.4388	4.5407	17.14
4.5180	4.6199	16.05
4.6150	4.7169	13.98
4.7400	4.8419	12.01
4.9160	5.0179	10.04
5.2170	5.3189	5.17
5.3139	5.4158	5.19
5.5400	5.6419	3.40
5.6149	5.7168	2.50
5.7118	5.8137	2.12
5.8368	5.9387	1.55
6.0100	6.1119	0.73
6.3139	6.4158	0.31

TABLE: A79 Surface pressure vs. activity data

Compd	Temp	Medium	-log f_{X^+}	γ°(mNm^{-1})
$C_{12}EO_2SO$	10°C	0.5 M NaCl	0.1464	69.80

-log C_{R^-}	-log a_{R^-}	π(mNm^{-1})
3.9159	4.0623	41.70
3.9573	4.1037	41.43
4.0100	4.1564	40.86
4.1377	4.2841	38.00
4.3130	4.4594	34.89
4.4388	4.5852	32.12
4.6150	4.7614	28.10
4.9159	5.0623	22.59
5.1376	5.2840	17.97
5.2100	5.3564	15.60
5.4388	5.5852	13.28
5.6149	5.7613	10.09
5.8367	5.9831	6.46
6.0128	5.1592	4.36
6.1677	6.3141	2.03
6.2347	6.3811	1.40
6.3138	6.4602	2.03
6.4107	6.5571	1.08

TABLE: A80 Surface pressure vs. activity data

Compd	Temp	Medium	-log f_{X^+}	γ°(mNm^{-1})
$C_{12}EO_2SO$	25°C	0.5 M NaCl	0.1500	73.06

-log C_{R^-}	-log a_{R^-}	π(mNm^{-1})
3.9159	4.0659	40.10
3.9573	4.1073	40.00
4.0100	4.1600	39.66
4.1377	4.2877	37.52
4.3130	4.4630	34.04
4.4388	4.5888	31.17
4.6150	4.7650	27.42
4.9159	5.0659	21.47
5.1376	5.2876	17.02
5.2100	5.3600	14.99
5.4388	5.5888	12.42
5.6149	5.7649	9.19
5.8367	5.9867	6.19
6.0128	6.1628	4.16
6.1677	6.3177	2.10
6.2347	6.3847	2.71
6.3138	6.4738	1.66
6.4107	6.5607	1.16

TABLE: A81 Surface pressure vs. activity data

Compd	Temp	Medium	-log f_{X^+}	γ°(mNm^{-1})
$C_{12}EO_2SO$	40°C	0.5 M NaCl	0.1544	70.66

-log C_R-	-log a_R-	π(mNm^{-1})
3.9159	4.0703	38.48
3.9573	4.1117	38.27
4.0100	4.1644	37.45
4.1377	4.2921	35.42
4.3130	4.4674	31.72
4.4388	4.5932	29.03
4.6150	4.7694	25.11
4.9159	5.0703	19.36
5.1376	5.2920	14.82
5.2100	5.3644	13.00
5.4388	5.5932	10.28
5.6149	5.7693	7.34
5.8367	5.9911	4.56
6.0128	6.1672	2.84
6.1677	6.3221	1.59
6.2347	6.3891	0.98
6.3138	6.4682	0.96
6.4107	6.5651	0.84

TABLE: A82 Surface pressure vs. activity data

log (CMC.f_-) vs log ($C_{X^+}.f_+$) data for $C_{10}S$

T	I	-log CMC	-log C_{X+}	-log f_-	-log f_+
10°C	H_2O	1.3194	1.3194	0.0759	0.0894
	0.1 M	1.5902	1.0000	0.0966	0.1207
	0.5 M	2.0998	0.3010	0.1464	0.2067
25°C	H_2O	1.3690	1.3690	0.0746	0.0873
	0.1 M	1.6754	1.0000	0.0990	0.1226
	0.5 M	2.1400	0.3010	0.1500	0.2117
40°C	H_2O	1.4000	1.4000	0.0749	0.0873
	0.1 M	1.7396	1.0000	0.1019	0.1262
	0.5 M	2.1847	0.3010	0.1544	0.2179

TABLE: A83 Surface pressure vs. activity data

log (CMC.f_-) vs log ($C_{X^+}.f_+$) data for $C_{12}S$

T	I	-log CMC	-log C_{X+}	-log f_-	-log f_+
25°C	H_2O	1.9060	1.9060	0.0464	0.0510
	0.1 M	2.6078	1.0000	0.0990	0.1226
	0.5 M	-.----	--.--	--.--	--.--
40°C	H_2O	1.9427	1.9427	0.0462	0.0406
	0.1 M	2.6157	1.000	0.1019	0.12625
	0.5 M	3.0996	0.3010	0.1544	0.2179

TABLE: A84 Surface pressure vs. activity data

log (CMC.f_-) vs log ($C_{X^+}.f_+$) data for $C_{10}EOS$

T	I	-log CMC	-log C_{X+}	-log f_-	-log f_+
10°C	H_2O	1.6870	1.6870	0.0555	0.0624
	0.1 M	2.1870	1.0000	0.0966	0.0120
25°C	H_2O	1.8070	1.8000	0.0514	0.0571
	0.1 M	2.2600	1.0000	0.0990	0.0300
	0.5 M	2.6870	0.3010	0.1500	0.2110
40°C	H_2O	1.8120	1.8150	0.0522	0.0579
	0.1 M	2.2970	1.0000	0.1019	0.1262
	0.5 M	2.7000	0.3010	0.1544	0.2179

TABLE: A85 Surface pressure vs. activity data

log (CMC.f_-) vs log ($C_{X^+}.f_+$) data for $C_{12}EOSO$

T	I	-log CMC	-log C_{X+}	-log f_-	-log f_+
10°C	H_2O	2.3247	2.3247	0.0300	0.3200
	0.1 M	3.3170	1.0000	0.0966	0.0120
	0.5 M	3.8660	0.3010	0.1464	0.2067
25°C	H_2O	2.4074	2.4074	0.0283	0.0300
	0.1 M	3.3659	1.0000	0.0990	0.1226
	0.5 M	3.8830	0.3010	0.1500	0.2117
40°C	H_2O	2.3826	2.3826	0.0299	0.0317
	0.1 M	3.3100	1.0000	0.1019	0.1262
	0.5 M	3.8170	0.3010	0.1544	0.2179

TABLE: A86 Surface pressure vs. activity data

log (CMC.f_-) vs log ($C_{X^+}.f_+$) data for $C_{12}EO_2SO$

T	I	-log CMC	-log C_{X+}	-log f_-	-log f_+
10	H_2O	2.5100	2.5100	0.0249	0.0262
	0.1 M	3.5000	1.0000	0.0966	0.0120
	0.5 M	3.9600	0.3010	0.1464	0.2067
25	H_2O	2.5400	2.5400	0.0469	0.0259
	0.1 M	3.5300	1.0000	0.9900	0.1226
	0.5 M	3.9801	0.3010	0.1500	0.2117
40	H_2O	2.5560	2.5560	0.0250	0.0263
	0.1 M	3.5501	1.0000	0.1019	0.1262
	0.5 M	3.9901	0.3010	0.1544	0.2179

TABLE: B1, Surface tension vs concentration data for EO_2 in water

C, (mol $dm^{-3}x10^3$)	γ (mNm^{-1}) 10°C	25°C	40°C	-log C
10.349	--.--	26.32	--.--	3.9851
9.3110	27.10	--.--	25.95	4.0310
6.3008	27.05	26.30	--.--	4.2006
4.4658	28.01	26.15	26.04	4.3501
3.8908	--.--	26.58	--.--	4.4100
3.5017	--.--	26.86	--.--	4.4557
3.1989	--.--	26.71	--.--	4.4950
3.1622	29.40	--.--	--.--	4.5000
2.9512	--.--	27.21	27.27	4.5300
2.2908	32.71	--.--	--.--	4.6400
2.0137	34.30	29.84	--.--	4.6960
0.9143	45.36	41.19	42.19	5.0389
0.4581	--.--	49.71	49.34	5.3390

TABLE: B2, Surface tension vs concentration data for EO3 in water

C, (mol $dm^{-3}x10^{3}$)	γ (mNm^{-1}) 10°C	25°C	40°C	-log C
22.3870	29.00	--.--	26.40	3.65
14.9620	--.--	27.68	--.--	3.8290
8.7096	28.92	27.70	26.51	4.06
5.3579	--.--	27.75	--.--	4.271
4.2452	--.--	28.80	--.--	4.3721
4.7863	--.--	29.80	--.--	4.3721
3.8019	33.75	30.81	29.00	4.42
2.6302	--.--	34.20	--.--	4.580
2.4547	38.50	--.--	33.92	4.610
1.6218	--.--	40.40	--.--	4.790
1.3963	--.--	40.28	--.--	4.855
1.2560	--.--	42.14	--.--	4.901
1.1220	46.16	--.--	41.40	4.950
0.9290	--.--	44.57	--.--	5.032
0.6280	--.--	48.27	--.--	5.202
0.4785	54.82	--.--	49.33	5.3201
0.4677	53.71	53.01	51.20	5.3300
0.3251	--.--	54.40	--.--	5.4880
0.3162	--.--	55.30	--.--	5.5000
0.2323	--.--	58.90	--.--	5.6340

TABLE: B3, Surface tension vs concentration data for EO4 in water

C, (mol $dm^{-3}x10^{3}$)	γ (mNm^{-1}) 10°C	25°C	40°C	-log C
22.3820	30.15	28.61	27.61	2.6501
11.4280	30.22	28.50	27.59	3.9420
5.3703	--.--	--.--	--.--	--.--
3.8708	34.21	30.21	30.65	4.2700
3.8708	36.89	33.28	30.84	4.4122
1.9350	37.88	32.82	30.37	4.4122
1.9350	--.--	39.71	37.91	4.7133
0.9601	43.90	39.52	37.61	4.7133
0.3871	50.18	45.36	43.69	5.0177
0.3890	--.--	53.51	43.70	5.4122

TABLE: B4, Surface tension vs concentration data for EO5 in water

C, (mol $dm^{-3}x10^{3}$)	γ (mNm^{-1}) 10°C	25°C	40°C	-log C
23.7130	32.40	30.56	28.45	3.6250
11.7220	32.45	30.50	28.50	3.9310
6.8391	--.--	30.45	--.--	4.1650
5.8210	35.71	31.40	29.00	4.2350
3.7325	--.--	34.69	--.--	4.4280
2.6302	42.32	--.--	34.59	4.5800
1.8620	--.--	41.03	--.--	4.7300
1.8620	--.--	40.64	--.--	4.7300
1.3182	47.86	--.--	41.50	4.8800
0.9290	--.--	46.76	--.--	5.0320
0.9290	--.--	45.78	--.--	5.0320
0.6607	52.70	--.--	47.45	5.1800
0.3698	--.--	53.54	--.--	5.4320
0.3699	--.--	52.39	--.--	5.4320

TABLE: B5, Surface tension vs concentration data for EO7 in water

C, (mol $dm^{-3} x10^5$)	γ (mNm^{-1}) 10°C	25°C	40°C	-log C
164.05	36.05	33.48	31.92	2.7850
54.701	36.10	33.63	31.75	3.2620
23.388	35.98	33.83	31.83	3.6310
13.740	36.00	33.42	31.80	3.8620
7.4131	39.05	34.40	31.01	4.1300
5.8479	--.--	36.42	--.--	4.2330
5.1880	--.--	36.47	--.--	4.2850
5.6221	41.25	36.20	33.05	4.2501
2.9512	45.44	--.--	37.78	4.5300
2.9512	--.--	41.00	--.--	4.5300
1.4791	49.95	46.32	42.63	4.8300
2.5941	--.--	42.10	--.--	4.5860
1.2971	--.--	46.98	--.--	4.8870
1.2971	--.--	46.74	--.--	4.8870
0.7413	53.67	50.27	47.53	5.1300
0.5188	--.--	52.43	--.--	5.2850
0.2951	58.62	--.--	53.02	5.5300

TABLE: B6, Surface tension vs concentration data for EO8 in water

C, (mol $dm^{-3} x 10^5$)	γ (mNm^{-1}) 10°C	25°C	40°C	-log C
19.4980	36.98	34.60	32.37	3.7200
12.3020	--.--	34.67	--.--	3.9100
9.3540	40.42	35.17	33.12	4.0290
7.5683	--.--	37.06	--.--	4.1210
7.0794	42.95	37.45	34.05	4.1500
3.4665	--.--	41.71	--.--	4.4601
3.0199	46.76	42.60	29.42	4.5200
2.2908	48.83	--.--	41.44	4.6400
1.8832	--.--	46.64	--.--	4.7257
1:5135	51.24	46.15	44.28	4.8200
0.7497	54.97	51.32	48.33	5.1251
0.3794	--.--	55.01	--.--	5.4209

TABLE: B7, Surface tension vs concentration data for C_8BMT in water

C, (mol $dm^{-3}x10^3$)	γ (mNm^{-1}) 10°C	25°C	40°C	-log C
2.5118	--.--	57.67	--.--	2.6000
2.1877	--.--	58.75	--.--	2.6600
3.3884	57.64	55.81	54.71	2.4700
1.1481	49.32	47.41	46.30	1.9400
19.9500	45.33	43.60	42.41	1.7000

TABLE: B8, Surface tension vs concentration data for C_{10}BMT in water

C, (mol $dm^{-3}x10^4$)	γ (mNm^{-1}) 10°C	25°C	40°C	-log C
69.183	--.--	--.--	38.23	2.16
63.095	--.--	--.--	34.54	2.20
50.118	--.--	--.--	34.50	2.30
38.904	--.--	--.--	34.54	2.41
30.199	--.--	--.--	34.50	2.52
12.022	--.--	45.45	44.81	2.92
8.9125	48.70	47.56	46.96	3.05
6.9183	50.44	49.07	48.56	3.16
5.6234	52.01	50.85	50.25	3.25
3.4673	55.27	54.00	53.38	3.46
1.3803	60.56	59.28	58.91	3.86

TABLE: B9, Surface tension vs concentration data for C_{12}BMT in water

C, (mol $dm^{-3} \times 10^5$)	γ (mNm^{-1}) 10°C	25°C	40°C	-log C
7.0794	--.--	46.01	45.90	4.15
3.1622	52.24	51.09	50.73	4.45
2.7542	53.81	52.97	52.27	4.56
1.7782	56.80	55.71	54.30	4.75
1.4125	58.31	57.09	56.75	4.85
7.0794	63.10	61.97	60.84	5.15

TABLE: B10, Surface tension vs concentration data for C_{12}BMG in water

C, (mol $dm^{-3} \times 10^4$)	γ (mNm^{-1}) 10°C	25°C	40°C	-log C
23.442	34.40	32.72	31.81	2.6300
10.471	34.51	32.93	32.00	2.9800
5.7016	35.22	32.96	32.71	3.2440
5.1168	37.22	33.51	32.01	3.2910
2.3496	41.42	39.07	37.90	3.6290
1.5995	44.31	41.72	40.98	3.7960
0.4898	52.91	50.53	54.81	4.3100
0.2290	57.86	55.95	49.61	4.6400

TABLE: B11, Surface tension vs concentration data for C_{10}BMG in water

	γ (mNm^{-1})			
C, (mol $dm^{-3}x10^{3}$)	10°C	25°C	40°C	-log C
10.2329	35.53	34.02	33.24	1.99
19.9526	35.60	34.13	33.30	1.70
3.4673	39.95	36.78	35.51	2.46
2.0417	43.53	40.74	39.00	2.69
1.1749	47.56	44.84	43.53	2.93
3.4673	39.95	36.78	35.51	2.46
0.8318	49.52	46.96	45.32	3.08
0.5248	52.88	50.58	49.28	3.28

TABLE: B12, Surface tension vs concentration data for $C_{12}NCl$ in water

C, (mol $dm^{-3}x10^3$)	γ (mNm^{-1}) 10°C	25°C	40°C	-log C
42.599	44.76	43.73	42.90	1.3706
42.5991	44.45	43.71	42.55	1.3706
16.6648	44.70	43.74	42.87	1.7782
13.4555	48.13	46.05	44.08	1.8711
8.53100	52.75	50.78	49.34	2.0690
6.3694	56.28	54.98	53.62	2.1959
2.7548	64.92	62.98	61.42	2.5599
2.7548	64.27	63.00	61.66	2.5599
1.9829	66.92	65.05	63.46	2.7027
1.1127	--.--	68.64	--.--	2.9536
1.1127	--.--	68.55	--.--	2.9536
1.0183	70.70	68.57	66.42	2.9921
0.6230	71.76	69.71	67.44	3.2055
0.6231	71.99	69.75	67.38	3.2055
0.4754	72.72	70.45	68.18	3.3229
0.3023	73.01	70.86	68.38	3.5195

TABLE: B13, Surface tension vs concentration data for $C_{12}NCl$ in 0.1 M NaCl

C, (mol $dm^{-3}x10^4$)	γ (mNm^{-1}) 10°C	25°C	40°C	-log C
73.7220	42.71	41.90	40.85	2.1324
55.2960	42.98	41.99	40.78	2.2573
55.2960	42.71	41.92	40.72	2.2573
36.8630	45.27	43.61	42.07	2.4334
24.5750	48.52	46.75	45.68	2.6095
14.7430	51.84	49.80	48.31	2.8314
36.8630	60.80	59.16	57.84	3.4334
29.4910	61.80	59.90	58.81	3.5303
22.1150	63.62	62.04	60.69	3.6553
1.4743	51.84	49.80	48.31	2.8314
0.7372	68.03	16.28	64.35	4.1324
0.2949	71.11	69.18	67.12	4.5303
0.2949	70.87	68.71	67.21	4.5303
0.2949	70.87	68.71	67.21	4.5303
0.1474	72.35	70.16	68.18	4.8314
0.7372	73.21	71.20	69.20	5.1324
0.7372	72.99	70.91	68.76	5.1324

TABLE: B14, Surface tension vs concentration data for $C_{12}NCl$ in 0.5 M NaCl

C, (mol $dm^{-3} \times 10^4$)	γ (mNm^{-1}) 10°C	25°C	40°C	-log C
32.9450	41.02	40.09	38.92	2.4822
32.9450	--.--	40.02	38.84	2.4822
18.1210	41.21	40.00	38.83	2.7418
18.1210	40.83	40.10	38.81	2.7418
14.8680	43.06	41.00	40.20	2.8277
11.1530	45.07	43.48	42.61	2.9526
11.1530	44.80	42.98	42.02	2.9526
5.7095	50.00	48.80	42.40	3.2434
2.8549	55.37	53.80	52.60	3.5444
1.4275	59.14	57.89	56.64	3.8454
1.1420	60.14	58.42	57.41	3.9423
0.5709	63.90	62.85	61.39	4.2434
0.2857	67.97	65.83	64.27	4.5444
0.1142	70.00	68.61	66.79	4.9423
0.6588	72.09	70.44	68.52	5.1812
0.6589	72.17	70.67	68.40	5.1812
0.0571	72.15	70.53	68.52	5.2434
0.0571	72.15	70.53	68.56	5.2434

TABLE: B15, Surface tension vs concentration data for $C_{12}NBr$ in water

C, (mol $dm^{-3}x10^{3}$)	γ (mNm^{-1}) 10°C	25°C	40°C	-log C
29.4850	39.47	39.10	--.--	1.5304
31.5420	--.--	--.--	38.90	1.5011
14.7300	39.82	39.18	38.80	1.8318
9.8380	--.--	40.90	--.--	2.0071
9.1432	43.10	42.42	41.65	2.0389
8.2281	44.47	43.65	42.77	2.0847
6.7577	46.29	45.64	44.40	2.1702
6.4639	49.00	47.91	48.56	2.1895
5.0280	--.--	51.84	--.--	2.2986
4.9970	53.00	--.--	52.48	4.9970
4.5321	53.02	52.17	51.22	2.3437
3.0262	59.10	58.33	57.22	2.5191
2.9187	--.--	57.75	--.--	2.5348
2.0244	--.--	61.86	--.--	2.6937
2.0244	--.--	62.00	--.--	2.6937
1.5682	65.74	64.87	62.82	2.8046
1.5682	--.--	--.--	--.--	--.--
8.0612	--.--	68.44	--.--	3.0936
0.6428	71.68	69.64	67.54	3.1919
0.5022	--.--	69.94	--.--	3.2991
0.4185	72.42	71.18	68.25	3.3783
0.3523	72.97	71.35	67.90	3.4531

3.0853	73.09	70.78	68.68	0.3085
0.2783	70.95	70.95	--.--	3.5554
0.2782	--.--	70.90	--.--	3.5557
0.1762	72.90	70.71	68.40	3.6623

TABLE: B16, Surface tension vs concentration data for $C_{12}NBr$ in 0.1 M NaBr

C, (mol $dm^{-3}x10^{3}$)	γ (mNm^{-1}) 10°C	25°C	40°C	-log C
64.1210	37.75	37.16	36.45	2.1930
38.4760	37.89	37.22	36.55	2.4148
38.4760	37.65	37.12	36.46	2.4148
32.0620	37.90	37.21	36.55	2.4940
25.6500	38.34	37.67	37.38	2.5909
19.2390	40.60	39.93	39.52	2.7158
12.8260	43.84	43.64	43.02	2.8919
6.4121	49.35	49.03	48.22	3.1930
3.2062	54.75	53.84	53.71	3.4940
1.2826	61.22	59.89	59.59	3.8919
0.6412	65.42	64.58	63.86	4.1930
0.5130	66.53	65.84	64.80	4.2899
0.5130	66.23	--.--	64.28	4.2899
0.5098	--.--	64.80	--.--	4.2926
0.2565	69.57	68.76	67.02	4.5909
0.1539	71.56	70.03	68.31	4.8128
0.1539	31.14	69.00	67.84	4.8128
0.1026	72.52	70.90	68.76	4.9888

TABLE: B17, Surface tension vs concentration data for $C_{12}NBr$ in 0.5 M NaBr

C, (mol $dm^{-3} \times 10^3$)	γ (mNm^{-1}) 10°C	25°C	40°C	-log C
368.00	36.38	35.77	34.89	2.4332
184.37	36.28	35.44	34.68	2.7343
147.50	36.56	35.83	34.83	2.8312
111.76	--.--	35.40	--.--	2.9517
73.750	38.74	38.74	39.00	3.1322
36.880	44.28	44.17	44.06	3.4332
18.437	49.38	49.35	49.20	3.7343
11.176	53.51	53.40	53.02	3.9517
7.3756	57.34	57.21	56.99	4.1322
3.6880	62.24	61.80	61.66	4.4332
3.6880	62.10	61.46	61.39	4.4332
2.9505	62.91	--.--	--.--	4.5301
2.9322	--.--	61.96	61.83	4.5328
1.4750	67.49	66.90	65.98	4.8312
0.8851	69.84	68.71	67.68	5.0530
0.5901	71.41	70.26	68.59	5.2291
0.4426	72.45	71.35	69.14	5.3540
0.4426	72.10	70.28	69.18	5.3540

TABLE: B18, Surface tension vs concentration data for $C_{10}S$ in water

C, (mol $dm^{-3} x 10^3$)	γ (mNm^{-1}) 10°C	25°C	40°C	-log C
58.9658	41.15	40.90	40.22	1.2294
46.7735	44.63	--.--	40.61	1.3300
39.5731	44.83	42.49	40.62	1.4026
39.0481	--.--	--.--	41.57	1.4084
30.7256	47.59	45.07	44.06	1.5125
15.3638	58.05	56.41	54.71	1.8135
10.2424	63.09	61.13	59.57	1.9896
7.7481	65.30	63.48	61.57	2.1108
6.1404	67.30	65.51	63.54	2.2118
3.7153	71.25	68.51	66.28	2.4300
3.0732	70.94	68.83	66.55	2.5124
2.4547	72.15	69.48	67.50	2.6100
1.8620	72.86	70.27	68.21	2.7300
1.2302	73.12	70.87	68.62	2.9100
0.6146	73.66	71.37	68.92	3.2115

TABLE: B19, Surface tension vs concentration data for $C_{10}S$ in 0.1 M NaCl

C, (mol $dm^{-3} \times 10^3$)	γ (mNm^{-1}) 10°C	25°C	40°C	-log C
38.5479	40.16	39.50	38.90	1.4140
31.0957	39.98	39.41	38.76	1.5073
22.3872	41.02	39.78	38.83	1.6500
18.6638	42.96	39.88	38.45	1.7290
15.5597	45.02	42.41	40.17	1.8080
15.4882	44.80	41.70	41.02	1.8100
12.8529	47.23	45.07	43.13	1.8910
10.3753	48.06	46.03	43.88	1.9840
7.7803	50.94	47.87	46.09	2.1090
6.1659	52.60	51.09	47.80	2.2100
3.8547	57.60	55.00	52.87	2.4140
3.1117	59.02	56.77	55.21	2.5070
1.8663	62.07	59.52	58.45	2.7290
1.2445	64.44	62.54	61.03	2.9050
0.9333	66.37	64.28	62.75	3.0300
0.6223	68.24	66.16	64.59	3.2060
0.3112	71.20	68.58	65.92	3.5070
0.2489	71.38	69.10	66.50	3.6040
0.1991	72.12	70.11	67.69	3.7010
0.1742	72.50	70.23	67.70	3.7590
0.9954	73.08	70.66	68.63	4.0020

TABLE: B20, Surface tension vs concentration data for $C_{10}S$ in 0.5 M NaCl

C, (mol $dm^{-3}x10^4$)	γ (mNm^{-1}) 10°C	25°C	40°C	-log C
53.345	41.34	38.81	36.38	2.2729
35.563	45.50	43.23	41.64	2.4490
26.674	48.36	46.00	45.56	2.5739
21.379	50.02	47.25	46.05	2.6700
10.668	56.23	54.76	53.52	2.9719
7.4679	58.97	57.44	56.60	3.1268
5.3493	61.90	60.23	59.18	3.2717
4.2658	62.40	60.46	58.83	3.3700
2.1399	67.31	65.62	63.30	3.6696
1.0697	71.10	69.10	67.10	3.9707
0.8558	71.83	69.98	68.15	4.0676
0.6847	72.41	69.97	68.29	4.1645
0.5998	72.92	70.90	68.76	4.2220
0.5135	73.16	70.95	66.22	4.2894

TABLE: B21, Surface tension vs concentration data for $C_{12}S$ in water

C, (mol $dm^{-3}x10^{3}$)	γ (mNm^{-1}) 10°C	25°C	40°C	-log C
5.8762	49.81	47.80	46.73	2.2309
5.3505	53.33	50.78	49.30	2.2716
3.2643	57.80	55.80	55.31	2.4862
2.9383	58.19	56.24	55.56	2.5319
1.7627	64.15	62.53	61.12	2.7538
1.1751	68.10	65.66	65.00	2.9299
0.7381	71.17	68.77	67.21	3.1319
0.5876	72.25	70.17	67.70	3.2309
0.4701	72.52	70.27	68.34	3.3278
0.3978	72.69	70.62	68.44	3.4003
0.3525	73.08	70.42	68.38	3.4528
0.2938	73.28	71.24	68.77	3.5320
5.2480	50.74	49.40	48.54	2.2800
7.7803	--.--	45.45	--.--	2.1090
3.7844	--.--	54.11	--.--	2.422
2.3933	--.--	59.10	--.--	2.6210
8.5782	--.--	42.98	41.60	2.0666
11.5345	--.--	40.05	39.29	1.9380
26.1216	--.--	39.19	38.76	1.5830
23.0675	--.--	39.17	38.76	1.6370

TABLE: B22, Surface tension vs concentration data for $C_{12}S$ in 0.1 M NaCl

C, (mol $dm^{-3}x10^4$)	γ (mNm^{-1}) 10°C	25°C	40°C	-log C
1.5135	60.53	58.68	57.40	3.8199
1.0597	63.77	62.39	60.87	3.9748
0.7570	66.21	64.69	63.22	4.1209
0.4541	69.04	67.44	65.77	4.3428
0.3028	70.63	68.75	66.90	4.5188
0.2110	71.79	69.76	67.73	4.6757
0.1514	72.48	70.41	68.22	4.8199
0.1060	73.14	71.03	68.84	4.9748
0.1060	73.27	70.80	68.77	4.9748
0.0757	73.67	71.28	69.07	5.1209
5.2480	51.64	50.31	49.85	3.2800
3.6559	54.60	53.34	53.01	3.4370
2.6121	57.50	56.30	55.65	3.5830
8.2603	46.98	--.--	--.--	3.0830
28.793	--.--	35.84	35.05	2.5407
26.187	--.--	35.57	35.09	2.5819
13.094	--.--	41.27	40.44	2.8829
78.559	--.--	45.80	45.45	2.1048
23.993	--.--	35.95	35.44	2.6199

TABLE: B23, Surface tension vs concentration data for $C_{12}S$ in 0.5 M NaCl

C, (mol dm^{-5})x10^5)	γ (mNm^{-1}) 10°C	25°C	40°C	-log C
8.7902	54.04	52.77	52.80	4.0560
6.1523	57.54	56.29	56.25	4.2109
4.3954	59.97	59.02	58.80	4.3570
2.6369	63.30	62.73	61.83	4.5789
1.7579	66.12	65.36	64.28	4.7550
1.2305	69.07	67.59	66.19	4.9099
1.0546	70.35	68.84	67.88	4.9769
0.8790	71.04	69.36	67.88	5.0560
0.6152	72.61	70.83	69.12	5.2109
0.4395	73.46	71.46	69.50	5.3570
0.2637	74.43	72.08	70.25	5.5789
26.121	43.65	42.29	42.60	3.5830
18.285	46.86	46.16	45.89	3.7379
13.061	50.37	49.23	49.41	3.8840
68.865	--.--	--.--	32.77	3.1620
38.264	--.--	--.--	38.06	3.4172
160.69	--.--	--.--	31.45	2.7940
206.53	--.--	--.--	31.55	2.685
103.27	--.--	--.--	31.93	2.9860

TABLE: B24, Surface tension vs concentration data for $C_{10}EOS$ in water

C, (mol $dm^{-3} \times 10^2$)	γ (mNm^{-1}) 10°C	25°C	40°C	-log C
2.3014	41.23	41.01	40.78	1.6380
1.5918	45.77	14.60	40.74	1.7981
0.6027	59.60	55.31	54.12	2.2199
0.7745	56.98	52.40	51.38	2.1110
1.0471	52.26	47.80	46.80	1.9800
1.2589	49.33	44.80	--.--	1.9000
0.8710	--.--	50.60	--.--	2.0600
2.6303	--.--	41.10	40.68	1.5800
1.3490	--.--	--.--	42.05	1.8700

TABLE: B25:

Surface tension vs concentration data for $C_{10}EOS$ in 0.1 M NaCl

C, (mol $dm^{-3} \times 10^3$)	γ (mNm^{-1}) 10°C	25°C	40°C	-log C
7.7624	37.81	37.40	36.78	2.1100
3.9810	42.93	31.51	39.07	2.4000
1.5595	52.09	22.51	48.49	2.8070
1.2465	53.90	20.62	50.44	2.9043
2.3383	47.56	26.95	44.08	2.6311
6.9183	37.73	37.34	36.66	2.1600

TABLE: B26: Surface tension vs concentration data for $C_{10}EOS$ in 0.5 M NaCl

C, (mol $dm^{-3}x10^{3}$)	γ (mNm^{-1}) 10°C	25°C	40°C	-log C
2.7101	--.--	33.97	33.10	2.5670
1.5135	38.68	36.59	35.77	2.8200
0.7586	45.59	43.65	42.93	3.1200
0.7145	51.90	49.89	49.27	3.4301
2.2882	--.--	33.98	33.01	2.6405
1.1558	41.27	39.44	38.66	2.9371

TABLE: B27, Surface tension vs concentration data for $C_{12}EOS$ in water

C, (mol $dm^{-3}x10^3$)	γ (mNm^{-1}) 10°C	25°C	40°C	-log C
3.5301	--.--	41.82	42.40	2.4522
2.9010	46.98	45.20	44.92	2.5375
2.6920	--.--	45.98	--.--	2.5699
1.9230	52.80	50.82	50.81	2.7160
1.4130	57.15	55.41	55.30	2.8498
1.0470	61.31	59.38	58.87	2.9800

TABLE: B28, Surface tension vs concentration data for $C_{12}EOS$ in 0.1 M NaCl

C, (mol $dm^{-3}x10^3$)	γ (mNm^{-1}) 10°C	25°C	40°C	-log C
27.1860	--.--	--.--	41.56	3.5656
13.5930	48.67	46.90	47.70	3.8668
9.2432	51.93	50.82	50.95	4.0343
6.7905	54.85	53.72	53.99	4.1681
5.4372	57.05	55.97	55.71	4.2650
4.0780	59.75	58.48	58.00	4.3904

TABLE: B29, Surface tension vs concentration data for $C_{12}EOS$ in 0.5 M NaCl

C, (mol $dm^{-3}x10^5$)	γ (mNm^{-1}) 10°C	25°C	40°C	-log C
2.8996	49.70	49.03	49.55	4.5377
2.3197	52.38	51.38	51.57	4.6346
2.0297	53.73	53.03	53.09	4.5272
1.4498	56.72	55.80	55.80	4.8387
1.1598	58.48	57.76	57.78	4.9356

TABLE: B30, Surface tension vs concentration data for $C_{12}EOSO$ in water

C, (mol $dm^{-3} x 10^3$)	γ (mNm^{-1}) 10°C	25°C	40°C	-log C
10.5974	38.70	39.00	39.07	1.9748
7.6050	38.85	39.12	39.20	2.1189
5.3112	39.09	39.41	39.46	2.2748
3.9003	40.79	39.62	40.20	2.4089
2.7656	46.25	44.17	44.81	2.5582
2.2599	48.52	45.95	46.70	2.6459
2.2407	48.84	46.00	47.35	2.6496
2.0017	50.45	48.76	48.91	2.6986
1.6113	53.45	--.--	51.76	2.7928
0.9360	59.30	58.00	58.20	3.0287
0.6285	60.87	--.--	--.--	3.2017
0.5744	63.87	62.85	62.69	3.2400
0.5744	63.07	62.13	63.30	3.2400
0.5248	64.16	63.33	62.51	3.2800
0.4980	64.77	63.39	62.82	3.3028
0.4491	65.44	64.27	63.45	3.3476
0.4467	65.53	64.39	63.82	3.3500
0.3713	67.91	66.73	65.78	3.4303
0.3713	68.55	66.86	65.85	3.4303
0.2630	69.93	68.13	67.46	3.5800
0.2072	70.95	69.39	67.85	3.6835

TABLE: B31, Surface tension vs concentration data for $C_{12}EOSO$ in 0.1 M NaCl

C, (mol $dm^{-3}x10^4$)	γ (mNm^{-1}) 10°C	25°C	40°C	-log C
28.0670	33.70	33.44	33.20	2.5518
13.8990	33.85	33.59	33.44	2.8570
13.8990	33.56	33.33	33.26	2.8570
11.0150	33.69	33.55	33.31	2.9580
5.5975	33.74	33.61	33.35	3.2520
4.4463	34.19	33.78	33.51	3.3520
3.8931	35.45	34.61	35.20	3.4097
3.8931	--.--	--.--	35.39	3.4097
2.7810	39.05	37.99	38.92	3.5558
2.7810	--.--	--.--	38.65	3.5558
1.3867	45.15	44.51	45.81	3.8580
1.1746	46.63	45.44	46.14	3.9301
0.8342	50.28	49.68	49.68	4.0787
0.6934	51.21	50.65	50.82	4.1590
0.4477	55.89	55.03	55.15	4.4771
0.2937	58.16	57.47	57.31	4.5320
0.1770	62.16	61.41	60.41	4.7540
0.1175	64.91	64.09	63.27	4.9301
0.8222	66.58	65.38	65.00	5.0850
0.0587	68.32	66.75	65.79	5.2310
0.0470	70.01	68.38	66.70	5.3280

0.0352	71.02	69.24	67.58	5.4529
0.0235	72.19	70.29	68.28	5.6290
0.0117	73.20	71.23	69.26	5.9301
0.0047	74.03	71.97	69.60	6.3280

TABLE: B32, Surface tension vs concentration data for $C_{12}EOSO$ in 0.5 M NaCl

C, (mol $dm^{-3} \times 10^5$)	γ (mNm^{-1}) 10°C	25°C	40°C	-log C
93.8210	30.54	30.01	29.92	3.0277
46.9130	30.54	30.11	30.08	3.3287
46.9130	31.01	30.65	--.--	3.3287
23.4420	31.03	30.54	30.08	3.6300
13.1250	32.08	30.69	31.34	3.8819
12.3390	31.79	31.22	32.26	3.9087
12.3390	31.10	30.57	32.17	3.9087
10.5020	32.30	32.07	33.57	3.9787
7.8759	36.42	35.93	37.02	4.1037
6.5629	38.15	37.89	38.55	4.1829
5.2504	40.79	40.26	41.20	4.2798
3.9810	43.14	43.14	42.21	4.4000
2.6254	48.26	47.75	48.65	4.5808
1.3125	53.54	53.47	54.27	4.8819
0.6563	60.17	59.66	59.61	5.1829
0.3938	64.84	63.70	63.80	5.4047
0.2625	67.28	66.20	65.73	5.5808
0.3100	69.08	67.85	66.97	5.6778
0.2099	68.59	67.10	66.65	5.6778
0.1640	70.12	68.86	67.65	5.7850
0.1312	71.05	69.89	68.24	5.8819

0.1125	72.30	70.60	69.12	5.9485
0.1126	72.06	70.39	68.93	5.9485
0.0938	73.17	71.31	69.30	6.0277

TABLE: B33, Surface tension vs concentration data for $C_{12}EO_2SO$ in water

C, (mol $dm^{-3}x10^4$)	γ (mNm^{-1}) 10°C	25°C	40°C	-log C
74.8500	41.65	41.40	40.86	2.1258
38.5030	41.66	41.48	41.10	2.4145
24.3380	44.82	42.91	42.42	2.6237
1.9815	49.12	47.04	46.55	2.7030
19.3370	46.--	45.62	45.86	2.7136
15.0450	51.79	49.09	48.70	2.8826
13.2370	52.41	50.80	51.06	2.8782
10.4281	54.72	52.92	52.54	2.9818
7.5509	56.09	55.32	55.80	3.1220
5.4827	59.75	58.06	58.15	3.2610
4.6174	61.31	59.88	59.11	3.3356
3.9445	65.33	61.90	61.25	3.4040
2.0202	68.20	67.47	66.11	3.6946
1.9719	67.23	65.72	--.--	3.7051
1.4302	70.85	68.94	67.59	3.8446
1.0967	70.55	68.76	67.04	3.9599
0.8236	72.18	70.21	68.14	4.0843
0.6492	72.59	70.45	68.44	4.1876
0.4809	72.49	70.49	68.24	4.3179

TABLE: B34, Surface tension vs concentration data for $C_{12}EO_2SO$ in 0.1 M NaCl

C, (mol $dm^{-3}x10^5$)	γ (mNm^{-1}) 10°C	25°C	40°C	-log C
60.6730	36.30	35.38	35.02	3.2170
45.5090	36.46	35.68	34.96	3.3419
30.3380	37.38	35.80	35.05	3.5180
24.2710	39.35	37.54	36.96	3.6149
18.2010	41.47	40.35	39.87	3.7399
12.1330	45.33	43.82	43.20	3.9160
6.2086	50.90	49.45	48.75	4.2070
3.6408	54.90	53.53	52.66	4.4388
3.0338	55.56	54.59	53.75	4.5180
2.4266	58.07	56.57	55.82	4.6150
1.8197	59.86	58.50	57.79	4.7400
1.2133	62.03	60.92	59.76	4.9160
0.6067	66.11	64.65	63.53	5.2170
0.4854	67.20	65.64	64.61	5.3139
0.2884	69.97	68.32	66.40	0.2884
0.2427	70.59	69.01	67.30	5.6149
0.1942	71.28	69.51	67.68	5.7118
0.1456	72.01	70.02	68.25	5.8368
0.0970	73.35	70.94	69.07	6.0130
0.0485	73.81	71.64	69.49	6.3139

TABLE: B35, Surface tension vs concentration data for $C_{12}EO_2SO$ in 0.5 M NaCl

C, (mol $dm^{-3} \times 10^5$)	γ (mNm^{-1}) 10°C	25°C	40°C	-log C
12.136	33.64	32.96	32.18	3.9159
11.033	33.91	33.06	32.39	3.9573
9.7723	34.48	33.40	33.21	4.0100
7.2828	37.34	35.54	35.24	4.1377
4.8640	40.45	39.02	38.94	4.3130
3.6408	43.22	41.89	41.63	4.4388
2.4266	47.24	45.64	45.55	4.6150
1.2136	52.75	51.59	51.30	4.9159
0.7284	57.37	56.04	55.84	5.1376
0.6166	59.74	58.07	57.66	5.2100
0.3641	62.06	60.64	60.38	5.4388
0.2427	65.25	63.87	63.32	5.6149
0.1456	68.88	66.87	66.10	5.8367
0.9709	70.98	68.90	67.82	6.0128
0.0608	73.31	70.96	69.07	6.1677
0.0582	73.94	70.35	69.68	6.2347
0.0485	73.31	71.40	69.70	6.3138
0.0388	74.26	71.90	69.82	6.4107

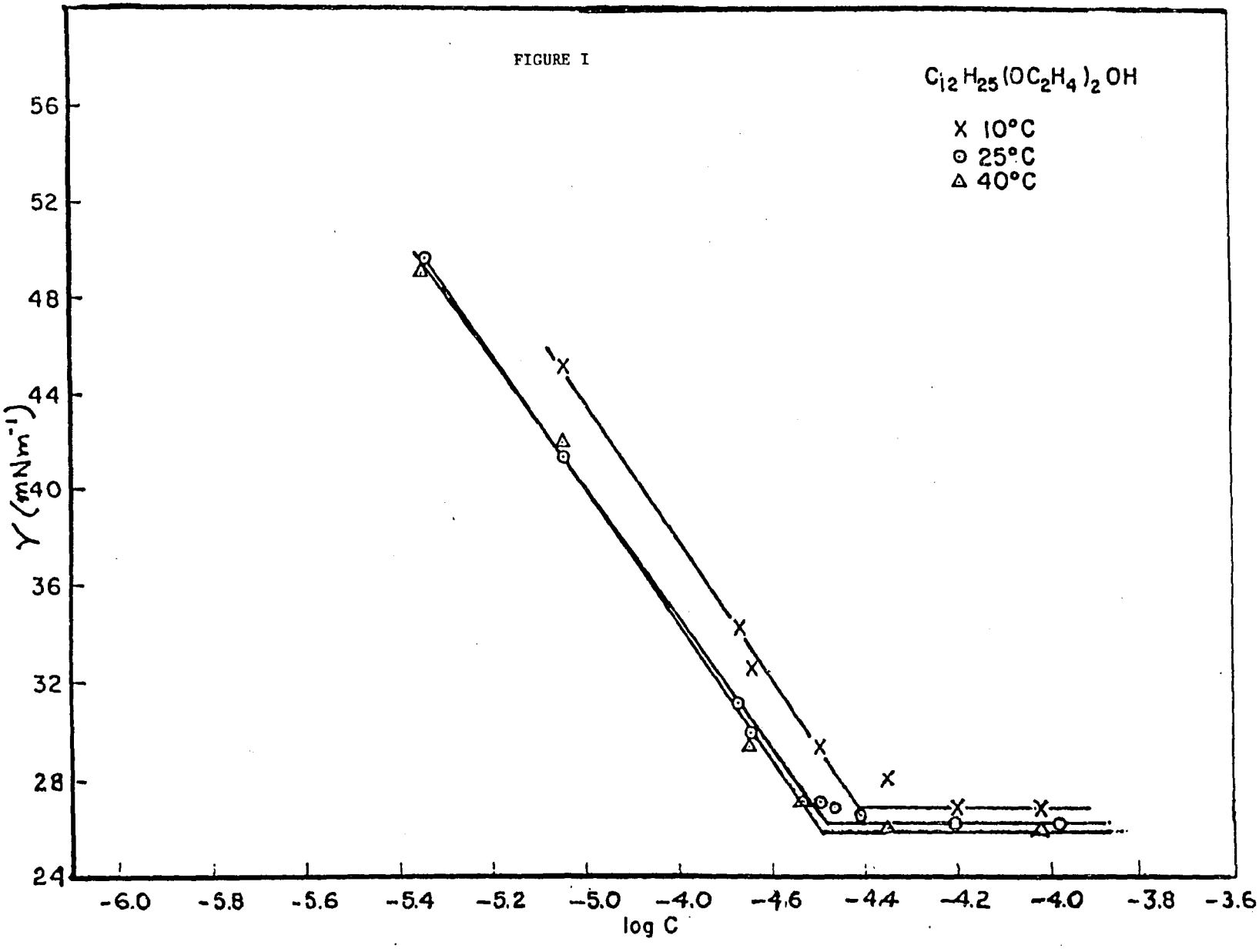
FIGURE I
$C_{12}H_{25}(OC_2H_4)_2OH$
X 10°C
⊙ 25°C
△ 40°C
56
52
48
44
40
36
32
28
24
γ (mNm⁻¹)
-6.0
-5.8
-5.6
-5.4
-5.2
-5.0
-4.0
-4.6
-4.4
-4.2
-4.0
-3.8
-3.6
log C

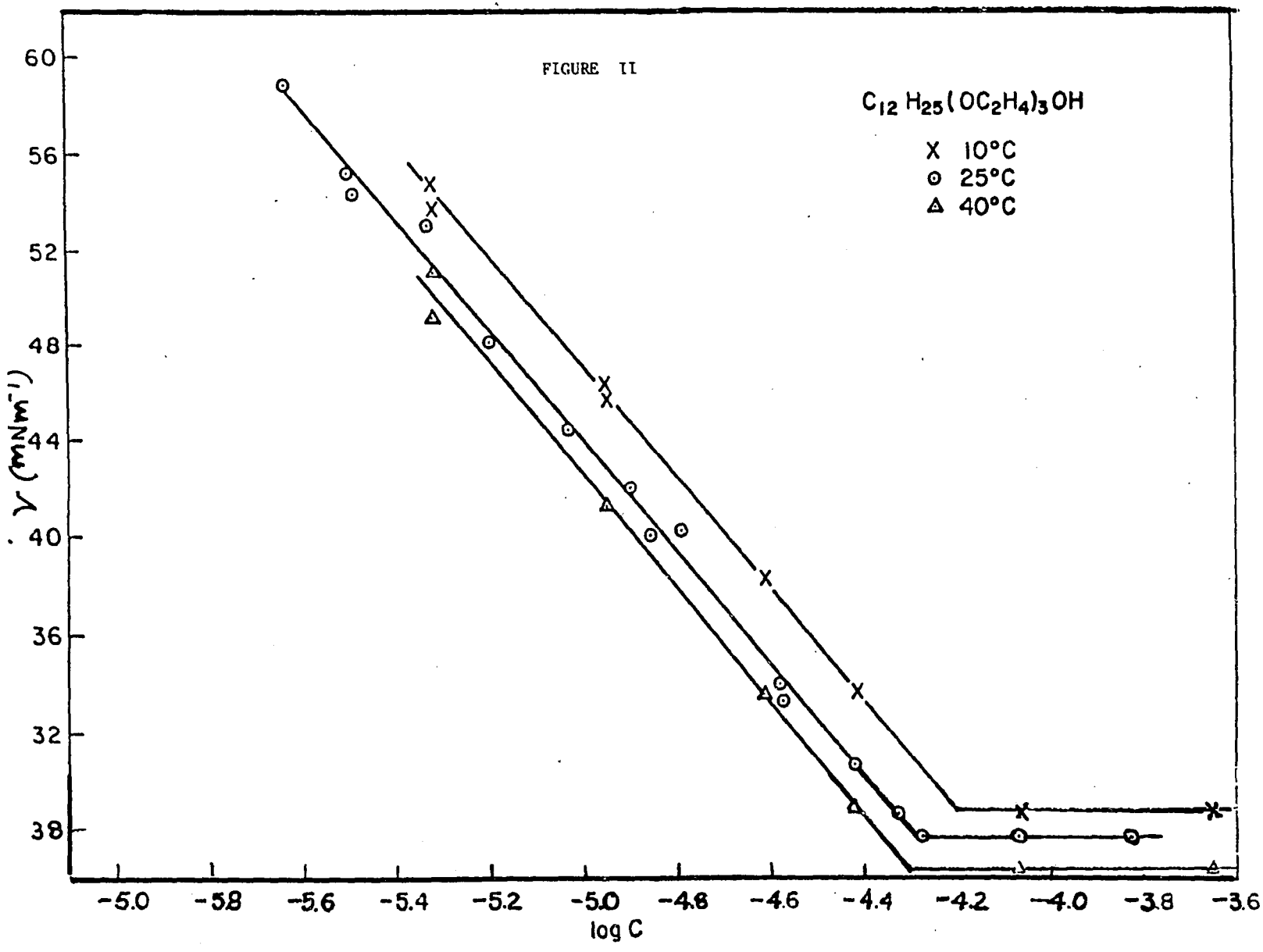
FIGURE II
$C_{12}H_{25}(OC_2H_4)_3OH$
X 10°C
⊙ 25°C
△ 40°C
γ (mNm⁻¹)
60
56
52
48
44
40
36
32
38
-5.0
-5.8
-5.6
-5.4
-5.2
-5.0
-4.8
-4.6
-4.4
-4.2
-4.0
-3.8
-3.6
log C

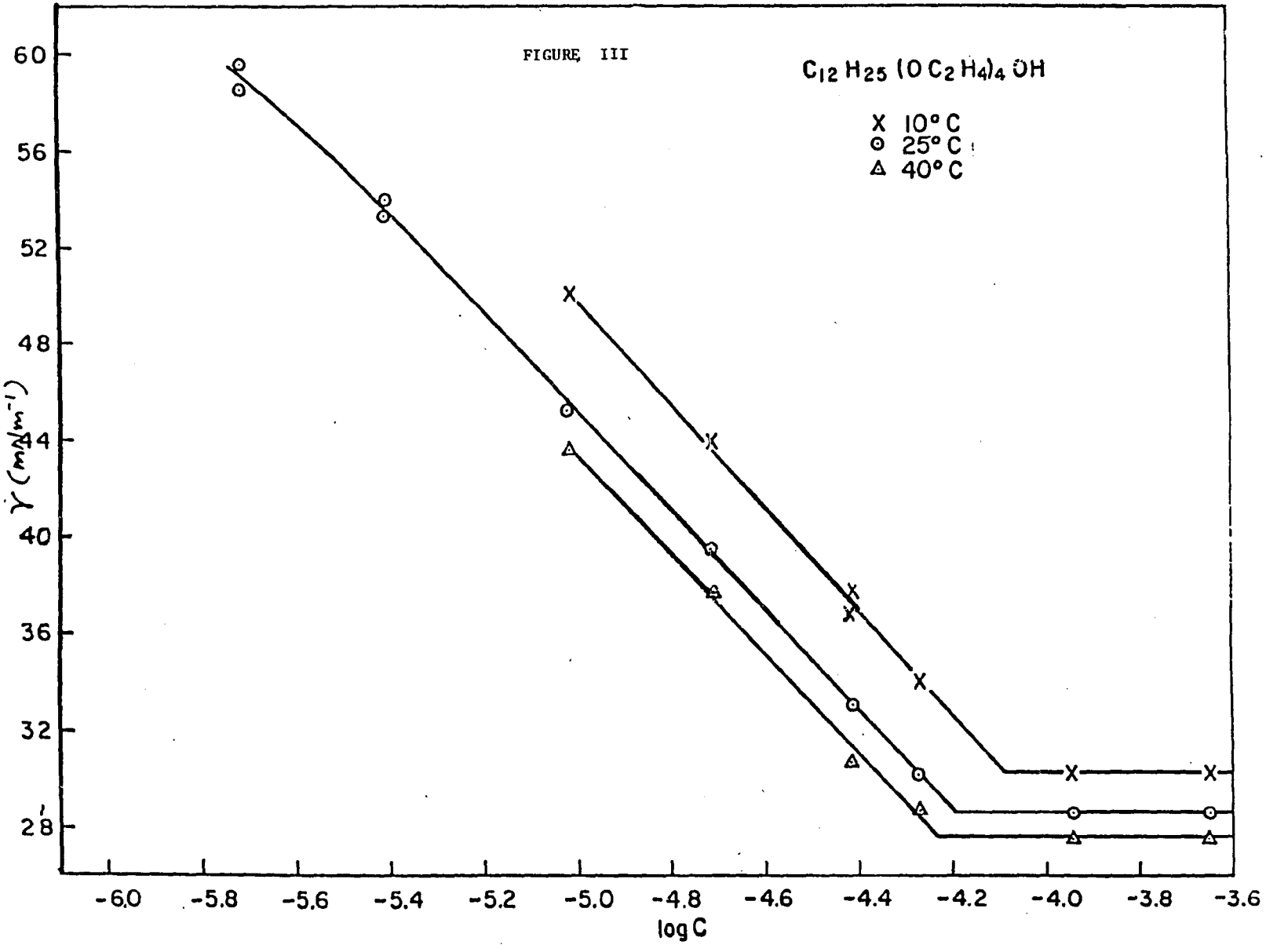
FIGURE III
$C_{12}H_{25}(OC_2H_4)_4OH$
X 10° C
⊙ 25° C
△ 40° C
60
56
52
48
44
40
36
32
28
γ (mN m⁻¹)
-6.0
-5.8
-5.6
-5.4
-5.2
-5.0
-4.8
-4.6
-4.4
-4.2
-4.0
-3.8
-3.6
log C

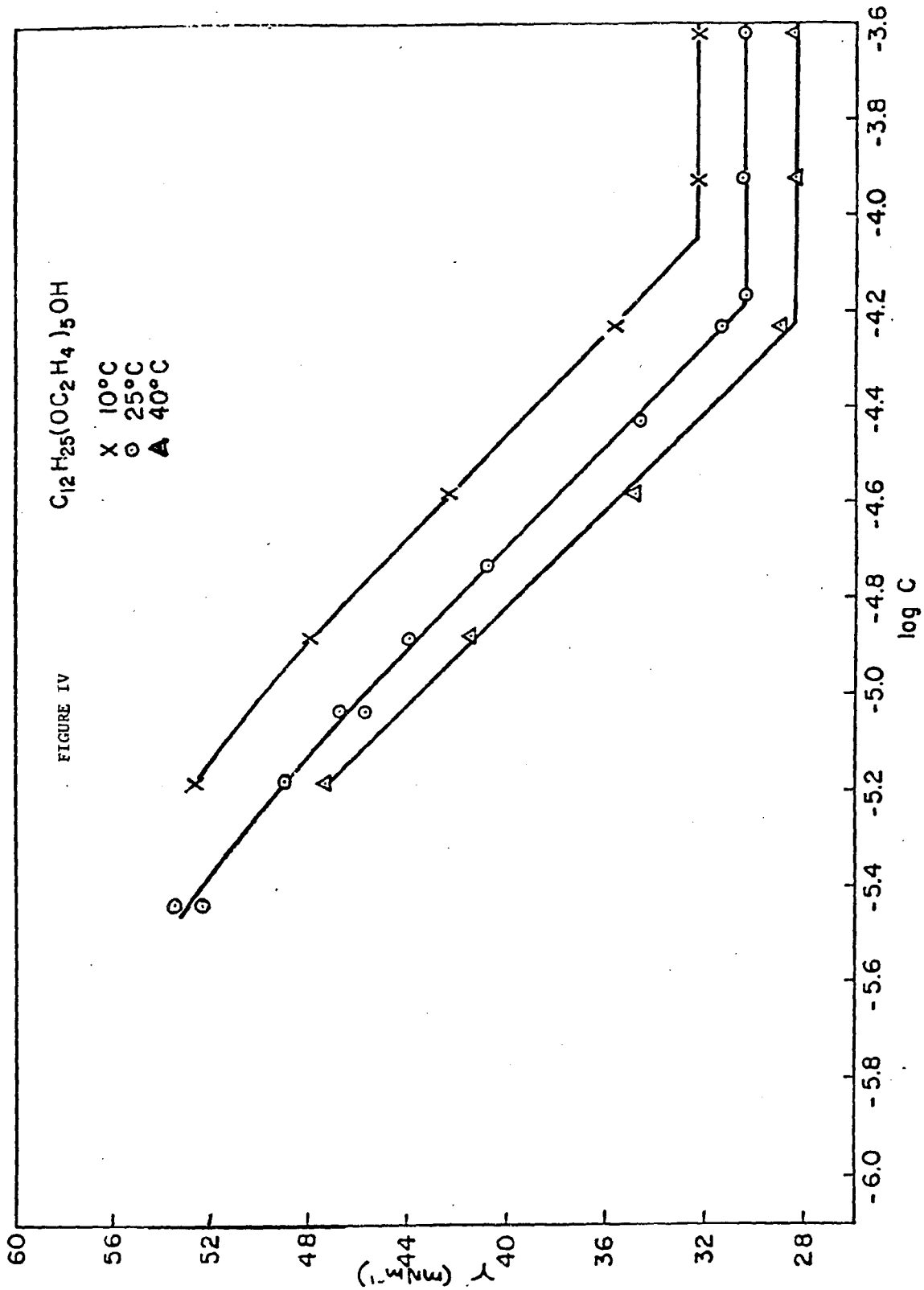
$C_{12}H_{25}(OC_2H_4)_5OH$
X 10°C
⊙ 25°C
▲ 40°C
60
56
52
48
44
40
36
32
28
γ (mN/m)
-6.0
-5.8
-5.6
-5.4
-5.2
-5.0
-4.8
-4.6
-4.4
-4.2
-4.0
-3.8
-3.6
log C

FIGURE IV

FIGURE V

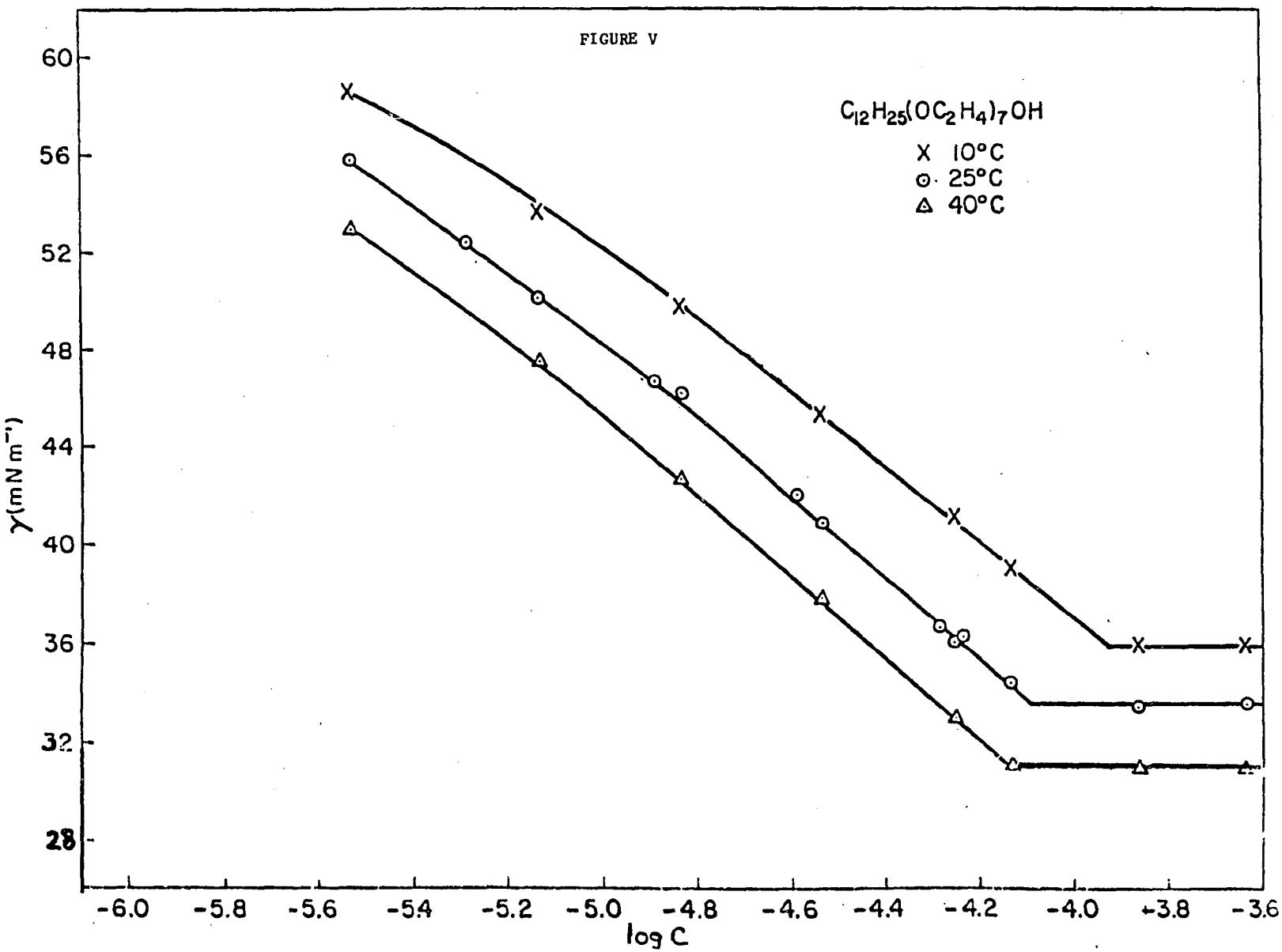
$C_{12}H_{25}(OC_2H_4)_7OH$
X 10°C
⊙ 25°C
△ 40°C
γ(mN m⁻¹)
60
56
52
48
44
40
36
32
28
-6.0
-5.8
-5.6
-5.4
-5.2
-5.0
-4.8
-4.6
-4.4
-4.2
-4.0
-3.8
-3.6
log C

FIGURE VI

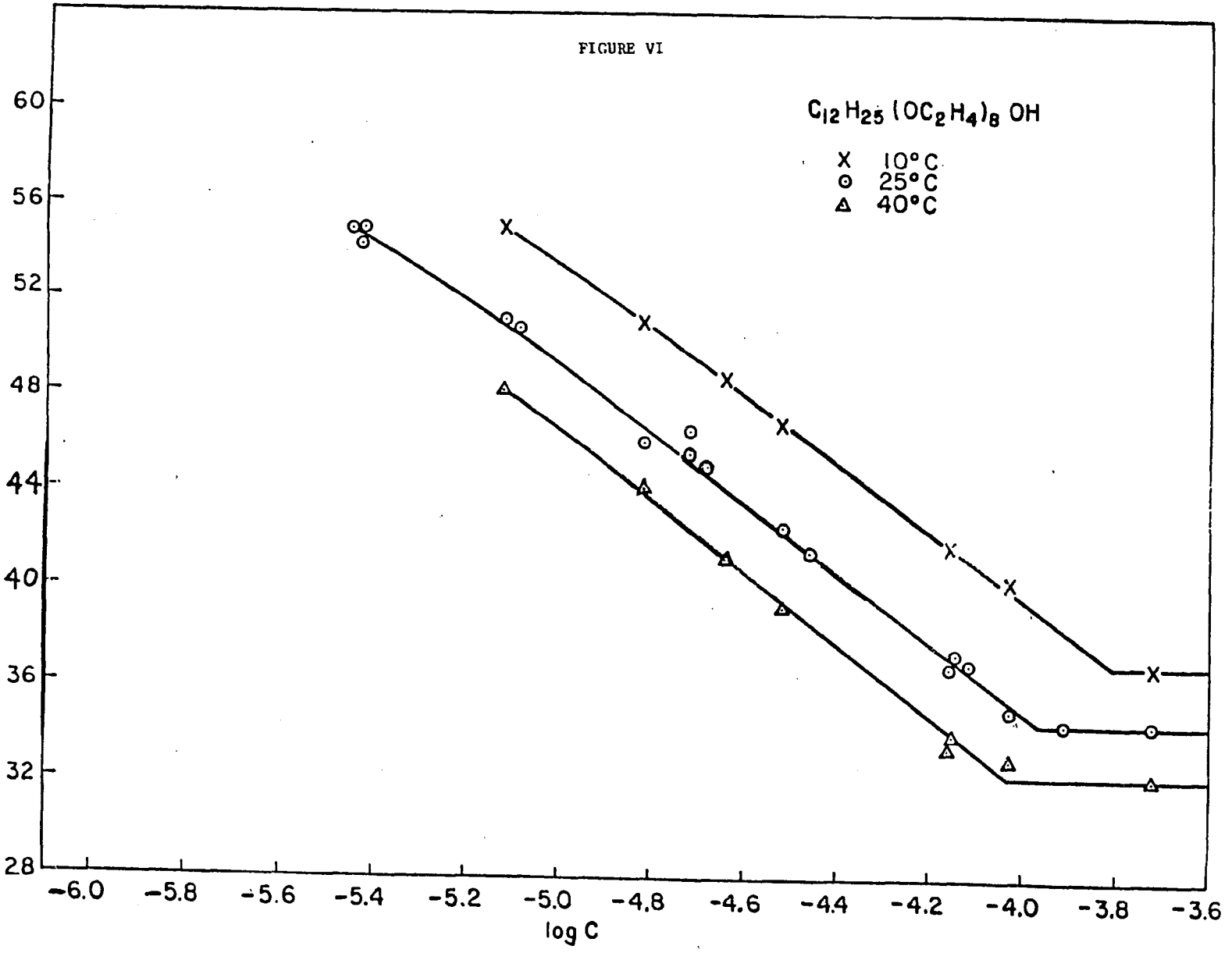
$C_{12}H_{25}(OC_2H_4)_8OH$
X 10°C
⊙ 25°C
△ 40°C
60
56
52
48
44
40
36
32
28
-6.0
-5.8
-5.6
-5.4
-5.2
-5.0
-4.8
-4.6
-4.4
-4.2
-4.0
-3.8
-3.6
log C

FIGURE VII

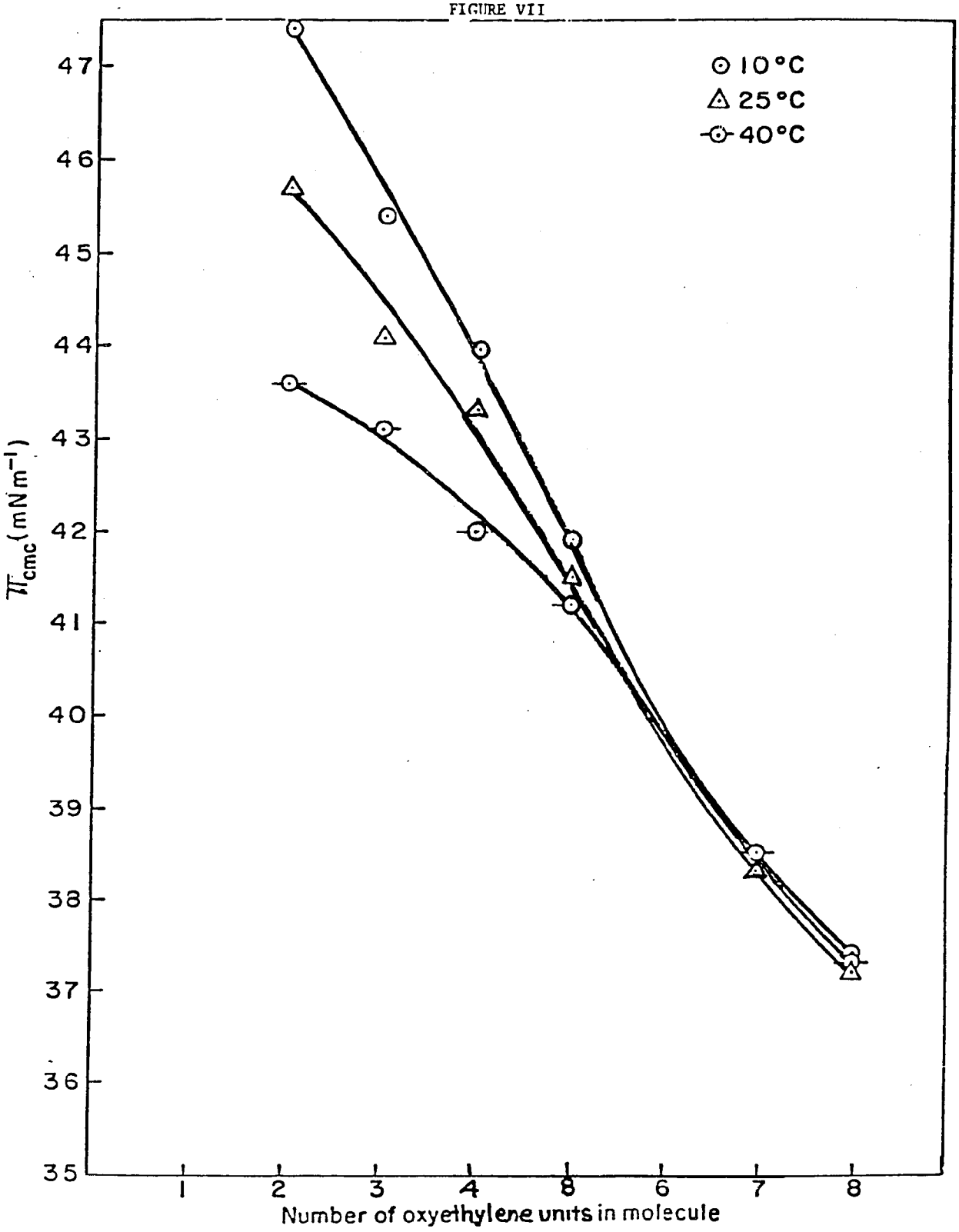
10°C
25°C
40°C
47
46
45
44
43
42
41
40
39
38
37
36
35
Π_{cmc} (mNm^{-1})
1
2
3
4
8
6
7
8
Number of oxyethylene units in molecule

FIGURE VIII

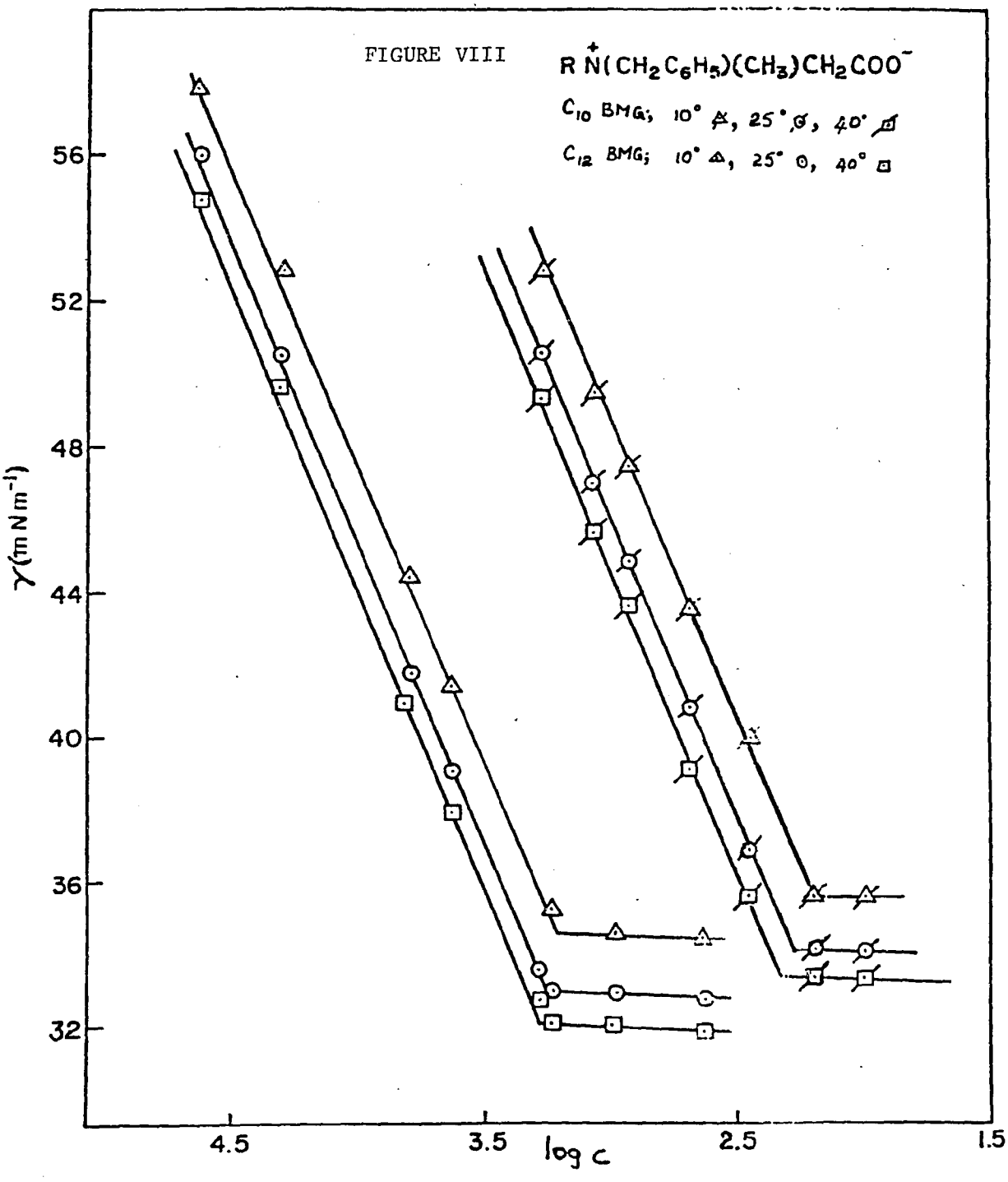
$R\overset{+}{N}(CH_2C_6H_5)(CH_3)CH_2COO^-$
C_{10} BMG; 10°, 25°, 40°
C_{12} BMG; 10°, 25°, 40°
56
52
48
44
40
36
32
γ(mN m⁻¹)
4.5
3.5
log c
2.5
1.5

FIGURE IX

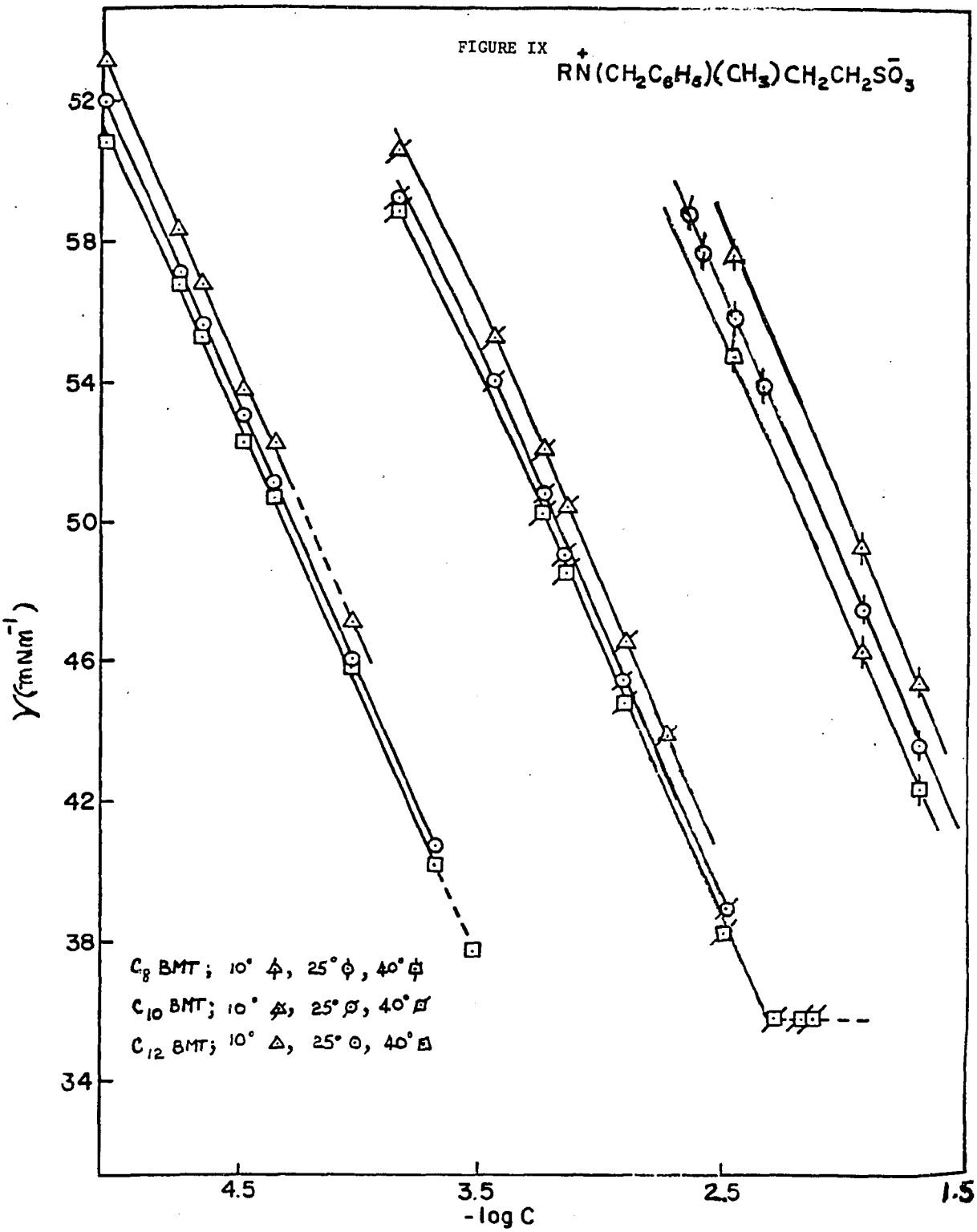
RN⁺(CH2C6H5)(CH3)CH2CH2SO3⁻
52
58
54
50
46
42
38
34
γ (mNm⁻¹)
C8 BMT; 10° Δ, 25° ϕ, 40° ϕ
C10 BMT; 10° Δ, 25° ϕ, 40° ϕ
C12 BMT; 10° Δ, 25° ⊙, 40° ⊡
4.5
3.5
2.5
1.5
-log C

FIGURE X

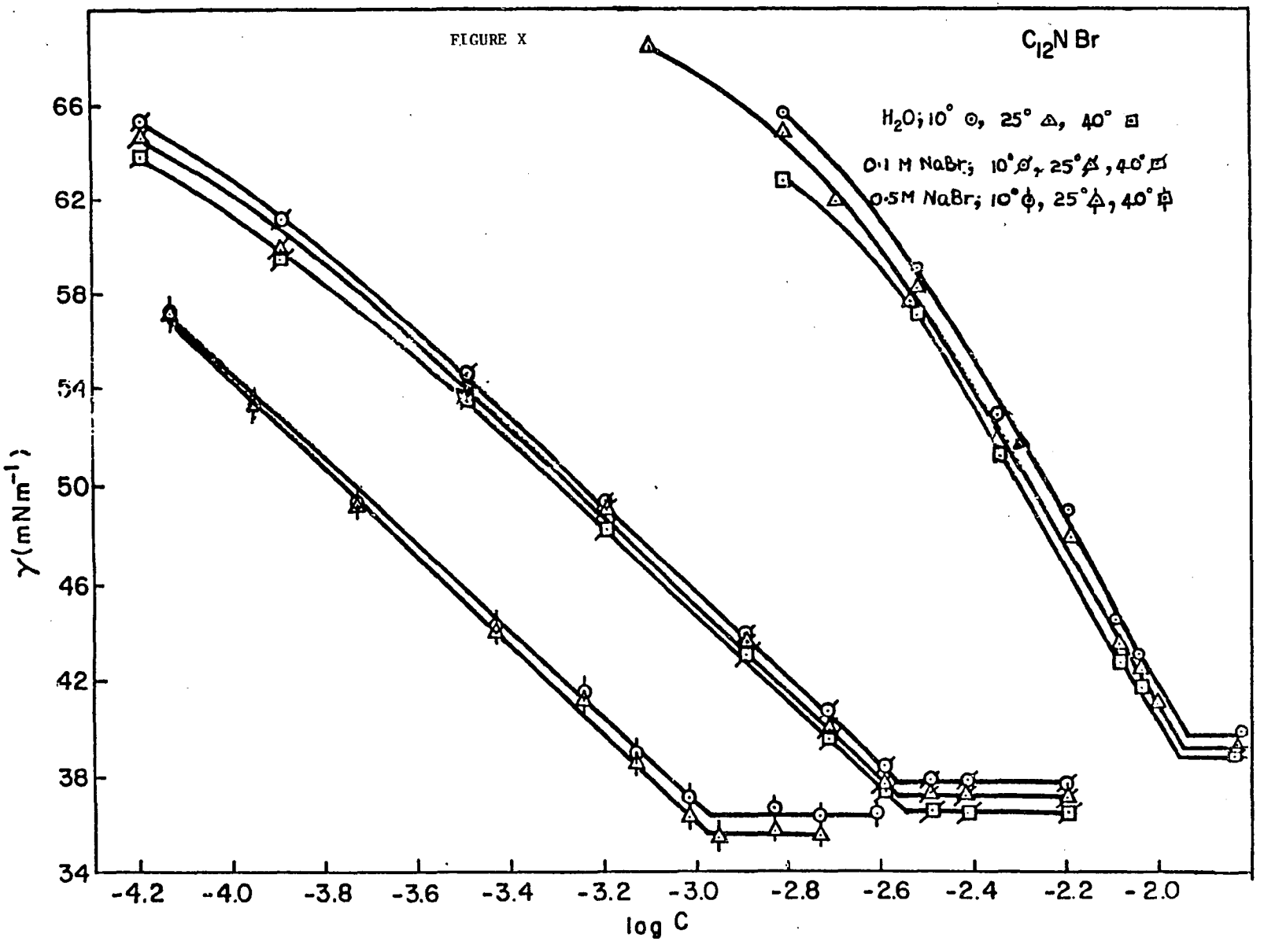
$C_{12}N\,Br$
H_2O; 10° ⊙, 25° △, 40° ⊡
0·1 M NaBr; 10°, 25°, 40°
0·5M NaBr; 10°, 25°, 40°
γ(mNm⁻¹)
66
62
58
54
50
46
42
38
34
-4.2
-4.0
-3.8
-3.6
-3.4
-3.2
-3.0
-2.8
-2.6
-2.4
-2.2
-2.0
log C

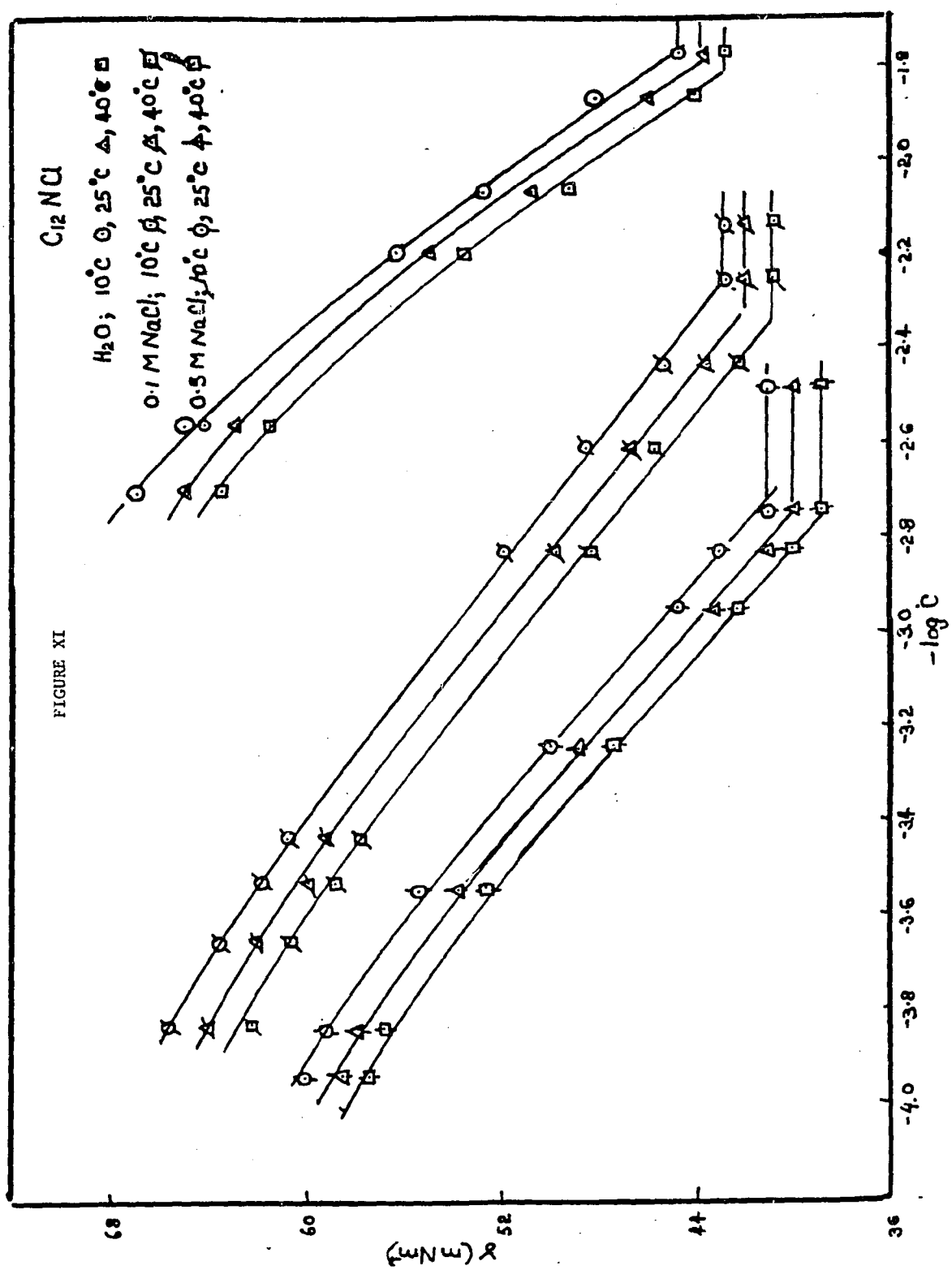
$C_{12}NCl$
H_2O; 10°C ○, 25°C △, 40°C □
0·1 M NaCl; 10°C ⊙, 25°C ▲, 40°C ■
0·5 M NaCl; 10°C ◑, 25°C ◭, 40°C ◧
γ (mN m⁻¹)
68
60
52
44
36
-4·0
-3·8
-3·6
-3·4
-3·2
-3·0
-2·8
-2·6
-2·4
-2·2
-2·0
-1·8
-log c

FIGURE XI

FIGURE XII

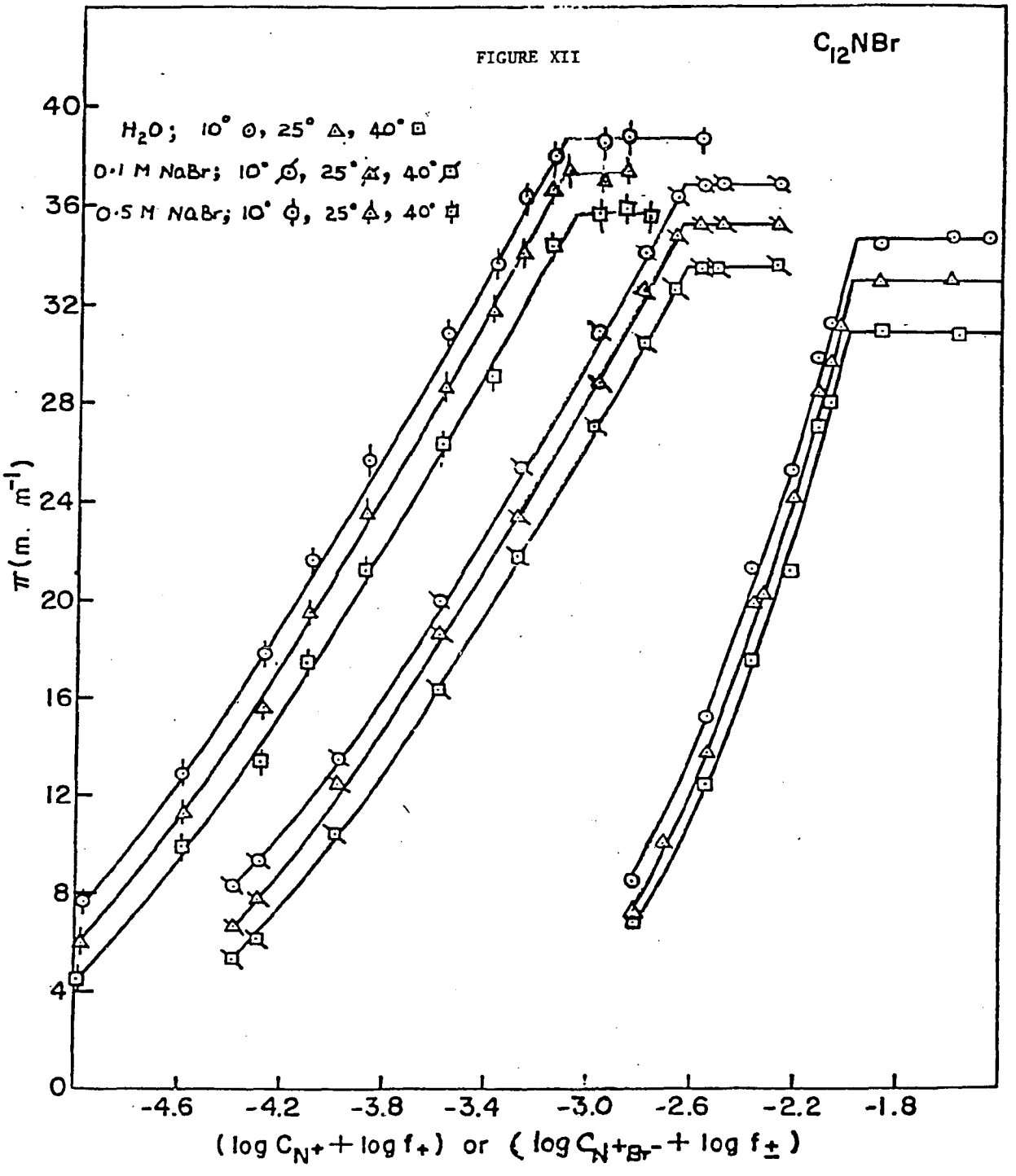
$C_{12}NBr$
H_2O; 10° ⊙, 25° △, 40° ⊡
0·1 M NaBr; 10° ⊙, 25° △, 40° ⊡
0·5 M NaBr; 10° ⊙, 25° △, 40° ⊡
π (m. m^{-1})
0
4
8
12
16
20
24
28
32
36
40
-4.6
-4.2
-3.8
-3.4
-3.0
-2.6
-2.2
-1.8
(log C_{N^+} + log f_+) or (log $C_{N^+Br^-}$ + log $f_\pm$)

FIGURE XIII

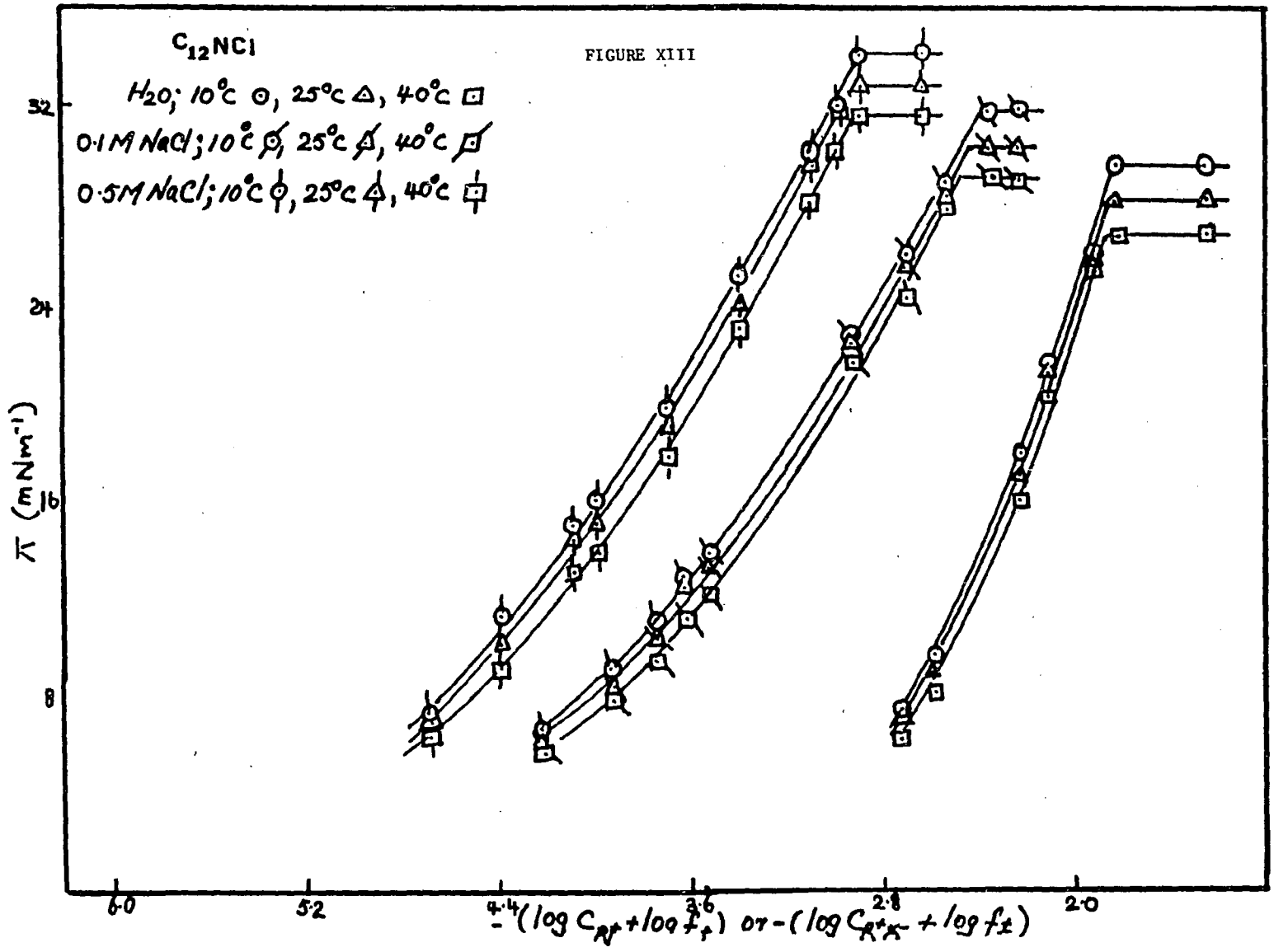
$C_{12}NCl$
H_2O; 10°C ⊙, 25°C △, 40°C □
0·1M NaCl; 10°C ⊙, 25°C △, 40°C □
0·5M NaCl; 10°C ⊙, 25°C △, 40°C □
32
24
16
8
π (mNm^{-1})
6·0
5·2
4·4
3·6
2·8
2·0
$-(\log C_{Na^+} + \log f_+)$ or $-(\log C_{R^+X^-} + \log f_\pm)$

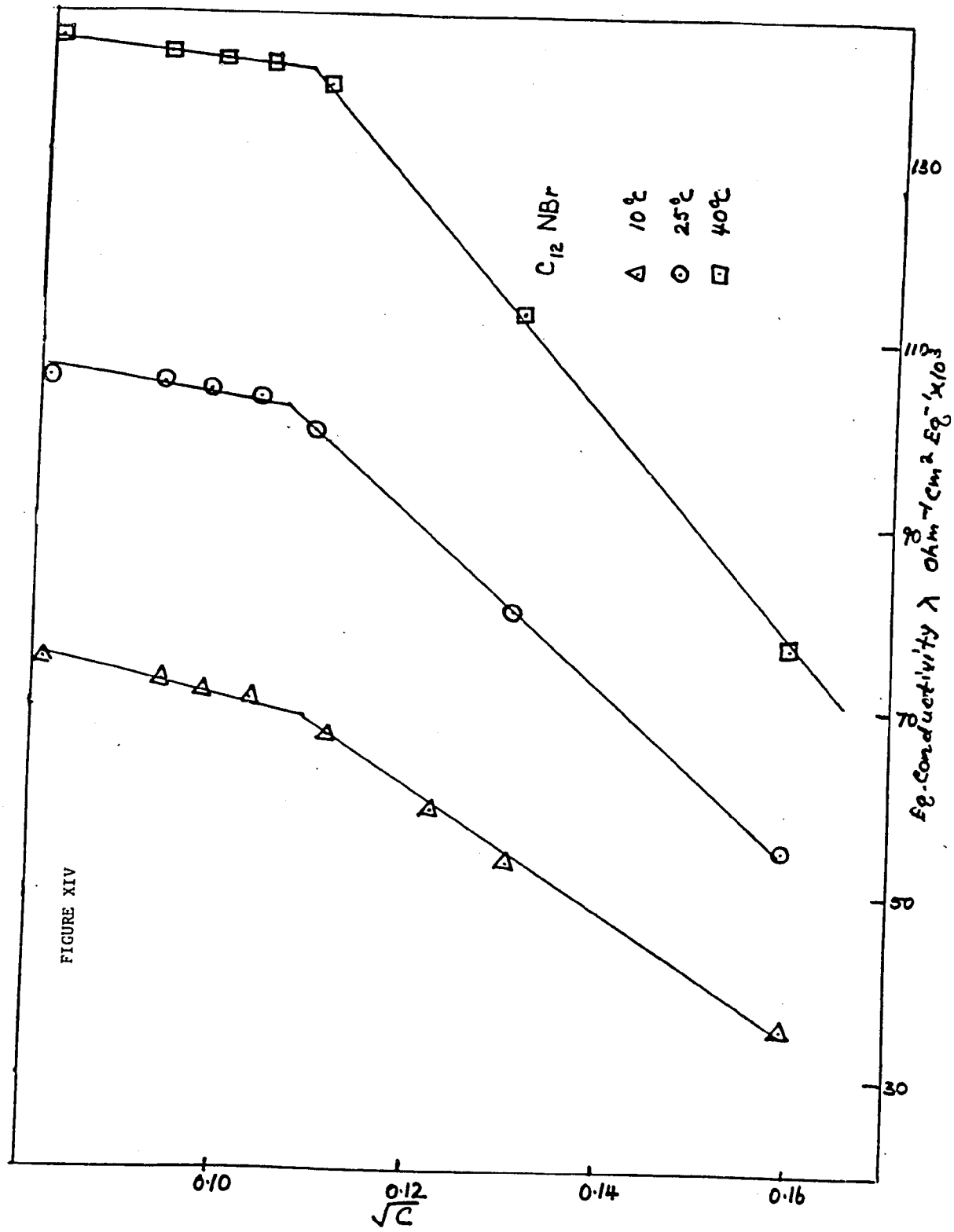
C_{12} NBr
10°c
25°c
40°c
130
110
90
70
50
30
Eq. conductivity λ ohm⁻¹cm² Eq⁻¹ x10³
0·10
0·12
0·14
0·16
$\sqrt{C}$

FIGURE XIV

FIGURE XV

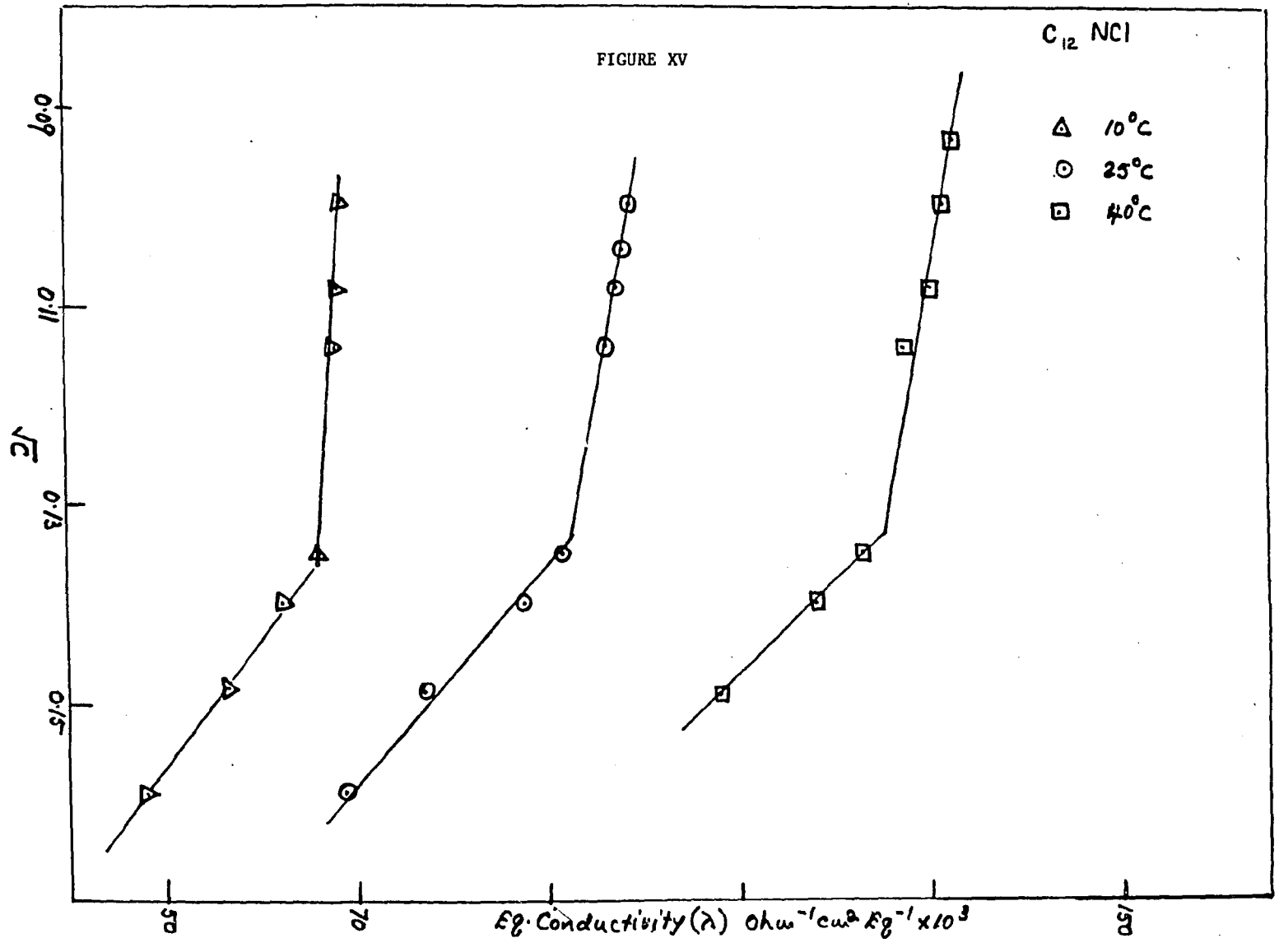
C_{12} NCl
10°C
25°C
40°C
$\sqrt{C}$
0.09
0.11
0.13
0.15
50
70
Eq. Conductivity (λ) $Ohm^{-1}cm^2Eq^{-1}\times10^3$
90

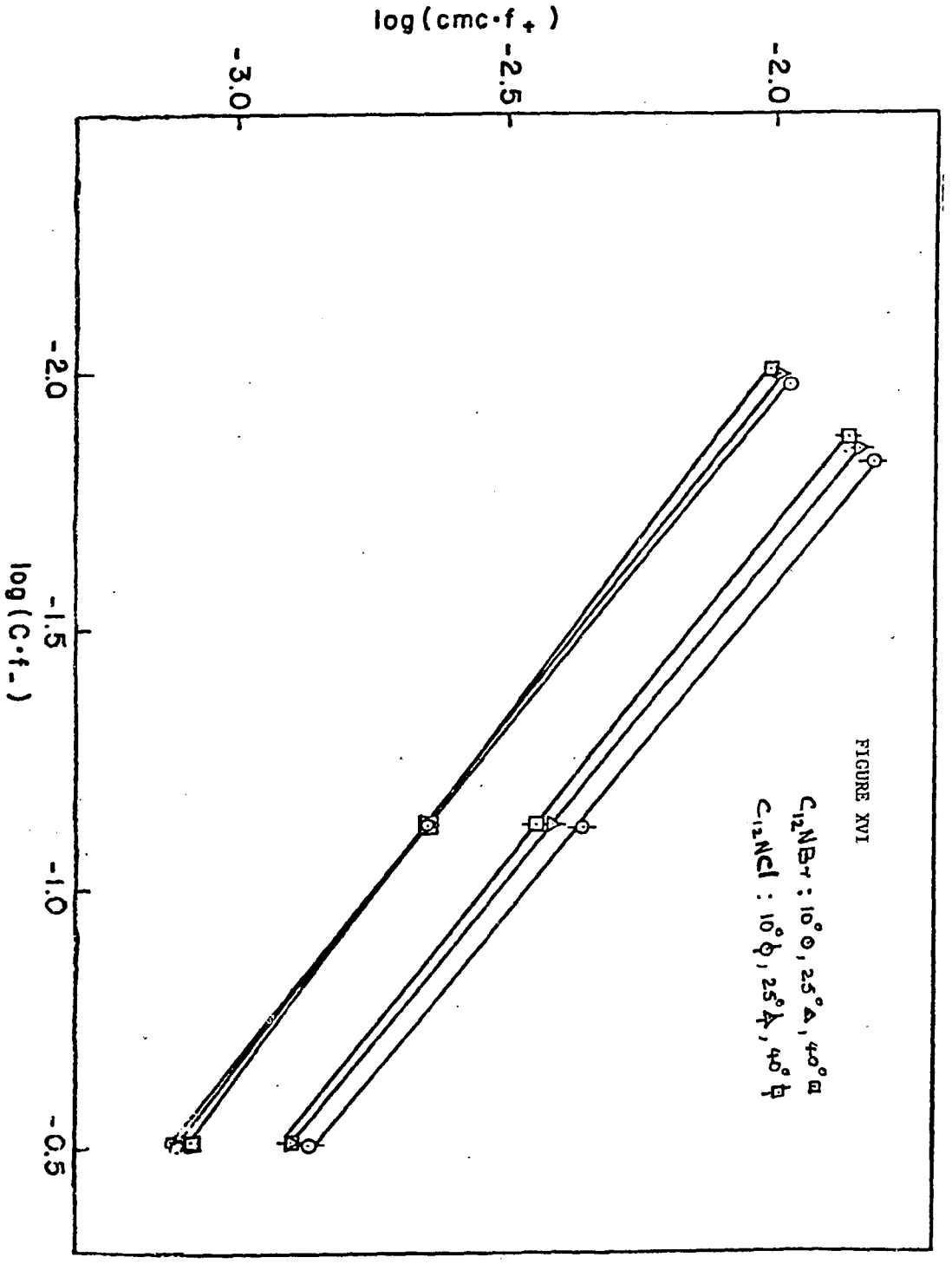
log(cmc·f+)
-3.0
-2.5
-2.0
log(C·f-)
-2.0
-1.5
-1.0
-0.5
C12NBr : 10°○, 25°△, 40°□
C12NCl : 10°◑, 25°▲, 40°■

FIGURE XVI

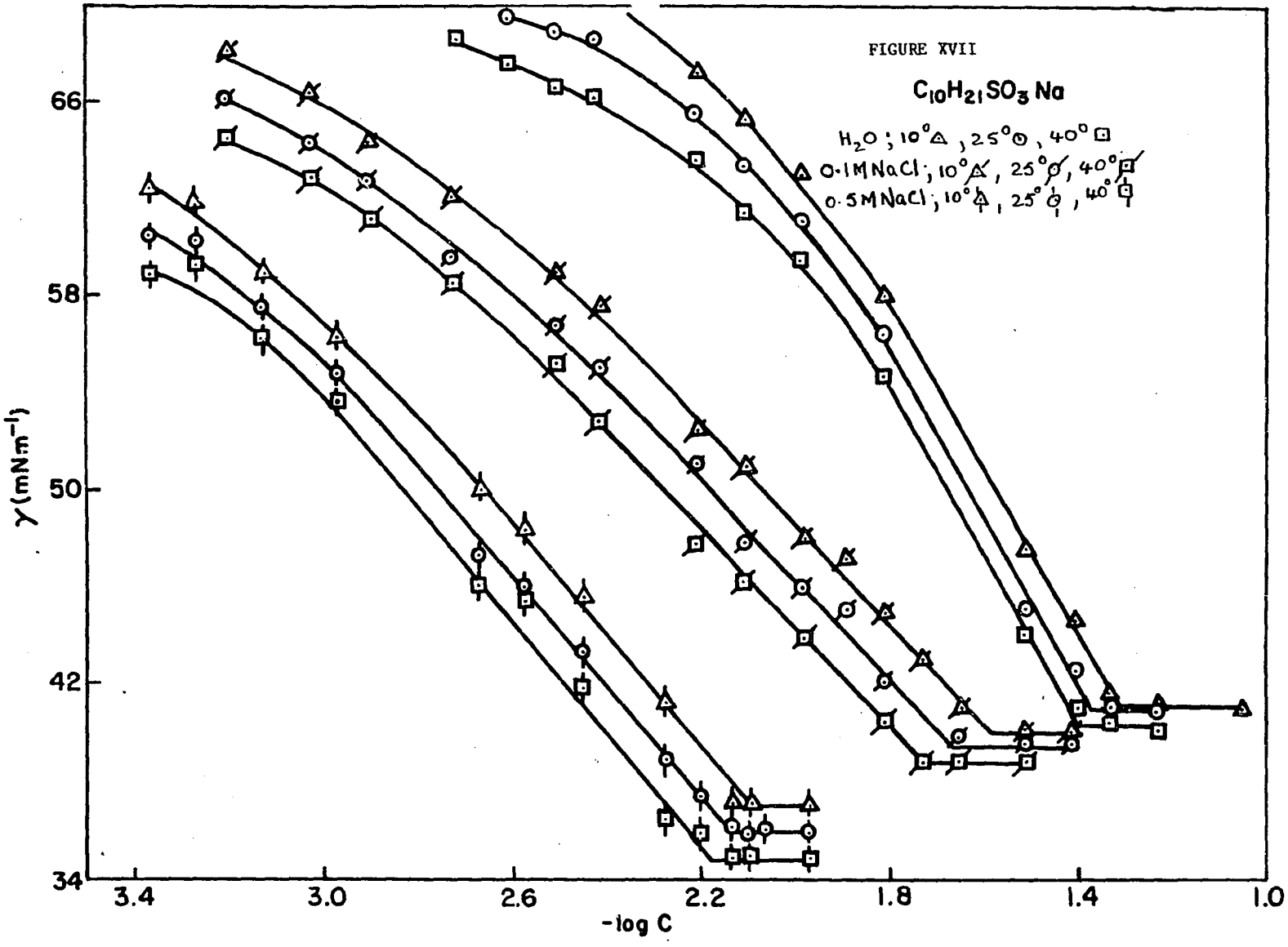
FIGURE XVII
$C_{10}H_{21}SO_3Na$
H_2O ; 10° △ , 25° ⊙ , 40° □
0·1M NaCl ; 10° ⊿ , 25° ⊘ , 40° ⊡
0·5M NaCl ; 10° ⧋ , 25° ⊜ , 40° ⊟
γ (mNm⁻¹)
66
58
50
42
34
3.4
3.0
2.6
2.2
1.8
1.4
1.0
-log C

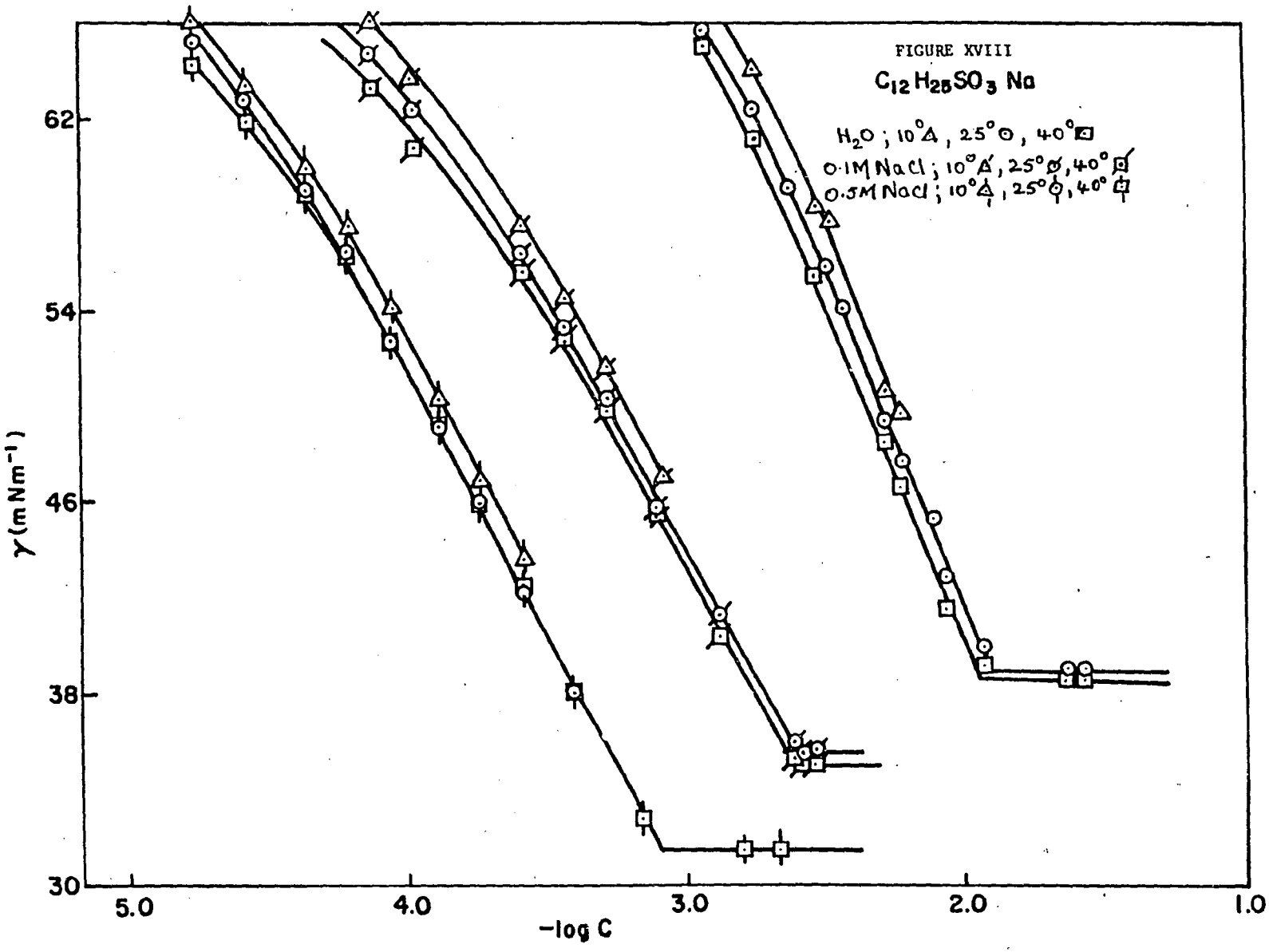
FIGURE XVIII
$C_{12}H_{25}SO_3Na$
H_2O ; 10°Δ , 25°○ , 40°□
0·1M NaCl ; 10°Δ, 25°Ø, 40°⊡
0·5M NaCl ; 10°Δ, 25°Ø, 40°⊡
62
54
46
38
30
γ (m Nm⁻¹)
5.0
4.0
3.0
2.0
1.0
−log C

FIGURE XIX

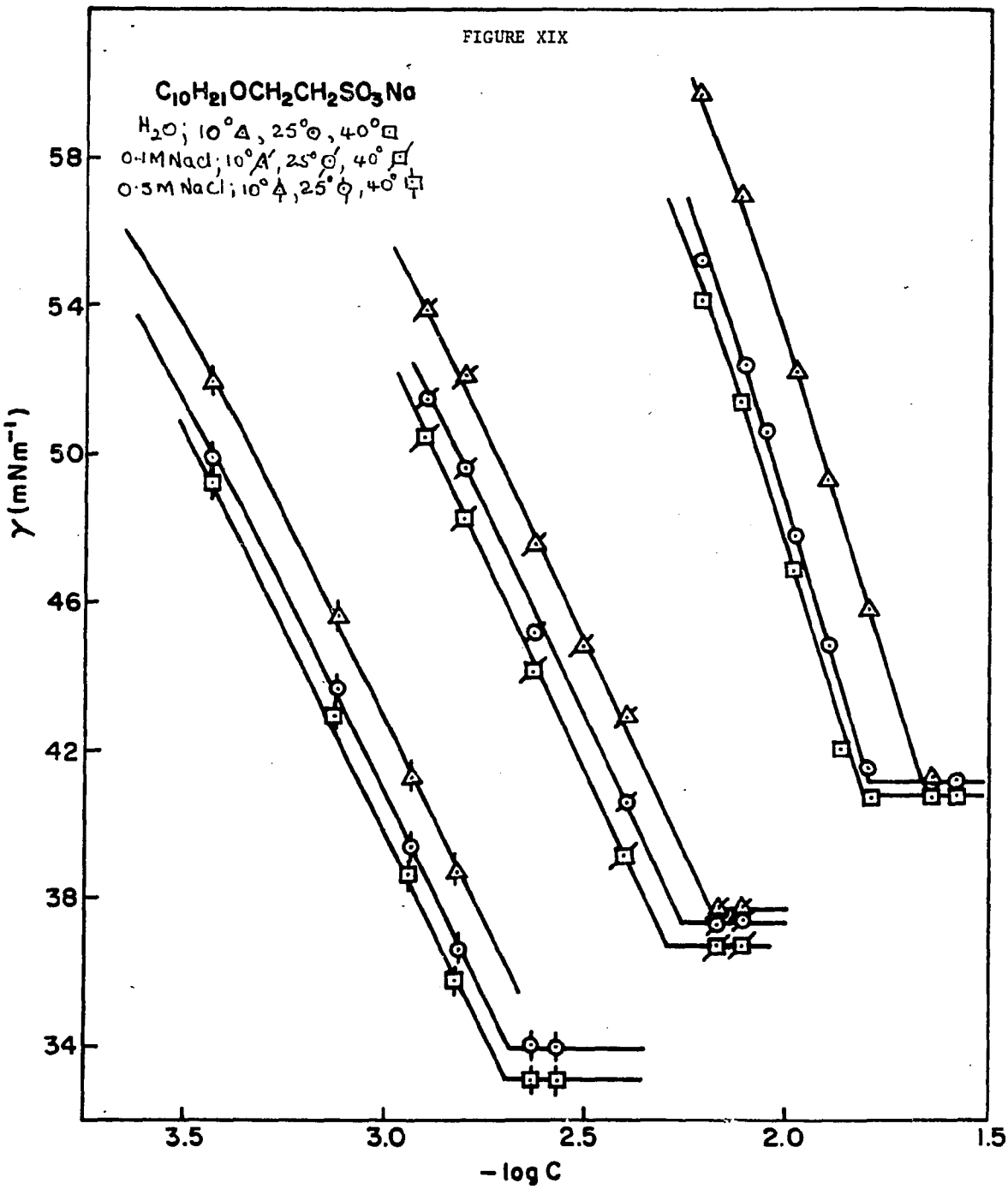
$C_{10}H_{21}OCH_2CH_2SO_3Na$
H_2O; 10° Δ, 25° ○, 40° □
0·1M NaCl; 10° Δ, 25° ○, 40° □
0·5M NaCl; 10° Δ, 25° ○, 40° □
γ (mNm⁻¹)
58
54
50
46
42
38
34
3.5
3.0
2.5
2.0
1.5
− log C

FIGURE XX

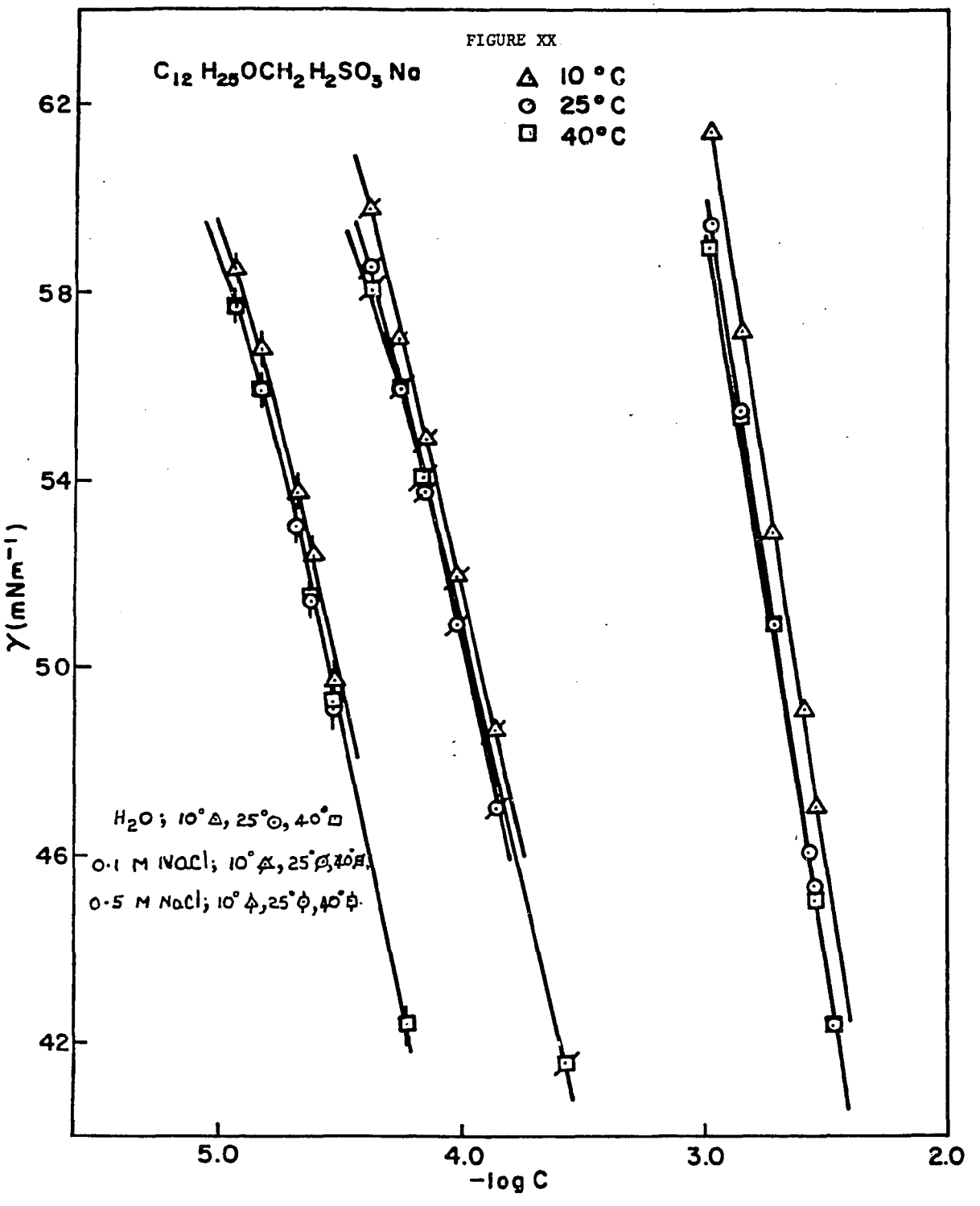
$C_{12}H_{25}OCH_2H_2SO_3Na$
10 °C
25°C
40°C
62
58
54
50
46
42
γ(mNm⁻¹)
H2O; 10°△, 25°○, 40°□
0·1 M NaCl; 10°▲, 25°●, 40°■
0·5 M NaCl; 10°◭, 25°◮, 40°◪
5.0
4.0
3.0
2.0
−log C

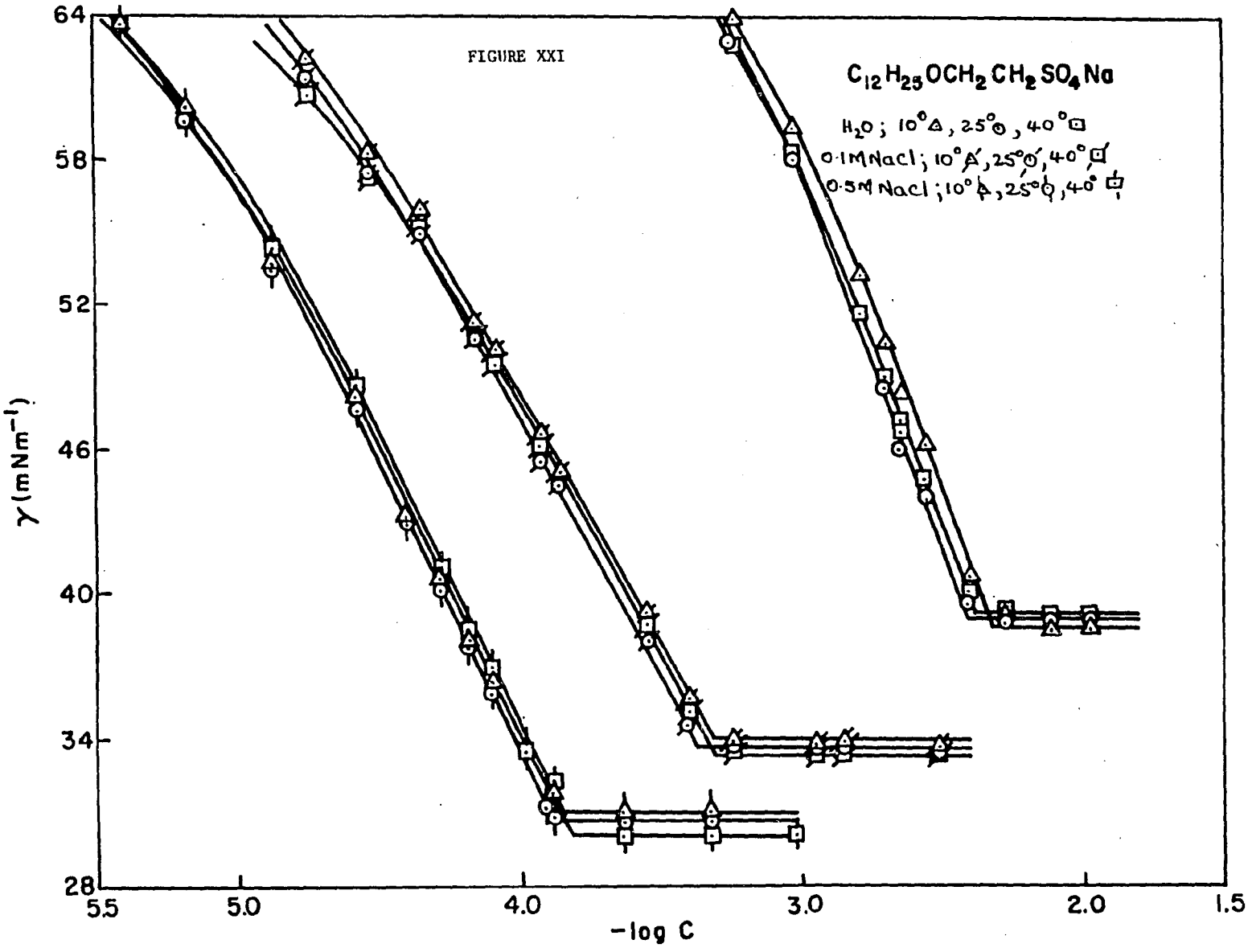
FIGURE XXI
$C_{12}H_{25}OCH_2CH_2SO_4Na$
H_2O; 10°Δ, 25°○, 40°□
0·1M NaCl; 10°Δ, 25°○, 40°□
0·5M NaCl; 10°Δ, 25°○, 40°□
γ (mNm⁻¹)
64
58
52
46
40
34
28
5.5
5.0
4.0
3.0
2.0
1.5
-log C

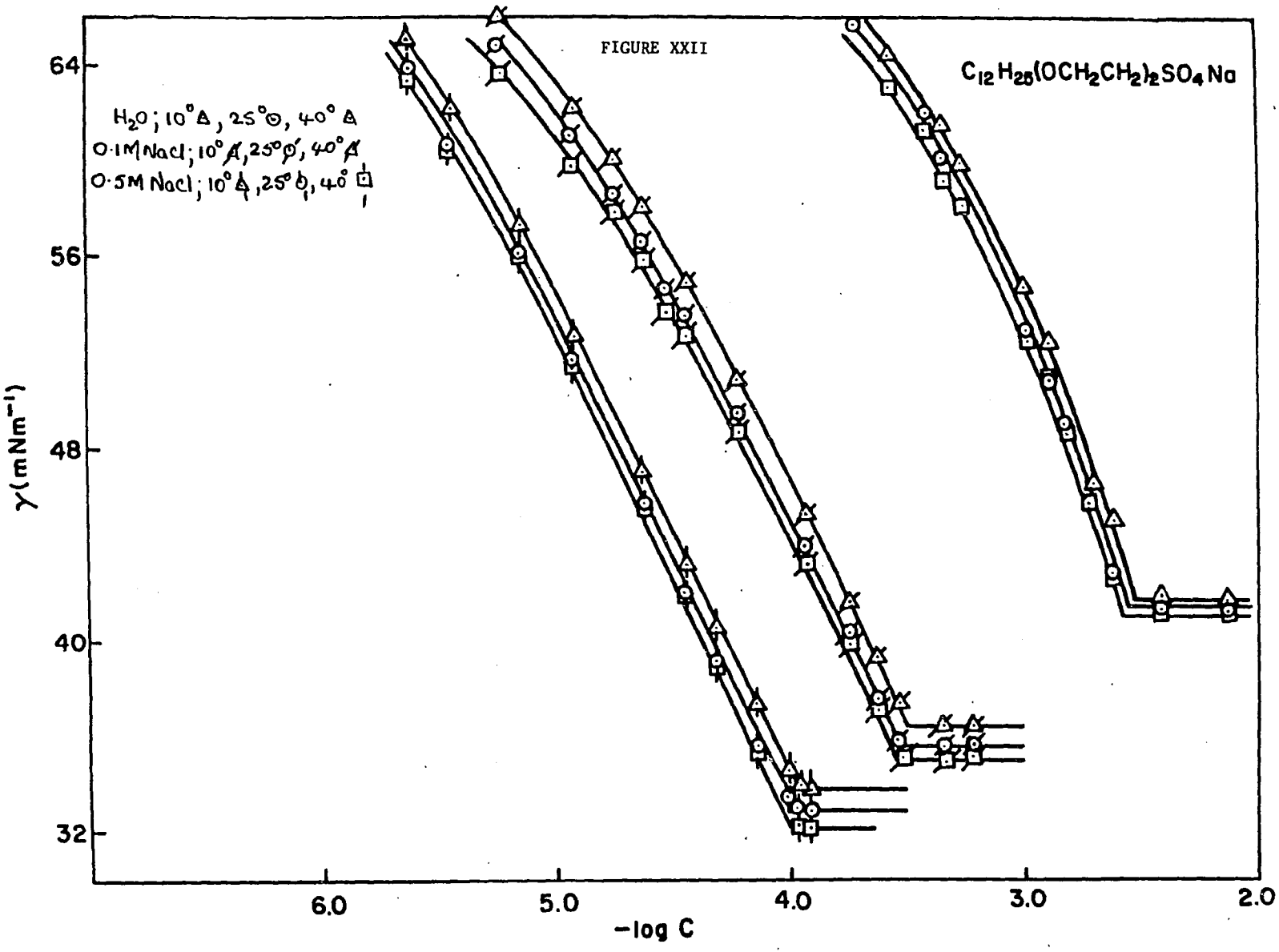
FIGURE XXII
$C_{12}H_{25}(OCH_2CH_2)_2SO_4Na$
H_2O; 10°Δ, 25°Θ, 40° Δ
0·1M NaCl; 10°Δ, 25°Θ, 40°Δ
0·5M NaCl; 10°Δ, 25°Θ, 40° Δ
γ (mNm⁻¹)
64
56
48
40
32
6.0
5.0
4.0
3.0
2.0
−log C

FIGURE XXIII

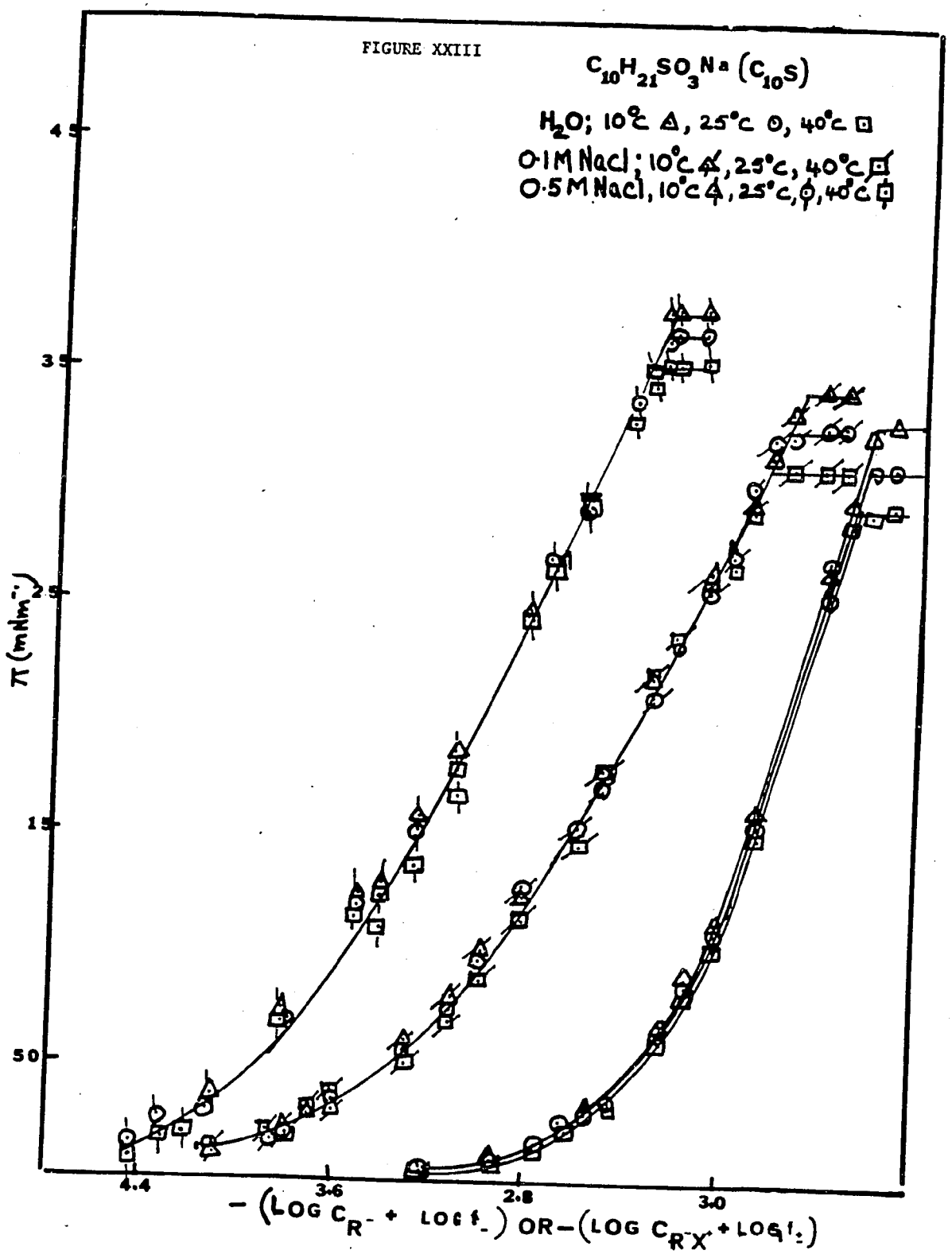

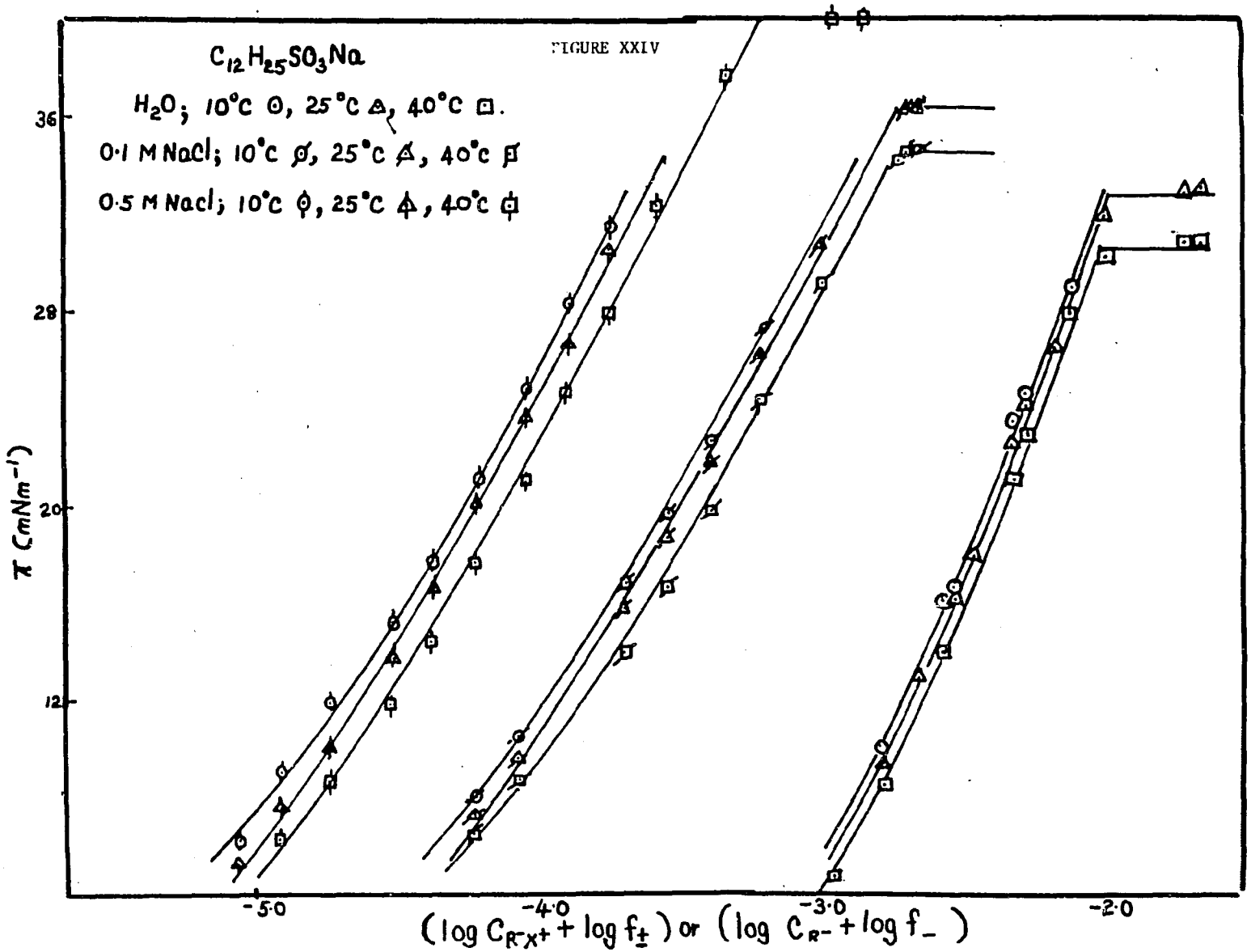
$C_{12}H_{25}SO_3Na$
H_2O; 10°C ⊙, 25°C △, 40°C □.
0·1 M NaCl; 10°C ⊘, 25°C ⧋, 40°C ⧈
0·5 M NaCl; 10°C ⊕, 25°C ⧊, 40°C ⧇
36
28
20
12
π (mNm^{-1})
-5·0
-4·0
-3·0
-2·0
(log $C_{R^-X^+}$ + log $f_\pm$) or (log C_{R^-} + log f_-)
FIGURE XXIV

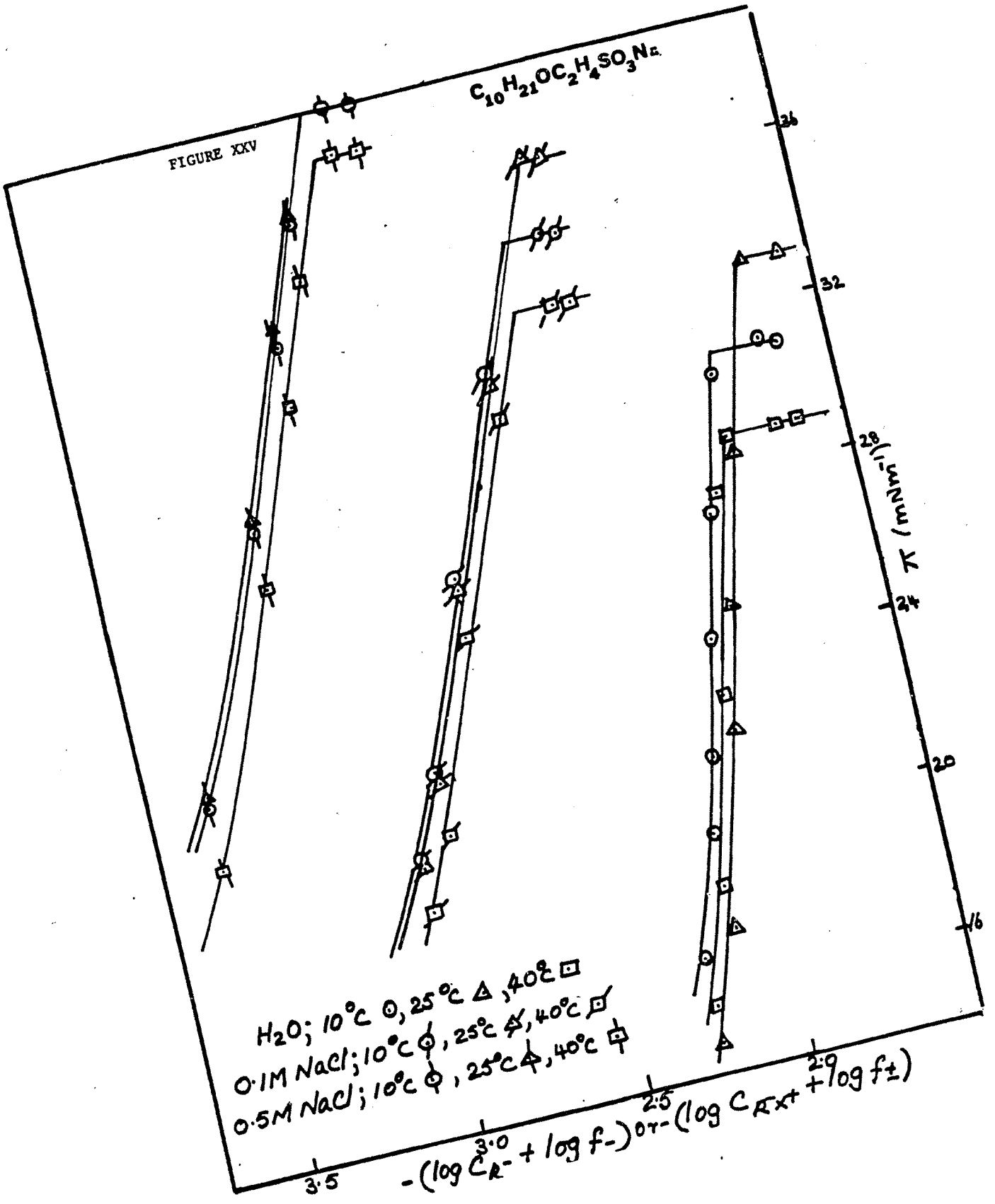
FIGURE XXV
$C_{10}H_{21}OC_2H_4SO_3Na$
H_2O; 10°C ⊙, 25°C △, 40°C ⊡
0·1M NaCl; 10°C ⊙, 25°C △, 40°C ⊡
0·5M NaCl; 10°C ⊙, 25°C △, 40°C ⊡
$-(\log C_{R^-} + \log f_-)$
$-(\log C_{RX^+} + \log f_\pm)$
3·5
3·0
2·5
2·9
26
32
28
24
20
16
K (mN/m)

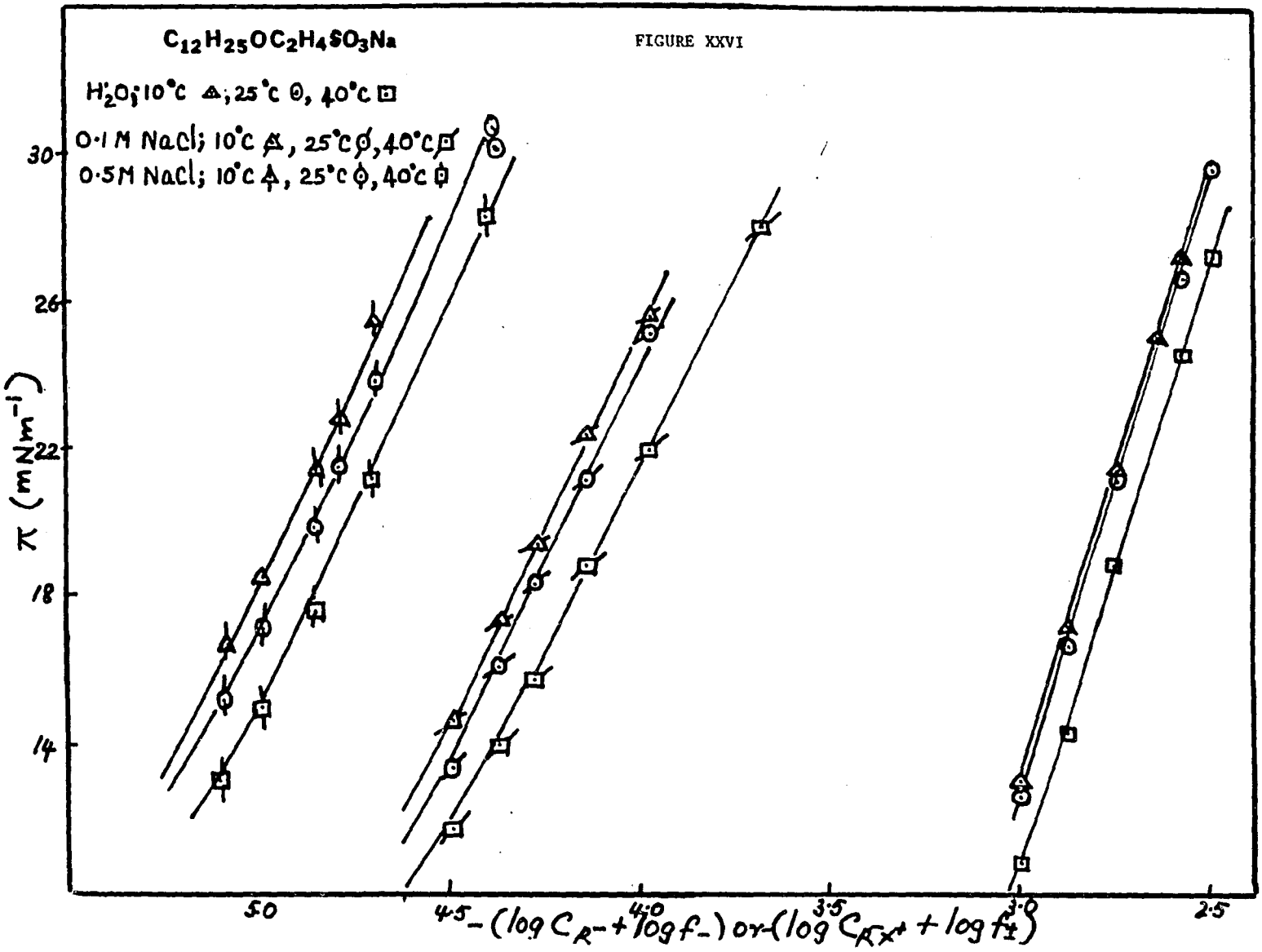
$C_{12}H_{25}OC_2H_4SO_3Na$
H_2O; 10°C △; 25°C ○, 40°C □
0·1 M NaCl; 10°C △, 25°C ◇, 40°C □
0·5M NaCl; 10°C ▲, 25°C ◆, 40°C ■
π (mNm⁻¹)
30
26
22
18
14
5·0
4·5
4·0
3·5
3·0
2·5
$-(\log C_{R^-} + \log f_-)$ or $-(\log C_{RX} + \log f_\pm)$

FIGURE XXVI

FIGURE XXVII

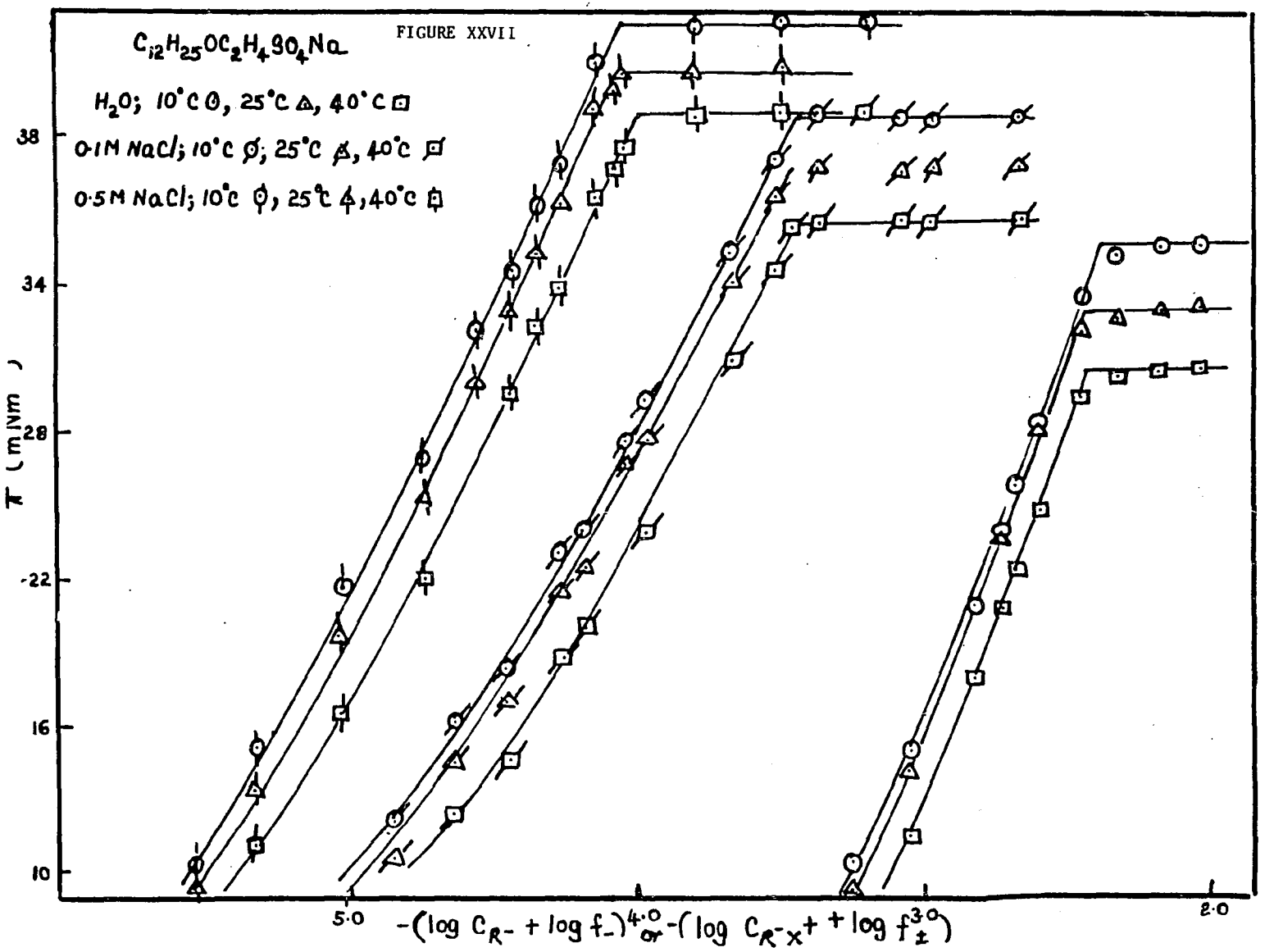

FIGURE XXVIII

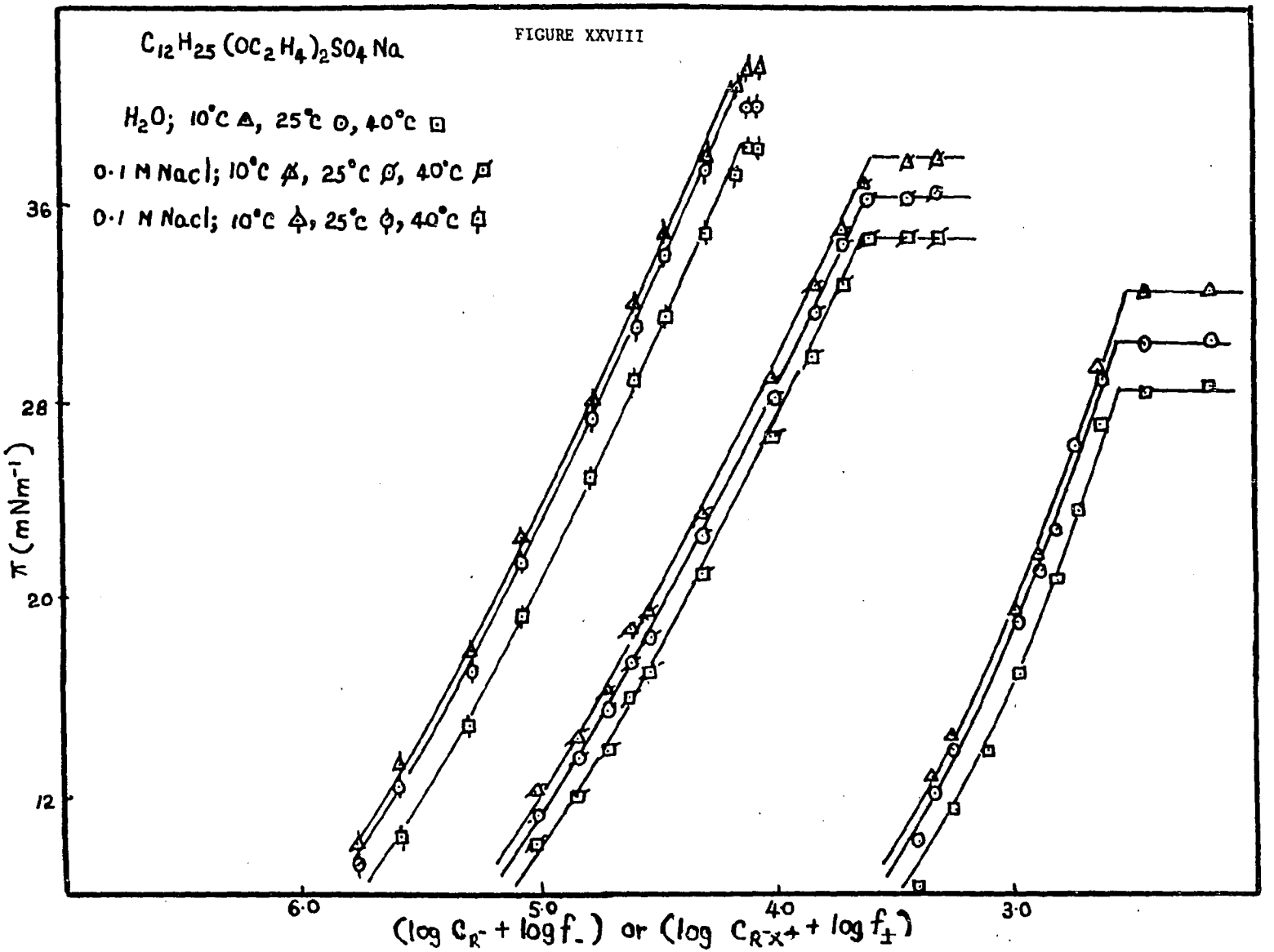

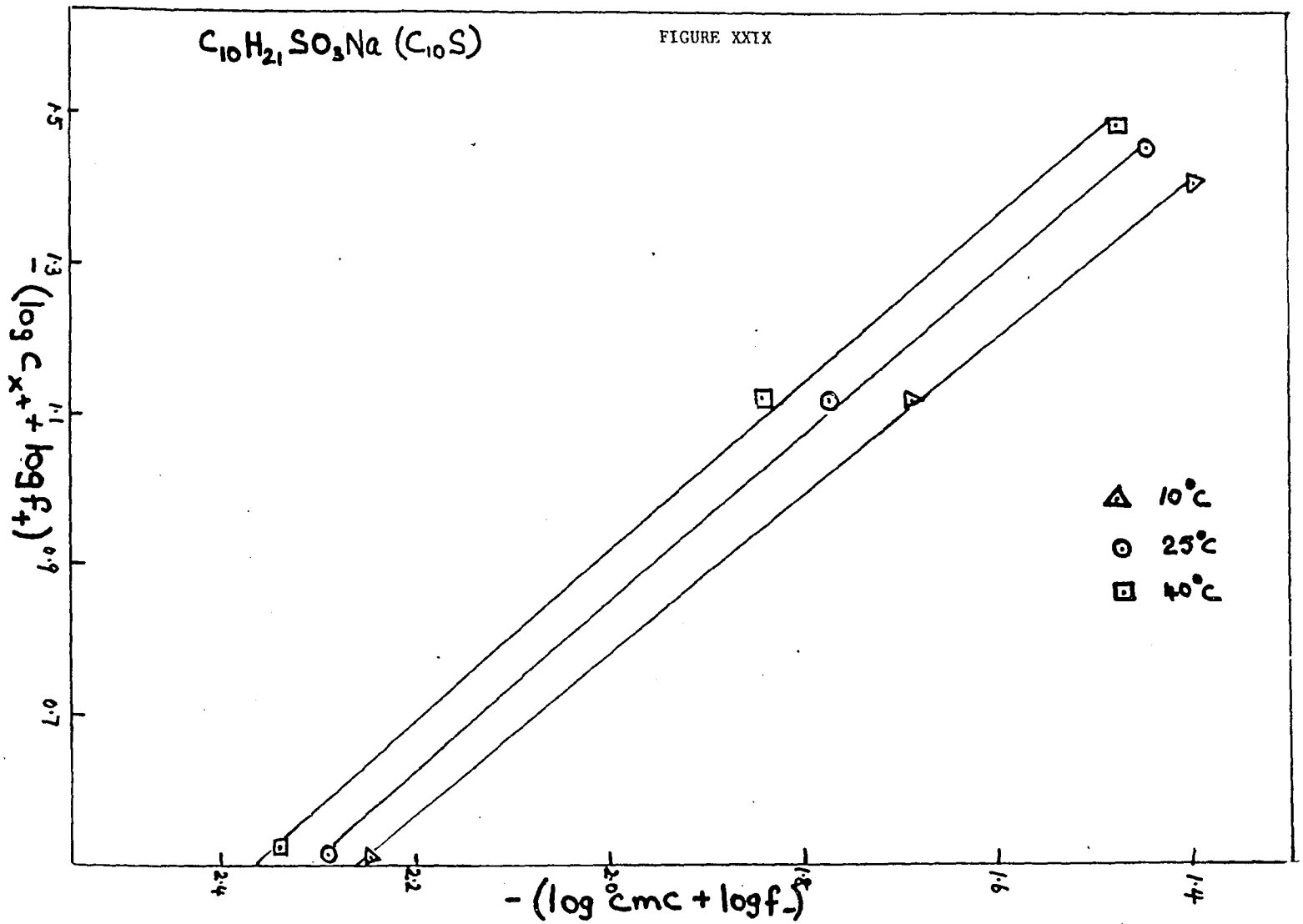
$C_{10}H_{21}SO_3Na$ ($C_{10}S$)
FIGURE XXIX
$-(\log c_{x^+} + \log f_+)$
$-(\log c_{mc} + \log f_-)$
10°C
25°C
40°C
0·7
0·9
1·1
1·3
1·5
2·4
2·2
2·0
1·8
1·6
1·4

FIGURE XXX

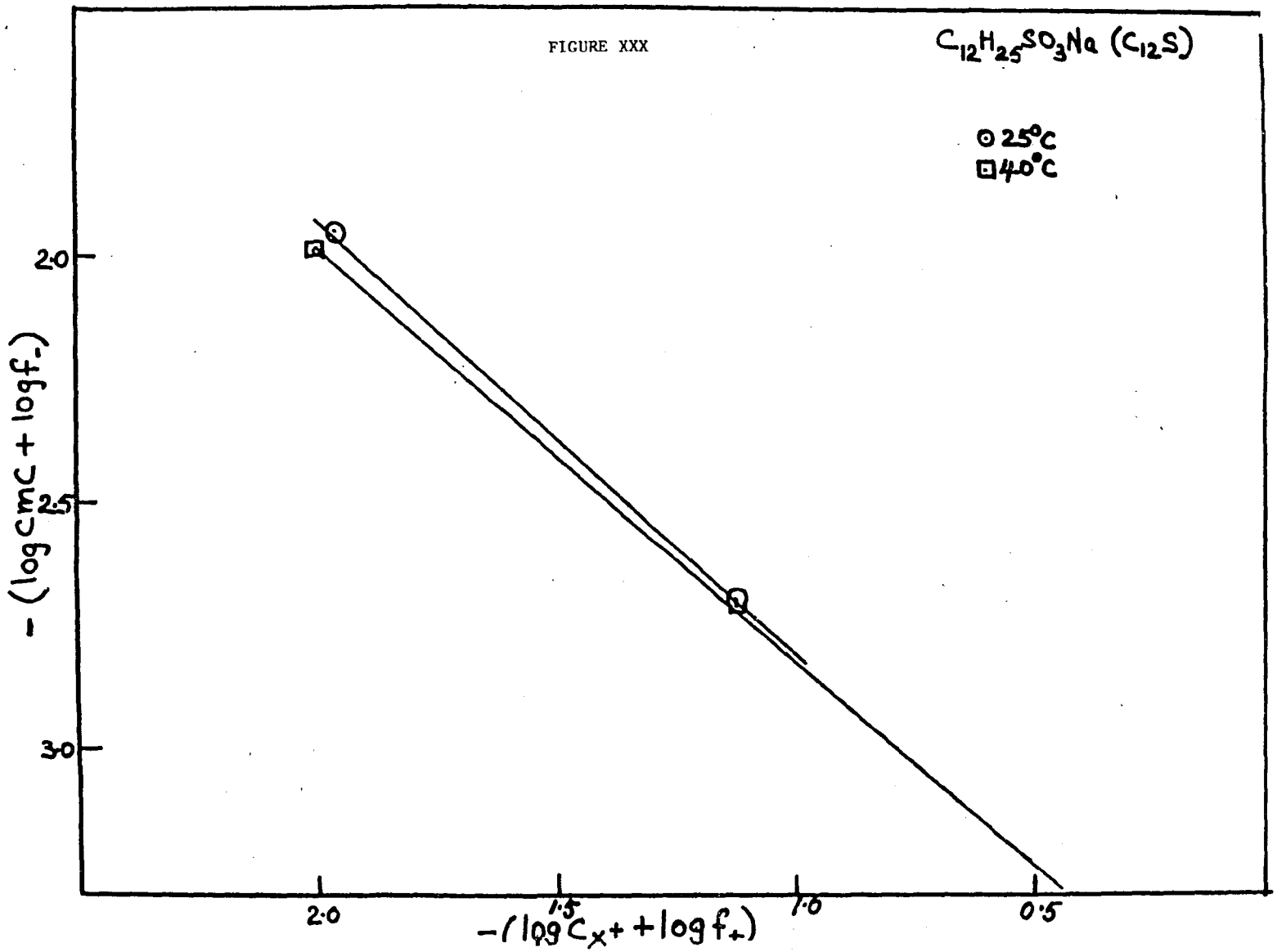
$C_{12}H_{25}SO_3Na$ ($C_{12}S$)
⊙ 25°C
⊡ 40°C
2·0
2·5
3·0
$-(\log cmc + \log f_-)$
2·0
1·5
1·0
0·5
$-(\log C_{x+} + \log f_+)$

FIGURE XXXI

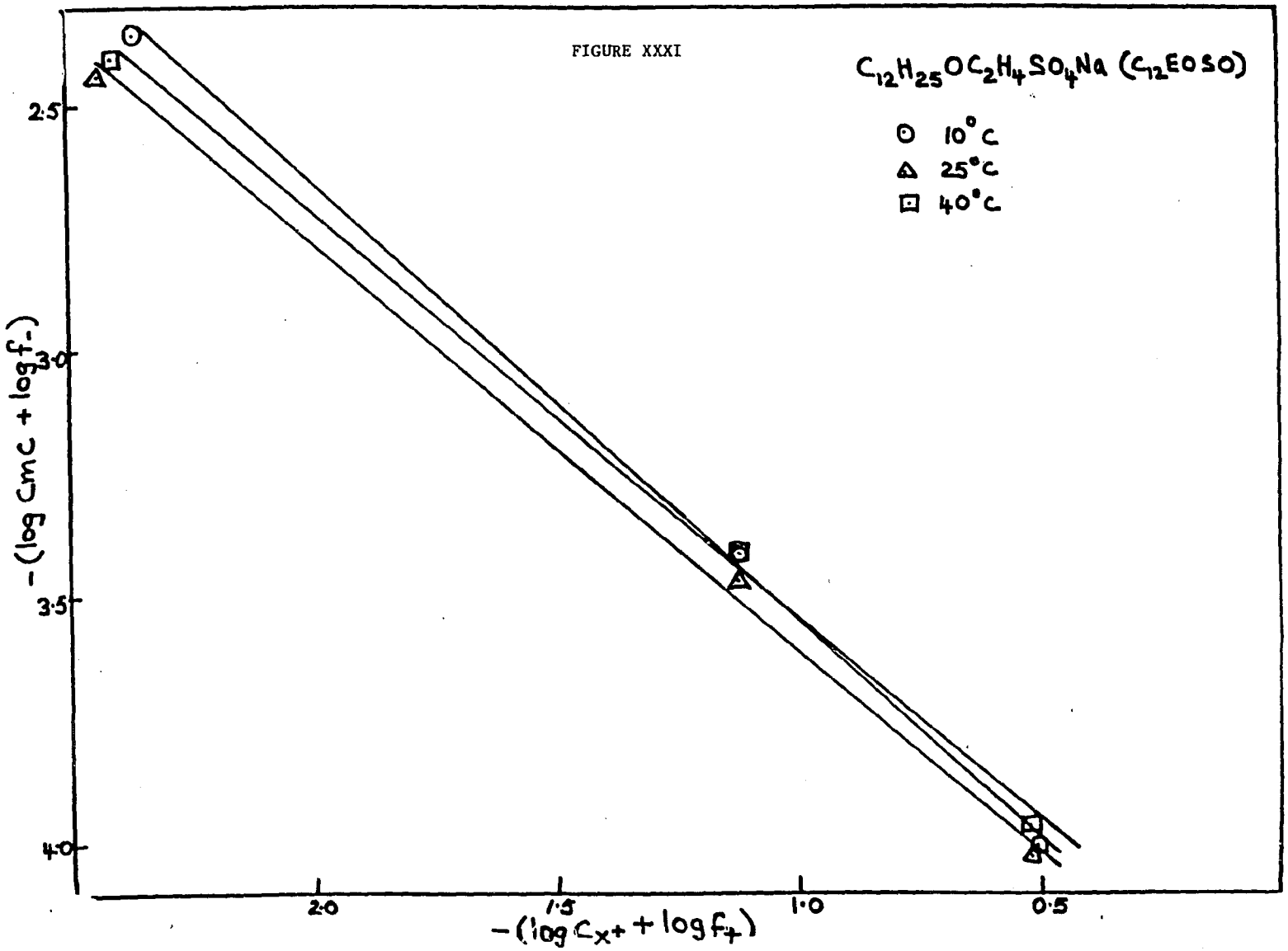
$C_{12}H_{25}OC_2H_4SO_4Na$ ($C_{12}EOSO$)
10°C
25°C
40°C
2·5
3·0
3·5
4·0
$-(\log cmc + \log f_-)$
2·0
1·5
1·0
0·5
$-(\log c_{x+} + \log f_+)$

FIGURE XXXII

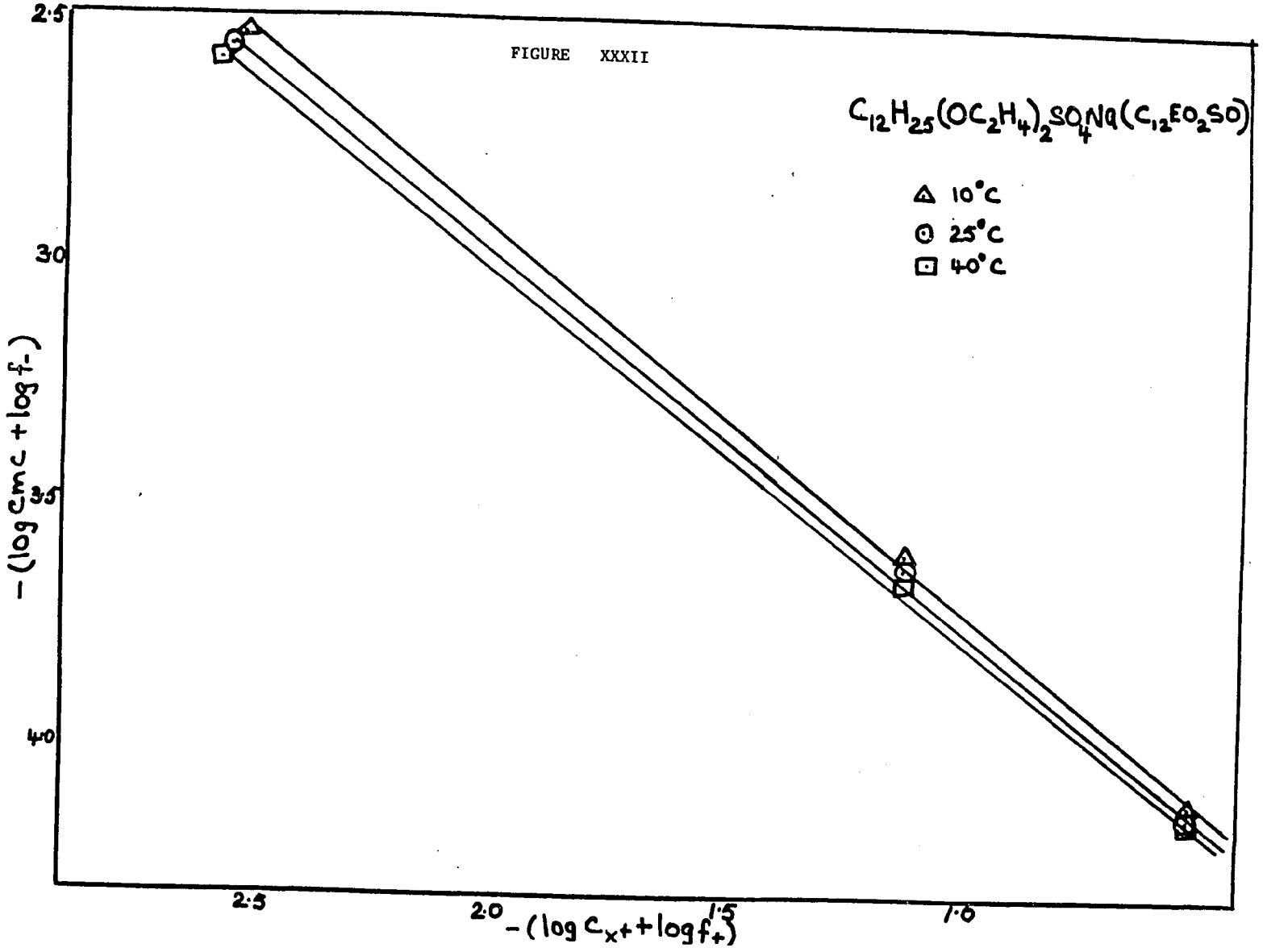

FIGURE XXXIII

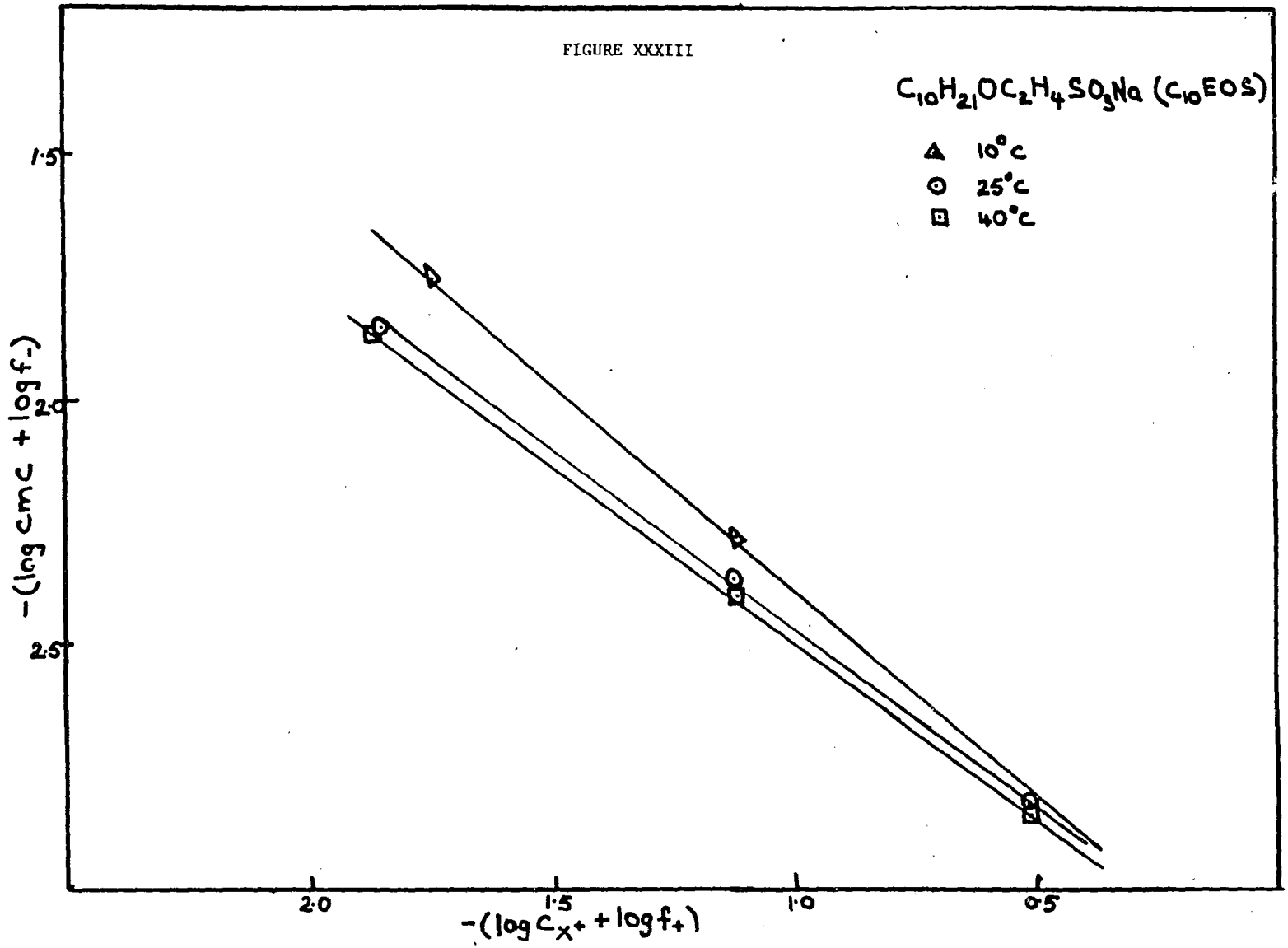

FIGURE XXXIV

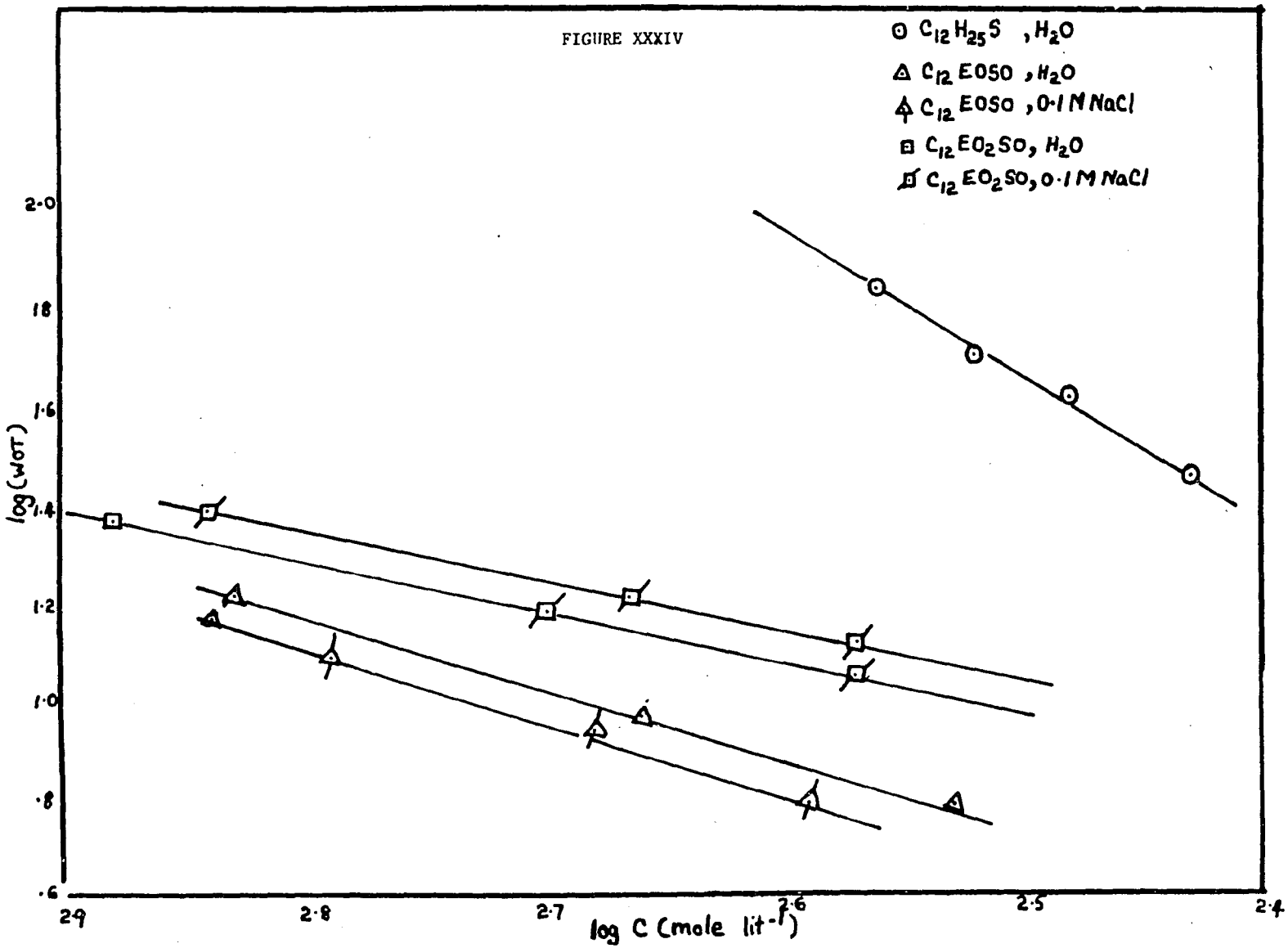

Bibliography

1. Black, W., "Recent Progress in Surface Science," Vol.1, Academic Press, New York, 1964. pg 59.

2. Chemical & Engineering News, Jan 23, 1984, 17.

3. Adamson, A.W., "Physical Chemistry of Surfaces", 2nd edition Interscience Publishers, New York, 1967. Pg 72.

4. Aveyard, R., Haydon, D.A.,"An introduction to the principles of Surface chemistry", Cambridge London, London, 1973 pg 3.

5. Boucher, E.S., Grinchuk, T.M., Zettlemoyer, A.C., J. Am. OilChem Soc., 1968, 49, 45.

6. Rosen, M.J., "Surfactant & Interfacial Phenomena", Wiley Interscience, N.Y., 1976, pg. 60.

7. Matijevic, E., Pethica B.A., Trans. Faraday Soc., 1958, 54, 1384.

8. Posner, A.M.; Anderson. J.R. Alexander A.E., J. Colloid Sci., 1952, 7, 623.

9. Betts, J.J.; Pethica, B.A., Trans. Faraday Soc., 1960, 56, 1515.

10. Tamaki, N.D., Bull. Chem Soc. Japan, 1967, 38,40.

11. Gillap, W.R; Weiner, N.D; Gibaldi, M., J. Phys Chem., 1968,72 2218-2222.

12. Clint, J.M.; Corkill, J.M.; Goodman, J.F; Tate, J.R.,J. Colloid interface Sci., 1968, 28, 522.

13. Tokiwa, K.; Ohki, K.; J. Colloid Interface Sci., 1968, 26, 457.

14. Langmuir, I., J. Am. Chem. Soc., 1917, 39, 1848.

15. Betts, J.J.; Pethica, B.A.,Proceeding of the second international congress of surface activity, Vol 1, London, 1957, pg 152.

16. Betts, J.J.; Pethica, B.A., Trans. Faraday Soc., 1960, 56, 1515.

17. Ward, A.T.H., Trans. Faraday. Soc., 1946, 42, 399

18. Ward, A.T.H.; Tordai, L., Trans. Faraday Soc., 1946, 42,408.

19. Lange, H., in "Nonionic Surfactants", Shick, M. J., Ed., Deckker, New York., 1967, pg. 443-477.

20. Rosen, M. J.; Aronson, S., Colloids Surf., 1981, 3, 201.

21. Mukerjee, P., Advan. Colloid Interface Sci., 1967, 1, 241.

22. Fendler, E.; Fendler, J., Catalysis in Micellar and Macromolecular systems, Acadamic, N.Y., 1975, pg 271-397.

23. Shinoda, K.; Nakagawa, T.; Tamamushi, B.; Isemura, T.,"Colloidal Surfactants.", Acadamic press, New York, 1963, pg 1-80.

24. Mukerjee, P.; Mysels, K.J.,Critical micelle concentration of aqueous surfactant systems, NSRDS-NBS 36, U.S. Dept. of commerce, Washington D.C., 1971.

25. Corkill, J.M.; Goodman, J.F.; Walker, T., Trans. Faraday, Soc. 1067. 63, 768.

26. Benjamin, L., J. Phys. Chem., 1966, 70, 3790.

27. Walker, T., J. Colloid Interface Sci., 1971, 45, 372.

28. White, P.; Benson, G.C., Trans. Faraday, Soc., 1959, 55, 1025.

29. Corkill, J.M.; Goodman, J.F.; Tate, J.R., Trans. Faraday, Soc., 1964,60 996.

30. Benjamin, L., J. Phys. Chem., 1964, 68, 3575.

31. Goddard, E.D.; Hoeve, C.A.J.; Benson, G.C., J. Phys. Chem., 1957, 61, 593.

32. Goddard, E.D.; Benson, G.C., Can. J. Chem., 1957, 35, 986.

33. Flockhart, B.D., J. Colloid Sci., 1961, 16, 484.

34. Corkill, J.M.; Goodmann, J.F.; Harrold, S.P., Trans. Faraday. Soc., 1964, 60, 202.

35. White, P.; Benson, G.C., Trans. Faraday, Soc., 1959, 55 1025.

36. Nasho, J. Colloid Sci., 1959, 59, 14.

37. Poland, D.C.; Sheraja, H.A., J. Phys. Chem., 1965, 69, 2431.

38. Phillips, J.N., Trans. Faraday. Soc. 1955, 51, 561.

39. Shinoda, K., J. Phys. Chem., 1956, 60, 1439.

40. Matigevic, E.; Pethica, B.A., Trans. Faraday. Soc., 1957, 54, 587.

41. White, P.; Benson, G.C., J. Phys. Chem. 1960, 64, 599.

42. Shinoda, K.; Hutchinson., E., J.Phys. Chem., 1962, 66, 577.

43. Mukerjee, P., J. Phys. Chem., 1962, 66, 1375.

44. Schick, M.J., J. Phys. Chem., 1963, 67, 1796.

45. Corkill, J.M.; Goodmann, J.F.; Harrold, S.P., Trans. Faraday, Soc., 1964,60, 202.

46. Mukerjee, P., J. Phys. Chem., 1965, 69, 4038.

47. Corkill, J. M.; Goodmann, J.F.; Harrold, S.P.; Tate, J.R.,Trans. Faraday. Soc., 1967, 63, 240.

48. Benjamin, L., Colloid. interface Sci., 1966, 22, 386.

49. Stanisby, G.; Alexander, A.E., Trans. Faraday. Soc., 1950, 46, 587.

50. Aranow, R.H., J. Phys. Chem., 1963, 67, 556.

51. Hoeve, C.A.J.; Benson, G.C., J. Phys. Chem., 1957, 61, 1149.

52. Shinoda, K.; Nakagawa, T.; Tamaushi, B.; Isemura, T.,"Colloidal Surfactants", Acadamic press, New York, 1963, pg 20-21.

53. Corrin, M.L., J. Colloid Sci., 1948, 3, 333.

54. Shedlovsky, L.; Jacob, C.W.; Epstein, M.B., J. Phys. Chem. 1963,67, 2075.

55. Botre, C.; Cresenzi.; Mele, A., J. Phys. Chem., 1969, 63, 650.

56. Ingram, T.; Jones, M.N., Trans. Faraday Soc., 1969, 65, 297.

57. Andersen, J.E.; Taylor, H., J. Pharm. Pharmcol., 1971, 23, 311.

58. Phillips, J.N.; Mysels, K.J., J. Phys. Chem., 1955, 59, 325.

59. McBain, J.W.; Brady, A.P., J. Am. Chem. Soc., 1943, 65, 2072.

60. Mysels, K.J.; Mukerjee, P.; Abudiyyah, M., J. Phys. Chem., 1963,67, 1943.

61. Elworthy, P.H.; Mysels, K.J., J. Colloid. Sci., 1966, 21, 33.

62. Williams, E.T.; Woodberry, N.T.; Dixon, J.K., J. Colloid Sci., 1957, 12., 452.

63. Hoyer, H. W., J. Phys. Chem., 1957, 61, 1283.

64. Shinoda, K.; Katsura, K., J. Phys. Chem., 1964, 68, 1568.

65. Rosen, M.J., J. Am. Oil Chem. Soc., 1974, 51, 461.

66. Rosen, M.J., J. Colloid. Interface. Sci., 1976, 56, 320.

67. Miles, G.D.; Shedlovsky, L., J. Phys Chem., 1944, 57.

68. Williams, R.J.; Phillips, J.N.; and Mysels, K.J., Trans. Faraday Soc., 1955, 51, 728.

69. Vijayendran, B.R., J. Colloid. Interface. Sci., 1977, 60, 418.

70. Rosen, M.J., J.Colloid Interface Sci., 1981, 79, 587.

71. Crook, E.H.; Fordyce, D.B.; Trebbi, G.F., J. Phys. Chem., 1963, 67, 1987.

72. Crook, E.H.; Trebbi, G.F.; Fordyce, D.B., J. Phys. Chem., 1964, 68, 3592.

73. Corkill, J.M.; Goodman, J.F.; Ottewill, R.H., Trans. Faraday Soc., 1961, 57, 1627.

74. Meguro, K; Takasawa, Y; Kawahashi, N; Tabata, Y; Ueno, M.,J.Colloid interface sci, 1981, 83, 50.

75. Schick, M.J.; Gilbert, A.H., J. Colloid Sci., 1965, 20, 464.

76. Erust, R; Miller, E.J., Jr., "Amphoteric Surfactants" Bluestein,B.R; Hilton, C.L., Ed; Marcel Dekker: New York, 1982; pg. 137-150.

77. Kaminski, M.; Linfield, W.M., J. Am. Oil Chem. Soc. 1979,56,7711.

78. Tori, K.; Nakagawa, T., Kolloid - Z.Z Polym. 1963, 50, 187.

79. Tori, K.; Nakagawa, T., Kolloid - Z.Z Polym., 1963, 188, 47.

80. Tori, K.; Nakagawa, T., Kolloid - Z.Z Polym., 1963, 189, 50.

81. Tori, K.; Nakagawa, T., Kolloid - Z.Z Polym., 1963, 191, 42.

82. Tori, K.; Nakagawa, T., Kolloid - Z.Z Polym., 1963, 191, 48.

83. Beckett, A.H.; Woodward, R.J., J.Pharm. Pharmecol., 1963, 15, 422.

84. Herrmann, K.W., Colloid Interface Sci., 1966, 22, 352.

85. Molyneux, P.; Rhodes C.T.; Swarbrick, J., Trans. Faraday Soc., 1965,61, 1043.

86. Swarbrick, J.; Daruwala, J., J. Phys. Chem., 1969, 73, 2627

87. Swarbrick, J., J. Pharm. Sci., 1969, 58, 147.

88. Jungermann, E., "Cationic Surfactants", Ed Marcel Dekker: New York, 1970; pg 1 to 5.

89. Samis, C.S.; Hartley, G.S., Trans. Faraday Soc., 1938, 34,1288.

90. Ford, W.P.J.; Ottewill, R.H.; Parreira, H.C.,J.Colloid interface Sci., 1966, 21,522.

91. Goddard, E.D.; Harva, O.; Jones, T.G., Trans. Faraday Soc., 1953, 49, 980.

92. Venable, R.L.; Nauman, R.V., J. Phys. Chem., 1964, 68, 3498.

93. Anacher, E.W.; Gouse, H.M., J. Phys. Chem., 1963, 67, 1713.

94. Tamaki, K., Bull Chemical Soc. of Japan, 1967, 38 - 40.

95. Anderson, J.E.; Taylor, H., J.Colloid Sci., 1964, 19, 495.

96. Bistline, R.G.; Stirton, A.J.; Weil, J.K.; Maurer, E.W.,J. Am. oil Chem. Soc., 1957, 34, 516.

97. Weil, J.K.; Bistline, R.G.; Stirton, A.J., J. Am. Oil Chem. Soc., 1958, 62, 1083.

98. Tokiwa, F., J. Phys. Chem., 1967, 71, 1214.

99. Lange, H.; Schwuger, Kolloid-z.z.-Polymere:, 1968, 223, 145.

100. Rosen, M.J.; and Goldsmith, H.A.,Systematic Analysis of Surface-Active Agents, 2nd ed., Wiley-Interscience New York, 1972, pg. 427.

101. Rosen, M.J.; Hua, X.Y.; Bratin, P.; Cohen, A.W.,Anal Chem., 1981, 53, 1981.

102. Wilhelmy, L., Ann. Phys., 1863, 119, 177.

103. Hsiao, L.; Dunning, H.N.; Lorenz, P.B., J.Phys. Chem., 1956, 60, 657.

104. Shinoda, K.; Yamanaka, T.; Kinoshita, K., J. Phys. Chem., 1959, 63, 648.

105. Rosen, M.J., "Solution Chemistry of Surfactants", Vol. I, K.L. Mittal, Ed., Plennm, New York, 1979, pg. 45-61.

106. McAuliffe, C., Nature (LONDON), 1963, 200, 1092

107. Kwan, C.; Rosen, M.J., J. Phys. Chem., 1980, 84, 547.

108. Rosen, M.J.; Cohen, A.W.; Dahanayake, M.; Hua, X.Y., J.Phys. Chem., 1982, 86, 541.

109. Caskey, J.A.; Barlage W.B.Jr., J.Colloid interface Sci., 1971, 35, 46.

110. Klevens, H.B., J. Phys. Colloid Chem., 1953, 74, 30.

111. Choux, G.; Benoit, R.C., J. Am. Chem. Soc., 87 (969) 6221

112. Hua, X.Y; Rosen, M.J., J. Colloid, Sci., 1982, 87, 469.

113. Rosen, M.J.; and Zhao, F., J. Colloid Interface Sci., 1983,95, 443.

114. Stigter, D., J. Phys Chem., 1974, 78, 2480.

115. Klevens, H.B., J. Am. Oil Chem. Soc., 1953, 30, 74.

116. Draves, C.Z., Am. Dyestuff Rep 1938, 28, 425.

117. Fowkes, F.M., J. Phys. Chem., 1953, 98, 57.

118. Crook, E.H.; Fordyce, D.B.; Trebbi, G.F., J. Am. Oil Chem. Soc., 1964, 41,231.

119. Rosen, M.J.; Zhu, B.Y., in"Structure/Performance Relationships of Surfactants", Rosen, M.J., Ed ACS Symposium Series, 253, Washington, D.C., 1983; pg. 61-70.

120. Ross, J; Miles, G., Oil Soap, 1941, 18, 99.

121. American Society for Testing and Materials, Method D 1173-53, Philadelphia, 1953.